Fall 2009

A control-theoretical fault prognostics and accommodation framework for a class of nonlinear discrete-time systems

Balaje T. Thumati

Department: Electrical and Computer Engineering

A CONTROL-THEORETIC FAULT PROGNOSTICS AND ACCOMMODATION FRAMEWORK FOR A CLASS OF NONLINEAR DISCRETE-TIME SYSTEMS

by

BALAJE T. THUMATI

A DISSERATION

Presented to the Faculty of the Graduate Studies of the

MISSOURI UNIVERSITY OF SCIENCE AND TECHNOLOGY

In Partial Fulfillment of the Requirements for the Degree

DOCTOR OF PHILOSOPHY

in

ELECTRICAL ENGINEERING

2009

Approved by

Jagannathan Sarangapani, Advisor
Kelvin Erickson
Cihan Dagli
Chengshan Xiao
S. N. Balakrishnan
Al Salour

PUBLICATION DISSERTATION OPTION

This dissertation consists of the following six articles that have been accepted/submitted for publication as follows:

Paper 1, Balaje T. Thumati and S. Jagannathan, "A Fault Detection and Prediction Scheme Using Asymptotic Estimators for Non-affine Nonlinear Discrete-time Systems with State Faults," under review in the International Journal of Control.

Paper 2, Balaje T. Thumati and S. Jagannathan, "A Robust Fault Detection and Prognostics Scheme for Nonlinear Discrete Time Input-Output Systems," to appear in the December issue of International Journal of Computational Intelligence in Control.

Paper 3, Balaje T. Thumati and S. Jagannathan, A Model Based Fault Detection and Prediction Scheme for Nonlinear Multivariable Discrete-time Systems with Asymptotic Stability Guarantees", accepted in IEEE Transactions on Neural Networks.

Paper 4, Balaje T. Thumati and S. Jagannathan, "A Novel Prognostics Scheme for Nonlinear Discrete-time Systems with Multiple State Faults and Fault Types," Intended for submission to IEEE Transaction on Neural Networks.

Paper 5, Balaje T. Thumati and S. Jagannathan, "An Asymptotically Stable Online Fault Detection and Accommodation Scheme for Nonlinear Discrete-time Systems," under revision in Automatica.

Paper 6, Gary R. Halligan, Balaje T. Thumati and S. Jagannathan, "A Novel Fault Detection and Prediction Scheme in Discrete-time Using a Nonlinear Observer and Artificial Immune System as an Online Approximator," Intended for submission to IEEE Transaction on Control Systems and Technology.

ABSTRACT

Fault diagnostics and prognostics schemes (FDP) are necessary for complex industrial systems to prevent unscheduled downtime resulting from component failures. Existing schemes in continuous-time are useful for diagnosing complex industrial systems and no work has been done for prognostics. Therefore, in this dissertation, a systematic design methodology for model-based fault prognostics and accommodation is undertaken for a class of nonlinear discrete-time systems. This design methodology, which does not require any failure data, is introduced in six papers.

In Paper I, a fault detection and prediction (FDP) scheme is developed for a class of nonlinear system with state faults by assuming that all the states are measurable. A novel estimator is utilized for detecting a fault. Upon detection, an online approximator in discrete-time (OLAD) and a robust adaptive term are activated online in the estimator wherein the OLAD learns the unknown fault dynamics while the robust adaptive term ensures asymptotic performance guarantee. A novel update law is proposed for tuning the OLAD parameters. Additionally, by using the parameter update law, time to reach an a priori selected failure threshold is derived for prognostics. Subsequently, the FDP scheme is used to estimate the states and detect faults in nonlinear input-output systems in Paper II and to nonlinear discrete-time systems with both state and sensor faults in Paper III.

Upon detection, a novel fault isolation estimator is used to identify the faults in Paper IV. It was shown that certain faults can be accommodated via controller reconfiguration in Paper V. Finally, the performance of the FDP framework is demonstrated via Lyapunov stability analysis and experimentally on the Caterpillar hydraulics test-bed in Paper VI by using an artificial immune system as an OLAD.

ACKNOWLEDGMENTS

I would like to express my deep thanks to my advisor, Dr. Jagannathan Sarangapani for his valuable guidance, time and support. I also would like to thank Dr. Kelvin Erickson, Dr. Chengshan Xiao, Dr. Cihan Dagli, Dr. S. N. Balakrishnan, and Dr. Al Salour for serving on my doctoral committee. I also thank the Intelligent System Center (ISC) and the NSF Intelligent Maintenance System Center (IMS) at Missouri S & T for funding my education through a graduate research assistantship.

I am greatly thankful to my father, Dr. T. S. Thandavamoorthy for his encouragement and also dedicate this dissertation to my beloved late mother, T. T. Vijayanthimala. I also express my sincere gratitude to rest of my family members back home in India for their understanding and love. I also thank all my friends here in the US and as well back home for their time and support.

I also would like to thank all my fellow colleagues who made my time in Ph.D. program fun and exciting. I also would like to extend a special thanks to Dr. Maciej Zawodniok and Jeff Birt for their support and time.

Finally, I would like thank the staff of ECE department for their continuous assistance and also would like to thank the staff of Curtis Laws Wilson Library for providing me with the necessary literature.

TABLE OF CONTENTS

Page

LIST OF ILLUSTRATIONS

SECTION

1. INTRODUCTION

In the past few decades, with the availability of cheap and reliable embedded computer hardware along with sensors, scientists and engineers have developed complex engineering systems such as automotive vehicles, UAVs, aircrafts, power plants, DoD vehicles etc. These technological advancements have improved our quality of life but with the potential risk of component failures. For instance, faults undetected in an aircraft, blackout of 2003 in the northeast due to power system faults, could be disastrous and may cost heavily.

In the earlier days, in industrial plants, a structured maintenance plan is not utilized costing the manufacturer dearly. Subsequently, a scheduled maintenance plan was implemented to reduce machine down. However, this has lead to increased false and missed alarms. Therefore, a proactive maintenance scheme is being developed by monitoring the complex industrial systems and in the event of a fault, an alarm is generated. Such a maintenance scheme is expected to minimize missed and false alarms and as well reduce machine down time and cost. Early fault detection schemes were soon found to be unreliable and required human intervention. Later, many developed data driven schemes heavily relied on sensor information for decision making. But, due to low reliability of sensors, these schemes soon faded out.

With the progress of research, it was determined that any development on fault detection and prediction should take into account the inherent system nonlinearities,

disturbances or noise. Thus robust fault detection (FD) schemes which reduce missed or false alarms are being introduced in the literature.

In general, fault diagnosis and prognosis of complex industrial nonlinear systems comprise of four major tasks: i) *fault detection*; ii) *fault isolation*; iii) *fault accommodation*; and iv) *prognostics*. Detection of an abrupt, incipient and intermittent fault in a given system is normally referred to as fault detection whereas isolation involves determining the root cause and identifying the fault upon detection. In other words, fault detection and isolation will render diagnostics. Moreover, in certain applications it may be possible to reconfigure the controller in order to accommodate the effects of the fault, which is known as fault accommodation. Finally, estimating the remaining useful life of a system after a fault has occurred is referred to as prognostics. Therefore, prognostics include fault isolation and time to failure determination.

In general, literature indicates that two most prominent fault detection methodologies exist: *hardware redundancy* and *analytical redundancy-based framework.* In the hardware redundancy framework, redundant hardware is used for detecting a fault in the system. For example, in a process, two sensors of the same kind measuring the same process variable can be deployed. When the measurements from one sensor deviate from the other, a fault is alerted. However, such a scheme is not only expensive but also consumes space.

Among the analytical-based fault detection framework, the two prominent methods, qualitative and quantitative, are introduced. In the qualitative technique, process or experimental data is used for detection. Qualitative techniques are generally referred to as data-driven techniques. Figure 1.1 illustrates the detection of fault using signals,

where the process is monitored using sensors. Subsequently, features are extracted from the measured signals using techniques such as Fourier analysis, Wavelet analysis etc. These features are compared against normal signatures to detect faults in the process. Additionally, to understand the failures better, data have to be obtained continuously from the system. Therefore, this technique is found to be time consuming and expensive. The detection depends upon the quality of the collected data. Finally, the data driven techniques are sensitive to system and operational changes.

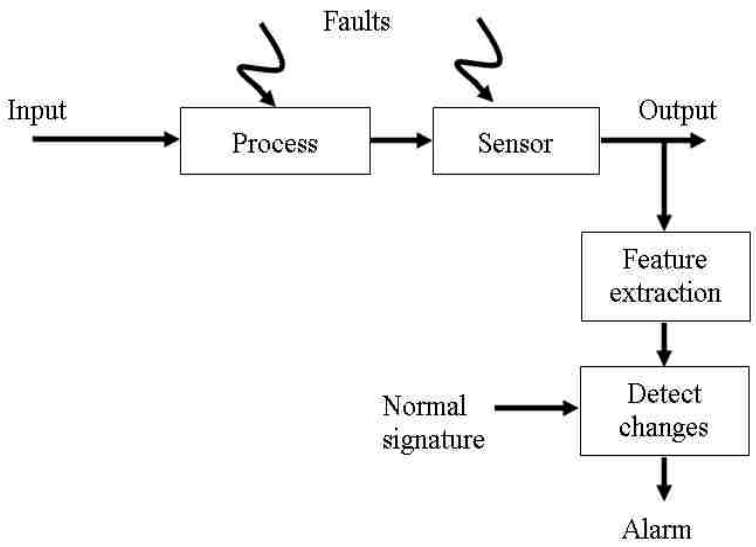

Fig. 1.1: A qualitative technique based fault detection.

By contrast, in the quantitative method, a model representative of the system is utilized for detecting faults. This model is typically derived from either first principles or borrowed from control scientists/engineers. The system model provides an estimate of the system states by observing the inputs and measured outputs of the nonlinear system. A residual signal is then generated by comparing the output of the model with that of the

system. A fault is detected in a robust manner even under system uncertainties when the residual deviates beyond a predefined threshold value. The selection of the threshold is a challenging task since an improper threshold selection might lead to false and missed alarms; however, several attempts have been made to address this issue using analytical methods. One such residual based FD design is shown in Fig. 1.2, where an observer with online fault learning capabilities is used for fault detection. As explained above, the fault is detected by comparing the generated residual against *apriori* chosen threshold. Subsequently, the online approximator (OLA) such as neural networks, fuzzy systems etc., are initiated online to learn the unknown fault dynamics. Additionally, the OLA scheme is tuned online without any offline training. Therefore, in this way the fault is successfully detected and learned in real-time without any offline training. The advantage of using a quantitative based FD scheme is reduced cost and space requirements, and also generic. Consequently, this online framework can be used for a range of applications.

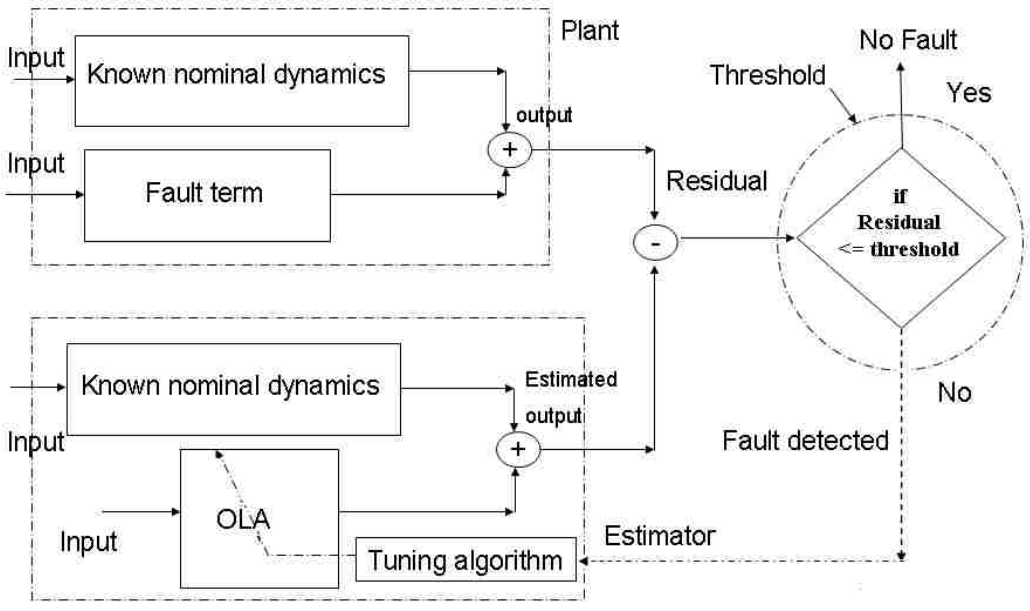

Fig. 1.2: Block diagram representation of a model-based fault detection scheme.

Next, an overview of current methodologies for fault diagnosis and prognosis is presented, and their shortcomings are exposed. Subsequently, the organization of this dissertation along with the contributions of this work is introduced.

1.1 OVERVIEW OF THE FAULT DETECTION METHODOLOGIES

There have been numerous research activities focusing on solving the problem of fault diagnosis and prognosis. However, in the past couple of decades, many researchers developed fault detection (FD) schemes by considering a linear representation of the nonlinear system. Popular FD schemes include parity relations [1], geometric relationships [2], and observers or estimators [3].

Recently, with better understanding of nonlinear systems, several quantitative-based FD schemes, which include geometric [4], adaptive estimation [5, 6], are introduced for nonlinear continuous-time systems. Other techniques include the use of sliding mode observer [7] and diagonal observer [8]. Additionally, FD schemes have been developed for engineering applications such as robot manipulators, hydraulic systems, flight control etc [9]. Moreover, numerous survey papers [10] providing an excellent overview of the state-of-the art developments have been published on model-based FD techniques.

Guaranteeing the stability of FD schemes using Lyapunov theory has gained interest in the past few years. However, the existing FD schemes [4-8] render only uniform ultimate bounded (UUB) stability due to the presence of system disturbances. However, in the recent literature, some work on the asymptotic convergence of the

identification error in continuous-time is demonstrated for robot manipulators with actuator faults [11].

Another aspect which lacked in the previously reported quantitative-based schemes for nonlinear systems [4-11] is prognostics or predicting the remaining useful life of the system. However, in certain data-driven techniques, TTF approaches [12-14] assumed a specific degradation model which has been found to be limited to the system or material type under consideration. Another scheme [15] employs a deterministic polynomial and a probabilistic method for prognosis by assuming that certain parameters are affected by the fault while others [16] use a black box approach using neural network (NN) on the failure data. All these schemes [12-16] while being data-driven address only TTF prediction, require offline training and do not offer performance guarantees. Therefore, it is envisioned that a unified FDP scheme will be necessary to alert an impending failure and provide the remaining useful life.

It is worth noting that most of the above discussed schemes [4-8] were developed for continuous time nonlinear systems. However, FDP schemes in discrete-time are necessary due to the stability problems incurred in the direct conversion of the continuous time FD schemes [17]. Recent developments in discrete-time include [17], where a FD scheme is introduced by using the persistent of excitation (PE) condition. Since it is very difficult to verify or guarantee PE, in our earlier work [18], a FD scheme using linearly parameterized online approximators is introduced by relaxing the PE requirement. However, bounded stability of all the signals is demonstrated similar to the case of fault detection algorithms in continuous-time.

In summary, the problem of fault diagnosis deals with detecting and isolating faults in the system (root-cause analysis). On the other hand, prognostics deal with fault isolation and predicting the remaining useful life of the system. In other words, prognostics include detection, isolation and remaining useful life prediction while accommodation aims at minimizing the risk due to the fault by reconfiguring the controller. Each of the major tasks is challenging and involved, as there are issues relating to sensitivity, robustness, and stability. However, in this dissertation, mathematically rigorous schemes are outlined to address these issues pertaining to quantitative or model-based fault detection, diagnosis, prognostics, and accommodation. Additionally, stability guarantees are provided for the schemes developed in the dissertation when compared to the previously reported FDP schemes.

1.2 ORGANIZATION OF THE DISSERTATION

This dissertation deals exclusively on fault prognostics and accommodation respectively for a class of nonlinear discrete-time systems and is presented in the form of six papers as illustrated in Fig. 1.3.

In this dissertation, the two most commonly classified faults: incipient (slowly growing) and abrupt (sudden), are considered. Paper I details the fault detection and prediction scheme for a class of nonlinear discrete-time systems with state or process faults. Additionally, the scheme is based on the assumption that all states are measurable. The proposed fault detection scheme is guaranteed to be asymptotically stable due to a novel nonlinear estimator comprising of the online approximator and a robust adaptive term. It is also noted that the robust adaptive term is a function of the parameters of the

online approximator. In addition, a deterministic method for estimating the time to failure by using the parameter vector of the online approximator is proposed. In comparison to our previous work [18], the proposed method achieves asymptotic stability using novel estimator design.

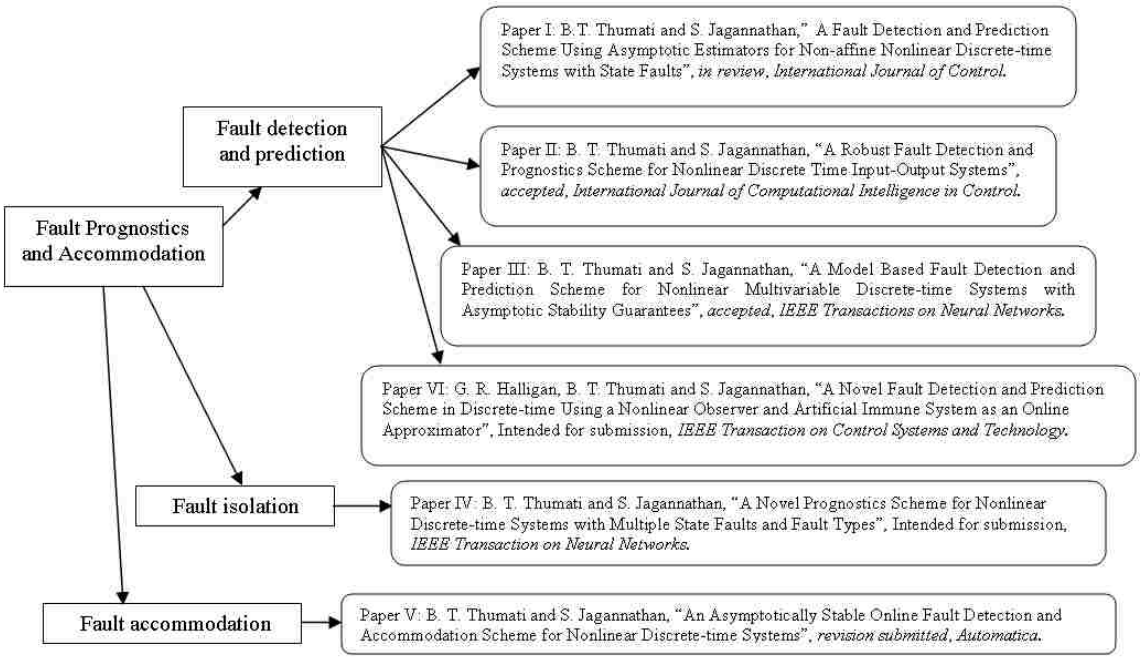

Fig. 1.3: Dissertation overview.

Subsequently, the fault detection and prediction scheme has been extended in Paper II to a multivariable input-output nonlinear discrete-time system, and also to a multi-input-multi-output (MIMO) nonlinear discrete time system with state and sensor faults in Paper III. Due to the availability of outputs, in Paper II, not all the states are needed whereas the detection scheme becomes more challenging. Additionally, the TTF scheme is developed using only the output signals. On the other hand, addition of sensor faults in Paper III complicates the stability of the MIMO system. However, suitable

performance guarantees is still shown. Separate TTF schemes are developed for process and sensor faults, respectively.

By contrast, in Paper IV, a novel fault isolation framework is addressed wherein a fault isolation estimator is designed to isolate the fault in the system. It is noted that the system could have more than one fault at a given time instance. Additionally, in the worst case scenario, every system state can incur multiple faults and fault types. Therefore, this complicates the design of a fault isolation scheme; however, it is still undertaken. In the event of a new fault, the fault dynamics are characterized by the online approximator and will be added to the fault isolation estimator. In addition, a prognostics scheme based on the online estimation of the isolation estimator parameter vector is used for predicting the time to failure. The prognostics scheme is based on an explicit mathematical equation and an iterative algorithm.

On the other hand, Paper V introduces the idea of fault accommodation for a general class of nonlinear discrete-time systems with state or process faults. In this paper, for fault detection, a nonlinearly linearly parameterized online approximator such as multi-layer neural network (MNN) is used instead of the linearly parameterized approximators. This complicates the stability proof but is still offered. Subsequently, using the online estimate of the unknown fault dynamics, a corrective control signal is proposed, which could accommodate the effects of the fault in the system. This fault accommodation scheme is developed for a nonlinear system under the assumption that all the states are available for measurement.

Finally, Paper VI considers a new FD design using artificial immune system (AIS) as online approximator. The fault detection process remains same as that of the

above given in Paper I. However, AIS is used for the online learning of the fault dynamics. Conventionally, AIS has been considered as an offline tool for applications such as classification, pattern recognition and detection. In this paper, an adaptive online parameter update law is proposed for tuning the AIS parameters. Using Lyapunov theory, mathematically, the asymptotic convergence of the residuals and the parameter estimation errors are demonstrated. Due to the asymptotic performance guarantees of the parameter estimation errors, we use AIS parameters to develop a TTF scheme.

In summary, novel fault prognostics and accommodation framework is introduced in this dissertation. Different fault classes and fault types are considered. The proposed scheme is deterministic when compared to other schemes in the literature. Finally, both simulation and Caterpillar hydraulics test-bed environments are used to illustrate the performance of the proposed schemes.

1.3 CONTRIBUTIONS OF THE DISSERTATION

This dissertation introduces online model-based fault diagnosis, prognosis and accommodation schemes for nonlinear discrete-time systems. In all of the designs presented in this dissertation, asymptotic stability results are derived in the presence of system uncertainties and faults. Asymptotic convergence of the residual is stronger when compared to boundedness which is typical in other fault detection, diagnosis, and accommodation schemes [6, 12-16, 17]. The proposed design does not require any *apriori* offline training unlike other fault diagnosis schemes [1].

The contributions of paper I include the design of a FDP scheme that detects and learns, online the state or process faults using suitable online approximators.

Additionally, a new parameter based TTF scheme was introduced, unlike other data driven or probabilistic approach [15]. This implies that the proposed TTF technique is deterministic and accurate in estimating the system behavior. Next, these results are extended to nonlinear systems with minimal state measurements, i.e., a FD scheme to detect and learn state faults using output measurements alone is introduced in Paper II. Another contribution includes the design of a FD scheme to detect both the state and sensor faults.

In addition, an online fault isolation (root-cause analysis) method is developed to identify the simultaneously occurring faults in a nonlinear discrete-time system. Moreover, the performance of the fault isolation scheme is demonstrated for multiple faults. In paper V, a single layer NN and a MNN design is proposed for fault accommodation design. Additionally, asymptotic tracking performance is shown even in the presence of system uncertainties and faults. Finally, a new fault detection scheme using AIS as an online approximator is introduced for capturing the fault dynamics. Adaptive parameter update law is proposed to tune the AIS scheme online, which obviates the need of any *apriori* offline training as used in the conventional approach.

1.4 REFERENCES

[1] J. Chen and R. J. Patton, *Robust Model-based Fault Diagnosis for Dynamic Systems*, Kluwer Academic publishers, MA, USA, 1999.

[2] M. Massoumnia, G. C. Verghese, and A. S. Willsky,"Failure detection and identification," *IEEE Trans. on Automatic Control*, vol. 34, no. 3, pp. 316-322, 1989.

[3] C. Edwards, S. K. Spurgeon, and R. J. Patton,"Sliding mode observers for fault detection and isolation," *Automatica*, vol. 36, pp. 541-553, 2000.

[4] C. De Persis and A. Isidori,"A geometric approach to nonlinear fault detection and isolation," *IEEE Trans. on Automatic Control*, vol. 46, no. 6, pp. 853 – 865, 2001.

[5] M. A. Demetriou and M. M. Polycarpou,"Incipient fault diagnosis of dynamical systems using online approximators," *IEEE Trans. on Automatic Control*, vol. 43, no. 11, pp. 1612-1617, 1998.

[6] H. A. Talebi, S. Tafazoli, and K. Khorasani,"A recurrent neural-network-based sensor and actuator fault detection and isolation for nonlinear systems with application to the satellite's attitude control subsystem," *IEEE Trans. on Neural Networks*, vol. 20, no.1, pp. 45- 60 , 2009.

[7] X. G. Yan and C. Edwards,"Nonlinear robust fault reconstruction and estimation using a sliding mode observer," *Automatica*, vol. 43, no. 9, pp. 1605-1614, 2007.

[8] S. Narasimhan, P. Vachhani, and R. Rengaswamy,"Nonlinear residual feedback observer for fault diagnosis in nonlinear systems," *Automatica*, vol. 44, no. 9, pp.2222-2229, 2008.

[9] F. Caccavale and L. Villani, *Fault Diagnosis and Fault Tolerance for Mechatronic Systems: Recent Advances*, Springer, UK, 2003.

[10] R. Isermann,"Model-based fault-detection and diagnosis–status and applications," *Annual Reviews in Control*, vol. 29, no.1, pp. 71-85, 2005.

[11] M. L. McIntyre, W. E. Dixon, D. M. Dawson, and I. D. Walker,"Fault identification for robot manipulators," *IEEE Trans. on Robotics and Automation*, vol. 21, no. 5, pp. 1028-1034, 2005.

[12] J. Luo, M. Namburu, K. Pattipati, L. Qiao, M. Kawamoto, and S, Chigusa,"Model-based prognostic techniques," *AUTOTESTCON 2003: IEEE Systems Readiness Technology Conference*, Anaheim, California, USA, pp. 330-340, 2003.

[13] J. Luo, A. Bixby, K. Pattipati, L. Qiao, M. Kawamoto, and S. Chigusa,"An interacting multiple model approach to model-based prognostics," *IEEE International Conference on Systems, Man and Cybernetics*, Washington, D.C., USA, vol. 1, pp. 189-194, 2003.

[14] E. Phelps, P. Willett, and T. Kirubarajan,"Useful lifetime tracking via the IMM," *Components and System Diagnostics, Prognostics, and Health Management II, Proc. of SPIE*, vol. 4733, pp. 145-156, 2002.

[15] M. J. Roemer and D. M. Ghiocel,"A probabilistic approach to the diagnosis of gas turbine engine faults," *53rd Machinery Prevention Technologies (MFPT) Conference*, Virginia Beach, VA, USA, pp. 325-336, 1999.

[16] Y. Shao and K. Nezu,"Prognosis of remaining bearing life using neural networks," *Proc. of the Institution of Mechanical Engineers, Part I: Journal of Sys. and Control Engg.*, vol. 214, no. 3, pp. 217-230, 2000.

[17] F. Caccavale and L. Villani,"An adaptive observer for fault diagnosis in nonlinear discrete-time systems," *Proc. of the American Control Conference*, June 30 -July 2, pp. 2463-2468, Boston, MA, 2004.

[18] B. T. Thumati and S. Jagannathan,"An online approximator-based fault detection framework for nonlinear discrete-time systems," *Proc. of 46th IEEE Conference on Decision and Control (CDC),* New Orleans, LA, USA, pp. 2608-2613, 2007.

PAPER

1. A Fault Detection and Prediction Scheme Using Asymptotic Estimators for Non-Affine Nonlinear Discrete-Time Systems with State Faults

Balaje T. Thumati* and S. Jagannathan

Abstract—In this paper, an asymptotic state estimator comprising of an online approximator in discrete-time (OLAD) along with a robust term, which is a function of the parameter vector of the approximator, is proposed for monitoring and detecting state faults in a nonlinear discrete-time system although the states are considered measurable. A fault in the system is detected by comparing the residual against a mathematically chosen threshold.

Upon detecting a fault, the OLAD and the robust term are initiated and the OLAD parameter vector is tuned online using a suitable update law in order to learn the unknown fault dynamics, while the robust term is used to ensure local asymptotic stability of the fault detection scheme, unlike other FD schemes rendering bounded stability. Subsequently, the fault detection time and a parameter based time to failure (TTF) prediction schemes are developed. Finally, the proposed FDP scheme is simulated on two examples.

Keywords: fault detection, prediction scheme, nonlinear discrete-time system, Lyapunov stability.

* Corresponding author: bttr74@mst.edu

Research supported in part by NSF I/UCRC on Intelligent Maintenance Systems Award and Intelligent Systems Center.

1. Introduction

Complex engineering systems require automatic control methods to minimize human intervention and attain the desired productivity. However, such systems are prone to failures due to unnoticed wear and tear in the systems resulting in huge losses and at times catastrophic problems. Therefore, a robust fault detection and prediction scheme has to be designed to predict an impending fault which can be used to alert the operator by providing the remaining useful life of the component or the system.

In the past (see, Chen and Patton (1999), Frank and Keller (1990), Gertler (1988)) analytical and hardware redundancy techniques were developed whereas a hardware redundancy technique is found to be not practically feasible for many applications due to its incurred cost. Therefore, analytical redundancy techniques reined more interest from the fault detection community. Quantitative and qualitative methodologies were used within the analytical redundancy framework. In the qualitative method (Dash and Venkatasubramanian 2000), a simple rule based and/or a fault tree analysis is used to detect a fault in the system. An associated drawback is the need of data for failure mode analysis and also there is no opportunity to learn new faults (Liu *et al.* 2006). Data-driven approaches (Luh and Cheng 2005) also have the same weakness that newer faults for detection require a priori data which is expensive (Luh and Cheng 2005).

However, in the quantitative method, a model representative of the given system is used for fault detection, where the models could be derived from physics of system operation or borrowed from control engineers (see, Chen and Patton (1999), Frank and Keller (1990), Gertler (1988)). Certain fault detection (FD) schemes developed under quantitative approach, use parity-relations (Chen and Patton 1999) whereas others (see,

Chen and Patton (1999), Frank and Keller (1990), Gertler (1988), Hermans and M. Zarrop (1996), Edwards *et al.* (2000)) employ an observer for fault detection. Alternatively, a geometric based approach was developed (Massoumnia *et al.* 1989). Along the similar lines, an FD scheme has been developed for stochastic systems (Chen and Speyer 2003). However, all of these schemes are useful for linear systems.

Recently, the FD schemes have been extended to nonlinear continuous time systems. For instance, the geometric approach used is extended to a nonlinear system (see, Hammouri *et al.* (1999), Hammouri *et al.* (2002), Persis and Isidori (2001), Hammouri *et al.* (2001)), whereas, an adaptive estimation technique is proposed (see, Demetriou and Polycarpou (1998), Jiang and Chowdhury (2005), Talebi *et al.* (2009)). Others use sliding mode observer (Yan and Edwards 2007) whereas (Lopez-Toribio and Patton 1998, Lopez-Toribio and Patton 1999) employ a fuzzy based observers. In (Dixon *et al.* 2000) FD schemes for robot manipulators have been developed and in (Caccavle and Villani 2003), a compilation of the FD schemes for numerous engineering applications such as hydraulic systems, flight control etc. are given. A recent survey in (Isermann 2005) on model based FD techniques gives an excellent overview of the state-of-the art developments which indicates that stability and performance of FD schemes are gaining interest within the community. Therefore, most of the reported schemes (see, Demetriou and Polycarpou (1998), Hammouri *et al.* (1999), Jiang and Chowdhury (2005), Yan and Edwards (2007), Hammouri *et al.* (2002), Persis and Isidori (2001), Hammouri *et al.* (2001)) have utilized Lyapunov theory to study the stability and performance of FD schemes. However, a uniform ultimate boundness (UUB) of the signals is ensured with the schemes (Demetriou and Polycarpou (1998), Jiang and

Chowdhury 2005). A recently proposed continuous time FD work renders asymptotic stability (McIntyre *et al.* 2005), but is only for robotic manipulators with specific types of actuator faults.

For real-time applications, a discrete-time scheme would be more natural to implement on a computer rather than a continuous-time scheme. In addition, a continuous time scheme can be prone to instability without an appropriate sampling rate. Therefore, in the literature (Mahmoud (2008), Kabore and Wang (1999), Caccavle *et al.* (2008), Zhang *et al.* (2007)), there have been FD schemes developed for both linear and nonlinear discrete-time systems. The nonlinear FD presented in (Caccavle *et al.* 2008) is based on the adaptive estimation, but the stability is proven to be UUB under a stringent persistency of excitation (PE) condition. In our recent work (Thumati and Jagannathan 2007), this assumption was relaxed when an online approximator is used although UUB stability of the residual is proven.

Finally, it is important to note that all the above mentioned schemes (see, Demetriou and Polycarpou (1998), Hammouri *et al.* (1999), Thumati and Jagannathan (2007), Jiang and Chowdhury (2005), Mahmoud (2008), Talebi *et al.* (2009), Kabore and Wang (1999), Caccavle *et al.* (2008), Hammouri *et al.* (2001), Zhang *et al.* (2007)) address fault detection and no attempt has been made to predict the impending faults. In order to determine remaining useful life, time to failure (TTF) prediction is a first step. However, in certain data-driven schemes (Luo *et al.* 2003), TTF is determined by assuming a specific degradation model which has been found to be limited to the system or material type under consideration. Another scheme relied on a deterministic polynomial and a probabilistic method for prognosis (Roemer and Ghiocel (1999) and

Phelps *et al.* (2002)) by assuming that certain parameters are affected by the fault. On the other hand, a black box approach using neural network (NN) was developed in (Shao and Nezu 2000). All these schemes (see, Luo *et al.* (2003), Roemer and Ghiocel (1999), Phelps *et al.* (2002), Shao and Nezu (2000)) address only prognostics, and there is no method to learn the fault dynamics online, which is usually required for improving system design and for fault accommodation. Moreover, obtaining data a priori for each fault is expensive.

Developing FDP schemes in discrete-time is difficult due to stability analysis as it is relatively easier to show stability using Lyapunov theory in continuous time since the first derivative is linear with respect to the states whereas the first difference of a Lyapunov function in discrete-time is quadratic with respect to the states (Jagannathan 2006). Lack of a robust discrete-time FDP scheme that offers better performance is the main motivation of this paper.

In this paper, a FDP scheme is designed using the adaptive estimation techniques for non-affine nonlinear MIMO discrete-time systems. All the states of the system are assumed to measurable, and a FD estimator is used for generating the residual for monitoring and fault detection. Unlike in control theory, where the estimator is used to supplement the unknown states for controller design, the purpose of the proposed FD estimator is to generate the residual signal. Since the states are measurable, the faults are assumed to be a function of the system states and input. In addition, the faults considered could be slowly growing (incipient fault) or suddenly occurring (abrupt fault). The nonlinear estimator consists of an online approximator in discrete-time (OLAD) and a robust term to monitor the nonlinear discrete-time system.

A dead-zone operator with a mathematically derived threshold is utilized to detect the occurrence of the fault even in the presence of bounded uncertainties and approximation errors thus ensuring robust detection. When a fault is detected, the OLAD and the robust term are initiated while the OLAD learns the dynamics of the unknown fault. An adaptive parameter update law is proposed for tuning the unknown parameters of the OLAD and the robust term. Additionally, the uniqueness of the proposed parameter update law is the relaxation of the PE condition. By using the Lyapunov theory, the local asymptotic stability of the proposed fault detection scheme is demonstrated, which is unique in comparison to the previously reported FD schemes (see, Demetriou and Polycarpou (1998), Hammouri *et al.* (1999), Thumati and Jagannathan (2007), Caccavle *et al.* (2008)) that guarantees only bounded stability. In addition, the robust term used in the nonlinear estimator facilitate the asymptotic convergence of the residual and the parameter estimation errors.

The asymptotic convergence of the residual or state estimation error helps in developing a prediction scheme or TTF determination based on the parameter trajectories. When an unknown fault is detected, TTF is determined in tandem with the online approximation of the fault dynamics. It is essential to understand that a system may remain functional after a fault, whereas it cannot continue to function after a failure (Isermann 2006). In other words, a fault is a first step in the failure occurrence. To predict the remaining useful life of a system, the parameter update law used for tuning the OLAD is utilized. For TTF, the parameters are projected to their limits where the system operation beyond the limits is considered to be unsafe. Alternatively, knowledge of state trajectories in real time could be used as well for prediction using the approach given

here. The limits could also be obtained from simulation or by using tools such as in (Phelps *et al.* (2002), Mathur *et al.,* 1998).

Therefore, the contributions of this paper include the design of a FDP scheme rendering asymptotic stability for a class of non-affine nonlinear discrete-time systems even in the presence of system uncertainties and reconstruction errors. The proposed FDP scheme considers nonlinear state faults while other schemes (Caccavle *et al.* (2008), McIntyre *et al.* (2005)) consider only structured faults.

In addition, the online learning feature provided by the OLAD could assist in fault isolation and accommodation; however, it is not addressed in this paper. Published literature, however, (Gertler (1988), Persis and Isidori (2001)), presents fault isolation and accommodation schemes.

In terms of organization, Section 2 introduces the non-affine system under consideration whereas Section 3 presents the proposed fault detection scheme in detail. In Section 4, the stability and performance of the fault detection scheme are introduced and Section 5 discusses the prediction scheme. Finally, in Section 6, a real-time example of a magnetic levitation system and a mass damper system are considered. Section 7 presents some concluding remarks and discusses future work.

2. Problem Statement

Consider a class of non-affine nonlinear discrete time system described by

$$\begin{aligned} x_1(k+1) &= p_1(x(k),u(k)) + \eta_1(x(k),u(k)) + h_1(x(k),u(k)) \\ x_2(k+1) &= p_2(x(k),u(k)) + \eta_2(x(k),u(k)) + h_2(x(k),u(k)) \\ &\vdots \\ x_n(k+1) &= p_n(x(k),u(k)) + \eta_n(x(k),u(k)) + h_n(x(k),u(k)) \end{aligned} \tag{1}$$

where $x = [x_1, ..., x_n] \in \Re^n$ is the state vector, $u \in \Re^m$ is the input vector, $p_i : \Re^n \times \Re^m \to \Re$, $\eta_i : \Re^n \times \Re^m \to \Re$, $h_i : \Re^n \times \Re^m \to \Re$ are smooth vector fields, and $i = 1, 2, ..., n$. Additionally, p_i is the known system dynamics, η_i is the system uncertainty, $h_i(x(k),u(k)) = \Pi_i(k-T) f_i(x(k),u(k))$ represents unknown fault function with $f_i(x(k),u(k))$ represents the unknown nonlinear state or process fault dynamics. Further, $\Pi_i \in \Re$ for $i = 1, 2, ..., n$ denotes the time profile of the state or process faults, which is given by

$$\Pi_i(k-T) = \Omega_i(k-T) = \begin{cases} 0 \text{ if } k < T \\ 1 - e^{-\kappa_i (k-T)}, \text{ if } k \geq T \end{cases} \qquad i=1, 2 \ldots n$$

where $\kappa_i > 0$ is an unknown constant representing the rate at which the fault evolves in the state x_i (Zhang and Morris 1994). Here the use of an exponential term in the time profile is to characterize the incipient and abrupt faults. Thus for small values of κ_i, this term describes an incipient fault, whereas for large values it represents abrupt faults. Additionally, T denotes the unknown time of occurrence of state or process faults (see, Demetriou and Polycarpou (1998), Thumati and Jagannathan (2007), Caccavle *et al.*

(2008)), Talebi *et al.* (2009)). In certain previous works on FD (see, Chen and Patton (1999), Frank and Keller (1990), Gertler (1988), Isermann (2005)), structured faults are assumed, which makes it easier to use other techniques like parity relation to decouple the uncertainty from the fault. However, we relax such assumptions here.

Remark 1: The nonlinear fault function is modeled in terms of the system states and inputs. This is a common means of representing nonlinear system faults (Demetriou and Polycarpou 1998), unlike actuator faults (Caccavle *et al.* (2008)), which is a function of the system inputs.

Typically, in an actuator fault (see, Chen and Patton (1999), Frank and Keller (1990), Gertler (1988), Jiang and Chowdhury (2005)), part of its dynamics is assumed to be known; however, in this case, the fault type assumed is nonlinear, thus encompassing the various possible state or process faults.

Additionally, by using an assumption such as linear in the unknown parameters (Jagannathan 2006), the fault dynamics in (1) could be expressed as $h_i(x(k),u(k)) = \theta_i^T \phi_i(x(k),u(k)) + \varepsilon_{1_i}(k)$, where $\theta_i \in \Re^{l\times 1}$ is an ideal and unknown parameter (or weight) matrix such that the approximation error, $\varepsilon_{1_i}(k)$, is bounded (Barron 1993). The ideal parameter vector or weights are considered bounded, i.e., $\|\theta_i\| \le \theta_{i\max}$ (Jagannathan 2006). In this case, $\phi_i \in \Re^{l\times 1}$ is a known nonlinear basis function assumed to be upper bounded by $\|\phi\| \le \phi_{i\,max}$. This is true for activation functions such as RBF, sigmoid etc. The following assumption is standard in the fault detection literature:

Assumption 1: The state and the input vectors are bounded prior to and after the fault occurrence consistent with the past literature (see, Demetriou and Polycarpou (1998), Thumati and Jagannathan (2007), Caccavle *et al.* (2008), Jiang and Chowdhury (2005), Yan and Edwards (2007), Talebi *et al.* (2009), Kabore and Wang (1999), Alessandri (2003)). Moreover, the system in (1) could have single and multiple state faults.

Figure 1 clarifies Assumption 1 by using a state trajectory to illustrate the difference between a fault and the failure. Before the fault occurrence, the system states are considered bounded for a given system uncertainty. After the occurrence of the fault, the system behavior degrades and reaches a maximum limit beyond which the system is considered to have failed. The system degradation behavior is described by an increase in the system parameters, which also increases the magnitude of the states. As the states enlarge, a maximum limit, or failure threshold, is reached beyond which the system will be unable to perform its assigned task. The states or parameters that approximate the uncertain nonlinear dynamics increase substantially while they still remain bounded. However, the bound could be large. This bounding value is used to predict TTF and to avoid any catastrophic failures. Therefore it is most important to detect a fault at the incipient stage by learning its dynamics accurately so that TTF can be determined. This also implies that the class of nonlinear discrete-time systems (1) considered here is assumed to have slower escape time upon the occurrence of a fault so that Assumption 1 is still valid. Next the following assumptions are required before we proceed.

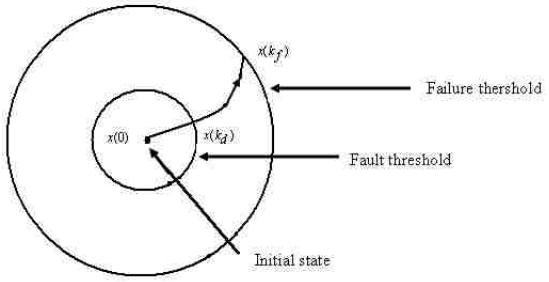

Figure 1: State trajectories from initial state to failure.

Assumption 2: The modeling uncertainty is unstructured and bounded (Demetriou and Polycarpou 1998), i.e., $\|\eta_i(x(k),u(k))\| \le \eta_{i_M}$, $\forall (x,u) \in (\chi \times U)$ where there exist the compact sets $\chi \subset \Re^n$ and $U \subset \Re^m$, with $\eta_{i_M} \ge 0$ a known constant, for $i = 1, 2, ..., n$.

In some of the previous works (see, Chen and Patton (1999), Frank and Keller (1990), Gertler (1988), Edwards *et al.* (2000), Yan and Edwards (2007)), bounded and structured system uncertainties are considered, which simplifies the development of fault detection.

Assumption 3: The initial system states are available, i.e., $x_i(0) = x_{i_0}$.

The representation given in (1) provides a general framework for a broad class of nonlinear discrete-time systems with state or process faults. Now, the following section introduces the fault detection scheme. Subsequent sections will present the prediction scheme and TTF determination.

3. Asymptotic Fault Detection Estimator

In this model based technique, it is required to generate residuals to monitor and detect faults in (1). Therefore, a nonlinear asymptotic estimator that serves the purpose of residual generation will be introduced. This clearly implies that the purpose of the estimator is not to estimate the systems states as in the case of a controller design (Jagannathan 2006) whereas it will be utilized solely for detection and prediction. This is similar to the case of using observers or estimators (Demetriou and Polycarpou (1998), Caccavle *et al.* (2008)) in the literature in lieu of the proposed asymptotic state estimator. Following is the design of the nonlinear estimator, which is used for monitoring and detecting faults in the system defined in (1)

$$\begin{aligned}
\hat{x}_1(k+1) &= a_{11}(x_1(k) - \hat{x}_1(k)) + p_1(x(k), u(k)) + \hat{h}_1(x(k), u(k); \hat{\theta}_1(k)) - v_1(k) \\
\hat{x}_2(k+1) &= a_{22}(x_2(k) - \hat{x}_2(k)) + p_2(x(k), u(k)) + \hat{h}_2(x(k), u(k); \hat{\theta}_2(k)) - v_2(k) \\
&\vdots \\
\hat{x}_n(k+1) &= a_{nn}(x_n(k) - \hat{x}_n(k)) + p_n(x(k), u(k)) + \hat{h}_n(x(k), u(k); \hat{\theta}_n(k)) - v_n(k)
\end{aligned} \tag{2}$$

where $\hat{x} = [\hat{x}_1, ..., \hat{x}_n] \in \Re^n$ is the estimated state vector, $\hat{h}_i : \Re^n \times \Re^m \times \Re^{l\times 1} \to \Re$ for $i = 1, 2, ..., n$, represents the OLAD used to approximate the unknown fault dynamics, A is a diagonal design matrix (i.e., $A = diag(a_{11}, ..., a_{nn})$), and $\hat{\theta}_i \in \Re^{l\times 1}$ represents the adjustable parameters for approximating unknown fault dynamics. Since the type of faults considered in (1) is linearly parameterized, the structure of the OLAD could be written as $\hat{h}_i(x(k), u(k); \hat{\theta}_i(k)) = \hat{\theta}_i^T(k)\phi_i(x(k), u(k))$. Finally, $v_i \in \Re$ represents the robust term which is defined as

$$v_i(k) = \frac{\hat{\theta}_i^T(k) b_i}{b_i^T \hat{\theta}_i(k) \hat{\theta}_i^T(k) b_i + c_i} \tag{3}$$

where $c_i > 0$ is a user defined constant and b_i is an appropriate dimensioned constant vector and its selection is addressed later in the text. The use of the robust term in the nonlinear estimator is one of the important design changes from other FD observers/estimators (Demetriou and Polycarpou (1998), Caccavle *et al.* (2008)).

Next, define the state estimation error or residual as $e_i(k) = x_i(k) - \hat{x}_i(k)$. Using equations (1) and (2), the residual dynamics can be written as

$$e_i(k+1) = a_{ii} e_i(k) + \tilde{\theta}_i^T(k) \phi_i(x,u) + v_i(k) + \varepsilon_i(k) \tag{4}$$

where $\varepsilon_i(k) = \varepsilon_{1_i}(k) + \eta_i(x(k), u(k))$, and the parameter estimation error is given as $\tilde{\theta}_i(k) = \theta_i - \hat{\theta}_i(k)$. In order to detect faults in the system, the residual is compared with a known threshold via a dead-zone operator. This dead-zone operator and the threshold improve robustness of the fault detection scheme (see, Chen and Patton (1999), Frank and Keller (1990), Gertler (1988)) in the presence of bounded disturbances and other uncertainties. Selection of a threshold guarantees reliable performance in the presence of system uncertainties. The threshold selection (Demetriou and Polycarpou 1998) is difficult even for continuous-time systems; however, a mathematical procedure is presented in this paper for discrete-time systems to simplify the process.

Prior to the occurrence of the fault, the residual, $e_i(k)$, remains within the threshold provided a suitable threshold is selected. In the event of a fault, however, the residual increases and eventually crosses the threshold. Once the residual exceeds the threshold, a fault is considered to have occurred through the dead-zone operator. Upon

detecting a fault, the OLAD and the robust term are initiated online. The threshold operator $D[\cdot]$ is defined in terms of the residual as

$$D[e_i(k)] = \begin{cases} 0, & \text{if } |e_i(k)| \le \rho_i \\ e_i(k), & \textit{Otherwise} \end{cases} \tag{5}$$

where $\rho_i > 0$ is the threshold for $i = 1, 2, ..., n$, $\rho = [\rho_1, ..., \rho_n]^T \in \Re^n$, and $D[e(k)] = [D[e_1], ..., D[e_n]]^T \in \Re^n$. The selection of the dead-zone size ρ_i clearly provides a tradeoff between reducing the possibility of false alarms (robustness) and improving the sensitivity of the faults. The selection of an appropriate value for ρ_i is addressed in the following section.

Remark 2: Since the OLAD and the robust term are not initiated until a fault is detected, the proposed FD estimator guarantees a bounded residual prior to the fault. Therefore, any unforeseen incipient or abrupt state fault can only drive the residual to exceed the threshold thus enabling the FD scheme to detect them. Consequently, the OLAD or the robust adaptive terms do not compensate the residual prior to fault detection.

Next, to guarantee a stable learning of the fault function, the following weight update law is used to tune the parameters of the OLAD

$$\hat{\theta}_i(k+1) = \hat{\theta}_i(k) + \alpha_i \phi_i(k) \mathrm{D}[e_i(k+1)] - \Gamma_i \left\| I - \alpha_i \phi_i(k) \phi_i^T(k) \right\| \hat{\theta}_i(k) \tag{6}$$

where $\alpha_i > 0$ is the learning rate, $\Gamma_i > 0$ is the design constant, and $\phi_i(k) = \phi_i(x(k), u(k))$ is the OLAD basis function, which could be an RBF, a sigmoid, etc. (Farrell and Polycarpou 2006). This online tuning law relaxes the need of PE condition, which is required for some of the previously reported discrete-time FD scheme (Caccavle *et al.* 2008). Later, it would be seen that the additional term commonly referred to as epsilon-modification in

(6) not only relaxes PE but also renders a stable parameter based prediction scheme, which is a uniqueness of the proposed update law. The following lemma is needed before proceeding any further.

Lemma 1: The term ($\varepsilon_i(k)$), comprising of the reconstruction error ($\varepsilon_{1_i}(k)$), the bounded system uncertainty ($\eta_i(x(k),u(k))$) are bounded above by a function of residual and the weight estimation errors (see, Dawson *et al.* (1991), Kwan *et al.* (1995), Xian *et al.* (2004), Patre *et al.* (2007), Lewis *et al.* (1999)), i.e.,

$$\left(1+5(2+1/\delta_i)\alpha_i\phi_i^T\phi_i\right)\varepsilon_i^2(k) \le \varepsilon_{i_M} = b_{i_0} + b_{i_1}\left\|e_i(k)\right\|^2 + b_{i_2}\left\|e_i(k)\right\|\left\|\tilde{\theta}_i(k)\right\| + b_{i_3}\left\|\tilde{\theta}_i(k)\right\|^2 \qquad (7)$$

where $b_{i_0}, b_{i_1}, b_{i_2}$ and b_{i_3} are known positive constants.

Proof: Please refer to Appendix.

Remark 3: In most of the previous schemes (Demetriou and Polycarpou (1998), Thumati and Jagannathan (2007), Caccavle *et al.* (2008)), the approximation error and the system uncertainty are considered to be upper bounded by a known constant, thus rendering UUB results. On the other hand, certain stringent assumptions such as the approximation errors satisfy a conic sector (Hayakawa *et al.* 2008) is not needed here. Instead, a novel procedure is proposed to take into account the approximation errors and the system uncertainties in a more reasonable fashion, thus resulting in improved stability without any assumptions.

Remark 4: In (Xian *et al.* 2004), disturbances are also included along with the reconstruction errors and asymptotic stability of the tracking error is demonstrated provided the disturbances are bounded above. In this paper, bounded disturbances and round-off errors can be included with the OLAD reconstruction errors and asymptotic

stability can still be shown. Next, by adding and subtracting $\frac{\left(\theta_i^T b_i - C_i\right)}{b_i^T \hat{\theta}_i(k)\hat{\theta}_i^T(k) b_i + c_i}$ in (4), where C_i is an appropriate dimensioned constant vector, the residual dynamics is rewritten as

$$e_i(k+1) = a_{ii} e_i(k) + \Psi_{1_i}(k) - \Psi_{2_i}(k) + \varepsilon_i(k) - \frac{\left(\theta_i^T b_i - C_i\right)}{b_i^T \hat{\theta}_i(k)\hat{\theta}_i^T(k) b_i + c_i} \tag{8}$$

where $\Psi_{1_i}(k) = \tilde{\theta}_i^T(k)\phi_i(x,u)$, and $\Psi_{2_i}(k) = \frac{\left(\tilde{\theta}_i^T(k) b_i - C_i\right)}{b_i^T \hat{\theta}_i(k)\hat{\theta}_i^T(k) b_i + c_i}$ for convenience.

The uniqueness of the proposed FD scheme is the online learning feature of the OLAD to learn the unknown fault dynamics and the asymptotic stability guarantees in contrast with available fault detection schemes in both continuous (Demetriou and Polycarpou 1998) and discrete-time (Thumati and Jagannathan (2007), Caccavle *et al.* (2008), Alessandri (2003)) where UUB is only ensured. This implies that the residual derived using the estimator is robust to system uncertainties and would render effective fault detection. Unlike other schemes (Liu *et al.* (2006), Luh and Cheng (2005)), no prior offline training is needed to tune the OLAD and thus facilitating the learning of unknown fault dynamics online. Next, the performance of the FD scheme using the OLAD and the robust term is examined mathematically.

4. Analytical Results

In this section, analytical results in terms of the performance of the detection scheme and time to detection are discussed. First, prior to the occurrence of the fault, the stability is examined to guarantee the boundedness of the residual thus ensuring the

design of the estimator. In addition, based on the uncertainty, the selection of the threshold is derived.

A) Stability Analysis

To begin with, assume first that the system in (1) has no uncertainties and with no faults present, the system (1) is rewritten as $x_i(k+1) = p_i(x(k), u(k))$.The estimator in (2) is reduced to

$$\hat{x}_i(k+1) = a_{ii}(x_i(k) - \hat{x}_i(k)) + p_i(x(k), u(k))$$

and the residual dynamics is obtained as

$$e_i(k+1) = a_{ii} e_i(k) \tag{9}$$

where the eigen values of a_{ii} is selected within the unit circle. Hence the stability of (9) follows trivially, i.e., $e_i \to 0$ as $k \to \infty$. Next, the system described in (1) in the presence of uncertainties and prior to the fault occurrence, is given by

$$x_i(k+1) = p_i(x(k), u(k)) + \eta_i(x(k), u(k)) \tag{10}$$

The proposed estimator to monitor the system (1) becomes

$$\hat{x}_i(k+1) = a_{ii}(x_i(k) - \hat{x}_i(k)) + p_i(x(k), u(k)) \tag{11}$$

To derive a suitable threshold for detecting a fault and to show the stability of the estimator prior to the fault occurrence, the residual dynamics are obtained from (10) and (11) as

$$e_i(k+1) = a_{ii} e_i(k) + \eta_i(x(k), u(k)) \tag{12}$$

Using (Chen 1999), we solve (12) such that $e_i(k) = \sum_{j=0}^{k-1} a_{ii}^{k-j} \eta_i(x(k), u(k))$ provided the initial conditions are zero. Since a_{ii} is selected to remain within the unit circle and using the upper bound on the system uncertainty, there exist two positive constants μ_i and β_{t_i} such that $\left|a_{ii}^k\right| \leq \beta_{t_i} \mu_i^k \leq 1$. Therefore, $|e_i(k)| \leq \beta_{c_i} \eta_{i_M} \frac{(1-\mu_i^k)}{(1-\mu_i)}$, where $\beta_{c_i} = \beta_{t_i} \mu_i$. This implies that if the size of the dead-zone is selected as $\rho_i = \frac{\beta_{c_i} \eta_{i_M}}{(1-\mu_i)}$, the residual, $e_i(k)$, remains within the dead-zone for all $k \leq T$. Given the individual thresholds, the overall threshold ρ can be determined by using Frobenious norm which is compatible with the Euclidean norm (DePree and Swartz 1988). This demonstrates that the estimator is bounded prior to the fault.

Subsequent to the detection of a fault, the OLAD is used to learn the unknown fault dynamics. To guarantee a stable learning environment in the presence of faults by the OLAD-robust term, the update law proposed in (6) is exerted. To show that the parameter update law in (6) renders a stable system, the following theorem is proposed.

Theorem 1 (Stability Analysis of the Fault Detector After a Fault Occurrence): Let the proposed fault estimator design in (2) be used to monitor the system (1), and the parameter update law given in (6) be used for tuning OLAD parameter vector. Additionally, let the initial conditions be bounded in a compact set *B*. In the presence of bounded OLAD reconstruction error and uncertainties, by using the adaptive robust term (3), the residual, $e_i(k)$, and $\tilde{\theta}_i(k)$ are locally asymptotically stable.

Proof: Please refer to Appendix.

Remark 5: The above theorem demonstrates that the first difference of the Lyapunov function is negative definite even in the presence of NN reconstruction vector provided if the robust adaptive term is used in (2). By contrast, a uniformly ultimately bounded (UUB) result will be observed in the literature (Demetriou and Polycarpou (1998), Thumati and Jagannathan (2007), Caccavle *et al.* (2008)) if the robust term is not applied. This robust term and Lemma 1 enables one to express the system uncertainties and unmodeled dynamics as a function of tracking and estimation errors which are combined with other negative terms for ensuring negative definiteness of the first difference in the Lyapunov function.

Remark 6: Theorem 1 indicates that the fault detection scheme developed in this effort would ensure stable learning of the fault function or dynamics in the presence of system uncertainties while rendering asymptotic stability. The asymptotic convergence of the residual in fact ensures that the fault function is approximated in a more accurate fashion provided the initial parameters are within the compact set. The dead-zone operator is still necessary even if system uncertainties are not present due to bounded disturbances and or computer round off errors. Even if they are present, similar to continuous-time (Hayakawa 2008), these bounded disturbances and round-off errors can be accommodated while guaranteeing asymptotic stability of the residual and parameter vector. In contrast, only asymptotic stability of the tracking error (Hayakawa 2008) can be demonstrated in continuous-time.

Remark 7: An Euler discretization of the continuous time fault detection scheme cannot be used here for discrete-time system since the update laws cannot be derived from the continuous-time counterpart.

B) Fault Detection Time

Besides stability, an additional metric to evaluate the performance of a fault detection scheme is the detection time which is defined as how quickly a fault is detectable once it has occurred. Previous works in discrete-time do not provide a measure of the fault detection time (Thumati and Jagannathan (2007), Caccavle *et al.* (2008)) unlike their continuous-time counterparts. This paper presents a mathematical procedure to determine the fault detection time for nonlinear discrete time systems due to incipient and abrupt faults. The explicit equation for deriving fault detection time is shown in the following theorem, once a fault has occurred in the i^{th} state. For faults in multiple states, the fault detection time is given by $k_{dt} = \min(k_{di}), i = 1.....n$.

Theorem 2 (**Fault Detection Time):** During the time interval $k \in [T + k_1, T + k_d]$, if the i^{th} fault dynamics satisfies $f_i(x(k), u(k)) \geq 2\eta_{i_M}$, the upper bound on the fault detection time for incipient and abrupt faults can be obtained by solving:

For incipient fault:

$$\left(1 - a_{ii}^{\,k_d - k_1}\right) - (1 - a_{ii}) a_{ii}^{k_d} (e^{-\kappa_i} / a_{ii}) \left(\frac{(e^{-\kappa_i} / a_{ii})^{k_1} - (e^{-\kappa_i} / a_{ii})^{k_d}}{1 - (e^{-\kappa_i} / a_{ii})} \right) = \frac{2\eta_{i_M}}{\beta_i} \tag{13}$$

For abrupt fault:

$$k_d = \frac{\log\left(1 - \dfrac{2\eta_{i_M}}{\beta_i}\right)}{\log(a_{ii})} + k_1 \tag{14}$$

Proof: Please refer to Appendix.

The above mathematical equations (13)-(14) determines the fault detection time explicitly. Next, a new parameter based prediction scheme is proposed.

5. Prediction Scheme

Thus far, a fault detection scheme has been presented, its performance analyzed and the fault detection time derived analytically. Now TTF can be determined using the behavior of the parameter trajectories before and after the occurrence of a fault. The following assumption holds in deriving the TTF.

Assumption 4: The parameter vector $\hat{\theta}_i(k)$ is an estimate of the actual system parameters.

Remark 8: This assumption is satisfied when a system can be expressed as linear in the unknown parameters (LIP). For example, in a mass damper system, or in civil infrastructure such as a bridge, the mass, damping constant and spring constant may be expressed as linear in the unknown parameters. In the event of a fault, system parameters change, and tend to reach their limits. When any one of the parameters exceeds its limit, operation is considered unsafe. TTF is defined as the time elapsed when the first parameter reaches its limit. The TTF can also be analyzed with lower limits.

The parameter update law given in (6) is used to estimate the system parameter online and will be used in this section to develop an explicit mathematical equation for predicting TTF. This equation is then used to develop an algorithm for the continuous prediction of TTF iteratively at every time instant. Alternatively, estimated state trajectories can be employed as well if the states can be related to physical quantities. Next, the mathematical equation is presented in the following theorem.

Theorem 3 (Time to Failure): If the system in (1) can be expressed as LIP, the TTF for the j^{th} system parameter at the k^{th} time instant can be determined using

$$k_{f_j} = \frac{\left| \log\left(\left| \frac{\left(\gamma_i \left\| I - \alpha_i \phi_i \phi_i^T \right\| \theta_{i_{j\max}} - \alpha_i \phi_{i_j} e_i \right)}{\left(\gamma_i \left\| I - \alpha_i \phi_i \phi_i^T \right\| \theta_{i_{j_0}} - \alpha_i \phi_{i_j} e_i \right)} \right| \right) \right|}{\left| \log(1 - \gamma_i \left\| I - \alpha_i \phi_i \phi_i^T \right\|) \right|} + k_{0_j} \tag{15}$$

where k_{f_j} is the TTF, k_{0_j} is the time instant when the prediction starts (bearing in mind that k_{dt} was the initial value, which increases incrementally), $\theta_{i_{j\max}}$ is the maximum value of the system parameter, and $\theta_{i_{j_0}}$ is the value of the system parameter at the time instant k_{0_j}.

Proof: Please refer to Appendix.

Remark 9: The mathematical equation (15) presents the TTF for the j^{th} system parameter. In general, for a given system with a parameter vector, the TTF would be $k_{ft} = \min(k_{f_j}),\ j = 1, 2, ...l$, where l denotes the number of parameters. The TTF is defined as the time elapsed when the first parameter reaches its limit. The speed at which the actual parameters approach their target values is dictated by the learning rate or adaptation gain and the design constant in the parameter update law (6). A small value for the learning rate implies that slower convergence which further means that the TTF is not as accurate when the learning rate is lower. However, a large value of the learning rate can speed up the convergence. Increasing the learning rate can cause hunting problems which will result in inaccurate prediction of TTF.

Remark 10: Although the proposed prediction scheme is based on the parameter trajectory, estimated system states could also be used for prediction since asymptotic stability is proven. A relationship similar to (15) can be derived for TTF using (2).

However, for brevity, no further discussions on the use of state trajectories for prediction are included in this paper.

Remark 11: This prediction scheme could be applied to unknown systems that satisfy LIP. It could also be applied to systems with partial information that satisfy LIP. Such systems were given in Section 2.

Figure 2 provides a flow chart of the iterative algorithm to determine TTF (k_{ft}) for each system parameter. The TTF is calculated at each time instant starting when a fault is detected until the system parameter reaches its maximum value (threshold). Therefore, it is logical that the TTF decreases as the parameters approach their corresponding limits.

By tuning the system parameter estimate ($\hat{\theta}_i(k)$) to update the TTF recursively, the system could be more accurately monitored than would be possible with other methods (Roemer and Ghiocel (1999), Phelps *et al.* (2002)). In fact, the TTF will not be accurate when the parameter estimate vector is just started. Over time when the parameter vector starts converging to its true values, the TTF prediction starts improving. Additionally, no prior offline training is required to estimate the system parameters, which significantly reduces the burden of collecting data.

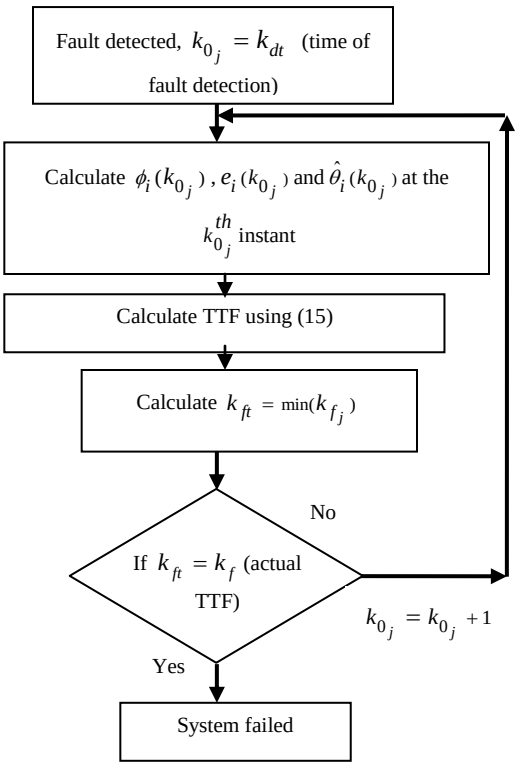

Figure 2: Flow chart indicating the TTF determination.

Next the performance of this FDP scheme is tested on a practical application. The simulation results presented below will indeed show that the performance of the FDP scheme as indicated in the theorems can be demonstrated in simulation.

6. Simulation Results

In this section, two different simulation examples are considered to study the proposed FDP scheme. In both the simulations, the detection, online learning, and TTF are illustrated. The first example is a magnetic suspension system and the second example considered is a mass-damper system. Next, we introduce the first example.

Example 1: Magnetic levitation system

The following modified nonlinear discrete-time model is considered (Barie and Chiasson 1996)

$$
\begin{aligned}
x_1(k+1) &= \Delta t(x_2(k)) + x_1(k) \\
x_2(k+1) &= \Delta t(g - (C_p / m)(x_3(k) / x_1(k))^2) + x_2(k) \\
x_3(k+1) &= \Delta t(-(R(k) / L)x_3(k) + (2C_p / L)(x_2(k)x_3(k) / x_1^2(k))) + (u(k) / L) + \eta(x(k)) + x_3(k)
\end{aligned} \tag{16}
$$

where $x(k) = [x_1(k), x_2(k), x_3(k)]^T$ is the state vector, and $\eta(x(k))$ is the system uncertainty. Prolonged use of the magnetic coil may cause wear and tear thus changing its resistance nonlinearly. Hence, we consider an incipient fault that would change the resistance nonlinearly. Moreover, the fault is seeded at the 60th second of system operation and the fault is defined by

$$
R(k) = \begin{cases} 27.7 & for\ 0 < k < 60 \text{ sec} \\ R(k-1) - ((k + \exp(-k)) / 5000) & k \geq 60 \text{ sec} \end{cases}
$$

Finally, the input is taken as

$$
u(k) = L(\sin(0.1k) - \Delta t(-(R_1 / L)x_3(k) - (2C_p / L)(x_2(k)x_3(k) / x_1^2(k))) - (1 / \Delta t)x_3(k))
$$

To monitor the system defined in (16) and to generate residual, the following nonlinear FD estimator is used

$$
\begin{aligned}
\hat{x}_1(k+1) &= \Delta t(x_2(k)) + x_1(k) + 0.1(x_1(k) - \hat{x}_1(k)) \\
\hat{x}_2(k+1) &= \Delta t(g - (C_p / m)(x_3(k) / x_1(k))^2) + x_2(k) + 0.1(x_2(k) - \hat{x}_2(k)) \\
\hat{x}_3(k+1) &= \Delta t(-(\hat{\theta}(k) / L)x_3(k) + (2C_p / L)(x_2(k)x_3(k) / x_1^2(k))) + (u(k) / L) + x_3(k) + 0.1(x_3(k) - \hat{x}_3(k)) + v(k)
\end{aligned} \tag{17}
$$

where the estimated state vector is given by $\hat{x}(k) = [\hat{x}_1(k), \hat{x}_2(k), \hat{x}_3(k)]^T$, and $A = 0.1I_m$ with I_m is an appropriately dimensioned identity matrix. Additionally, the robust term used to

guarantee the convergence of the residual is given by $v(k) = \frac{\hat{\theta}(k) b_f}{b_f^2 \hat{\theta}^2(k) + c_f}$, but is not initiated until the fault is detected. The values of the system parameters used for this simulation are $m = 1, C_p = 1.24 \times 10^{-4} Nm^2 A^2, R_1 = 27.7 ohm, L = 0.65 Henry,$ $t_s = 0.01$, $x_1(0) = x_2(0) = 0.002$, $x_3(0) = 0.001$, $c_f = 1.5$, and $b_f = 0.008$. In this simulation, the system uncertainty is taken as $\eta(x(k)) = 0.25$ and is assumed to exist from the start of the system operation. The parameter $\hat{\theta}(k)$ is estimated online, and prior to the fault detection $\hat{\theta}(k) = 27.7$.

Since uncertainty is considered in the simulation, a fault detection threshold has to be utilized to avoid missed or false alarms. To overcome such problems, the threshold derived in Section 4 of this paper is used, where we have $\rho = \frac{\beta_c \eta_M}{(1-\mu)}$. Since $\eta_M = 0.25$, and taking $\beta_c = 0.935$, $\mu = 0.01$, we have a constant threshold value of $\rho = 0.27$. Fig. 3 depicts the residual and the detection threshold over the entire simulation interval.

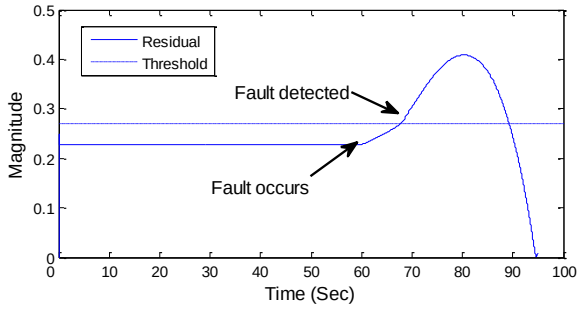

Figure 3: Residual signal with the detection threshold.

From the figure, it is obvious that for the designed threshold value, the residual remains always within the limit, but exceeds only after the occurrence of the fault. These could be observed from the two arrow heads showing the occurrence and detection of the fault. Upon detection of the fault, the residual converges to zero, which is attributed to the online learning of the unknown fault and the use of the robust term. Additionally, this shows that the proposed FD estimator tracks the actual system states accurately.

The online learning of the change in the fault parameter is shown in Fig. 4, where the estimate converges to the target value asymptotically in real-time, i.e., unlike other schemes (Liu *et al.* (2006), Luh and Cheng (2005)) neither apriori fault information nor offline training is needed to learn the change in the parameter. However, the initial variations in the parameter estimate may be attributed to the selection of the gains of the parameter update law in (6), where $\alpha = 0.58$ and $\gamma = 0.001$.

Using the online parameter estimate in Fig. 4 and setting a failure threshold value of 0.8 units, the TTF is estimated using the procedure outlined in Section 5, thus we have the TTF prediction as shown in Fig. 5. From the figure, the prediction seems to be satisfactory as it converges to the actual time of failure of 93.7 seconds. The TTF is estimated only after the detection of the fault and as seen in the figure, the estimated TTF is consistent with the actual time of failure.

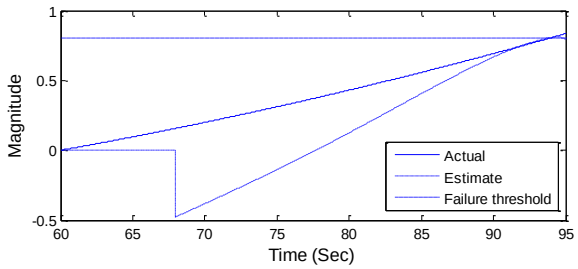

Figure 4: Online estimation of the system parameter.

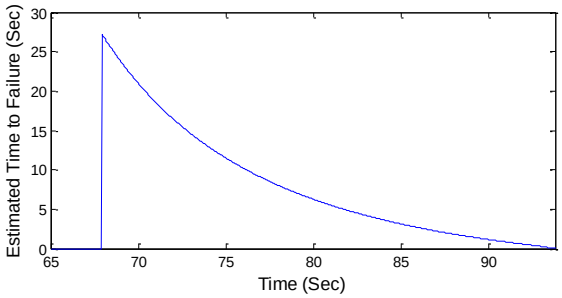

Figure 5: The TTF determination after the fault detection.

Hence, through this simulation, the theoretical results derived in this paper are verified. Additionally, another simulation example is introduced next to illustrate the usability of the proposed FDP scheme.

Example 2: Mass damper system

Some of the commonly known systems such as bridges, automobile suspension system etc., could be modeled as a mass damper system. Hence a FDP scheme to alert users about any impending faults is necessary. Consider the following discrete time states space model equivalent to a continuous time mass damper system (Demetriou and Polycarpou 1998)

$$x_1(k+1) = T_s x_2(k) + x_1(k)$$

$$x_2(k+1) = \frac{1}{m}\{T_s(F - c_1 x_2(k) - k_{c1}(k)x_1(k)\} + x_2(k) + \eta(k) \qquad (18)$$

where $x_1(k)$ and $x_2(k)$ are the system states, representing the displacement and velocity term of the mass damper system. The external force (input) applied to the system is defined as $F = 2\sin(kT_s)$. In this simulation, a spring stiffness fault is assumed, which is considered as a predominant fault (Demetriou and Polycarpou 1998). Hence, the fault is assumed to cause the spring constant to vary as given below

$$k_{c1}(k) = \begin{cases} 0.55 & for\ 0 < k < 15\ \text{sec} \\ k_{c1}(k-1) - (k/90000) & k \geq 15\ \text{sec} \end{cases}$$

To monitor and detect faults in (18), the following nonlinear FD estimator is considered

$$\hat{x}_1(k+1) = T_s \hat{x}_2(k) + \hat{x}_1(k) + 0.01(x_1(k) - \hat{x}_1(k))$$
$$\hat{x}_2(k+1) = \frac{1}{m}\{T_s(F - c_1 x_2(k) - \hat{\theta}_s(k)x_1(k)\} + v(k) + 0.01(x_2(k) - \hat{x}_2(k)) \qquad (19)$$

where $\hat{x}_1(k)$ and $\hat{x}_2(k)$ are estimated states of $x_1(k)$ and $x_2(k)$. For this simulation, the following values are considered $m = 1, c_1 = 0.5$, $x_1(0) = 0$, $x_2(0) = 0$, $\hat{x}_1(0) = 0, \hat{x}_2(0) = 0$, and $T_s = 0.01\,\text{sec}$. Additionally, $v(k)$ is the robust term which is given by $v(k) = \frac{\hat{\theta}_s(k) b_s}{b_s^2 \hat{\theta}_s^2(k) + c_s}$. We take $b_s = 0.4$ and $c_s = 0.05$. From the definition, the fault is seeded at the 15th second of operation. Initially, we calculate the residual and monitor constantly to detect faults in the system. In this simulation, we consider the following defined constant disturbance

$$\eta(k) = 0.48 \quad for \quad k > 0\ \text{sec}$$

Therefore, a threshold is required to avoid missed or false alarms. In this design, we have $\eta_M = 0.48$, and taking $\beta_c = 0.99$, $\mu = 0.01$, using $\rho = \frac{\beta_c \eta_M}{(1-\mu)}$, we would have a constant threshold value of $\rho = 0.49$. The above discussed results could be seen in Fig. 6, where the residual remains within the threshold prior to the occurrence of the fault. Consequently, after the fault, the residual tends to increase, which exceeds the chosen threshold. Subsequent to detection, the fault parameter, i.e., $\hat{\theta}_s(k)$ has to estimated online using (6), with $\alpha = 0.5$ and $\gamma = 0.001$. However, prior to the fault detection, we take $\hat{\theta}_s(k) = 0.55$. In addition, the robust term is triggered to guarantee asymptotic convergence of the residual, which is observed in Fig. 6, where the residual converges to zero eventually. This is true even with a disturbance.

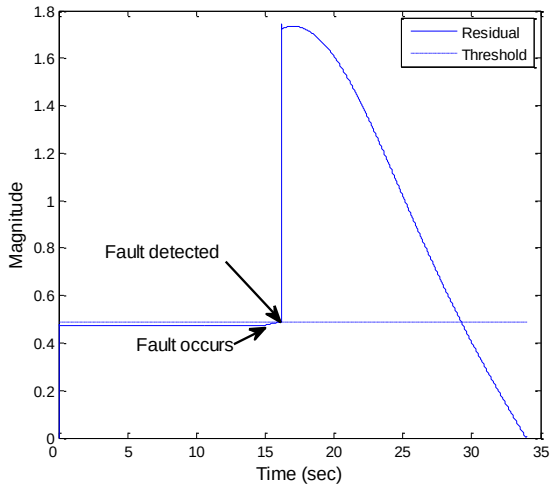

Figure 6: Residual signal with the fault detection threshold.

The online estimation of the fault parameter is shown in Fig. 7 along with the failure threshold value of 0.074. This implies that the induced fault causes the spring

constant to decrease and reach its lower limit beyond which the system is considered to have failed completely. Using this online estimate and the procedure outlined in Section 5, TTF is estimated in real-time and is shown in Fig. 8. The initial prediction may not be accurate, which is attributed to the random selection of the tuning parameter in (6). However, as the online estimation of the fault parameter improves, TTF estimation improves and is found to converge with the actual time of failure of 33 seconds.

The above two simulation examples demonstrate that the proposed FDP scheme performs reliably even in the presence of uncertainties. The scheme learns any unknown fault function and provides an estimate. It also predicts accurately the remaining useful life of the system. Moreover, no apriori training is needed to learn new faults or for estimating TTF (see, Liu *et al.* (2006), Luh and Cheng (2005), Luo *et al.* (2003), Roemer and Ghiocel (1999), Phelps *et al.* (2002), Shao and Nezu (2000), Mathur *et al.* (1998)). Additionally, in the first simulation example an increasing fault parameter was considered for TTF estimation, whereas, in the second simulation example, a decreasing fault parameter is considered to estimate TTF. This automatic FDP scheme, therefore, can alert maintenance personnel the need for preventive measures by providing the TTF. With a unified scheme, therefore, a system can be properly monitored from setup to failure.

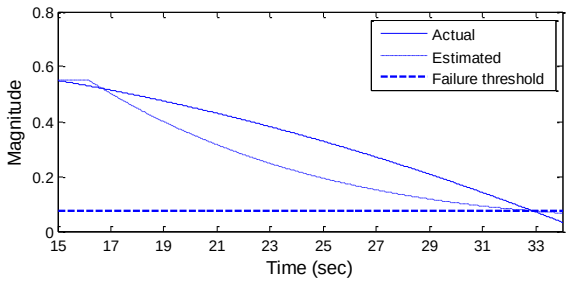

Figure 7: Estimated and actual system parameter trajectories along with the failure threshold.

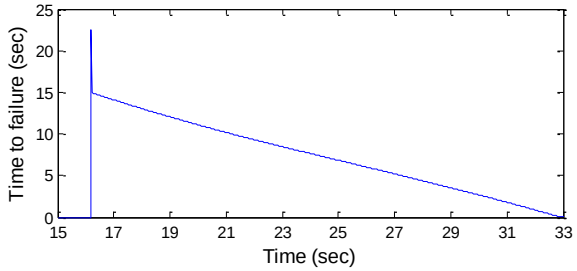

Figure 8: The TTF determination after the fault occurrence.

7. Conclusions and Future Work

In this paper, a new asymptotic FD estimator and a parameter based prediction scheme have been developed for a class of non-affine nonlinear discrete-time system with state faults. The proposed scheme detects and learns unknown incipient and abrupt state faults. By using a robust term and considering certain mild assumptions on the system uncertainties and reconstruction errors, the FDP scheme is guaranteed to render asymptotic stability in contrast with other schemes where a bounded stability is demonstrated. A dead-zone operator enhances robustness of the proposed scheme. A key feature of the proposed FDP scheme is the prediction of the remaining useful by using information on the real-time change in the system parameter. The scheme was developed

with the assumption that all states are measurable. Future work, therefore, would relax the need for measuring all the states.

Appendix

Proof of Lemma 1: Consider the residual dynamics given in (8), solving it would render

$$e_i(k) = a_{ii}^k e_i(0) + \sum_{j=0}^{k} a_{ii}^{k-j}\left[\tilde{\theta}_i^T(j)\phi_i(x(j),u(j)) + \frac{\tilde{\theta}_i^T(j)b_i - C_i}{b_i^T\hat{\theta}_i(j)\hat{\theta}_i^T(j)b_i + c_i} + \varepsilon_i(j) - \frac{\left(\theta_i^T b_i - C_i\right)}{b_i^T\hat{\theta}_i(j)\hat{\theta}_i^T(j)b_i + c_i}\right]$$

The above equation is rewritten as

$$\sum_{j=0}^{k} a_{ii}^{k-j}\varepsilon_i(j) = e_i(k) - a_{ii}^k e_i(0) - \sum_{j=0}^{k} a_{ii}^{k-j}\tilde{\theta}_i^T(j)\phi_i(x(j),u(j))$$

$$-\sum_{j=0}^{k} a_{ii}^{k-j}\frac{\left(\tilde{\theta}_i^T(j)b_i - C_i\right)}{b_i^T\hat{\theta}_i(j)\hat{\theta}_i^T(j)b_i + c_i} + \sum_{j=0}^{k} a_{ii}^{k-j}\frac{\left(\theta_i^T b_i - C_i\right)}{b_i^T\hat{\theta}_i(j)\hat{\theta}_i^T(j)b_i + c_i}\Bigg]$$

Apply Frobenius norm in the above equation to obtain the following

$$\left\|\sum_{j=0}^{k} a_{ii}^{k-j}\varepsilon_i(j)\right\| \le \left\|e_i(k)\right\| + \left\|a_{ii}^k e_i(0)\right\| + \left\|\sum_{j=0}^{k} a_{ii}^{k-j}\tilde{\theta}_i^T(j)\phi_i(j)\right\|$$

$$+\left\|\sum_{j=0}^{k} a_{ii}^{k-j}\frac{\tilde{\theta}_i^T(j)b_i}{b_i^T\hat{\theta}_i(j)\hat{\theta}_i^T(j)b_i + c_i}\right\| + \left\|\sum_{j=0}^{k} a_{ii}^{k-j}\frac{\theta_i^T b_i}{b_i^T\hat{\theta}_i(j)\hat{\theta}_i^T(j)b_i + c_i}\right\| \qquad \text{(A.1)}$$

The summation term in the above equation could be solved as $\left\|\sum_{j=0}^{k} a_{ii}^{k-j}\tilde{\theta}_i^T(j)\phi_i(j)\right\| \le \frac{\phi_{i_{\max}}\left\|\tilde{\theta}_i(k)\right\|}{(1-a_{ii_{\max}})}$. Constricting $a_{ii_{\max}} < 0.5$ in the unit disc, this makes the FD scheme even more stable. Then we obtain $\frac{\phi_{i_{\max}}\left\|\tilde{\theta}_i(k)\right\|}{(1-a_{ii_{\max}})} \le \frac{\phi_{i_{\max}}\left\|\tilde{\theta}_i(k)\right\|}{a_{ii_{\max}}}$. Similarly bounds could be derived for the other terms in the above equation.

Also, $\frac{\tilde{\theta}_i^T(k)b_i}{b_i^T\hat{\theta}_i(j)\hat{\theta}_i^T(j)b_i + c_i} \le \tilde{\theta}_i^T(k)b_i$, $\frac{\theta_i^T b_i}{b_i^T\hat{\theta}_i(j)\hat{\theta}_i^T(j)b_i + c_i} \le \theta_i^T b_i$. Therefore (A.1) could be rewritten as

$$\frac{\left\|\varepsilon_i(k)\right\|}{a_{ii_{\max}}} \le \left\|e_i(k)\right\| + \left\|a_{ii}^k e_i(0)\right\| + \frac{\phi_{i_{\max}}\left\|\tilde{\theta}_i(k)\right\|}{a_{ii_{\max}}} + \frac{b_{i_{\max}}\left\|\tilde{\theta}_i(k)\right\|}{a_{ii_{\max}}} + \frac{b_{i_{\max}}\left\|\theta_i\right\|}{a_{ii_{\max}}}$$

Squaring both side and factoring $a_{ii_{\max}}^2$ would give us

$$\left\|\varepsilon_i(k)\right\|^2 \le a_{ii_{\max}}^2\left(\left\|e_i(k)\right\| + \left\|a_{ii}^k e_i(0)\right\| + \frac{\phi_{i_{\max}}\left\|\tilde{\theta}_i(k)\right\|}{a_{ii_{\max}}} + \frac{b_{i_{\max}}\left\|\tilde{\theta}_i(k)\right\|}{a_{ii_{\max}}} + \frac{b_{i_{\max}}\left\|\theta_i\right\|}{a_{ii_{\max}}}\right)^2$$

Take $b_0 = \left\|a_{ii}^k e_i(0)\right\| + \frac{b_{i_{\max}}\left\|\theta_i\right\|}{a_{ii_{\max}}}$, $b_1 = \phi_{i_{\max}} + b_{i_{\max}}$, then the above equation could be rewritten as

$$\left\|\varepsilon_i(k)\right\|^2 \le a_{ii_{\max}}^2\left(\left\|e_i(k)\right\| + b_0 + \frac{b_1\left\|\tilde{\theta}_i(k)\right\|}{a_{ii_{\max}}}\right)^2$$

Expanding the square term on the right hand side of the above equation and after some mathematical manipulation, the following equation is obtained

$$\left\|\varepsilon_i(k)\right\|^2 \le 3a_{ii_{\max}}^2 b_0^2 + 2a_{ii_{\max}}^2\left\|e_i(k)\right\|^2 + 2b_1^2\left\|\tilde{\theta}_i(k)\right\|^2 + 2a_{ii_{\max}}b_1\left\|e_i(k)\right\|\left\|\tilde{\theta}_i(k)\right\| \qquad \text{(A.2)}$$

Multiply (A.2) by $\left(1+5(2+1/\delta_i)\alpha_i\phi_{i_{\max}}^2\right)$ to render the following equation

$$\left(1+5(2+1/\delta_i)\alpha_i\phi_{i_{\max}}^2\right)\left\|\varepsilon_i(k)\right\|^2 \le 3\left(1+5(2+1/\delta_i)\alpha_i\phi_{i_{\max}}^2\right)a_{ii_{\max}}^2 b_0^2 + 2\left(1+5(2+1/\delta_i)\alpha_i\phi_{i_{\max}}^2\right)a_{ii_{\max}}^2\left\|e_i(k)\right\|^2$$

$$+2\left(1+5(2+1/\delta_i)\alpha_i\phi_{i_{\max}}^2\right)b_1^2\left\|\tilde{\theta}_i(k)\right\|^2 + 2\left(1+5(2+1/\delta_i)\alpha_i\phi_{i_{\max}}^2\right)a_{ii_{\max}}b_1\left\|e_i(k)\right\|\left\|\tilde{\theta}_i(k)\right\|$$

Take $b_{i_0} = 3\left(1+5(2+1/\delta_i)\alpha_i\phi_{i_{\max}}^2\right)a_{ii_{\max}}^2 b_0^2$, $b_{i_1} = 2\left(1+5(2+1/\delta_i)\alpha_i\phi_{i_{\max}}^2\right)a_{ii_{\max}}^2$,

$b_{i_2} = 2\left(1+5(2+1/\delta_i)\alpha_i\phi_{i_{\max}}^2\right)a_{ii_{\max}}b_1$, and $b_{i_3} = 2\left(1+5(2+1/\delta_i)\alpha_i\phi_{i_{\max}}^2\right)b_1^2$, would reveal equation (7). This completes the proof.

Proof of Theorem 1: Consider the Lyapunov function candidate as

$$V_i = \frac{1}{5}e_i^2(k) + \frac{1}{\alpha_i}[\tilde{\theta}_i^T(k)\tilde{\theta}_i(k)]$$

whose first difference is given by

$$\Delta V_i = \underbrace{\frac{1}{5}\left[e_i^2(k+1) - e_i^2(k)\right]}_{\Delta V_1} \underbrace{+\frac{1}{\alpha_i}[\tilde{\theta}_i^T(k+1)\tilde{\theta}_i(k+1) - \tilde{\theta}_i^T(k)\tilde{\theta}_i(k)]}_{\Delta V_2} \tag{A.3}$$

Substitute (8) in ΔV_1 of (A.3) to render

$$\Delta V_1 = \frac{1}{5}\left\{\left[a_{ii}e_i(k) + \Psi_{1_i}(k) - \Psi_{2_i}(k) + \varepsilon_i(k) - \frac{\left(\theta_i^T b_i - C_i\right)}{b_i^T\hat{\theta}_i(k)\hat{\theta}_i^T(k)b_i + c_i}\right]^2 - e_i^2(k)\right\}$$

Apply Cauchy-Schwarz inequality

$\left((a_1+a_2+...+a_n)^T(a_1+a_2+...+a_n) \le n(a_1^Ta_1 + a_2^Ta_2 + ...+ a_n^Ta_n)\right)$ in the above equation to get

$$\Delta V_1 \le \left[e_i^2(k)a_{ii}^2 + \Psi_{1_i}^2(k) + \varepsilon_i^2(k) + \Psi_{2_i}^2(k) + \frac{\left(\theta_i^Tb_i - C_i\right)^2}{\left(b_i^T\hat{\theta}_i(k)\hat{\theta}_i^T(k)b_i + c_i\right)^2}\right] - \frac{1}{5}e_i^2(k) \tag{A.4}$$

Next, substitute (6) in ΔV_2 of (A.4), to render

$$\Delta V_2 = \frac{1}{\alpha_i}\left\{\left[\left(I - \gamma_i\left\|I - \alpha_i\phi_i(k)\phi_i^T(k)\right\|I\right)\tilde{\theta}_i(k) - \alpha_i\phi_i(x(k))e_i(k+1) + \gamma_i\left\|I - \alpha_i\phi_i(k)\phi_i^T(k)\right\|\theta_i\right)\right]^T$$

$$\times\left[\left(I - \gamma_i\left\|I - \alpha_i\phi_i(k)\phi_i^T(k)\right\|I\right)\tilde{\theta}_i(k) - \alpha_i\phi_i(x(k))e_i(k+1) + \gamma_i\left\|I - \alpha_i\phi_i(k)\phi_i^T(k)\right\|\theta_i\right)\right] - \tilde{\theta}_i^T(k)\tilde{\theta}_i(k)\right\}$$

After some mathematical manipulation, the above equation becomes

$$\Delta V_2 = \frac{1}{\alpha_i}\{-2\gamma_i \left\| I-\alpha_i\phi_i(k)\phi_i^T(k)\right\| \tilde{\theta}_i^T(k)\tilde{\theta}_i(k) + \gamma_i^2 \left\| I-\alpha_i\phi_i(k)\phi_i^T(k)\right\|^2 \tilde{\theta}_i^T(k)\tilde{\theta}_i(k)$$

$$\underbrace{-2\alpha_i\tilde{\theta}_i^T(k)\left(I-\gamma_i\left\|I-\alpha_i\phi_i(k)\phi_i^T(k)\right\|I\right)\phi_i(x(k))e_i(k+1)}_{1} + \underbrace{2\gamma_i\left\|I-\alpha_i\phi_i(k)\phi_i^T(k)\right\|\tilde{\theta}_i^T(k)\left(I-\gamma_i\left\|I-\alpha_i\phi_i(k)\phi_i^T(k)\right\|I\right)\theta_i}_{1}$$

$$+\alpha_i^2\phi_i^T(x(k))\phi_i(x(k))e_i^2(k+1) \underbrace{-2\alpha_i\gamma_i\left\|I-\alpha_i\phi_i(k)\phi_i^T(k)\right\|e_i(k+1)\phi_i^T(x(k))\theta_i}_{1} + \gamma_i^2\left\|I-\alpha_i\phi_i(k)\phi_i^T(k)\right\|^2\theta_i^T\theta_i\Big\}$$

Apply Cauchy-Schwarz inequality $(2ab \le a^2+b^2)$ to terms numbered as 1 in the above equation to obtain the following

$$\Delta V_2 \le \frac{1}{\alpha_i}\{-2\gamma_i\left\|I-\alpha_i\phi_i(k)\phi_i^T(k)\right\|\tilde{\theta}_i^T(k)\tilde{\theta}_i(k) + \gamma_i^2\left\|I-\alpha_i\phi_i(k)\phi_i^T(k)\right\|^2\tilde{\theta}_i^T(k)\tilde{\theta}_i(k) + 2\delta_i\tilde{\theta}_i^T(k)\left(I-\gamma_i\left\|I-\alpha_i\phi_i(k)\phi_i^T(k)\right\|I\right)$$

$$\left(I-\gamma_i\left\|I-\alpha_i\phi_i(k)\phi_i^T(k)\right\|I\right)\tilde{\theta}_i(k) + \underbrace{(2+1/\delta_i)\alpha_i^2\phi_i^T(x(k))\phi_i(x(k))e_i^2(k+1)}_{1} + (2+1/\delta_i)\gamma_i^2\left\|I-\alpha_i\phi_i(k)\phi_i^T(k)\right\|^2\theta_i^T\theta_i\Big\}$$

where $\delta_i > 0$ is a constant. Substitute the residual dynamics (8), apply the Cauchy-Schwarz inequality $(((a_1+a_2+...+a_n)^T.(a_1+a_2+...+a_n) \le n(a_1^Ta_1+a_2^Ta_2+..+a_n^Ta_n)))$ to terms numbered as 1 in the above equation and after some mathematical manipulation, we would have the following equation

$$\Delta V_2 \le \frac{1}{\alpha_i}\Big[-2(1+2\delta_i)\gamma_i\left\|I-\alpha_i\phi_i(k)\phi_i^T(k)\right\|\tilde{\theta}_i^T(k)\tilde{\theta}_i(k) + (1+2\delta_i)\gamma_i^2\left\|I-\alpha_i\phi_i(k)\phi_i^T(k)\right\|^2\tilde{\theta}_i^T(k)\tilde{\theta}_i(k) + 2\delta_i\tilde{\theta}_i^T(k)\tilde{\theta}_i(k)\Big]$$

$$+5(2+1/\delta_i)\alpha_i\phi_i^T\phi_i\Psi_{1_i}^2(k) + 5(2+1/\delta_i)\alpha_i\phi_i^T\phi_i\varepsilon_i^2(k) + 5(2+1/\delta_i)\alpha_i\phi_i^T\phi_i\frac{\left(\theta_i^Tb_i-C_i\right)^2}{\left(b_i^T\hat{\theta}_i(k)\hat{\theta}_i^T(k)b_i+c_i\right)^2} + 5(2+1/\delta_i)\alpha_i\phi_i^T\phi_i\Psi_{2_i}^2(k)$$

$$+5(2+1/\delta_i)\alpha_i\phi_i^T\phi_ie_i^2(k)a_{ii}^2 + (2+1/\delta_i)\frac{\gamma_i^2}{\alpha_i}\left\|I-\alpha_i\phi_i(k)\phi_i^T(k)\right\|^2\theta_i^T\theta_i \qquad \text{(A.5)}$$

Since $\Delta V = \Delta V_1 + \Delta V_2$ from (A.4) and (A.5), the first difference of the Lyapunov function candidate is given by

$$\Delta V \le \left[e_i^2(k)a_{ii}^2 + \Psi_{1_i}^2(k) + \varepsilon_i^2(k) + \underbrace{\Psi_{2_i}^2(k)}_{1} + \underbrace{\frac{\left(\theta_i^T b_i - C_i\right)^2}{\left(b_i^T \hat{\theta}_i(k)\hat{\theta}_i^T(k)b_i + c_i\right)^2}}_{2} \right]$$

$$+\frac{1}{\alpha_i}\left[-2(1+2\delta_i)\gamma_i \left\| I - \alpha_i \phi_i(k)\phi_i^T(k) \right\| \tilde{\theta}_i^T(k)\tilde{\theta}_i(k) + (1+2\delta_i)\gamma_i^2 \left\| I - \alpha_i \phi_i(k)\phi_i^T(k) \right\|^2 \tilde{\theta}_i^T(k)\tilde{\theta}_i(k) + 2\delta_i \tilde{\theta}_i^T(k)\tilde{\theta}_i(k) \right]$$

$$+5(2+1/\delta_i)\alpha_i \phi_i^T \phi_i \Psi_{1_i}^2(k) + 5(2+1/\delta_i)\alpha_i \phi_i^T \phi_i \varepsilon_i^2(k) + \underbrace{5(2+1/\delta_i)\alpha_i \phi_i^T \phi_i \frac{\left(\theta_i^T b_i - C_i\right)^2}{\left(b_i^T \hat{\theta}_i(k)\hat{\theta}_i^T(k)b_i + c_i\right)^2}}_{2}$$

$$+\underbrace{5(2+1/\delta_i)\alpha_i \phi_i^T \phi_i \Psi_{2_i}^2(k)}_{1} + 5(2+1/\delta_i)\alpha_i \phi_i^T \phi_i e_i^2(k)a_{ii}^2 + (2+1/\delta_i)\frac{\gamma_i^2}{\alpha_i}\left\| I - \alpha_i \phi_i(k)\phi_i^T(k) \right\|^2 \theta_i^T \theta_i - \frac{1}{5}e_i^2(k) \quad \text{(A.6)}$$

Consider only terms numbered as 1 and 2 in (A.6), would result in the following

$$\left(1+5(2+1/\delta_i)\alpha_i \phi_i^T \phi_i\right)\Psi_{2_i}^2(k) = \left(1+5(2+1/\delta_i)\alpha_i \phi_i^T \phi_i\right)\frac{\left(\tilde{\theta}_i^T(k)b_i - C_i\right)^2}{\left(b_i^T \hat{\theta}_i(k)\hat{\theta}_i^T(k)b_i + c_i\right)^2}$$

$$\le \left(1+5(2+1/\delta_i)\alpha_i \phi_i^T \phi_i\right)\left(\tilde{\theta}_i^T(k)b_i - C_i\right)^2$$

$$\le 2\left(1+5(2+1/\delta_i)\alpha_i \phi_i^T \phi_i\right)\left(b_i^T \tilde{\theta}_i(k)\tilde{\theta}_i^T(k)b_i + C_i^2\right) \quad \text{(A.7)}$$

Next, consider only terms numbered as 2 in (A.6), which is given by

$$\left(1+5(2+1/\delta_i)\alpha_i \phi_i^T \phi_i\right)\frac{\left(\theta_i^T b_i - C_i\right)^2}{\left(b_i^T \hat{\theta}_i(k)\hat{\theta}_i^T(k)b_i + c_i\right)^2} \le \left(1+5(2+1/\delta_i)\alpha_i \phi_i^T \phi_i\right)\left(b_i^T \theta_i \theta_i^T b_i - 2C_i \theta_i^T b_i + C_i^2\right) \quad \text{(A.8)}$$

Next, using (A.7), (A.8), and Lemma 1 in (7) in (A.6), would render the following equation

$$\Delta V \le \left[e_i^2(k)a_{ii}^2 + \Psi_{1_i}^2(k) \right] - \frac{1}{5}e_i^2(k) + \frac{1}{\alpha_i}\left[-2(1+2\delta_i)\gamma_i \left\| I - \alpha_i \phi_i(k)\phi_i^T(k) \right\| \tilde{\theta}_i^T(k)\tilde{\theta}_i(k) \right.$$

$$\left. +(1+2\delta_i)\gamma_i^2 \left\| I - \alpha_i \phi_i(k)\phi_i^T(k) \right\|^2 \tilde{\theta}_i^T(k)\tilde{\theta}_i(k) + 2\delta_i \tilde{\theta}_i^T(k)\tilde{\theta}_i(k) \right] + 5(2+1/\delta_i)\alpha_i \phi_i^T \phi_i e_i^2(k)a_{ii}^2 + 5(2+1/\delta_i)\alpha_i \phi_i^T \phi_i \Psi_{1_i}^2(k)$$

$$+(2+1/\delta_i)\frac{\gamma_i^2}{\alpha_i}\left\| I - \alpha_i \phi_i(k)\phi_i^T(k) \right\|^2 \theta_i^T \theta_i + 2\left(1+5(2+1/\delta_i)\alpha_i \phi_i^T \phi_i\right)\left(b_i^T \tilde{\theta}_i(k)\tilde{\theta}_i^T(k)b_i + C_i^2\right)$$

$$+\left(1+5(2+1/\delta_i)\alpha_i \phi_i^T \phi_i\right)\left(b_i^T \theta_i \theta_i^T b_i - 2C_i \theta_i^T b_i + C_i^2\right)$$

$$+b_{i_0}+b_{i_1}\left\|e_i(k)\right\|^2+\underbrace{b_{i_2}\left\|e_i(k)\right\|\left\|\tilde{\theta}_i(k)\right\|}_{1}+b_{i_3}\left\|\tilde{\theta}_i(k)\right\|^2 \tag{A.9}$$

Apply Cauchy-Schwarz inequality ($ab \le a^2 + b^2$) to the term numbered as 1 in the above equation and apply Frobenius norm would result in the following first difference of the Lyapunov function

$$\Delta V \le -\left(\frac{1}{5}-a_{ii_{\max}}^2-5(2+1/\delta_i)\alpha_i\phi_{i_{\max}}^2 a_{ii_{\max}}^2-b_{i_1}-\frac{b_{i_1}}{2}\right)\left\|e_i(k)\right\|^2-\left(\frac{2(1+2\delta_i)\gamma_i}{\alpha_i}\left\|I-\alpha_i\phi_i^T(k)\phi_i(k)\right\|-\phi_{i_{\max}}^2-\frac{2\delta_i}{\alpha_i}-\frac{(1+2\delta_i)\gamma_i^2}{\alpha_i}\left\|I-\alpha_i\phi_i(k)\phi_i^T(k)\right\|^2\right.$$

$$\left.-5(2+1/\delta_i)\alpha_i\phi_{i_{\max}}^4-\frac{3b_{i_3}}{2}-2(1+5(2+1/\delta_i)\alpha_i\phi_{i_{\max}}^2)b_{i_{\max}}^2\right)\left\|\tilde{\theta}_i(k)\right\|^2$$

$$+2(1+5(2+1/\delta_i)\alpha_i\phi_{i_{\max}}^2)C_{i_{\max}}^2+(2+1/\delta_i)\frac{\gamma_i^2}{\alpha_i}\left\|I-\alpha_i\phi_i(k)\phi_i^T(k)\right\|^2\theta_i^T\theta_i+b_{i_0}$$

$$+(1+5(2+1/\delta_i)\alpha_i\left\|\phi_i(k)\right\|^2)\left(b_{i_{\max}}^2\theta_{i_{\max}}^2-2C_{i_{\min}}b_{i_{\min}}\theta_{i_{\min}}+C_{i_{\max}}^2\right) \tag{A.10}$$

Take

$$b_{i_{\min}}=\frac{\left([(2+1/\delta_i)\frac{\gamma_i^2}{\alpha_i}\left\|I-\alpha_i\phi_i(k)\phi_i^T(k)\right\|^2\theta_{i_{\max}}^2+b_{i_0}]/(1+5(2+1/\delta_i)\alpha_i\left\|\phi_i(k)\right\|^2)\right)}{2C_{i_{\min}}\theta_{i_{\min}}}+\frac{\left(3C_{i_{\max}}^2+b_{i_{\max}}^2\theta_{i_{\max}}^2\right)}{2C_{i_{\min}}\theta_{i_{\min}}}$$

and $b_{i_{\max}}=\frac{\delta_i}{\sqrt{2(1+15\alpha_i\phi_{i_{\max}}^2)}}$,

then (A.10) could be rewritten as

$$\Delta V \le -\left(\frac{1}{5}-a_{ii_{\max}}^2-5(2+1/\delta_i)\alpha_i\phi_{i_{\max}}^2 a_{ii_{\max}}^2-b_{i_1}-\frac{b_{i_1}}{2}\right)\left\|e_i(k)\right\|^2-\left(\frac{2(1+2\delta_i)\gamma_i}{\alpha_i}\left\|I-\alpha_i\phi_i^T(k)\phi_i(k)\right\|-\phi_{i_{\max}}^2-\frac{2\delta_i}{\alpha_i}-\frac{(1+2\delta_i)\gamma_i^2}{\alpha_i}\left\|I-\alpha_i\phi_i(k)\phi_i^T(k)\right\|^2\right.$$

$$\left.-5(2+1/\delta_i)\alpha_i\phi_{i_{\max}}^4-\frac{3b_{i_3}}{2}-2(1+5(2+1/\delta_i)\alpha_i\phi_{i_{\max}}^2)b_{i_{\max}}^2\right)\left\|\tilde{\theta}_i(k)\right\|^2 \tag{A.11}$$

This implies that the first difference in the Lyapunov function candidate $\Delta V < 0$ in (A.11)

provided if the gains are selected as $a_{ii_{\max}} \le \sqrt{\frac{1/5}{(4+20(2+1/\delta_i)\alpha_i\phi_{i_{\max}}^2)}}$, $0<\alpha_i<1$, $0<\delta_i<1$, and

$$\frac{1-\sqrt{1-C_{r_i}}}{\left\|I-\alpha_i\phi_i(k)\phi_i^T(k)\right\|} \le \gamma_i \le 1/\left\|I-\alpha_i\phi_i(k)\phi_i^T(k)\right\|,$$

where

$$C_{r_i} = \frac{\alpha_i}{(2+1/\delta_i)}\left(\frac{2\delta_i}{\alpha_i}+\phi_{i_{\max}}^2+5\alpha_i(2+1/\delta_i)\phi_{i_{\max}}^4+\frac{3b_{i_3}}{2}+2\left(1+5\alpha_i(2+1/\delta_i)\phi_{i_{\max}}^2\right)b_{i_{\max}}^2\right).$$ Since

$V>0$ and the first difference is less than zero provided the gains are selected as above and $e_i(k_0)$ and $\tilde{\theta}_i(k_0)$ are bounded in a compact set *B*. This concludes that $e_i(k)$ and $\tilde{\theta}_i(k)$ converges to zero asymptotically. □

Proof of Theorem 2: After the i^{th} fault occurs, and prior to triggering the i^{th} OLAD and the robust term, the residual equation in (12) is given by

$$e_i(k+1) = a_{ii}e_i(k)+\eta_i(x(k),u(k))+h_i(x(k),u(k)) \tag{A.12}$$

Incipient faults: Solve for $e_i(k)$ in (A.12) during the time interval $k\in[T+k_1, T+k_d]$, would render

$$e_i(T+k_d) = a_{ii}^{(T+k_d-T-k_1)}e_i(T+k_1)+\sum_{m=T+k_1+1}^{T+k_d} a_{ii}^{(T+k_d-m)}\eta_i(x(m-1),u(m-1))$$

$$+\sum_{m=T+k_1+1}^{T+k_d} a_{ii}^{(T+k_d-m)}(1-e^{-\kappa_i(m-T)})f_i(x(m-1),u(m-1))$$

Use the triangle inequality and $\left|e_i(T+k_1)\right|<\rho_i$, would reveal

$$\left|e_i(T+k_d)\right| \geq -a_{ii}{}^{(k_d-k_1)}\rho_i - \left|\sum_{m=T+k_1+1}^{T+k_d} a_{ii}{}^{(T+k_d-m)}\eta_i(x(m-1),u(m-1))\right|$$

$$+\left|\sum_{m=T+k_1+1}^{T+k_d} a_{ii}{}^{(T+k_d-m)}(1-e^{-\kappa_i(m-T)})\,f_i(x(m-1),u(m-1))\right|$$

From Assumption 2, the maximum bound on the system uncertainty is given by $\left|\eta_i(x(k),u(k))\right| \leq \eta_{i_M}$, thus we have

$$\left|e_i(T+k_d)\right| \geq -a_{ii}{}^{(k_d-k_1)}\rho_i - \sum_{m=T+k_1+1}^{T+k_d} a_{ii}^{(T+k_d-m)}\eta_{i_M}$$

$$+\left|\sum_{m=T+k_1+1}^{T+k_d} a_{ii}{}^{(T+k_d-m)}(1-e^{-\kappa_i(m-T)})\,f_i(x(m-1),u(m-1))\right|$$

Since $\sum_{m=T+k_1+1}^{T+k_d} a_{ii}^{(T+k_d-m)}\eta_{i_M} = \beta_{c_i}\eta_{i_M}\dfrac{(1-\mu_i^{k_d-k_1})}{(1-\mu_i)}$ and solve further to have

$$\left|e_i(T+k_d)\right| \geq -\rho_i + \left|\sum_{m=T+k_1+1}^{T+k_d} a_{ii}{}^{(T+k_d-m)}(1-e^{-\kappa_i(m-T)})\,f_i(x(m-1),u(m-1))\right|$$

Hence a fault is detected only if $\left|(1-a_{ii})\sum_{m=T+k_1+1}^{T+k_d} a_{ii}{}^{(T+k_d-m)}(1-e^{-\kappa_i(m-T)})\,f_i(x(m-1),u(m-1))\right| \geq 2\eta_{i_M}$ and therefore $\left|e_i(T+k_d)\right| \geq \rho_i$. The fault term is assumed to satisfy $f_i(x(k),u(k)) \geq 2\eta_{i_M}$. Thus there exists a new constant $\beta_i \geq 2\eta_{i_M}$, such that $\left|f_i(x(k),u(k))\right| \geq \beta_i$, and

$$\left|(1-a_{ii})\sum_{m=T+k_1+1}^{T+k_d} a_{ii}{}^{(T+k_d-m)}(1-e^{-\kappa_i(m-T)})\,f_i(x(m-1),u(m-1))\right|$$

$$\geq \beta_i\left|(1-a_{ii})\sum_{m=T+k_1+1}^{T+k_d} a_{ii}{}^{(T+k_d-m)}(1-e^{-\kappa_i(m-T)})\right|$$

$$= \beta_i \left| (1-a_{ii}) \sum_{m=k_1+1}^{k_d} {a_{ii}}^{(k_d-m)} (1-e^{-\kappa_i(m)}) \right|$$

Now if the inequality

$\left| (1-a_{ii}) \sum_{m=k_1+1}^{k_d} {a_{ii}}^{(k_d-m)} (1-e^{-\kappa_i(m)}) \right| \geq \frac{2\eta_{i_M}}{\beta_i}$ holds, then the fault detection time can be obtained as

$$(1-a_{ii}) \sum_{m=k_1+1}^{k_d} {a_{ii}}^{(k_d-m)} (1-e^{-\kappa_i(m)}) = \frac{2\eta_{i_M}}{\beta_i} \tag{A.13}$$

$$(1-a_{ii})\left(\sum_{m=k_1+1}^{k_d} {a_{ii}}^{(k_d-m)} - \sum_{m=k_1+1}^{k_d} {a_{ii}}^{(k_d-m)} e^{-\kappa_i m} \right) = \frac{2\eta_{i_M}}{\beta_i}$$

Solve further to get

$$(1-a_{ii})\left(\left(\frac{1-{a_{ii}}^{k_d-k_1}}{1-a_{ii}} \right) - \sum_{m=k_1+1}^{k_d} {a_{ii}}^{(k_d-m)} e^{-\kappa_i m} \right) = \frac{2\eta_{i_M}}{\beta_i}$$

It is easy to see that solving the above equation further would render (13).

Abrupt faults: For abrupt faults, $\kappa_i \to \infty$ using (A.13), therefore,

$(1-a_{ii}) \sum_{m=k_1+1}^{k_d} {a_{ii}}^{(k_d-m)} = \frac{2\eta_{i_M}}{\beta_i}$. Solve further to derive $\left(1-{a_{ii}}^{k_d-k_1}\right) = \frac{2\eta_{i_M}}{\beta_i}$.

After performing some mathematical manipulations in the above equation, (14) could be derived. □

Proof of Theorem 3: In general, for any system satisfying *Assumption 6*, the maximum value of the system parameter in the event of a fault is determined by their physical

limitations. Thus $\hat{\theta}_{i_j}(k_{f_j}) = \theta_{i_{j\max}}$. Equation (15) holds only in the time interval $k \in [k_d, k_f]$. Consequently, the update equation in (6) can be written as

$$\hat{\theta}_i(k+1) = (I - \gamma_i \left\| I - \alpha_i \phi_i(k) \phi_i^T(k) \right\| I) \hat{\theta}_i(k) + \alpha_i \varphi_i(k)\, e_i(k+1)$$

The above equation is a linear time varying equation which can be written as

$$\overline{x}(k+1) = \overline{A}(k).\overline{x}(k) + \overline{B}.\overline{u}(k) \qquad \text{(A.14)}$$

where $\overline{x}(k+1) = \hat{\theta}_i(k+1)$, $\overline{A}(k) = (I - \gamma_i \left\| I - \alpha_i \phi_i(k) \phi_i^T(k) \right\| I)$ is a diagonal matrix, $\overline{x}(k) = \hat{\theta}_i(k)$, $\overline{B} = \alpha_i$, and $\overline{u}(k) = \phi_i(k)\, e_i(k+1)$. Since the above defined $\overline{A}$ matrix is diagonal, (A.14) can be written as

$$\overline{x}_j(k+1) = \overline{a}_{jj}(k)\overline{x}_j(k) + \overline{b}_j \overline{u}_j(k) \qquad \text{(A.15)}$$

where $\overline{a}_{jj}(k) = 1 - \gamma_i \left\| I - \alpha_i \phi_i(k) \phi_i^T(k) \right\|$, $\overline{b_j} = \alpha_i$, and $\overline{u}_j(k) = \phi_{i_j}(k) e_i(k+1)$, is a product of the basis function and the residual, additionally $j = 1, 2, ...l$.

The solution of the system defined in (A.15) is given by

$$\overline{x}_j(k) = \prod_{t=k_{0j}}^{k} \overline{a}_{jj}(t) \overline{x}_j(k_{0_j}) + \sum_{r=k_{0j}}^{k} \left(\prod_{t=r}^{k} \overline{a}_{jj}(t) \right) \overline{b_j} \overline{u}_j(r)$$

Since the j^{th} system parameter reaches its maximum value at the time of failure, i.e., k_{f_j}, then $\hat{\theta}_{i_j}(k_{f_j}) = \theta_{i_{j\max}}$. Additionally, the value of $\hat{\theta}_{i_j}(k_{0_j}) = \theta_{i_{j_0}}$; hence the above equation becomes

$$\theta i_{j\max} = \prod_{t=k_{0j}}^{k_{fj}} \overline{a}_{jj}(t)\theta i_{j_0} + \sum_{r=k_{0j}}^{k_{fj}} \left(\prod_{t=r}^{k_{fj}} \overline{a}_{jj}(t) \right) \overline{b}_j \overline{u}_j(r)$$

In the above equation, for the time interval $[k_{0_j}, k_{f_j}]$, $\overline{a}_{jj}(k)$ and $\overline{u}_j(k)$ are assumed to be constant. This suggests that the system defined above can be considered as a linearly time invariant system. This assumption is reasonable since $0 < \overline{a}_{jj} < 1$ and it is stable and the input $\overline{u}_j(k)$ would be bounded due to the guaranteed stability of the parameter update law in (6). Also, TTF is continuously updated at each time instant in the interval $k \in [k_d, k_f]$, as explained below. Hence the above equation becomes

$$\theta i_{j\max} = \overline{a}_{jj}^{(k_{fj}-k_{0j})} \theta i_{j_0} + \overline{b}_j \overline{u}_j \sum_{t=k_{0j}+1}^{k_{fj}} \overline{a}_{jj}^{(k_{fj}-t)} \tag{A.16}$$

Using results of geometric series, (A.16) then becomes

$$\theta i_{j\max} = \overline{a}_{jj}^{(k_{fj}-k_{0j})} \theta i_{j_0} + \overline{b}_j \overline{u}_j \left(\frac{1-\overline{a}_{jj}^{(k_{fj}-k_{0j})}}{1-\overline{a}_{jj}} \right)$$

With some simple mathematical manipulation, one obtains

$$\overline{a}_{jj}^{(k_{fj}-k_{0j})} = \frac{\left[\theta i_{j\max}(1-\overline{a}_{jj}) - \overline{b}_j \overline{u}_j \right]}{\left[\theta i_{j_0}(1-\overline{a}_{jj}) - \overline{b}_j \overline{u}_j \right]}$$

Finally, after performing some mathematical manipulation, we have

$$k_{f_j} = \frac{\left| \log\left(\left| \frac{\theta i_{j\max}(1-\overline{a}_{jj}) - \overline{b}_j \overline{u}_j}{\theta i_{j_0}(1-\overline{a}_{jj}) - \overline{b}_j \overline{u}_j} \right| \right) \right|}{\left| \log(\overline{a}_{jj}) \right|} + k_{0_j}.$$

Since $\overline{a}_{jj}(k) = 1 - \gamma_i \left\| I - \alpha_i \phi_i(k) \phi_i^T(k) \right\|$, $\overline{b}_j = \alpha_i$, and $\overline{u}_j(k) = \phi_{i_j}(k) e_i(k+1)$, equation (15) results. □

References

A. Alessandri,"Fault diagnosis for nonlinear systems using a bank of neural estimators," *Comp. in Ind.*, vol. 52, no. 3, pp. 271-289, 2003.

W. Barie and J. Chiasson,"Linear and nonlinear state-space controllers for magnetic levitation," *International Journal of Systems Science*, vol. 27, no. 11, pp. 1153-1163, 1996.

A. R. Barron,"Universal approximation bounds for superposition of a sigmoidal function," *IEEE Trans. on Information Theory*, vol. 39, no. 3, pp. 930-945, 1993.

F. Caccavale and L. Villani, *Fault Diagnosis and Fault Tolerance for Mechatronic Systems: Recent Advances*, Springer, UK, 2003.

F. Cacccavale, F. Pierri, and L. Villani,"Adaptive observer for fault diagnosis in nonlinear discrete-time systems," *ASME Journal of Dynamic Syst. Meas. and Control*, vol. 130, no. 2, pp. 1-9, 2008.

C. T. Chen, *Linear System Theory and Design*, 3rd Ed., Oxford University Press, NY, USA, 1999.

J. Chen and R. J. Patton, *Robust Model-based Fault Diagnosis for Dynamic Systems*, Kluwer Academic publishers, MA, USA, 1999.

R. H. Chen and J. L. Speyer,"Stochastic fault detection filter," *Automatica* , vol. 39, no. 3, pp. 377-390, 2003.

S. Dash and V. Venkatasubramanian,"Challenges in the industrial applications of fault diagnostic systems," *Computers and Chemical Engineering*, vol. 24, no. 2-7, pp. 785-791, 2000.

D. M. Dawson, Z. Qu, and S. Lim,"Re- thinking the robust control of robot manipulators," *Proc. of the Conf. on Decision and Control* pp. 1043-1045, 1991.

M. A. Demetriou and M. M. Polycarpou,"Incipient fault diagnosis of dynamical systems using online approximators," *IEEE Trans. on Automatic Control*, vol. 43, no. 11, pp. 1612-1617, 1998.

J. D. DePree and C. W. Swartz, *Introduction to Real Analysis*, Wiley, NY, USA, 1988.

C. Edwards, S. K. Spurgeon, and R. J. Patton,"Sliding mode observers for fault detection and isolation," *Automatica*, vol. 36, pp. 541-553, 2000.

W. E. Dixon, I. D. Walker, D. M. Dawson, and J. P. Hartranft, "Fault detection for robot manipulators with parametric uncertainty: A prediction-error-based approach," *IEEE Trans. on Robotics and Automation*, vol. 16, no. 6, pp. 689-699, 2000.

J. A. Farrell and M. M Polycarpou, *Adaptive Approximation Based Control-Unifying Neural, Fuzzy and Traditional Adaptive Approximation Approaches*, Wiley Interscience, NJ, USA, 2006.

P. M. Frank and L. Keller,"Fault diagnosis in dynamic systems using analytical and knowledge-based redundancy–a survey and some new results," *Automatica*, vol. 26, pp. 459-474, 1990.

J. Gertler,"Survey of model-based failure detection and isolation in complex plants," *IEEE Control Sys. Magazine*, vol. 8, pp. 3-11, 1988.

H. Hammouri, M. Kinnaert, and E. H. El Yaagoubi,"Observer-based approach to fault detection and isolation for nonlinear systems," *IEEE Trans. on Automatic Control*, vol. 44, no. 10, pp. 1879-1884, 1999.

H. Hammouri, P. Kabore, and M. Kinnaert,"A geometric approach to fault detection and isolation for bilinear systems," *IEEE Trans. on Automatic Control*, vol. 46, no. 9, pp. 1451 – 1455, 2001.

H. Hammouri, P. Kabore, S. Othman, and J. Biston,"Failure diagnosis and nonlinear observer- application to a hydraulic process," *Journal of The Franklin Institute*, vol. 339, no. 4-5, pp. 455-478, 2002.

T. Hayakawa, W. M. Haddad, and N. Hovakimyan,"Neural network adaptive control for a class of nonlinear uncertain dynamical systems with asymptotic stability guarantees," *IEEE Trans. on Neural Networks*, vol. 19, no. 1, pp. 80-89, 2008.

F. Hermans and M. Zarrop,"Sliding mode observers for robust sensor monitoring," *Proc. of the IFAC world congress*, pp.211-216, 1996.

R. Isermann,"Model-based fault-detection and diagnosis–status and applications,"*Annual Reviews in Control*, vol. 29, no.1, pp. 71-85, 2005.

R. Isermann, *Fault-Diagnosis Systems-An Introduction from Fault Detection to Fault Tolerance*, Springer, Berlin, Germany, 2006.

S. Jagannathan, *Neural Network Control of Nonlinear Discrete–Time Systems*, CRC publications, NY, USA, 2006.

B. Jiang and F. N. Chowdhury,"Parameter fault detection and estimation of a class of nonlinear systems using observers," *Journal of the Franklin Institute*, vol. 342, no. 7, pp. 725-736, 2005.

P. Kabore and H. Wang,"Using an equivalent feedback control of the residuals for fault detection and identification," *Proc. of the 38th IEEE Conf. on Decision and Control*, vol. 5, pp. 4466 – 4471, 1999.

C. M. Kwan, D. M. Dawson, and F. L. Lewis, "Robust adaptive control of robots using neural network: global tracking stability," *Proc. of the Conf. on Decision and Control*, pp. 1846-1851, 1995.

F. L. Lewis, S. Jagannathan, and A. Yesilderek,"*Neural Network Control of Robotics and Nonlinear Systems*," Taylor and Francis, UK, 1999.

J. Liu, D. Djurdjanovic, K. A. Marko, Jun Ni, and Pu Sun,"Growing structure multiple model system for anomaly detection and fault diagnosis," *Proc. of International Symposium on Flexible, Automation*, Osaka, Japan, pp. 396-405, 2006.

C. J. Lopez-Toribio and R. J. Patton,"Fuzzy observers for nonlinear dynamic systems fault diagnosis," *Proc. of the 37th IEEE Conference on Decision and Control (CDC)*, vol. 1, pp. 84-89, 1998.

C. J. Lopez-Toribio and R. J. Patton,"Takagi-Sugeno fuzzy fault-tolerant control for a non-linear system," *Proc. of the 38th IEEE Conference on Decision and Control*, vol. 5, pp. 4368-4373, 1999.

G. C. Luh and W. C. Cheng,"Immune model-based fault diagnosis," *Math and Computers in Simulation*", vol. 67, no. 6, pp. 515 – 539, 2005.

J. Luo, M. Namburu, K. Pattipati, L. Qiao, M. Kawamoto, and S, Chigusa,"Model-based prognostic techniques," *AUTOTESTCON Proc. of the IEEE Systems Readiness Technology Conference*, Anaheim, California, USA, pp. 330-340, 2003.

J. Luo, A. Bixby, K. Pattipati, L. Qiao, M. Kawamoto, and S. Chigusa,"An interacting multiple model approach to model-based prognostics," *IEEE International Conference on Systems, Man and Cybernetics*, Washington, D.C., USA, vol. 1, pp. 189-194, 2003.

M. Mahmoud,"Sufficient conditions for the stability of input delayed discrete time fault tolerant control systems," *IEEE International Conference on Control Applications*, pp. 504 -509, 2008.

M. Massoumnia, G. C. Verghese, and A. S. Willsky,"Failure detection and identification," *IEEE Trans. on Automatic Control*, vol. 34, no. 3, pp. 316-322, 1989.

A. Mathur, S. Deb, and K. R. Pattipati,"Modeling and real-time diagnostics in TEAMS-RT," *Proc. of the American Control Conf.*, Philadelphia, PA, USA, pp.1610-1614, 1998.

M. L. McIntyre, W. E. Dixon, D. M. Dawson, and I. D. Walker,"Fault identification for robot manipulators," *IEEE Trans. on Robotics*, vol. 21, no. 5, pp. 1028-1034, 2005.

P. M. Patre, W. MacKunis, K. Kaiser, and W. E. Dixon,"Asymptotic tracking for uncertain dynamics systems via a multilayer NN feed forward and RISE feedback control structure," *Proc. of the American Control conf.*, New York City, NY, USA, pp. 5989-5994, 2007.

C. De Persis and A. Isidori,"A geometric approach to nonlinear fault detection and isolation," *IEEE Trans. on Automatic Control*, vol. 46, no. 6, pp. 853 – 865, 2001.

E. Phelps, P. Willett, and T. Kirubarajan, "Useful lifetime tracking via the IMM," *Proc. of SPIE Components and System Diagnostics, Prognostics, and Health Mgmt. II*, vol. 4733, pp. 145-156, 2002.

M. J. Roemer and D. M. Ghiocel,"A probabilistic approach to the diagnosis of gas turbine engine faults," *53rd Machinery Prevention Tech. (MFPT) Conf.*, Virginia Beach, VA, USA, pp. 325-336, 1999.

Y. Shao and K. Nezu,"Prognosis of remaining bearing life using neural networks," *Proc. of the Institution of Mech. Engineers, Part I: Journal of Syst. and Control Eng.*, vol. 214, no. 3, pp. 217-230, 2000.

H. A. Talebi, S. Tafazoli, and K. Khorasani,"A recurrent neural-network-based sensor and actuator fault detection and isolation for nonlinear systems with application to the satellite's attitude control subsystem," *IEEE Trans. on Neural Networks*, vol. 20, no.1, pp. 45- 60 , 2009.

B. T. Thumati and S. Jagannathan,"An online approximator-based fault detection framework for nonlinear discrete-time systems," *Proc. of the IEEE Conf. on Decision and Control*, pp. 2608-2613, 2007.

B. Xian, D. M. Dawson, M. S. de Queiroz, and J. Chen,"A continuous asymptotic tracking control strategy for uncertain nonlinear systems," *IEEE Trans. on Automatic Control*, vol. 49, no. 7, pp. 1206-1211, 2004.

X. G. Yan and C. Edwards,"Nonlinear robust fault reconstruction and estimation using a sliding mode observer," *Automatica*, vol. 43, no. 9, pp. 1605-1614, 2007.

J. Zhang and A. J. Morris,"On-line process fault diagnosis using fuzzy neural networks," *Int. Systems Engineering*, pp. 37-47, 1994.

D. Zhang, Z. Wang, and S. Hu,"Robust satisfactory fault-tolerant control of uncertain linear discrete-time systems: an LMI approach," *Int. Journal of Systems Science*, vol. 38, no.2, pp. 151-165, 2007.

2. A Robust Fault Detection and Prediction Scheme for Nonlinear Discrete Time Input-Output Systems[1]

Balaje T. Thumati* and S. Jagannathan

Abstract—Model-based fault detection (MFD) techniques are preferred over hardware based schemes due to low cost and minimal changes to the system when the system states are available. However, one of the major challenges in model based monitoring, diagnosis and prognosis (MDP) approach was to develop a detection and prognosis (DP) scheme in discrete-time in the presence of partial state information since discrete-time schemes are normally preferred for ease of implementation. Therefore, in this paper, we propose a unified fault detection and prediction (FDP) scheme for a nonlinear discrete-time input-output system in the presence of modeling uncertainties when certain states are not available for measurement. A nonlinear estimator with an online tunable approximator and a robust term is introduced to monitor the system. A residual is generated by comparing the output of the system with that of the estimator. A unknown fault is detected when the generated residual exceeds a mathematically derived threshold. Subsequently, the online approximator and the robust terms are initiated. The approximator uses the system input and output measurements while its own parameters are tuned online using a novel

[1] Balaje T. Thumati and S. Jagannathan are with the Electrical and Computer Engineering Department, Missouri University of Science and Technology (formerly University of Missouri, Rolla), Rolla, MO 65409, USA. Research supported in part by NSF I/UCRC on Intelligent Maintenance Systems and Intelligent Systems Center. *Corresponding author, e-mail: bttr74@mst.edu

update law. Additionally, robustness, sensitivity, and the stability of the fault detection scheme are rigorously examined. The proposed scheme is guaranteed to be asymptotically stable due to the introduction of the robust term and using some mild assumption on the system uncertainty. Subsequently the process of determining the time to failure (TTF) is introduced. Finally, the FDP scheme is simulated on a magnetic suspension system.

***Keywords: Fault detection and prognostics, nonlinear discrete time system, online approximator, Lyapunov stability*.**

I. Introduction

Traditionally, fault detection and prognostics schemes were developed individually due to lack in understanding of how to learn the fault dynamics. In general, the process of fault detection, prognosis and accommodation consists of: (a) detection deals with determining if a fault has occurred; (b) diagnosis considers the problem of root cause and location of the fault; (c) prognosis deals with the prediction of TTF and (c) accommodation attempts to correct a particular fault, through controller reconfiguration. In particular, prognostic schemes have been found to be vital since the prediction of TTF helps the maintenance personnel to take action in the event of a fault.

From the available fault detection (FD) schemes, the model based FD appear to be most preferred [5, 9] over any hardware based schemes due to reduced cost. In such an approach, a model representative of the nonlinear system behavior is first developed and residuals are obtained by comparing the response of the model with that of the actual system. A fault is detected when the residuals exceed a pre-determined threshold. However, modeling uncertainties can cause performance degradation of the FD scheme

rendering false alarms and missed detection thus demanding a robust FD scheme. Quantitative modeling schemes such as state-space [9], parity relations [5] as well as the qualitative schemes such as expert systems [10] have been introduced for linear systems [5, 9, 10] as a robust FD scheme.

With the development of advance nonlinear modeling techniques [8], it is now possible to develop FD schemes for nonlinear systems with nonlinear incipient or abrupt faults [1, 3, 7, 20, 23, 24]. This classification of faults is based on the time profile, where an incipient fault would be a slowly growing whereas an abrupt fault would be suddenly occurring [7]. However, most of the above discussed schemes [5, 9, 7, 10, 20, 24] of FD are for continuous-time systems. There has been limited previous work on FD of discrete time system [1, 3], but has mainly been on sensor or actuator faults, and requires the persistency of excitation (PE) condition to prove the stability of the scheme. It is noted that the development of a FD scheme in discrete-time is difficult due to the stability or convergence. In other words, the first difference of a Lyapunov function is quadratic with respect to the states which makes the detection scheme in discrete-time difficult whereas it is linear in the case of continuous-time systems. Therefore, the authors have recently introduced a robust FD framework for nonlinear discrete-time systems [8] by assuming that all the states are available for measurement and relaxing the requirement of the PE condition. However, availability of all the states means the need for more sensors, which makes the scheme expensive. This is the main focus of this paper.

One of the noted problems in the literature for the above mentioned schemes even for continuous-time systems is the lack of prognostics or TTF determination. One of the earlier works on prognostics [16, 17] assumed a specific degradation model of the system,

which is found to be quite limited to the system or material type under consideration. On the other hand, deterministic polynomial and a probabilistic method were developed for prognosis [19, 21] by assuming that only certain parameters affect the fault. The fault dynamics are not being learned online making the prediction inaccurate. Finally, a black box approach using NN was developed in [22] using failure data which is expensive to collect apriori.

By contrast, in this paper, we unify the development of the fault detection and prognostics (FDP) scheme for nonlinear discrete-time input-output systems [7, 20, 24]. Such an approach has not been previously developed either in continuous or discrete time systems [1, 3]. First, a systematic learning methodology and some analytical results for the FDP scheme are introduced for a class of nonlinear discrete time input-output systems by using a robust term and assuming an upper bound on the modeling uncertainties. As a consequence, the proposed FDP scheme guarantees asymptotic stability in contrast to other schemes where a bounded stability [1, 3, 7, 20, 23, 24] is ensured. The proposed FDP scheme could detect nonlinear system faults, which are modeled as a nonlinear function of the input and output variables rather than actuator faults [1, 3]. Subsequently, the TTF is introduced by using the learning methodology.

The main idea behind this methodology, is to monitor the system for any abnormal behavior (which could be due to the faults or modeling uncertainties) utilizing a nonlinear estimator consisting of an online approximator in discrete-time (OLAD) with adjustable parameters and a robust term. Commonly used OLAD models are neural network, fuzzy logic, and spline function. By comparing the output of the estimator and the system output, residuals are generated and compared against a mathematically derived

threshold for FD. After the detection of a fault, the OLAD and the robust term are initiated to learn the fault dynamics online. A stable adaptive update law is proposed for tuning the OLAD. Subsequently, the parameter update law is utilized to solve for the TTF. Further, the stability, the sensitivity, and the robustness of the FDP scheme are demonstrated through Lyapunov analysis in the presence of reconstruction errors and unmodeled dynamics. Finally, it is important to note that fault detection schemes and adaptation laws developed in continuous-time [7, 20, 24] cannot be directly applied to nonlinear systems represented in discrete-time.

This paper is organized as follows: In Section II the nonlinear discrete-time input-output system under consideration is explained. In Section III, the fault detection scheme is introduced. In Section IV, the robustness, the sensitivity, and the performance of the fault detection scheme is shown extensively with mathematical proofs by using the Lyapunov theory and in Section V the prognostics scheme is developed. In Section VI, a magnetic suspension system is used to illustrate the fault detection and prognostics scheme. Finally, in Section VII some concluding remarks and some possible future work are given. This paper introduces a fault detection and prediction algorithm in discrete-time and not a fault isolation and accommodation scheme. However, published literature on fault isolation and accommodation could be found elsewhere [10, 20, 26].

II. Problem Formulation

The discrete time input-output system under consideration is described by

$$x(k+1) = Ax(k) + \zeta(y(k), u(k)) + \eta(x(k), u(k)) + \Pi(k-T) f(y(k), u(k))$$

$$y(k) = Cx(k) \tag{1}$$

where $x \in \Re^n$ is the state vector, $y \in \Re$ is the output, ζ, $f : \Re \times \Re^m \to \Re^n$, $\eta : \Re^n \times \Re^m \to \Re^n$ are smooth vector fields, $T \geq 0$ is the starting time of the fault, $\zeta(y(k), u(k))$ represents the nominal dynamics of system, $\eta(x(k), u(k))$ is the modeling uncertainty, $f(y(k), u(k))$ is the fault dynamics, and $\Pi(k-T)$, a $n \times n$ square matrix function representing the time profiles of the fault.

A system fault typically changes the parameters of the system or its dynamics which is expressed as a nonlinear function of the output and input. It is important to note that (1) does not address sensor faults. The time profiles of the incipient faults are modeled by [23]

$$\Pi(k-T) = diag(\Omega_1(k-T), \Omega_2(k-T), ..., \Omega_n(k-T))$$

where

$$\Omega_i(\tau) = \begin{cases} 0 \text{ if } \tau < 0 \\ 1 - e^{-\kappa_i \tau}, \text{ if } \tau \geq 0 \end{cases} \quad i=1, 2 \ldots n \tag{2}$$

with $\kappa_i > 0$ is an unknown constant that represents the rate at which the fault in the state x_i occurs. For large values of κ_i, the time profile function $\Omega_i(\tau)$ approaches a step function to model an abrupt fault. In this paper, we address only abrupt faults.

Remark 1: Modeling of faults using time profile is commonly found in the fault detection literature [25], and is used extensively by researchers [1, 3, 7, 20, 23, 24].

Next, throughout this paper, we make the following assumptions.

Assumption 1: Initial state of the system is known, i.e., $x(0) = x_0$.

Assumption 2: The state and the inputs are bounded before and after the fault, a standard assumption often made in the literature [7].

Assumption 3: The nominal system is assumed to be observable [24] in some domain of interest.

Assumption 4: The modeling uncertainty is unstructured and bounded [7, 24], i.e.,

$$\left\|\eta(x(k),u(k))\right\| \le \eta_0,\ \forall (x,u) \in (\chi \times U)$$

where there exists the compact sets $\chi \subset \Re^n$ and $U \subset \Re^m$, with $\eta_0 \ge 0$ a known constant.

During the past decade, many design schemes so called the robust fault diagnosis schemes have resulted in a variety of tools in continuous-time for dealing with modeling uncertainties [5]. In these robust detection schemes, when the system dynamics change above a predefined threshold, then a fault is declared [7, 20, 24]. On the other hand, another approach [5] attempts to decouple the effects of faults and modeling errors as a way of improving robustness. In the following section, a fault detection scheme is developed by using a mathematically derived threshold and OLAD. Subsequently, the parameter tuning scheme of the OLAD is utilized for prediction.

III. Fault Detection Scheme

The input-output system with fault under study uses the following nonlinear estimator given by

$$\hat{x}(k+1) = (A-KC)\hat{x}(k) + \zeta(y(k),u(k)) + Ky(k) + \hat{f}(y(k),u(k);\hat{\theta}(k)) - v(k)$$

$$\hat{y}(k) = C\hat{x}(k) \qquad (3)$$

with $\hat{x}(0) = x_0$, where $\hat{x} \in \Re^n$ is the estimated state vector, $\hat{y} \in \Re$ is the estimated output, $\hat{f}$ is

the OLAD, $\hat{\theta} \in \Re^q$ is a set of adjustable parameters, v is a robust term and would be defined later in the text, and K is a design constant, which is chosen such that $G = A - KC$ has all its eigenvalues within the unit disc. The initial value of the OLAD in (3) is selected such that $\hat{\theta}(0) = \hat{\theta}_0$, so that $\hat{f}(y, u, \hat{\theta}_0) = 0$ for all $y \in Y$ and $u \in U$. Given the initial conditions, the next step involves the development of an adaptive law for the parameter $\hat{\theta}(k)$, so that the OLAD $\hat{f}(y(k), u(k); \hat{\theta}(k))$ reconstructs the fault dynamics $f(y(k), u(k))$. An accurate modeling of the nonlinear discrete-time system would enable us to track any changes in the system dynamics and helps in the development of a robust fault detection algorithm.

Remark 2: Only upon detection of a fault, the OLAD and the robust term are initiated.

During the last few years, several online approximation based models have been studied primarily in continuous-time in the context of intelligent and learning control. In addition to conventional approximation models like polynomials, spline functions etc., various neural networks such as sigmoidal activation functions, radial basis functions, CMAC etc and others such as fuzzy logic systems and wavelets, have emerged. For the OLAD, y and u are considered as the input vectors, $\hat{\theta}(k)$ is the vector of adjustable parameters, and $\hat{f}(y, u; \hat{\theta})$ is the output. In this paper, we consider a general class of sufficiently smooth online approximators, $\hat{f} \in C^{\infty}$.

Next define the state estimation error as $e = x - \hat{x}$. Also define $e_o = y - C\hat{x}$ as the output estimation error or residual. Under the ideal conditions with no modeling errors, a fault is declared active whenever the output of the online approximator $\hat{f}(y(k), u(k); \hat{\theta}(k))$ and the residual becomes nonzero. An intuitive way of generating robustness with respect to

modeling uncertainties is to start the adaptation whenever the residual is above a certain threshold. This can be easily implemented by using a dead-zone operator $D[.]$, which is defined for improving the robustness of the fault detection scheme as

$$D[e_o(k)] = \begin{cases} 0, \text{ if } |e_{o(k)}| \le \varepsilon \\ e_o(k), \text{if } |e_{o(k)}| > \varepsilon \end{cases} \tag{4}$$

where $e_o(k)$ is the residual and $\varepsilon > 0$ is a design constant. The dead-zone size ε clearly provides a tradeoff between reducing the possibility of false alarms (robustness) and improving the sensitivity of the faults.

In the next section, ε is derived in terms of the modeling uncertainty bound (η_0), which guarantees robustness in the presence of modeling uncertainty. Based on the estimation model in (3) and the dead-zone in (4), the following parameter update law is proposed for tuning the OLAD

$$\hat{\theta}(k+1) = \hat{\theta}(k) + \alpha Z \, \mathrm{B}_0 \mathrm{D}[e_o(k)] - \gamma \left\| I - \alpha Z Z^T \right\| \hat{\theta}(k) \tag{5}$$

where $\alpha > 0$ the learning rate or adaptation gain, $0 < \gamma < 1$ is a design parameter, $\mathrm{B}_0 \in \Re^n$ is a constant vector, and Z is a $q \times n$ matrix defined as

$$Z = \left[\frac{\partial \hat{f}(y,u;\hat{\theta})}{\partial \hat{\theta}} \right]^T \tag{6}$$

The key advantage of the proposed parameter update law is the relaxation of parameter drift, a phenomenon that may occur with standard adaptive laws in the presence of approximation errors and due to the lack of the persistency of excitation (PE) of input signals. The last term is similar to e-modification in continuous-time adaptive

control. Next we define the robust term as

$$v(k) = \frac{B_1^T \hat{\theta}(k)}{\hat{\theta}^T(k) B_1 B_1^T \hat{\theta}(k) + c_m} \tag{7}$$

where $B_1 \in \Re^{q \times n}$ is a constant matrix and its selection is addressed later in the paper and $c_m > 0$ is a design constant. The performance of the parameter update law is shown mathematically by using Lyapunov theory in the next section.

Remark 3: In our earlier work [23], the authors have developed a nonlinear estimator for robust fault detection in dynamic systems with full state feedback. In the case of full state measurement with *n* states and *m* inputs, the input to the online approximator will be (*n*+*m*) whereas it is (*1*+*m*) for the proposed work. This has a major impact on the online approximator especially for linearly parameterized approximators since for high dimensional input spaces, the number of adjustable parameters needed to achieve a given approximation accuracy increases with the input dimension [2]. Therefore, the use of output sensor data instead of full state vector has obvious practical advantages similar to the case of continuous-time systems.

IV. Analytical Results

In this section, the robustness, the sensitivity, and the stability of the nonlinear fault detection scheme is rigorously examined. The robustness analysis deals with the investigation of the behavior of the OLAD in the presence of modeling uncertainties prior to the occurrence of any faults. The sensitivity analysis examines the behavior of the OLAD after the occurrence of the fault and characterizes the class of faults that can be

detected by the robust fault detection scheme. On the other hand, the stability analysis included in this section deals with the asymptotic convergence of the system signals, even after the fault occurrence.

In an ideal case, where there is no modeling errors and prior to the occurrence of a fault, i.e., $k \in [0, T)$, from (1) and (3), the state estimation error satisfy

$$e(k+1) = Ge(k) \tag{8}$$

Since G is a stable matrix, hence the stability follows trivially, i.e., $e \to 0$ as $k \to \infty$. Next, in the presence of modeling errors, (8) becomes

$$e(k+1) = Ge(k) + \eta(x(k), u(k)) \tag{9}$$

To determine an appropriate value for ε, we derive an upper bound for $e_o(k)$ prior to the fault. From (9), we have $e(k) = \sum_{j=0}^{k-1} G^{k-1-j} \eta(x(j), u(j))$. Hence the residual is given by $e_o(k) = \sum_{j=0}^{k-1} CG^{k-1-j} \eta(x(j), u(j))$. Since the matrix G is stable, there exist two positive constants μ and β_c such that (Frobenius norm) $\|G^k\| \le \beta_c \mu^k \le 1$. Therefore by using $\|C\| = 1$ [9], and taking $\beta = \beta_c \mu$, we get $|e_o(k)| \le \beta \eta_o \dfrac{(1-\mu^k)}{(1-\mu)}$. Thus we choose the size of the dead-zone $\varepsilon = \dfrac{\beta \eta_o}{(1-\mu)}$. Next to show the robustness of the proposed scheme (using equations (3), (4), (5), (9)), the following theorem is proposed.

Theorem 1 (Robustness): The robust nonlinear fault detection scheme described by (3), (4), (5) and (9) guarantees that $\hat{f}(y(k), u(k), \hat{\theta}(k)) = 0$, for $k \le T$ prior to the occurrence of the fault.

Proof: Let us assume that there exists a time k_r, $0 < k_r < T$, such that $|e_o(k)| < \varepsilon$ for $k < k_r$ and

$$|e_o(k_r)| = \varepsilon = \frac{\beta\eta_0}{(1-\mu)} \tag{10}$$

It is could be seen that the parameter $\hat{\theta}(k)$ has not adopted in the time interval $[0, k_r)$ by using (5) and the continuity of $e_o(k)$ [24]. Hence, in the time interval $[0, k_r)$ the state estimation error $e(k)$ satisfies

$$e(k+1) = Ge(k) + \eta(x(k), u(k)) \tag{11}$$

Therefore, in the interval $[0, k_r)$, the residual or the output estimation error is given by

$$e_o(k) = Ce(k) = C\left[\sum_{j=0}^{k-1} G^{k-1-j}\eta(x(j), u(j))\right]$$

By using $\|C\| = 1, \left\|\sum_{j=0}^{k-1} G^{k-1-j}\right\| \le \frac{\beta(1-\mu^k)}{(1-\mu)}$ and $\|\eta(x(k), u(k))\| \le \eta_0$, we get

$$|e_o(k)| \le \beta\eta_o \frac{(1-\mu^k)}{(1-\mu)} = \varepsilon(1-\mu^k).$$

Hence, $|e_o(k)| \le \varepsilon(1-\mu^k)$ for all $k \in [0, k_r)$ Thus by using the continuity of $e_o(k)$ we obtain that $|e_o(k_r)| < \varepsilon$, which contradicts our assumption in (10). In other words, the residual remains within the dead-zone and the output of the OLAD remains zero.

Remark 4: The proof of the theorem is quite analogous to the continuous-time case [24].

Next after the occurrence of the fault at $k \geq T$, by using equations (3) and (4), the state estimation error satisfies

$$e(k+1) = Ge(k) + \eta(x(k), u(k)) + \Pi(k-T) f(y(k), u(k)) - \hat{f}(y(k), u(k); \hat{\theta}(k)) + v(k)$$

$$= Ge(k) + \eta(x(k), u(k)) + \Pi(k-T) \hat{f}(y(k), u(k), \theta)$$

$$- \hat{f}(y(k), u(k); \hat{\theta}(k)) + \varepsilon(k) + v(k)$$

where the approximation error is given by $\varepsilon(k) = \Pi(k-T)[f(y(k), u(k)) - \hat{f}(y(k), u(k), \theta)]$ and θ is an optimal value chosen such that it minimizes the L_2 norm distance between $\hat{f}(y, u; \hat{\theta})$ and $f(y, u)$ for all (y, u) in some compact domain $Y \times U$. Also θ is constrained to a compact set $w \subset \Re^q$. Based on the smooth assumptions on $\hat{f}(y, u, \hat{\theta})$ [7], further, the above defined error equation can be expressed as

$$e(k+1) = Ge(k) + \eta(x(k), u(k)) - [I - \Pi(k-T)]\hat{f}(y(k), u(k), \theta)$$

$$+ \frac{\partial \hat{f}(y, u; \hat{\theta})}{\partial \hat{\theta}} (\hat{\theta} - \theta) + \Delta(y, u; \hat{\theta}, \theta) + \varepsilon(k) + v(k) \qquad (12)$$

where $\Delta(y, u; \hat{\theta}, \theta) = -\hat{f}(y, u; \hat{\theta}) + \hat{f}(y, u, \theta) - \frac{\partial \hat{f}(y, u; \hat{\theta})}{\partial \hat{\theta}} (\hat{\theta} - \theta)$ with $\Delta(y, u; \hat{\theta}, \theta)$ represents the higher order terms of the Taylor series expansion of $\hat{f}(y, u; \hat{\theta})$ w.r.t to $\hat{\theta}$. Let $\tilde{\theta} = \theta - \hat{\theta}$ is the parameter estimation error, denote $\omega(k) = \Delta(y, u; \hat{\theta}, \theta) - [I - \Pi(k-T)]\hat{f}(y(k), u(k), \theta)$ $+\eta(x(k), u(k)) + \varepsilon(k)$, and $\Psi_1(k) = z^T(k)\tilde{\theta}(k)$, then the error equation (12) becomes

$$e(k+1) = Ge(k) + \Psi_1(k) + \omega(k) + v(k)$$

Now using the definition of the robust term from (7), we get

$$e(k+1) = Ge(k) + \Psi_1(k) + \omega(k) + \frac{B_1^T \hat{\theta}(k)}{\hat{\theta}^T(k) B_1 B_1^T \hat{\theta}(k) + c_m}$$

Add and subtract $\frac{\left(B_1^T \theta - C_1\right)}{\hat{\theta}^T(k) B_1 B_1^T \hat{\theta}(k) + c_m}$ in the above equation, where $C_1 \in \Re^n$ is a constant vector, to get

$$e(k+1) = Ge(k) + \Psi_1(k) + \omega(k) - \Psi_2(k) + \frac{\left(B_1^T \theta - C_1\right)}{\hat{\theta}^T(k) B_1 B_1^T \hat{\theta}(k) + c_m} \tag{13}$$

where $\Psi_2(k) = \frac{\left(B_1^T \tilde{\theta}(k) - C_1\right)}{\hat{\theta}^T(k) B_1 B_1^T \hat{\theta}(k) + c_m}$. Next we consider the sensitivity of the proposed fault detection scheme. The class of detectable fault is given by the sensitivity theorem and is shown below; this theorem is obtained under the worst-case detectable conditions [9].

Theorem 2 (Sensitivity): For some $k_d > 0$, if the fault dynamics $f(y(k), u(k))$ satisfies the following inequality

$$\left| \sum_{j=T}^{T+k_d-1} CG^{(T+k_d-1-j)} f(y(j), u(j)) \right| \geq (1+\beta_c)\varepsilon \tag{14}$$

Then the residual is given by $|e_o(T+k_d)| \geq \varepsilon$.

Proof: The state estimation error in the presence of a fault and prior to the OLAD adaptation is given by

$$e(k+1) = Ge(k) + \eta(x,u) + f(y,u)$$

Therefore, for $k > 0$, the residual is given by

$$e_o(T+k) = CG^k e(T) + \sum_{j=T}^{T+k-1} CG^{(T+k-1-j)}\eta(x(j),u(j)) + \sum_{j=T}^{T+k-1} CG^{(T+k-1-j)} f(y(j),u(j))$$

Using $|e_o(T)| < \frac{\beta\eta_0}{(1-\mu)}$, $\|G^k\| \le \beta_c \mu^k$ and the triangle inequality, we obtain

$$|e_0(T+k)| \ge -\frac{\beta\eta_0\beta_c\mu^k}{(1-\mu)} - \beta\eta_0\frac{(1-\mu^k)}{(1-\mu)} + \left|\sum_{j=T}^{T+k-1} CG^{(T+k-1-j)} f(y(j),u(j))\right|$$

$$\ge -\varepsilon\left[\beta_c\mu^k + (1-\mu^k)\right] + \left|\sum_{j=T}^{T+k-1} CG^{(T+k-1-j)} f(y(j),u(j))\right|$$

Using $\|C\| = 1, \|G^k\| \le \beta_c\mu^k \le 1$ and taking $k=0$, we obtain $\beta_c \le 1$. If $\beta_c = 1$, $\mu^k \le 1$ and also if there exists a time $k_d > 0$ and if the condition in (14) is satisfied then it can be concluded that $|e_0(T+k_d)| \ge \varepsilon$.

This theorem shows that the OLAD would start adapting, if $|e_0(T+k_d)| \ge \varepsilon$ and hence the output of the OLAD ($\hat{f}(y,u;\hat{\theta})$) becomes non-zero.

Remark 5: The above theorem characterizes the class of faults that are detectable by the robust nonlinear discrete-time fault detection scheme. Note that the left-hand side of (14) represents the fault function. Intuitively the sensitivity theorem states that if the magnitude of the fault function after some time k_d becomes greater than $(1+\beta_c)\varepsilon$, then such faults can be detected under worst-case detectability conditions. In other words, similar to the continuous-time case, the inequality (14) is a sufficient (but not necessary) condition for activating adaptation of the OLAD in the presence of any modeling

uncertainty satisfying Assumption 4.

One of the most important parameters in fault detection is the time interval between the occurrence of a fault and the detection of the fault which is referred to as fault detection time. The sensitivity theorem not only characterizes the class of faults but it also provides a measure of the detection time. In other words, the smallest k_d for which the inequality (14) holds is equal to the detection time under the worst case detectability conditions. Hence, k_d represents the maximum detection time over all allowable scenarios of modeling uncertainties.

Next the stability and performance of the fault detection scheme is examined. For the following results, it is taken that $|e_o(k)| > \varepsilon$. For a gradient-based tuning updates used in a fault detection scheme [1, 3] which cannot exactly reconstruct certain unknown parameters because of the presence of unmodeled nonlinearities or approximation errors, cannot be guaranteed to yield bounded estimates. Then the PE condition is required to guarantee boundedness of the parameter estimates. However, it is very difficult to guarantee or verify the PE. In the next theorem, improved parameter tuning schemes for the fault detection scheme is presented so that PE is not required.

Theorem 3 (Stability): (PE condition not required) let the initial conditions for the nonlinear estimator is bounded in a compact set $S \subset \Re^n$. In the event of a fault, the fault detection scheme guarantees robust stability in the presence of modeling and approximation errors, such that $e_o(k)$ and $\tilde{\theta}(k)$ are locally asymptotically stable.

Proof: Consider a Lyapunov candidate as

$$V = \frac{1}{5} e_o^2(k) + \frac{1}{3\alpha}[\tilde{\theta}^T(k)\tilde{\theta}(k)]$$

The first difference is given by

$$\Delta V = \underbrace{\frac{1}{5} e_o^2(k+1) - e_o^2(k)}_{\Delta V_1} + \underbrace{\frac{1}{3\alpha}[\tilde{\theta}^T(k+1)\tilde{\theta}(k+1) - \tilde{\theta}^T(k)\tilde{\theta}(k)]}_{\Delta V_2}$$

Consider the first term (ΔV_1) in the first difference ΔV and substituting $e_o = y - C\hat{x} = Cx - C\hat{x} = Ce$, using the error equation (13), and applying the Cauchy-Schwarz inequality ($(a_1 + a_2 + ... + a_n)^T . (a_1 + a_2 + ... + a_n)$

$\leq n.(a_1^T a_1 + a_2^T a_2 + ... + a_n^T a_n)$ gives us

$$\Delta V_1 \leq ((e^T(k) G^T C^T)^2 + (\Psi_1^T(k) C^T)^2 + (\omega^T(k) C^T)^2 + (\Psi_2^T(k) C^T)^2 + \left(\frac{\left(B_1^T \theta - C_1\right)^T C^T}{\left(\hat{\theta}^T(k) B_1 B_1^T \hat{\theta}(k) + c_m\right)^2} \right)^2 \Bigg] - \frac{1}{5}\left(Ce(k)\right)^2 \qquad (15)$$

Next, considering the second term (ΔV_2) in the first difference of the Lyapunov function ΔV

$$\Delta V_2 = \frac{1}{3\alpha}[\tilde{\theta}^T(k+1)\tilde{\theta}(k+1) - \tilde{\theta}^T(k)\tilde{\theta}(k)]$$

by using the parameter update law (5), applying the dead-zone operator in (4), and $\tilde{\theta} = \theta - \hat{\theta}$, one obtains

$$\Delta V_2 = \frac{1}{3\alpha}\Big\{\Big[(I - \gamma \left\| I - \alpha Z Z^T \right\| I)\tilde{\theta}(k) - \alpha Z \, \mathrm{B}_0 e_o(k) + \gamma \left\| I - \alpha Z Z^T \right\| \theta\Big]^T$$

$$\times \Big[(I - \gamma \left\| I - \alpha Z Z^T \right\| I)\tilde{\theta}(k) - \alpha Z \mathrm{B}_0 e_o(k) + \gamma \left\| I - \alpha Z Z^T \right\| \theta\Big] - \tilde{\theta}^T(k)\tilde{\theta}(k)\Big\}$$

Applying the Cauchy-Schwarz inequality $((a_1 + a_2 + ... + a_n)^T (a_1 + a_2 + ... + a_n)$

$\leq n.(a_1^T a_1 + a_2^T a_2 + ... + a_n^T a_n)$ in the above equation gives us

$$\Delta V_2 \leq \frac{1}{3\alpha}\left\{\left[3\tilde{\theta}^T(k)(I-\gamma\left\|I-\alpha ZZ^T\right\|I)(I-\gamma\left\|I-\alpha ZZ^T\right\|I)\tilde{\theta}(k)\right.\right.$$

$$\left.\left.+3\alpha^2 \mathrm{B}_0^{\mathrm{T}} Z^T e_o(k) Z \mathrm{B}_0 e_o(k) + 3\gamma^2\left\|I-\alpha ZZ^T\right\|^2 \theta^T\theta\right] - \tilde{\theta}^T(k)\tilde{\theta}(k)\right\}$$

In the above equation, performing some mathematical manipulations would result in the following equation

$$\Delta V_2 \leq \frac{2}{3\alpha}\tilde{\theta}^T(k)\tilde{\theta}(k) - \frac{2\gamma}{\alpha}\left\|I-\alpha ZZ^T\right\|\tilde{\theta}^T(k)\tilde{\theta}(k) + \frac{\gamma^2}{\alpha}\left\|I-\alpha ZZ^T\right\|^2 \tilde{\theta}^T(k)\tilde{\theta}(k)$$

$$+\alpha \mathrm{B}_0^{\mathrm{T}} Z^T Ce(k) Z \mathrm{B}_0 Ce(k) + \frac{\gamma^2}{\alpha}\left\|I-\alpha ZZ^T\right\|^2 \theta^T\theta \qquad (16)$$

Combining ΔV_1 from (15) and ΔV_2 from (16) results in the following equation

$$\Delta V \leq ((e^T(k)G^T C^T)^2 + (\Psi_1^T(k)C^T)^2 + (\omega^T(k)C^T)^2 + (\Psi_2^T(k)C^T)^2$$

$$\left.+\left(\frac{\left(B_1^T\theta - C_1\right)^T C^T}{\left(\hat{\theta}^T(k)B_1 B_1^T\hat{\theta}(k) + c_m\right)^2}\right)^2\right] - \frac{1}{5}\left(Ce(k)\right)^2 +$$

$$\frac{2}{3\alpha}\tilde{\theta}^T(k)\tilde{\theta}(k) - \frac{2\gamma}{\alpha}\left\|I-\alpha ZZ^T\right\|\tilde{\theta}^T(k)\tilde{\theta}(k) + \frac{\gamma^2}{\alpha}\left\|I-\alpha ZZ^T\right\|^2 \tilde{\theta}^T(k)\tilde{\theta}(k)$$

$$+\alpha \mathrm{B}_0^{\mathrm{T}} Z^T Ce(k) Z \mathrm{B}_0 Ce(k) + \frac{\gamma^2}{\alpha}\left\|I-\alpha ZZ^T\right\|^2 \theta^T\theta \qquad (17)$$

Next, we introduce the following Lemma

Lemma 1: The term $\omega(k)$ in (17) comprising of the approximation error and the basis function of the OLAD, is assumed to be upper bounded by a smooth nonlinear function of state estimation and parameter estimation errors [6, 11]

$$(\omega^T(k)C^T)^2 \le \varepsilon_M = \beta_0 + \beta_1 \left\|e(k)\right\|^2 + \beta_2 \left\|\tilde{\theta}(k)\right\|^2 + \beta_3 \left\|e(k)\right\| \left\|\tilde{\theta}(k)\right\|$$

where $\beta_0, \beta_1, \beta_2,$ and β_3 are computable positive constants.

Proof: Use some standard norm inequalities, Assumption 1, and the fact that the reconstruction error can be expanded as a function of the residual error and error in adaptive estimation parameters. The steps follow similar to the case in continuous-time in proving the boundedness for a NN controller [15].

Then taking the Frobenius norm and using lemma 1, equation (17) could be rewritten as

$$\Delta V \le -\left(\frac{1}{5} - G_{\max}^2 - \alpha B_{0_{\max}}^2 Z_{\max}^2 - \beta_1 - \beta_4\right)\left\|e(k)\right\|^2$$

$$-\left(\frac{2\gamma}{\alpha}\left\|I - \alpha ZZ^T\right\| - Z_{\max}^2 - 2B_{1_{\max}}^2 - \frac{2}{3\alpha} - \frac{\gamma^2}{\alpha}\left\|I - \alpha ZZ^T\right\|^2 - \beta_2 - \beta_4\right).$$

$$\left\|\tilde{\theta}(k)\right\|^2 + B_{1_{\max}}^2 \theta_{\max}^2 - 2B_{1_{\min}} \theta_{\min} C_{1_{\min}} + 2C_{1_{\max}}^2 + \frac{\gamma^2}{\alpha}\left\|I - \alpha ZZ^T\right\|^2 \theta_{\max}^2 + \beta_0 \qquad (18)$$

where $\theta_{\min} \le \left\|\theta\right\| \le \theta_{\max}$, $Z_{\min} \le \left\|Z\right\| \le Z_{\max}$, and $\beta_4 = \left(\beta_3 / 2\right)$.

Taking $B_{1_{\min}} = \dfrac{B_{1_{\max}}^2 \theta_{\max}^2 + 2C_{1_{\max}}^2 + \frac{\gamma^2}{\alpha}\left\|I - \alpha ZZ^T\right\|^2 \theta_{\max}^2 + \beta_0}{2\theta_{\min} C_{1_{\min}}}$

Using this definition in (18) results in the following equation

$$\Delta V \le -(\frac{1}{5} - G_{\max}^2 - \alpha B_{0_{\max}}^2 Z_{\max}^2 - \beta_1 - \beta_4)\left\|e(k)\right\|^2$$

$$-\left(\frac{2\gamma}{\alpha}\left\|I - \alpha ZZ^T\right\| - Z_{\max}^2 - 2B_{1_{\max}}^2 - \frac{2}{3\alpha} - \frac{\gamma^2}{\alpha}\left\|I - \alpha ZZ^T\right\|^2 - \beta_2 - \beta_4\right)\left\|\tilde{\theta}(k)\right\|^2$$

Hence in the above equation, $\Delta V < 0$ if we choose the following gains

$$B_{0_{\max}} = \frac{G_{\max}}{\sqrt{\alpha} Z_{\max}},\ G_{\max} \le \sqrt{\frac{\frac{1}{5} - \beta_1 - \beta_4}{2}},\ \beta_1 + \beta_4 < \frac{1}{5},\ \min(a) \le \gamma \le \frac{1}{\left\|I - \alpha ZZ^T\right\|},$$

$$a = \frac{1 \mp \sqrt{\frac{1}{3} - \alpha(Z_{\max}^2 + 2B_{1_{\max}}^2 + \beta_2 + \beta_4)}}{\left\|I - \alpha ZZ^T\right\|},\ \text{and}\ \alpha < 1.$$

Thus as long as the first difference $\Delta V < 0$ which indicates that the error signals are stable in the sense of Lyapunov. Additionally, in absence of measurement noise, $e_0(k) = Ce(k)$, hence $e_0(k)$ and $\tilde{\theta}(k)$ are bounded, provided $e_0(k_0)$ and $\tilde{\theta}(k_0)$ are bounded in a set *S*. Hence $e_0(k)$ and $\tilde{\theta}(k)$ converges asymptotically to zero.

Remark 6: From the above theorem, it is observed that by using the robust term and the lemma on the approximation error, we proved local asymptotic stability of the closed loop system.

Next we propose stability without using the robust term and also removing the lemma 1, thus we present the following corollary. In this corollary, we show that the FD scheme is only semi-globally uniformly ultimately bounded (SGUUB). Thus (13) without the robust term could be written as

$$e(k+1) = Ge(k) + \Psi(k) + \omega(k) \qquad (19)$$

where $\Psi(k) = Z^T(k)\tilde{\theta}(k)$ and $\omega(k) = \Delta(y,u;\hat{\theta},\theta) - [I - \Pi(k-T)]\hat{f}(y(k),u(k),\theta) + \eta(x(k),u(k)) + \varepsilon(k)$. Next the corollary on the stability is presented.

Corollary 1: Consider the hypothesis given in Theorem 3 with the robust term being removed. In the presence of bounded uncertainties and reconstruction or approximation errors, the output estimation error or residual $e_o(k)$ and the parameter estimation error $\tilde{\theta}(k)$ are SGUUB.

Proof: Consider a Lyapunov candidate as

$$V = \frac{1}{3}e_o^2(k) + \frac{1}{3\alpha}[\tilde{\theta}^T(k)\tilde{\theta}(k)]$$

The first difference is given by

$$\Delta V = \underbrace{\frac{1}{3}e_o^2(k+1) - e_o^2(k)}_{\Delta V_1} + \underbrace{\frac{1}{3\alpha}[\tilde{\theta}^T(k+1)\tilde{\theta}(k+1) - \tilde{\theta}^T(k)\tilde{\theta}(k)]}_{\Delta V_2}$$

Consider the first term (ΔV_1) in the first difference ΔV and substituting $e_o = y - C\hat{x} = Cx - C\hat{x} = Ce$, using the error equation (19), applying the Cauchy-Schwarz inequality ($(a_1 + a_2 + ... + a_n)^T(a_1 + a_2 + ... + a_n) \le n.(a_1^T a_1 + a_2^T a_2 + ... + a_n^T a_n)$) in the above equation gives us

$$\Delta V_1 \le \frac{2}{3}\left(CGe(k)\right)^2 + \left(C\Psi(k)\right)^2 + \left(C\omega(k)\right)^2 \qquad (20)$$

Next, considering the second term (ΔV_2) in the first difference of the Lyapunov function ΔV, we get

$$\Delta V_2 = \frac{1}{\alpha}[\tilde{\theta}^T(k+1)\tilde{\theta}(k+1) - \tilde{\theta}^T(k)\tilde{\theta}(k)]$$

by using the parameter update law (5), applying the dead-zone operator in (4), and

$\tilde{\theta} = \theta - \hat{\theta}$, one obtains

$$\Delta V_2 = \frac{1}{3\alpha}\left\{\left[(I - \gamma\left\|I - \alpha ZZ^T\right\| I)\tilde{\theta}(k) - \alpha Z\, \mathrm{B}_0 e_o(k) + \gamma\left\|I - \alpha ZZ^T\right\|\theta\right]^T\right.$$

$$\left.\times\left[(I - \gamma\left\|I - \alpha ZZ^T\right\| I)\tilde{\theta}(k) - \alpha Z\mathrm{B}_0 e_o(k) + \gamma\left\|I - \alpha ZZ^T\right\|\theta\right] - \tilde{\theta}^T(k)\tilde{\theta}(k)\right\}$$

Applying the Cauchy-Schwarz inequality

$((a_1 + a_2 + ... + a_n)^T(a_1 + a_2 + ... + a_n) \le n(a_1^T a_1 + a_2^T a_2 + ... + a_n^T a_n))$ in the above equation gives us

$$\Delta V_2 \le \frac{1}{3\alpha}\left\{\left[3\tilde{\theta}^T(k)(I - \gamma\left\|I - \alpha ZZ^T\right\| I)(I - \gamma\left\|I - \alpha ZZ^T\right\| I)\tilde{\theta}(k)\right.\right.$$

$$\left.\left.+3\alpha^2 \mathrm{B}_0^{\mathrm{T}} Z^T e_o(k) Z\mathrm{B}_0 e_o(k) + 3\gamma^2\left\|I - \alpha ZZ^T\right\|^2 \theta^T\theta\right] - \tilde{\theta}^T(k)\tilde{\theta}(k)\right\}$$

In the above equation, performing some mathematical manipulations would result in the following equation

$$\Delta V_2 \le \frac{2}{3\alpha}\tilde{\theta}^T(k)\tilde{\theta}(k) - \frac{2\gamma}{\alpha}\left\|I - \alpha ZZ^T\right\|\tilde{\theta}^T(k)\tilde{\theta}(k) + \frac{\gamma^2}{\alpha}\left\|I - \alpha ZZ^T\right\|^2\tilde{\theta}^T(k)\tilde{\theta}(k)$$

$$+\alpha \mathrm{B}_0^{\mathrm{T}} Z^T Ce(k) Z\mathrm{B}_0 Ce(k) + \frac{\gamma^2}{\alpha}\left\|I - \alpha ZZ^T\right\|^2\theta^T\theta \qquad (21)$$

Combining ΔV_1 from (20) and ΔV_2 from (21) results in the following equation

$$\Delta V \le \frac{2}{3}\left(CGe(k)\right)^2 + \left(C\Psi(k)\right)^2 + \left(C\omega(k)\right)^2 + \frac{2}{3\alpha}\tilde{\theta}^T(k)\tilde{\theta}(k)$$

$$-\frac{2\gamma}{\alpha}\left\|I-\alpha ZZ^{T}\right\|\tilde{\theta}^{T}(k)\tilde{\theta}(k)+\frac{\gamma^{2}}{\alpha}\left\|I-\alpha ZZ^{T}\right\|^{2}\tilde{\theta}^{T}(k)\tilde{\theta}(k)$$

$$+\alpha \mathrm{B}_{0}^{\mathrm{T}}Z^{T}Ce(k)Z\mathrm{B}_{0}Ce(k)+\frac{\gamma^{2}}{\alpha}\left\|I-\alpha ZZ^{T}\right\|^{2}\theta^{T}\theta$$

Applying Frobenius norm in the above equation gives us

$$\Delta V \le -(\frac{1}{3}-G_{\max}^{2}-\alpha B_{0_{\max}}^{2}Z_{\max}^{2})\left\|e(k)\right\|^{2}$$

$$-\left(\frac{2\gamma}{\alpha}\left\|I-\alpha ZZ^{T}\right\|-Z_{\max}^{2}-\frac{2}{3\alpha}-\frac{\gamma^{2}}{\alpha}\left\|I-\alpha ZZ^{T}\right\|^{2}\right)\left\|\tilde{\theta}(k)\right\|^{2}+D_{M}^{2}$$

where $D_{M}^{2}=\omega_{\max}^{2}+\frac{\gamma^{2}}{\alpha}\left\|I-\alpha ZZ^{T}\right\|^{2}\theta_{\max}^{2}$, $\left\|\omega(k)\right\|\le\omega_{\max}$. Then $\Delta V\le 0$ as long as the following conditions hold

$$\left\|e(k)\right\|\ge\frac{D_{M}}{\sqrt{\left(\frac{1}{3}-G_{\max}^{2}-\alpha B_{0_{\max}}^{2}Z_{\max}^{2}\right)}}\ \text{or}\ \left\|\tilde{\theta}(k)\right\|\ge\frac{D_{M}}{\sqrt{\left(\frac{2\gamma}{\alpha}\left\|I-\alpha ZZ^{T}\right\|-Z_{\max}^{2}-\frac{2}{3\alpha}-\frac{\gamma^{2}}{\alpha}\left\|I-\alpha ZZ^{T}\right\|^{2}\right)}}$$

also $B_{0_{\max}}=\frac{G_{\max}}{\sqrt{\alpha}Z_{\max}}$, $G_{\max}\le 0.408$, $b=\frac{1\mp\sqrt{\frac{1}{3}-\alpha Z_{\max}^{2}}}{\left\|I-\alpha ZZ^{T}\right\|}$,

$\min(b)\le\gamma\le\frac{1}{\left\|I-\alpha ZZ^{T}\right\|}$, $Z_{\max}<0.577$, and $\alpha<1$. (22)

Therefore, $\Delta V\le 0$ and it can be concluded that the residual or output estimation error $e_{o}(k)$ and the parameter estimation error $\tilde{\theta}(k)$ are SGUUB.

Remarks 7: It is important to note that in the above two theorems (Theorem 3 and Corollary 1) the requirement of the PE condition and certainty equivalence (CE) assumption are relaxed for the adaptive estimator, in contrast to standard work in discrete-time adaptive control [13]. In the latter, two separate Lyapunov functions are considered to show the bound on the state estimation error and the parameter estimation error [13, 23]. By contrast in our proof, the residual, $e_o(k)$ and the parameter estimation errors $\tilde{\theta}(k)$ are combined in one Lyapunov function. Hence the proof is exceedingly complex due to the presence of several different variables. However, it obviates the need for the CE assumption and it allows parameter-tuning algorithms to be derived during the proof, not selected a priori in an ad hoc manner.

Remark 8: The parameter updating rule (5) is a nonstandard scheme that was derived from Lyapunov analysis and does include an extra term referred to as discrete-time ε-mod [13], which is normally used to provide robustness due to the coupling in the proof between the residual and the parameter estimation error terms. The Lyapunov proof shows that the term is necessary. Unless the term is utilized, the time to failure cannot be derived.

In this section we presented the robustness, sensitivity, and the stability of the proposed FD scheme. Additionally, two different stability results were obtained, i.e., asymptotic stability and SGUUB under certain conditions. In the next section, we would introduce a new method of predicting TTF.

V. Prediction Scheme

The interest of most modern industrial maintenance is to predict impending faults and alert the concerned maintenance personal by predicting the TTF so that the failing component or system can be replaced thus avoiding any catastrophic failure. The prognosis scheme will help out in this regard so that costs can be controlled due to failures. Though it is usually difficult to predict failure, TTF can be approximately obtained by predicting time to limit, In other words, systems parameters are monitored with fault and the TTF is obtained by projecting the time at which the value of the parameters reach their maximum limit usually set by a designer. The maximum limit could be the value up to which the system could perform it's intend task or operation safely. In general for most physical systems, the system parameters could be related to physical parameters. Hence in the event of a fault, the parameters may tend to increase or decrease depending on the fault characteristics.

To predict the TTF by using the parameter update law in (5), we propose the following theorem. In this theorem, we show that an explicit mathematical formula could be derived to predict the TTF. Before proceeding any further, we make the following assumption.

Assumption 5: The parameter $\hat{\theta}(k)$ is an estimate of the actual system parameter.

Remark 9: This assumption is satisfied when a system can be expressed as linear in the unknown parameters (LIP). For example in a mass damper system or civil infrastructure such as a bridge, the mass, damping and spring constants can be expressed as unknown parameters. Hence in the event of a fault, we assume that system parameters change and

tend to reach their limits defined by the designer. When any one of the parameters exceeds its limit, it is considered unsafe to operate. TTF will be defined as the time that the first parameter reaches its maximum limit. Here the TTF analysis can be done with lower limits as well.

Theorem 4 (Time to failure): Assume that the parameter update law can be treated time invariant during the time interval *k* and *k+1* and consider system (1) can be expressed as LIP, the TTF for the i^{th} system parameter could be iteratively determined by solving

$$k_{f_i} = \frac{\left| \log\left(\left| \frac{\left(\gamma \left\| I - \alpha z z^T \right\| \theta_{i_{\max}} - \alpha \sum_{j=1}^{n} z_{ij} B_{0_j} e_0 \right)}{\left(\gamma \left\| I - \alpha z z^T \right\| \theta_{i_0} - \alpha \sum_{j=1}^{n} z_{ij} B_{0_j} e_0 \right)} \right| \right) \right|}{\left| \log(1 - \gamma \left\| I - \alpha z z^T \right\|) \right|} + k_{0_i} \tag{23}$$

where k_{f_i} is the TTF, k_{0_i} is the time instant when the prediction starts (starts at k_d and incremented with time), $\theta_{i_{\max}}$ is the maximum value of the system parameter, and θ_{i_0} is the value of the system parameter at the time instant k_{0_i}.

Remark 10: The mathematical equation (23) is derived for the i^{th} system parameter. In general for a given system, the TTF would be $k_{ft} = \min(k_{f_i}), i = 1, 2, ...l$, where l the number of system parameters. This also implies that for a fault that is occurring in the system, the TTF is obtained as the time that the first parameter reaches its limit.

Proof: In general for any system satisfying *Assumption 5*, the maximum value of the system parameter in the event of a fault is determined via physical limitation. Hence we take $\hat{\theta}_i(k_{f_i}) = \theta_{i_{\max}}$. Note that the equation (23) holds only in the time interval $k \in [k_d, k_f]$

when the residual and other terms are held constant at each k. Thus the values of Z and e_0 are known and would be held fixed for the k^{th} time instant. Under the assumption, the parameter update law shown in (5) could be written as

$$\hat{\theta}(m+1) = (I - \gamma \left\| I - \alpha Z Z^T \right\| I)\hat{\theta}(m) + \alpha Z\, B_0 e_0$$

where we use *m* as the time index to simplify the understanding of the theorem, and the above defined equation could be written as

$$\overline{x}(m+1) = \overline{A}.\overline{x}(m) + \overline{B}.\overline{u} \tag{24}$$

where $\overline{x}(m+1) = \hat{\theta}(m+1)$, $\overline{A} = (I - \gamma \left\| I - \alpha Z Z^T \right\| I)$ is a diagonal matrix, $\overline{x}(m) = \hat{\theta}(m)$, and $\overline{B} = \alpha$, and $\overline{u} = Z\, B_0 e_0$. Since the above defined $\overline{A}$ matrix is diagonal, (24) could be written as

$$\overline{x_i}(m+1) = \overline{a_{ii}}\,\overline{x_i}(m) + \overline{b_i}\,\overline{u_i} \tag{25}$$

where $\overline{a_{ii}} = 1 - \gamma \left\| I - \alpha Z Z^T \right\|$, $\overline{b_i} = \alpha$, and $\overline{u_i} = \sum_{j=1}^{n} z_{ij} B_{0_j} e_0$ with the elements of input being constant between the time instant *k* and *k+1*.

Solving (25) to determine TTF using [4], we get

$$\overline{x_i}(m) = \overline{a_{ii}}^{(m-m_0)}\overline{x_i}(m_0) + \sum_{j=m_0+1}^{m} \overline{b_i}\,\overline{a_{ii}}^{(m-j)}\overline{u_i} \tag{26}$$

Since at a given instance k, u_i is time-invariant in (26), thus the above equation becomes

$$\overline{x_i}(m) = \overline{a_{ii}}^{(m-m_0)}\overline{x_i}(m_0) + \overline{b_i}\,\overline{u_i} \sum_{j=m_0+1}^{m} \overline{a_{ii}}^{(m-m_0)}$$

Now using results of geometric series, the above equation could be written as

$$\overline{x_i}(m) = \overline{a_{ii}}^{(m-m_0)}\overline{x_i}(m_0) + \overline{b_i}\,\overline{u_i}\left(\frac{1-\overline{a_{ii}}^{m-m_0}}{1-\overline{a_{ii}}}\right)$$

After performing some simple mathematical manipulation, one obtains

$$\overline{a_{ii}}^{m-m_0} = \frac{[\overline{x_i}(m)(1-\overline{a_{ii}}) - \overline{b_i}\,\overline{u_i}]}{[\overline{x_i}(m_0)(1-\overline{a_{ii}}) - \overline{b_i}\,\overline{u_i}]}$$

Since $0 < \overline{a_{ii}} < 1$, take absolute value and logarithm on both sides and apply again the absolute operator to get

$$m = \frac{\left|\log\left(\left|\frac{\overline{x_i}(m)(1-\overline{a_{ii}}) - \overline{b_i}\,\overline{u_i}}{\overline{x_i}(m_0)(1-\overline{a_{ii}}) - \overline{b_i}\,\overline{u_i}}\right|\right)\right|}{\left|\log(\overline{a_{ii}})\right|} + m_0$$

Next we take $m = k_{f_i}$, and $m_0 = k_{0_i}$. Additionally, we have

$\overline{x_i}(m) = \overline{x_i}(k_{f_i}) = \theta_{i_{\max}}$, $\overline{x_i}(m_0) = \overline{x_i}(k_{0_i}) = \theta_{i_0}$, and we know that $\overline{a_{ii}} = 1 - \gamma\left\|I - \alpha ZZ^T\right\|$, $\overline{b_i} = \alpha$, and $\overline{u_i} = \sum_{j=1}^{n} z_{ij} B_{0_j} e_0$. Thus, we get equation (23). Hence completes the proof.

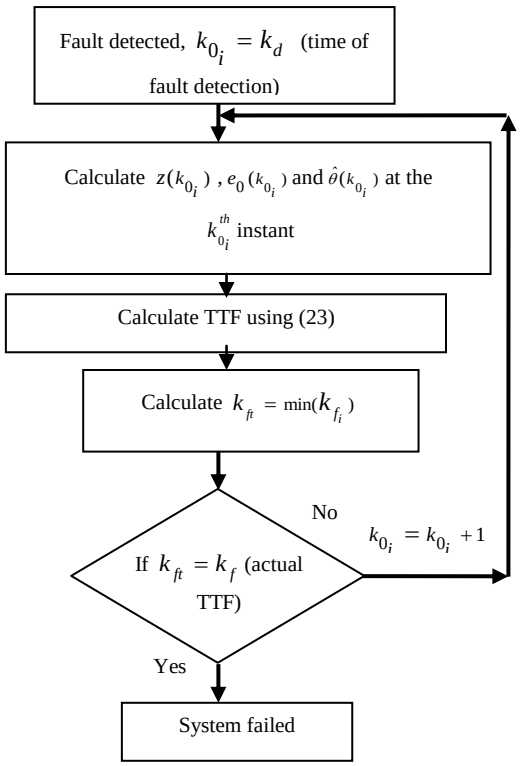

Figure 1: Procedure to iteratively update the TTF.

After fault detection, (23) is utilized iteratively to obtain TTF in the time interval $k \in [k_d, k_f]$. To better understand the idea of updating the TTF, refer to the flowchart in Fig. 1. From the flowchart, upon detecting the fault, at each time instance, $z(k)$, $\hat{\theta}(k)$ and $e_0(k)$ are calculated. Then TTF is estimated by using (23), as the parameter $\hat{\theta}(k) \to \theta_{\max}$ as $k \to k_f$. This iterative procedure allows one to accurately assess the TTF at every time instant more accurately when compared to probabilistic methods [21], where the change in the direction of the fault parameter is not known.

Next, the performance of the developed FDP scheme is simulated onto an application. The details of the simulation are given in the next section.

VI. Simulation Results

In this section the FDP scheme is simulated with a magnetic suspension system. The performance of the FDP scheme is shown with and without system uncertainty and measurement noise. The learning capability of the OLAD is also presented for the chosen example.

A. Fault Detection Scheme

To begin with, first we analyze the performance of the fault detection scheme. A simplified discrete time state space representation of a magnetic suspension system is given below [14]

$$x_1(k+1) = T_S x_2(k) + x_1(k) + \eta_1(x(k), u(k))$$

$$x_2(k+1) = T_S \left\{ \frac{1}{m}\left(-k_1 x_2(k) + 9.8 + f(y(k)) + F\right) \right\} + x_2(k)$$

$$y(k) = x_2(k) \tag{27}$$

where x_1 and x_2 are the system states, F is the input for the system in (27) and for the estimator in (28) which is taken as $F = 5\sin(kT_s)$. A fault induced by changing the coil resistance in a nonlinear fashion by simply adding it to the system in (27) using $f(y(k))$. The following nonlinear estimator is used to study the system described in (27)

$$\hat{x}_1(k+1) = T_s x_2(k) + x_1(k) + a_1 \hat{x}_2(k) + a_3 \hat{x}_1(k) + a_2 x_2(k)$$

$$\hat{x}_2(k+1) = T_s \left\{ \frac{1}{m} \left(-k_1 x_2(k) + 9.8 + F \right) \right\} + x_2(k) + \hat{f}(y(k), \hat{\theta}(k))$$

$$\hat{y}(k) = \hat{x}_2(k) \tag{28}$$

where $\hat{x}_1$ and $\hat{x}_2$ are the estimated states of the system in (27), and $\hat{f}(y(k), \hat{\theta}(k))$ is the OLAD. For this simulation, the OLAD is chosen to be a single layer sigmoid function network with sixteen neurons, and the initial weights of the network ($\hat{\theta}$) are chosen randomly. The system is simulated with an abrupt fault that occurs at $T = 15$ seconds and is given by

$$\Pi(k-T) f(y(k)) = \{5 \sin(0.01 y(k)), \textit{if } k \geq 15, \textit{else } 0 \textit{ if } k \leq 15\}$$

The parameter values for the actual system (27) and the estimator (28) are taken as follows $m = 1$, $k_1 = 0.5$, $a_1 = 0.0005$, $a_2 = 0.00005$, $a_3 = 0.009$, $a_4 = -0.5$, $a_5 = 0.000005$, $x_1(0) = 0$, $x_2(0) = 0$, $\hat{x}_1(0) = 0$, $\hat{x}_2(0) = 0$, and $T_S = 0.01$. In this simulation we present two different scenarios, where in the first scenario, it is assumed that no system uncertainty (i.e., $\eta_1(x(k), u(k)) = 0$) is present with no measurement noise and in the second scenario, a fixed system uncertainty and a measurement noise of Gaussian type is considered. For both the scenarios, to tune the OLAD, the parameter update law (5) is employed. The learning rate and the design constant in (5) are taken randomly as $\alpha = 0.03$ and $\gamma = 0.001$ respectively. The simulation results for the first scenario are shown in Figs. 2 and 3. Figure 2 shows the absolute value of the residual under normal operation wherein the residual appears to be zero. However, during a fault, this residual will increase above zero indicating the presence of a fault and by initiating the OLAD.

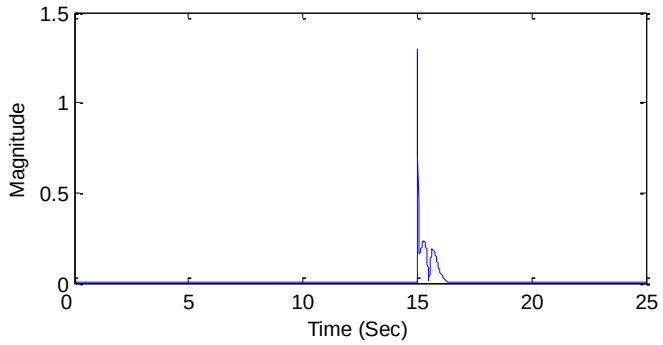

Figure 2: Absolute value of the residual.

Figure 3 shows the evolution of the fault term and the OLAD response. From this figure, it could be observed that the chosen OLAD learns the occurring fault dynamics satisfactorily. Such online fault estimates are useful for fault isolation. To study the robustness of the scheme, we introduce a fixed system uncertainty, i.e., $\eta_1(x(k), u(k)) = 0.5$ and a measurement noise of Gaussian type with a maximum amplitude of 0.02.

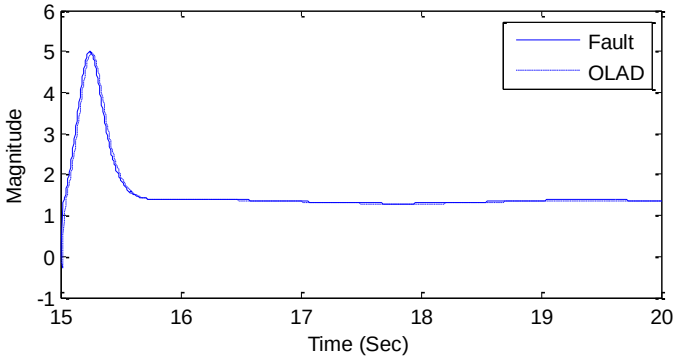

Figure 3: Evolution of the actual fault term ($f(y)$) and OLAD ($\hat{f}(y, \hat{\theta})$) response.

The simulation results for this scenario are shown in Figs. 4 and 5 wherein the absolute value of the residual is illustrated in Fig. 4 and due to the presence of the modeling uncertainty, to improve robustness, a threshold is introduced. A fixed threshold of 0.1 is considered as observed in Fig. 4. The threshold is chosen based on the procedure developed in Section IV, where $\varepsilon = \dfrac{\beta\eta_0}{(1-\mu)}$ and solving this equation using $\eta_0 = 0.5$, $\mu = 0.9$ and $\beta_c = 0.2$, to get $\beta = 0.18$ and $\varepsilon = 0.1$. A fault is detected when the residual exceeds the threshold, which is verified as seen in Fig. 4.

Figure 5 shows the performance of the OLAD during the fault in the presence of the system uncertainty and the measurement noise. Additionally from the figure, it could be seen that the learning of the fault dynamics by the OLAD appears to be highly satisfactory. An important point to be considered here is the selection of the design parameters, size and OLAD activation functions were kept unchanged from the previous simulation. Hence even in the presence of the uncertainty and noise, the performance of the fault detection scheme is not compromised.

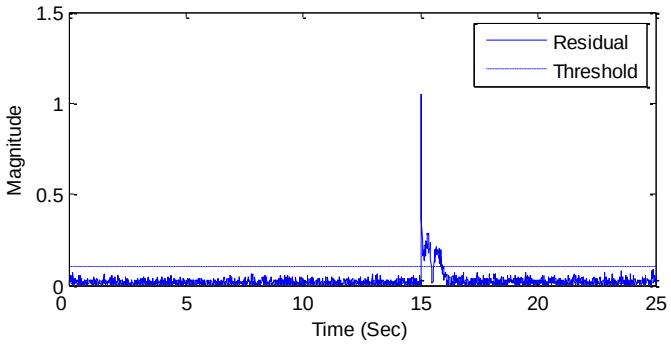

Figure 4: Absolute value of the residual and the fault detection threshold.

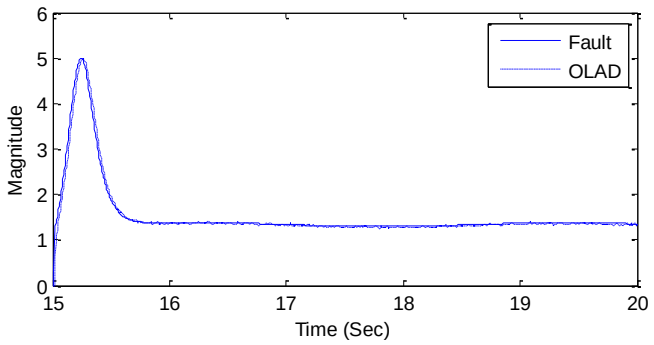

Figure 5: Evolution of the fault ($f(y)$) and OLAD ($\hat{f}(y,\hat{\theta})$) response in the presence of the system uncertainty and the measurement noise.

Thus, from the above simulation results, the robustness and the performance of the proposed fault detection scheme, and its learning capabilities of the OLAD were demonstrated. The scheme is able to learn online any type of unknown nonlinear faults, which is an inherent advantage. Although in this simulation, the system considered having abrupt faults, but still the fault detection scheme would be able to capture a wide range of fault conditions, which is evident from the mathematical results as seen in the previous section. This makes the OLAD based approach better than other quantitative or qualitative based methods [5, 10]. Next we illustrate the working of the prognostics scheme, where we assume the same type of fault, i.e., nonlinear change in coil resistance.

B. Prediction Scheme

For this simulation, a change in coil resistance in the form $f(y(k)) = 5\sin(0.01y(k))$ is considered at the 10^{th} second of operation in (1) and the prognostics scheme is now demonstrated. By using the procedure outlined in Section V, we determine the TTF. The spring constant (k_1) is considered to be unknown. Next, the parameter update law (5) is utilized to estimate the unknown system parameter. The learning rate and the design

constant in (5) are chosen as $\alpha = 0.35$, $\gamma = 0.0011$, respectively. The estimated system parameter is compared with the actual system parameter by defining a maximum acceptable limit (usually using safety limit) as shown in Fig. 6. As the fault continues to grow, the actual parameter tends to increase approaching the maximum defined parameter threshold value of 30. This value was chosen randomly to demonstrate the working of the proposed prediction scheme.

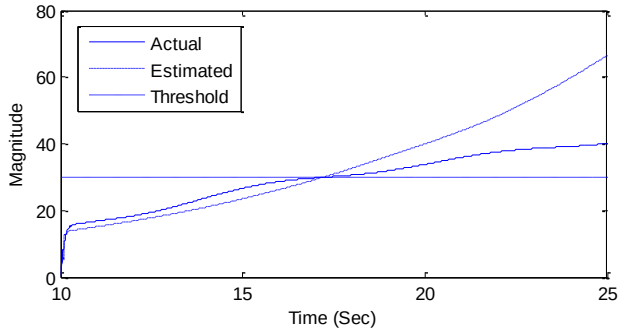

Figure 6: Comparison between the estimated and the actual system parameter, and also shown the safe threshold.

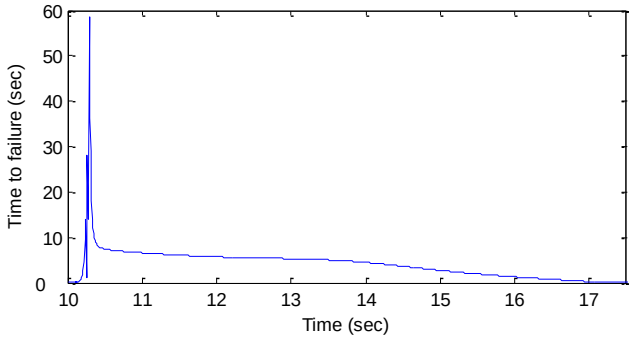

Figure 7: Prediction of TTF after the occurrence of the fault.

From the procedure outlined in the flowchart in Fig. 1, the TTF is estimated at each time instant after the occurrence of the fault and is shown in Fig. 7. From the figure, after the first prediction of TTF, for few seconds the prediction seems to increase, this could possibly be due to the random selection of the gains of the parameter update law in (5) which needs some time to converge. However the prediction of TTF improves as the scheme learns the change in the system dynamics and converges to the actual time of failure of 17.27 seconds. This could also be observed in Fig. 7, where the TTF decreases as the system parameter approaches the threshold.

Hence with the chosen example, the working of the FDP scheme was illustrated. The simulation results show promising performance of the proposed FDP scheme. Additionally, the robustness of the scheme was also studied by introducing uncertainty and measurement noise in the simulation results.

VII. Conclusion and Future Work

In this paper, we have shown a FDP algorithm for nonlinear discrete time system with input and output measurements. The scheme was developed based on the assumptions that the states and the input being bounded before and after the fault. The scheme also addressed the prediction of TTF. Further more it is assumed that not all the states of the system are available for measurement. A detailed mathematical analysis and the simulation results show the robustness and performance of the proposed FDP scheme. Further based on the proofs, it was seen that the proposed scheme could be used as a robust FDP scheme for nonlinear discrete time input-output systems. Future work

involves with developing fault isolation and fault accommodation techniques for a nonlinear discrete time input-output systems.

References

[1] G. Antonelli, F. Caccavale, and L. Villani,"Adaptive discrete-time fault diagnosis for a class of nonlinear systems: application to a mechanical manipulator," 2003 *IEEE International Symposium on Intelligent Control*, Oct. 5-8, 2003, Houston, TX, USA, pp. 667-672.

[2] A. R. Barron,"Universal approximation bounds for superpositions of a sigmoidal function," *IEEE Transaction on Information Theory*, vol. 39, no. 3, pp. 930-945, 1993.

[3] F. Caccavale and L. Villani,"An Adaptive Observer for Fault Diagnosis in Nonlinear Discrete-Time Systems," *Proceeding of the 2004 American Control Conference*, Boston, MA, June 30 -July 2, 2004.

[4] C. T. Chen, *Linear System Theory and Design*, 3rd Ed., Oxford University Press, New York, 1999.

[5] J. Chen and R. J. Patton, *Robust Model-based Fault Diagnosis for Dynamic Systems*, Kluwer Academic publishers, MA, USA, 1999.

[6] D. M. Dawson, Z. Qu, and S. Lim,"Re- thinking the robust control of robot manipulators," *Proc. of the 30th Conference on Decision and Control (CDC),* Dec., Brighton, England, pp. 1043-1045, 1991.

[7] M. A. Demetriou and M. M. Polycarpou,"Incipient fault diagnosis of dynamical systems using online approximators," *IEEE Transactions on Automatic Control*, vol. 43, no. 11, pp. 1612-1617, 1998.

[8] J. A. Farrell and M. M Polycarpou, *Adaptive Approximation based Control-Unifying Neural, Fuzzy and Traditional Adaptive Approximation Approaches*, Wiley Interscience, NJ, USA, 2006.

[9] P. M. Frank and L. Keller,"Fault diagnosis in dynamic systems using analytical and knowledge-based redundancy– A survey and some new results," *Automatica*, vol. 26, pp. 459-474, 1990.

[10] J. Gertler,"Survey of model-based failure detection and isolation in complex plants," *IEEE Contr. Syst. Mag.*, vol. 8, pp. 3-11, 1988.

[11] T. Hayakawa, W. M. Haddad, and N. Hovakimyan,"Neural network adaptive control for a class of nonlinear uncertain dynamical systems with asymptotic stability guarantees," *IEEE Transactions on Neural Networks*, vol. 19, no. 1, pp. 80-89, 2008.

[12] S. Jagannathan, *Neural Network Control of Nonlinear Discrete–Time Systems*, CRC publications, NY, 2006.

[13] S. Jagannathan and F. L. Lewis,"Robust implicit self-tuning regulators," *Automatica*, vol. 32, no. 12, pp. 1629-1644, 1996.

[14] H. K. Khalil, *Nonlinear systems 3rd ed.*, Prentice Hall, NJ, USA, 2002.

[15] F. L. Lewis, S. Jagannathan, and A. Yesilderek,"*Neural network control of robotics and nonlinear systems*," Taylor and Francis, UK, 1999.

[16] J. Luo, A. Bixby, K. Pattipati, L. Qiao, M. Kawamoto, and S. Chigusa,"An interacting multiple model approach to model-based prognostics," *IEEE International Conference on Systems, Man and Cybernetics*, Washington, D.C., USA, vol. 1, pp. 189-194, 2003.

[17] J. Luo, M. Namburu, K. Pattipati, L. Qiao, M. Kawamoto, and S, Chigusa,"Model-based prognostic techniques," *AUTOTESTCON 2003: IEEE Systems Readiness Technology Conference*, 22-25 Sept., Anaheim, California, USA, pp. 330-340, 2003.

[18] A. Mathur, S. Deb, and K. R. Pattipati,"Modeling and real-time diagnostics in TEAMS-RT," *Proceedings of the American Control Conference*, June, Philadelphia, PA, USA, pp.1610-1614, 1998.

[19] E. Phelps, P. Willett, and T. Kirubarajan,"Useful lifetime tracking via the IMM," *Components and System Diagnostics, Prognostics, and Health Management II, proceedings of SPIE*, vol. 4733, pp. 145-156, 2002.

[20] M. M. Polycarpou and A. J. Helmicki,"Automated fault detection and accommodation: a learning systems approach," *IEEE Transactions on Systems, Man, and Cybernetics*, vol. 25, no. 11, pp. 1447-1458, 1995.

[21] M. J. Roemer and D. M. Ghiocel,"A probabilistic approach to the diagnosis of gas turbine engine faults," *53rd Machinery Prevention Technologies (MFPT) Conference*, April, Virginia Beach, VA, USA , pp. 325-336, 1999.

[22] Y. Shao and K. Nezu,"Prognosis of remaining bearing life using neural networks," *Proceedings of the Institution of Mechanical Engineers, Part I: Journal of Systems and Control Engineering*, vol. 214, no. 3, pp. 217-230, 2000.

[23] B. T. Thumati and S. Jagannathan,"An online approximator-based fault detection framework for nonlinear discrete-time systems," *46th IEEE Conference on Decision and Control (CDC) 2007*, New Orleans, LA, USA, pp. 2608-2613, 2007.

[24] A. T. Vemuri and M. M. Polycarpou,"Robust nonlinear fault diagnosis in input-output system," *International Journal of Control*, Vol. 68, no. 2, pp. 343 – 360, 1997.

[25] J. Zhang and A. J. Morris,"On-line process fault diagnosis using fuzzy neural networks," *Intelligent systems engineering*, pp. 37-47, 1994.

[26] X. Zhang, M. Polycarpou, and T. Parsini,"A robust detection and isolation scheme for abrupt and incipient fault in nonlinear systems," *IEEE Transactions on Automatic Control*, vol. 47, no. 4, pp. 576-593, 2002.

3. A Model Based Fault Detection and Prediction Scheme for Nonlinear Multivariable Discrete-Time Systems With Asymptotic Stability Guarantees

Balaje T. Thumati and S. Jagannathan

***Abstract*— In this paper, a novel, unified model-based fault detection and prediction (FDP) scheme is developed for nonlinear multi-input and multi-output (MIMO) discrete-time systems. The proposed scheme addresses both state and output faults by considering separate time profiles. The faults, which could be incipient or abrupt, are modeled using input and output signals of the system. The fault detection scheme comprises of online approximator in discrete-time (OLAD) with a robust adaptive term. An output residual is generated by comparing the fault detection estimator output with that of the measured system output. A fault is detected when this output residual exceeds a predefined threshold. Upon detecting the fault, the robust adaptive terms and the OLADs are initiated wherein the OLADs approximates the unknown fault dynamics online while the robust adaptive terms help in ensuring asymptotic stability of the FD design. Using the OLAD outputs, a fault diagnosis scheme is introduced. A stable parameter update law is developed not only to tune the OLAD parameters but also to estimate the time-to-failure (TTF), which is considered as a first step for prognostics. The asymptotic stability of the FDP scheme enhances the detection and TTF accuracy.**

The effectiveness of the proposed approach is demonstrated using a fourth order

Research supported in part by NSF I/UCRC on Intelligent Maintenance Systems award. Contact author: bttr74@mst.edu

multi-input-multi-output satellite system.

***Keywords*—fault detection, prognostics, MIMO nonlinear discrete-time system, asymptotic stability.**

I. Introduction

Growing system complexity demands robust control schemes to mitigate system uncertainties and unknown disturbances. However, due to the high risk of component failures, reliable fault detection and prediction (FDP) schemes are normally required to guarantee safe operation even under the presence of system uncertainties. If the impending faults can be detected early through prediction, and via root cause analysis, prognostics can be performed.

Traditionally, a fault is detected by manual inspection, which in turn requires a knowledgeable operator. As a consequence, manual inspection is time consuming, offline and costly for highly complex industrial systems and therefore not well suited. Therefore, in order to minimize the increasing operating costs, researchers developed the prominent qualitative and quantitative fault detection techniques [1-2].

In the qualitative or data-driven schemes [2], experimental data are collected from the system and used for fault detection (FD). Previously reported data driven approaches [2] such as the immune system [3] require offline training and therefore do not have the online fault learning feature to approximate new faults. Moreover, generating data offline for each fault is time consuming and costly. By contrast, in the quantitative method, a model representative of the system is utilized for detecting faults. This model is typically derived from either first principles or borrowed from control scientists/engineers. The system model provides an estimate of the system states by observing the inputs and

measured outputs of the nonlinear system. A residual signal is then generated by comparing the output of the model with that of the system. A fault is detected in a robust manner even under system uncertainties when the residual deviates beyond a predefined threshold value. The selection of the threshold is a challenging task since an improper threshold selection might lead to false and missed alarms [1, 4-7]; however, several attempts have been made to address this issue [8-11] using analytical methods.

In previously suggested quantitative works [4, 5, 12], the FD techniques are developed by considering a linear representation of the nonlinear system. Other fault detection schemes use parity relations [1], geometric relationships [13, 14], observers or estimators [1, 4-7, 15]. On the other hand, FD schemes for linear stochastic system are reported in [16].

In the past decade, several quantitative methodology-based FD schemes, which include geometric [17, 18], and adaptive estimation [8-11, 19, 20] are introduced for nonlinear continuous-time systems while the authors in [21-24] use sliding mode observer or others [25, 26] use fuzzy based observers. In [27], FD schemes have been developed for robot manipulators. A compilation of FD schemes for hydraulic systems, flight control etc., are given in [28]. A recent survey [6] on model-based FD techniques presents an excellent overview of the state-of-the art developments.

A common issue that has been gaining interest is stability analysis using Lyapunov theory in the design of FD schemes [8-11, 14, 17-19, 29, 30]. However, the FD schemes [8-11, 19] render only uniform ultimate boundness (UUB) stability due to the presence of system uncertainties. However, in a recent work [31], asymptotic convergence of the

identification error in continuous-time is demonstrated for robot manipulators with actuator faults.

Another important feature in general unavailable in the previously reported schemes [8-36] is the time-to-failure determination (TTF) since TTF is the first step for prognostics assessment. While none of the Lyapunov-based schemes offer TTF [8-11, 19], certain TTF schemes in data-driven approaches [37-39], assumed a specific degradation model which has been found to be limited to the system or material type under consideration. Another scheme [40] employs a deterministic polynomial and a probabilistic method for prognosis by assuming that certain parameters are affected by the fault while others [41] use a black box approach using neural network (NN) on the failure data. All these schemes [37-41] while being data-driven address only TTF prediction, require offline training and do not offer performance guarantees. It is envisioned that a unified FDP scheme will be necessary to alert an impending failure and provide the remaining useful life.

On the other hand, implementation of the FD schemes using an embedded computer requires explicit discrete-time development since deriving a direct discrete-time equivalent of a continuous time scheme may cause stability issues [43]. However, due to the quadratic nature of first difference of the Lyapunov function, it is very hard to show stability [42] of the FD schemes in discrete-time. Therefore, limited FD schemes have been proposed in discrete-time [29, 33, 34, 43] out of which the ones proposed in [33, 34] consider nonlinear discrete-time systems with actuator faults and their stability is guaranteed only when persistency of excitation (PE) condition is satisfied. In our previous work [29], a novel FDP scheme is developed for nonlinear discrete-time systems with

state faults by relaxing the PE condition and assuming that all the states are measurable. By contrast, this assumption of state measurability is relaxed in this work in contrast with [8, 10, 11, 29, 33, 34, 43] for the proposed online-based FDP scheme while focusing on both state and output faults for a general class of nonlinear multi-input-multi-output (MIMO) discrete-time systems.

In this work, the state and output faults (sensor faults), which are incipient and abrupt in nature, are modeled as a nonlinear function of the inputs and measured outputs. These faults occur independently or simultaneously, and evolve at different rates while their time profiles are modeled by using exponential functions consistent with the literature [8-11]. A nonlinear fault detection estimator scheme, which is used to monitor and declare the presence of a fault in the nonlinear system, consists of an online approximator in discrete-time (OLAD) along with a robust adaptive term. One OLAD and a robust adaptive term are utilized to approximate the state faults whereas a second OLAD and another robust adaptive term for output faults. The robust adaptive terms use the corresponding parameters of the online approximators.

The fault detection (FD) estimator and the measured system outputs are utilized to generate an output residual which when compared against an analytically selected threshold will determine the presence of a fault. Upon detection, the unknown fault dynamics are approximated online using the appropriate OLADs. Subsequently, the detected fault is identified as a state or an output fault by asserting thresholds on the OLAD outputs. Due to presence of robust adaptive terms, the asymptotic stability of the proposed FDP scheme is demonstrated using Lyapunov theory in contrast with all other boundedness–based FD schemes [8-11, 17, 19, 29, 33, 34]. Asymptotic stability enables

accurate TTF determination since the parameter update law or state estimator will be utilized.

The TTF determination together with rigorous root cause or fault isolation will become prognostics. Therefore prognostics are relegated as part of future work. A mathematically derived TTF determination is presented using the developed parameter update law by projecting the current value to its limit provided the limiting parameter value is defined by the designer. This process is iteratively performed to continuously predict TTF up to the failure threshold beyond which the system is considered unsafe. For most practical systems, the unknown parameters could be tied to physical entities thus making the parameter-based TTF determination very useful. Alternatively, the state trajectories from the FD estimator can be utilized for TTF determination due to asymptotic convergence.

The contributions of this paper include an online fault detection and diagnosis scheme for multiple state or output faults for a class of nonlinear MIMO discrete-time systems using inputs and outputs, thus relaxing the need for state measurements. The scheme considers both incipient and abrupt, state and output faults. Unlike available adaptive estimation based fault detection schemes [8-11, 29, 33, 34, 43], asymptotic convergence of the state residual and the parameter estimation errors in discrete-time is demonstrated. In addition, by asserting suitable thresholds on the OLAD outputs, the declared fault is identified as a state or an output fault. Finally, an online parameter or state estimator-based TTF determination scheme is introduced.

The paper is organized as follows: Section II introduces the system under investigation whereas Section III presents the proposed fault detection scheme in detail. In

Section IV, the stability and performance of the fault detection scheme are introduced and Section V discusses the TTF determination. Finally, in Section VI, a fourth order MIMO satellite system is used to illustrate the performance of the proposed FDP scheme. Section VII presents some concluding remarks and discusses future work.

II. Problem Statement

The nonlinear MIMO discrete-time system under consideration is described by

$$x(k+1) = Ax(k) + \varphi_S(y(k), u(k)) + \eta_S(x(k), u(k)) + g_S(y(k), u(k))$$

$$y(k) = Cx(k) + \eta_y(x(k), u(k)) + g_y(u(k)) \quad (1)$$

where $x \in \Re^n$ represents state vector, $u \in \Re^m$ is the input vector, $y \in \Re^p$ denotes measurable system output, $\varphi_s : \Re^p \times \Re^m \to \Re^n$, $\eta_s : \Re^n \times \Re^m \to \Re^n$, $g_s : \Re^p \times \Re^m \to \Re^n$, $\eta_y : \Re^n \times \Re^m \to \Re^p$, $g_y : \Re^m \to \Re^p$ are smooth vector fields, $A \in \Re^{n \times n}$, and $C \in \Re^{p \times n}$ are known matrices. The system is assumed to be observable. The nonlinear function $\eta_S(x(k), u(k))$ represents the modeling uncertainties whereas $\eta_y(x(k), u(k))$ represents the sensor modeling uncertainties while $\varphi_S(y(k), u(k))$ represents known system dynamics. Moreover, $g_S(y(k), u(k)) = \Pi_S(k - T_s) f_S(y(k), u(k))$ represents the evolution of the nonlinear fault dynamics modeled in terms of the measurable inputs and outputs, whereas $g_y(u(k)) = \Pi_y(k - T_y) f_y(u(k))$ represents the nonlinear output fault dynamics modeled in terms of the input vector. The diagonal matrices $\Pi_s \in \Re^{n \times n}$ and $\Pi_y \in \Re^{p \times p}$ denote the time profiles of the state and output faults, which are given by

$$\Pi_s(k-T_s) = diag(\Omega_{s_1}(k-T_s), \Omega_{s_2}(k-T_s), ..., \Omega_{s_n}(k-T_s))$$

$$\Pi_y(k-T_y) = diag(\Omega_{y_1}(k-T_y), \Omega_{y_2}(k-T_y), ..., \Omega_{y_p}(k-T_y))$$

where

$$\Omega_{s_i}(k-T_s) = \begin{cases} 0 \text{ if } k < T_s \\ 1 - e^{-\kappa_{s_i}(k-T_s)}, \text{ if } k \geq T_s \end{cases} \qquad i=1, 2\ldots n$$

and

$$\Omega_{y_m}(k-T_y) = \begin{cases} 0 \text{ if } k < T_y \\ 1 - e^{-\kappa_{y_m}(k-T_y)}, \text{ if } k \geq T_y \end{cases} \qquad m=1, 2\ldots p$$

with $\kappa_{s_i} > 0$ and $\kappa_{y_m} > 0$ are unknown constants denoting the rate at which the fault in the state x_i and in output y_m evolves. For small values of κ_{s_i} and κ_{y_m}, the exponential term decays slowly, thus describing incipient faults whereas for large values of these terms, it decays faster thus represents abrupt faults, i.e., say $\kappa_{s_i} \to \infty$, then $e^{-\infty} = 0$. The use of exponential term is only to signify the fault growth rate. However, the nonlinear fault functions $f_s(.)$ and $f_y(.)$ denote the magnitude and type of fault, for example, they could be a stuck actuator, sensor fault etc. In addition, T_s and T_y denote the unknown time of occurrence of state and output faults, respectively. Its worth noting, that the proposed fault time profile encompasses most of the commonly occurring faults in a practical system [7].

Remark 1: Use of the time profiles to address incipient and abrupt faults is common in fault detection [44] and used extensively by other researchers [8-11, 19, 20, 29, 30, 32, 33, 35, 43].

Additionally, by asserting an assumption that the fault dynamics can be expressed as linear in the unknown parameters (LIP) [42], the fault dynamics in (1) could be written as $g_s(y(k),u(k)) = \theta_s^T \phi_s(y(k),u(k)) + \varepsilon_{1s}(k)$, where $\theta_s \in \Re^{l\times n}$ is the target and unknown parameter (or weight) matrix, $\phi_s \in \Re^{l\times 1}$ is a known nonlinear basis function vector such as RBF, sigmoid, sinusoidal etc, which is upper bounded by $\|\phi_s\| \le \phi_{s\,max}$ with the approximation error $\varepsilon_{1s}(k)$ is considered bounded above [45]. The target parameters are also bounded, such that $\|\theta_s\| \le \theta_{s_{\max}}$ [42]. Similarly, the output fault (sensor fault) dynamics can be written using LIP assumption as $g_y(u(k)) = \theta_y^T \phi_y(u(k)) + \varepsilon_{1y}(k)$, where $\theta_y \in \Re^{q\times p}$ is the target parameter matrix such that $\|\theta_y\| \le \theta_{y_{\max}}$, with $\phi_y \in \Re^{q\times 1}$ is a known nonlinear basis function , which is also upper bounded by $\|\phi_y\| \le \phi_{y\,max}$ with $\varepsilon_{1y}(k)$ being the approximation error vector. Finally, it is assumed that the initial system state vector is available, i.e., $x(0) = x_0$ and also the pair (A,C) is observable consistent with the literature. Other assumptions include:

Assumption 1: The modeling uncertainty is unstructured and bounded [10], i.e., $\|\eta_s(x(k),u(k))\| \le \tilde{\eta}_s$, $\forall (x,u) \in \mathrm{X}\times\Omega$ and $\|\eta_y(x(k),u(k))\| \le \tilde{\eta}_y$, $\forall (x,u) \in \mathrm{X}\times\Omega$, where $\tilde{\eta}_{s\ge 0}$ and $\tilde{\eta}_{y\ge 0}$ are known constants, $\mathrm{X} \subset \Re^n$, $\Omega \subset \Re^m$ are the state and control input regions of interest, respectively. Additionally, bounded time varying disturbances including process and sensor noise [41] could also be assumed to be present in the system defined in (1). However, the asymptotic stability guarantee depends upon the type of noise [46]. Note, in some of the previous works [15, 21], the modeling uncertainty is assumed to be structured,

thus simplifies the FD scheme design. Also, define $\mathbf{T} \subset \Re^+$ as the time interval prior to the occurrence of either state or sensor fault, i.e., $\mathbf{T} := \left[0, \min(T_s, T_y)\right]$ [10]. This assumption is consistent with the literature.

Unlike, other previously reported FD schemes [1, 4, 5, 14, 15], which considers only structured faults, the proposed framework addresses either process (or state) and sensor faults which are unstructured in nature. In the next section, the fault detection scheme and the parameter update law are introduced.

III. Fault Detection and Diagnosis Framework

Define the nonlinear FD estimator to monitor the system given in (1) as

$$\begin{aligned} \hat{x}(k+1) &= A\hat{x}(k) + \varphi_s(\hat{y}(k), u(k)) - Ke_y(k) + \hat{g}_s(\hat{y}(k), u(k); \hat{\theta}_s(k)) + v_{s_r}(k) \\ \hat{y}(k) &= C\hat{x}(k) + \hat{g}_y(u(k); \hat{\theta}_y(k)) + v_{y_r}(k) \end{aligned} \tag{2}$$

where $\hat{x} \in \Re^n$ is the estimated state vector, $\hat{y} \in \Re^p$ is the estimated output vector, $\hat{g}_s : \Re^p \times \Re^m \times \Re^{l \times n} \to \Re^n$ and $\hat{g}_y : \Re^m \times \Re^{h \times p} \to \Re^p$ are the OLAD outputs with $\hat{\theta}_s \in \Re^{l \times n}$ and $\hat{\theta}_y \in \Re^{h \times p}$ are the set of adjustable parameters, $e_y = y - \hat{y}$ is the output residual, $v_{s_r}(k)$ and $v_{y_r}(k)$ denote the robust adaptive terms, and $K \in \Re^{n \times p}$ is a design constant matrix, which is chosen such that the matrix $A + KC$ has all its eigenvalues within the unit disc [42]. The purpose of the FD estimator is to generate the residual and not to estimate the system states typical in control applications. Additionally, in comparison with discrete-time FD schemes [29, 33, 34, 43], proposed FD estimator includes robust adaptive terms.

Now to better understand the difference between a fault and a failure, we refer to Fig. 1. The design matrix *K* will ensure that the state residual is asymptotically stable in the absence of uncertainties and faults. However, with bounded uncertainties and in the absence of faults, it is not difficult to show that the system states will be bounded (see next section), which will be utilized to define the detection threshold. Now during faults of finite magnitude, the system parameter/state magnitudes change with time exceeding a failure threshold since the fault function can be viewed as an additional unwanted input. The failure threshold is used to determine TTF and to avoid any catastrophic failures. It is up to the maintenance personnel to define an appropriate failure threshold, which is normally tied with unacceptable drop in performance, since it is considered unsafe to operate the system beyond this value. On the other hand, a fault function magnitude that increases indefinitely with time can be considered here as well except the system will become ultimately unstable in the presence of such faults.

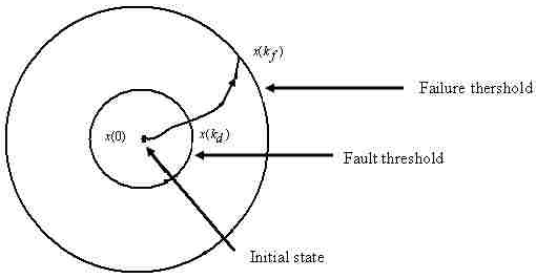

Figure 1: State trajectories from initial time to failure.

Define the state residual as $e_s = x - \hat{x}$. Since the system outputs are measurable, only the output residual will be used for fault detection. Moreover, we consider a general class of online approximators in discrete-time (OLAD) such as neural networks, radial

basis functions, fuzzy logic and so on where their parameters are tuned online with an adaptive law. Many papers [8-11, 47] discuss various online approximator schemes and therefore the discussion is omitted. The initial parameter vector of the OLAD is chosen such that $\hat{\theta}_s(0) = \hat{\theta}_{0s}$, $\hat{g}_s^T(y(k), u(k), \hat{\theta}_{0s}) = [0, 0, ..., 0]^T$ and $\hat{\theta}_y(0) = \hat{\theta}_{0y}$, $\hat{g}_y^T(u(k), \hat{\theta}_{0y}) = [0, 0, ..., 0]^T$ for all $y \in \mathcal{Y}$ and $u \in U$, where U and $\mathcal{Y}$ define the admissible range of inputs and outputs. Define $\tilde{\varphi}_s(k) = \varphi_s(y(k), u(k)) - \varphi_s(\hat{y}(k), u(k))$. Now before proceeding further, the following assumption is required.

Assumption 2: The function $\varphi_s(.)$ is Lipschitz in y and u with Lipschitz constant c_g, i.e., $\left\|\tilde{\varphi}_s(k)\right\| \le c_g \left\|e_y(k)\right\|$ [20].

Remark 2: This assumption allows one to relate the output OLAD basis function with the output residual.

In order to avoid false alarms due to unmodeled dynamics, the proposed fault detection scheme utilizes a dead-zone [1, 5] operator defined by $D[e_y(k)] = \begin{cases} 0, \text{ if } \left\|e_y(k)\right\| \le \varepsilon \\ e_y(k), \text{if } \left\|e_y(k)\right\| > \varepsilon \end{cases}$, with ε is the detection threshold obtained analytically in this section. The detection threshold is expressed in terms of the modeling error bounds viz. $\tilde{\eta}_s$ and $\tilde{\eta}_y$ presented in Assumption 1. By selecting the dead-zone based fault detection similar to continuous-time, which is absent in other model based schemes [4, 5], missed and false alarms can be minimized.

The dead-zone operator is utilized to turn the OLAD and robust adaptive terms online. Prior to the fault, *i.e.*, $\|e_y(k)\| \le \varepsilon$, $\hat{\theta}_s(k) = \begin{bmatrix} 0 & . & . & . & 0 \\ . & . & . & . & . \\ . & . & . & . & . \\ 0 & . & . & . & 0 \end{bmatrix}_{l\times n}$, $\hat{\theta}_y(k) = \begin{bmatrix} 0 & . & . & . & 0 \\ . & . & . & . & . \\ . & . & . & . & . \\ 0 & . & . & . & 0 \end{bmatrix}_{h\times p}$, $0 \le k \le T$, $v_{s_r}^T(k) = [0, 0, ..., 0]^T$ and $v_{y_r}^T(k) = [0, 0, ..., 0]^T$. This means $\hat{g}_s^T(y(k), u(k), \hat{\theta}_s(k)) = [0, 0, ..., 0]^T$, $\hat{g}_y^T(u(k), \hat{\theta}_y(k)) = [0, 0, ..., 0]^T$, $v_{s_r}^T(k) = [0, 0, ..., 0]^T$, and $v_{y_r}^T(k) = [0, 0, ..., 0]^T$ in the time interval $0 \le k \le T$ prior to a state or output fault. In the next section, the robustness theorem will indeed demonstrate that the OLAD's and the robust terms will not be initiated and tuned prior to the fault detection.

When the output residual exceeds the detection threshold, i.e., $\|e_y(k)\| > \varepsilon$, a fault is declared active and the OLAD schemes that generate, $\hat{g}_s(.)$ and $\hat{g}_y(.)$, are initiated and tuned online using the following update laws as

$$\hat{\theta}_s(k+1) = \hat{\theta}_s(k) + \alpha_s \phi_s(k)\, \mathrm{D}[e_y^T(k)]B - \gamma_s \left\| I - \alpha_s \phi_s(k)\phi_s^T(k) \right\| \hat{\theta}_s(k) \tag{3}$$

$$\hat{\theta}_y(k+1) = \hat{\theta}_y(k) + \alpha_y \phi_y(k)\, \mathrm{D}[e_y^T(k)] - \gamma_y \left\| I - \alpha_y \phi_y(k)\phi_y^T(k) \right\| \hat{\theta}_y(k) \tag{4}$$

where $\alpha_s > 0$ and $\alpha_y > 0$ are the learning rate or adaptation gains, $0 < \gamma_s < 1$ and $0 < \gamma_y < 1$ are the design parameters, and B is an appropriately sized constant matrix chosen such that $\|B\| \le \kappa$, with $\kappa > 0$.

Additionally, the robust adaptive terms $v_{s_r}(k)$ and $v_{y_r}(k)$ in (2) defined by as $v_{s_r}(k) = \dfrac{\hat{\theta}_s^T(k)B_1}{B_1^T \hat{\theta}_s(k)\hat{\theta}_s^T(k)B_1 + c_s}$ and $v_{y_r}(k) = \dfrac{\hat{\theta}_y^T(k)B_2}{B_2^T \hat{\theta}_y(k)\hat{\theta}_y^T(k)B_2 + c_y}$ respectively, are initiated

where B_1 and B_2 are constant vectors to be defined later, with $c_s > 0$ and $c_y > 0$ denote positive constants.

Remark 3: The parameter update laws proposed in (3) and (4) relaxes the critical requirement of the PE for non-ideal cases, i.e., system with modeling and approximation errors, and prevent parameter drift due to the extra terms embedded in them similar to other schemes [33, 34, 43]. Another important remark is that no prior offline training is needed for tuning the online approximators and therefore can be applied to learn new fault functions or dynamics [3].

Remark 4: The asymptotic stability proofs can be demonstrated even in the presence of unmodeled dynamics and OLAD reconstruction errors without these extra terms in (3) and (4) [42] due to the new robust adaptive term included herein. The proof is not included in here since it will be shown later that the extra terms are needed in (3) and (4) for the purpose of TTF determination.

Now for the purpose of diagnosis, once a fault is detected, it is identified as a state or an output fault based on the OLAD outputs. A state fault is considered to have occurred if the OLAD that approximates the state fault function exceeds a predefined threshold whereas an output fault has occurred if the OLAD output that approximates the output fault function has exceeded its threshold. When the OLAD outputs exceed their corresponding thresholds, then both state and output faults have considered to have occurred simultaneously. This result is explained in the form of a sensitivity theorem which is discussed in the next section.

Unless rigorous fault isolation can be performed, one cannot go beyond simply identifying a state or output fault. In other words, the proposed diagnosis scheme cannot

be utilized to identify which particular state or output a fault has occurred. Such rigorous fault isolation is outside the scope of this paper. Next analytical results on the detection and diagnosis scheme are introduced.

IV. Analytical Results

In this section, mathematical results for the sensitivity and the robustness of the FD scheme are derived in order to determine the class of detectable faults. Next, the stability of the FD scheme after the detection of a fault is introduced.

To derive the detection threshold, consider the residual dynamics prior to a fault obtained using (1) and (2) as

$$e_s(k+1) = Ae_s(k) + \tilde{\varphi}_s(k) + \eta_s(x(k), u(k)) + Ke_y(k) \tag{5}$$

$$e_y(k) = Ce_s(k) + \eta_y(x(k), u(k)) \tag{6}$$

Note prior to the fault, the OLAD and the robust terms in (2) are $\hat{g}_s^T(y(k), u(k), \hat{\theta}_{0s}) = [0, 0, ..., 0]^T$, $\hat{g}_y^T(u(k), \hat{\theta}_{0y}) = [0, 0, ..., 0]^T$, $v_{s_r}^T(k) = [0, 0, ..., 0]^T$ and $v_{y_r}^T(k) = [0, 0, ..., 0]^T$ in the time interval $0 \le k \le T$. Now by solving (5) for $e_s(k)$ first and then (6) for $e_y(k)$, we obtain

$$e_s(k) = \sum_{j=0}^{k} A_0^{k-j} \left[\eta_s(x(j), u(j)) + \tilde{\varphi}_s(j) + K\eta_y(x(j), u(j))\right]$$

and

$$e_y(k) = C\sum_{j=0}^{k} A_0^{k-j} \left[\eta_s(x(j), u(j)) + \tilde{\varphi}_s(j) + K\eta_y(x(j), u(j))\right] + \eta_y(x(j), u(j))$$

This in turn yields

$$\left\|e_y(k)\right\| \le \left\|C\sum_{j=0}^{k} A_0^{\,k-j}\right\|\tilde{\eta}_s + \left\|C\sum_{j=0}^{k} A_0^{\,k-j}K\right\|\tilde{\eta}_y + \left\|C\sum_{j=0}^{k} A_0^{\,k-j}\right\| c_g \left\|e_{y(k)}\right\| + \tilde{\eta}_y \qquad (7)$$

which could be written as

$$\left\|e_y(k)\right\| \le \mu_s\tilde{\eta}_s + (\mu_{y_1} + \mu_{y_2})\tilde{\eta}_y \qquad (8)$$

where $\mu_s := \dfrac{\left\|C\sum_{j=0}^{k} A_0^{\,k-j}\right\|}{\left(1 - c_g\left\|C\sum_{j=0}^{k} A_0^{\,k-j}\right\|\right)}$, $\mu_{y_1} := \dfrac{\left\|C\sum_{j=0}^{k} A_0^{\,k-j}K\right\|}{\left(1 - c_g\left\|C\sum_{j=0}^{k} A_0^{\,k-j}\right\|\right)}$,

and $\mu_{y_2} = 1\Big/\left(1 - c_g\left\|C\sum_{j=0}^{k} A_0^{\,k-j}\right\|\right)$. Thus if the detection threshold is selected as $\varepsilon = \mu_s\tilde{\eta}_s + (\mu_{y_1} + \mu_{y_2})\tilde{\eta}_y$, the output residual, $e_y(k)$, will remain within the dead zone for all $k \le T$ and the output of the OLADs and the robust adaptive terms would remain zero. Therefore, the FD scheme given in (2) is robust in the sense that it is not affected by the modeling errors provided their upper bounds are known apriori. If there are no modeling errors as in the ideal case, then the detection threshold will be zero as expected.

Remark 5: The detection threshold, ε, will be higher when an output residual based FD detection scheme is utilized due to the additional system uncertainties in the output equation in comparison to a state measurable FD scheme [8, 11, 29, 33, 34, 43]. This confirms that the output residual-based scheme will be less sensitive to incipient faults.

A key performance measure of a FD scheme is its sensitivity to faults. Sensitivity is defined as the ability of the FD scheme to correctly determine the existence of a fault. One approach to analyze the fault sensitivity properties of a FD scheme is to characterize the set of faults that can be reliably detected. The following theorem characterizes the set of state and output faults that can be detected by the FD scheme.

In this theorem, a suitable condition is derived for both state and output faults occurring independently or simultaneously. In the previous work [4, 5], the system uncertainties and the faults are assumed to be decoupled; however, in this paper, we relax this assumption by distinguishing the effects of the faults from those of uncertainties by using bounds on the uncertainties. Next, the sensitivity theorem is introduced.

Theorem 1 (Sensitivity): *Consider the system given by (1), detection estimator (2) and the OLAD tuning updates (3) and (4).* ***i)*** *If there exist a time instant* $k_s > 0$, *such that* $f_s(y(k),u(k))$ *satisfies*

$$\frac{1}{\mu_{y_2}}\left\|\sum_{i=T_S}^{T_S+k_S} CA_0^{(T_S+k_S-i)}\Pi_s(i-T_s)\,f_s(y(i-1),u(i-1))\right\| \geq 2\varepsilon, \tag{9}$$

Then the state fault will be detected, i.e., the output residual $\|e_y(T_s+k_s)\| \geq \varepsilon$.

ii) *Also if there exists a time instant* $k_y > 0$ *such that* $f_y(u(k))$ *satisfies*

$$\frac{1}{\mu_{y_2}}\left\|\Pi_y(k_y)\,f_y(u(T_y+k_y)) + \sum_{i=T_y}^{T_y+k_y} CA_0^{(T_y+k_y-i)}K\Pi_y(i-T_y)\,f_y(u(i-1))\right\| \geq 2\varepsilon \tag{10}$$

then the output fault will be detected, i.e., $\|e_y(T_y+k_y)\| \geq \varepsilon$.

*Proof***:** Refer to Appendix.

Inequalities (9) and (10) are derived for worst-case scenario of modeling uncertainties. Moreover, for the purpose of applicability, the actual fault functions can be replaced by their approximations.

Remark 6: From the sufficient conditions introduced in (9) or (10), the magnitude of the fault has to be sufficiently large to distinguish it from the modeling uncertainties. Upon detection, the magnitude of state or output OLAD would vary as per the conditions stated

above. Therefore, the OLAD with the highest magnitude is more sensitive towards the type of fault occurring in the system, thus helps in identifying the fault. Therefore by appropriately setting a threshold value defined in (9) and (10) on the OLAD outputs, one can identify whether or not a state or sensor fault has occurred. Subsequently, that particular OLAD will be used for the online estimation of the unknown fault dynamics and the other can be reset to zero. In the event that both state and output faults occur simultaneously, both the conditions will be satisfied and OLAD outputs will exceed the thresholds defined in (9) and (10). This approach is used in the fault diagnosis.

Next, the following theorem guarantees the robustness of the fault detection scheme. This theorem shows that the OLAD does not adapt prior to the fault and the FD scheme does not generate false alarms in the presence of uncertainties.

Theorem 2 (Robustness): *Consider the system given by (1), detection estimator (2) and the OLAD tuning updates (3) and (4). The proposed fault detection scheme ensures that the output of the online approximators (OLAD's) and the robust adaptive terms would remain at zero prior to the occurrence of a state or output fault for* $k \in [0, T)$ *,i.e.,* are $\hat{g}_s^T(y(k), u(k), \hat{\theta}_{0s}) = [0, 0, ..., 0]^T$, $\hat{g}_y^T(u(k), \hat{\theta}_{0y}) = [0, 0, ..., 0]^T$, $v_{s_r}^T(k) = [0, 0, ..., 0]^T$ and $v_{y_r}^T(k) = [0, 0, ..., 0]^T$.

Proof: Refer to Appendix.

As we understand from the above two theorems, only in the event of a fault, the output residual exceeds the threshold thus initiating the OLADs and the robust adaptive terms. As a consequence, the OLAD and the robust adaptive terms do not compensate for any faults prior to detection. Now assuming a worst case scenario of faults, then the state and the output residual dynamics from (1) and (2) are given by

$$e_S(k+1) = Ae_S(k) + \eta_S(x(k), u(k)) + g_S(y(k), u(k)) - \hat{g}_S(y(k), u(k), \hat{\theta}_S(k)) + \tilde{\varphi}_S(k) + Ke_y(k) - \frac{\hat{\theta}_S^T(k)B_1}{B_1^T\hat{\theta}_S(k)\hat{\theta}_S^T(k)B_1 + c_S},$$

$$e_y(k) = Ce_s(k) + \eta_y(x(k),u(k)) + g_y(u(k)) - \hat{g}_y(u(k),\hat{\theta}_y(k)) - \frac{\hat{\theta}_y^T(k)B_2}{B_2^T\hat{\theta}_y(k)\hat{\theta}_y^T(k)B_2 + c_y}$$

Asserting the LIP assumption, then the state and the output residuals are expressed as

$$e_s(k+1) = Ae_s(k) + \eta_s(x(k),u(k)) + Ke_y(k) + \theta_s^T\phi_s(y(k),u(k)) + \tilde{\varphi}_s(k) - \hat{\theta}_s^T(k)\phi_s(y(k),u(k))$$

$$+\varepsilon_s(k) - \frac{\hat{\theta}_s^T(k)B_1}{B_1^T\hat{\theta}_s(k)\hat{\theta}_s^T(k)B_1 + c_s}$$

$$e_y(k) = Ce_s(k) + \eta_y(x(k),u(k)) + \theta_y^T\phi_y(u(k)) - \hat{\theta}_y^T(k)\phi_y(u(k)) + \varepsilon_y(k) - \frac{\hat{\theta}_y^T(k)B_2}{B_2^T\hat{\theta}_y(k)\hat{\theta}_y^T(k)B_2 + c_y}$$

Define the parameter estimation errors as $\tilde{\theta}_s(k) = \theta_s - \hat{\theta}_s(k)$ and $\tilde{\theta}_y(k) = \theta_y - \hat{\theta}_y(k)$. Adding and subtracting $\frac{\left(\theta_s^T B_1 - C_3\right)}{B_1^T\hat{\theta}_s(k)\hat{\theta}_s^T(k)B_1 + c_s}$ and $\frac{\left(\theta_y^T B_2 - C_4\right)}{B_2^T\hat{\theta}_y(k)\hat{\theta}_y^T(k)B_2 + c_y}$ in the above equation, where C_3 and C_4 are appropriate dimensioned constant vectors, the state and the output residuals are given by

$$e_s(k+1) = Ae_s(k) + \eta_s(x(k),u(k)) + \tilde{\theta}_s^T(k)\phi_s(y(k),u(k)) + Ke_y(k) + \tilde{\varphi}_s(k) + \varepsilon_s(k) - \frac{\hat{\theta}_s^T(k)B_1}{B_1^T\hat{\theta}_s(k)\hat{\theta}_s^T(k)B_1 + c_s}$$

$$- \frac{(\theta_s^T B_1 - C_3)}{B_1^T\hat{\theta}_s(k)\hat{\theta}_s^T(k)B_1 + c_s} + \frac{\theta_s^T B_1 - C_3}{B_1^T\hat{\theta}_s(k)\hat{\theta}_s^T(k)B_1 + c_s},$$

$$e_y(k) = Ce_s(k) + \eta_y(x(k),u(k)) + \tilde{\theta}_y^T(k)\phi_y(u(k)) + \varepsilon_y(k) - \frac{\hat{\theta}_y^T(k)B_2}{B_2^T\hat{\theta}_y(k)\hat{\theta}_y^T(k)B_2 + c_y} + \frac{\theta_y^T B_2 - C_4}{B_2^T\hat{\theta}_y(k)\hat{\theta}_y^T(k)B_2 + c_y}$$

$$- \frac{(\theta_y^T B_2 - C_4)}{B_2^T\hat{\theta}_y(k)\hat{\theta}_y^T(k)B_2 + c_y}$$

The above dynamics can be rewritten as

$$e_s(k+1) = A_0e_s(k) + \eta_s(x(k),u(k)) + \tilde{\theta}_s^T(k)\phi_s(y(k),u(k)) + \varepsilon_s(k) + \tilde{\varphi}_s(k) + K\eta_y(x(k),u(k)) + K\tilde{\theta}_y^T(k)\phi_y(u(k)) + K\varepsilon_y(k)$$

$$+K\frac{\left(\tilde{\theta}_y^T(k)B_2 - C_4\right)}{B_2^T\hat{\theta}_y(k)\hat{\theta}_y^T(k)B_2 + c_y} - K\frac{\left(\theta_y^T B_2 - C_4\right)}{B_2^T\hat{\theta}_y(k)\hat{\theta}_y^T(k)B_2 + c_y} + \frac{\left(\tilde{\theta}_s^T(k)B_1 - C_3\right)}{B_1^T\hat{\theta}_s(k)\hat{\theta}_s^T(k)B_1 + c_s} - \frac{(\theta_s^T B_1 - C_3)}{B_1^T\hat{\theta}_s(k)\hat{\theta}_s^T(k)B_1 + c_s},$$

$$e_y(k) = Ce_s(k) + \eta_y(x(k),u(k)) + \tilde{\theta}_y^T(k)\phi_y(u(k)) + \varepsilon_y(k)$$

$$+\frac{\left(\tilde{\theta}_y^T(k)B_2 - C_4\right)}{B_2^T\hat{\theta}_y(k)\hat{\theta}_y^T(k)B_2 + c_y} - \frac{(\theta_y^T B_2 - C_4)}{B_2^T\hat{\theta}_y(k)\hat{\theta}_y^T(k)B_2 + c_y}$$

where $A_0 = A + KC$ .Denote $\Psi_s(k) = \tilde{\theta}_s^T(k)\phi_s(y(k),u(k))$, $\Psi_y(k) = \tilde{\theta}_y^T(k)\phi_y(u(k))$,

$v_s(k) = \frac{\left(\tilde{\theta}_s^T(k)B_1 - C_3\right)}{B_1^T\hat{\theta}_s(k)\hat{\theta}_s^T(k)B_1 + c_s}$, and $v_y(k) = \frac{\left(\tilde{\theta}_y^T(k)B_2 - C_4\right)}{B_2^T\hat{\theta}_y(k)\hat{\theta}_y^T(k)B_2 + c_y}$. Therefore, the dynamics become

$$e_s(k+1) = A_0e_s(k) + \eta_s(x(k),u(k)) + \Psi_s(k) + \varepsilon_s(k) + K\eta_y(x(k),u(k)) + K\Psi_y(k) + K\varepsilon_y(k) + Kv_y(k)$$

$$-K\frac{\left(\theta_y^T B_2 - C_4\right)}{B_2^T\hat{\theta}_y(k)\hat{\theta}_y^T(k)B_2 + c_y} + \tilde{\varphi}_s(k) + v_s(k) - \frac{(\theta_s^T B_1 - C_3)}{B_1^T\hat{\theta}_s(k)\hat{\theta}_s^T(k)B_1 + c_s},$$

$$e_y(k) = Ce_s(k) + \eta_y(x(k),u(k)) + \Psi_y(k) + \varepsilon_y(k) + v_y(k) - \frac{(\theta_y^T B_2 - C_4)}{B_2^T\hat{\theta}_y(k)\hat{\theta}_y^T(k)B_2 + c_y} \quad (11)$$

Before proceeding, the following lemma is required.

Lemma 1: The terms comprising of the OLAD approximation errors ($\varepsilon_s(k)$ and $\varepsilon_y(k)$) and the system uncertainties ($\eta_s(x(k),u(k))$ and $\eta_y(x(k),u(k))$) are bounded according to

$$\left\|\eta_s(x,u)\right\|^2 + \left\|\varepsilon_s(k)\right\|^2 + 3\left\|\eta_y(x,u)\right\|^2 K_{\max}^2 + 3\left\|\varepsilon_y(k)\right\|^2 K_{\max}^2 + 6c_g^2\left\|\eta_y(x,u)\right\|^2 + 6c_g^2\left\|\varepsilon_y(k)\right\|^2 \le 6\left(\left\|\eta_s(x,u)\right\|\right.$$

$$\left. + \left\|\varepsilon_s(k)\right\| + \left\|\eta_y(x,u)\right\|K_{\max} + \left\|\varepsilon_y(k)\right\|K_{\max} + c_g\left\|\eta_y(x,u)\right\| + c_g\left\|\varepsilon_y(k)\right\|\right)^2$$

$$\le \beta_0 + \beta_1\left\|e_s(k)\right\|^2 + \beta_2\left\|\tilde{\theta}_s(k)\right\|^2 + \beta_3\left\|\tilde{\theta}_y(k)\right\|^2 + \beta_4\left\|e_s(k)\right\|\left\|\tilde{\theta}_s(k)\right\| + \beta_5\left\|e_s(k)\right\|\left\|\tilde{\theta}_y(k)\right\|$$

where $\beta_0, \beta_1, \beta_2, \beta_3, \beta_4$ and β_5 are computable positive constants.

Proof: Refer to Appendix.

Remark 7: It is important to note that such relationships mentioned in Lemma 1, and not necessarily the same, are available in continuous-time [46, 48-50, 51, 52] whereas it is not shown for discrete-time case. This relationship will aid in the asymptotic stability analysis.

Proving asymptotic residual convergence implies a more accurate approximation of the unknown fault dynamics by the OLADs which in turn is necessary for the TTF determination. In the following theorem, the asymptotic stability of the proposed fault detection scheme is shown.

Theorem 3 (Asymptotic Stability Analysis after the Fault): *Let the initial conditions for the detection estimator be bounded in a region* $U \subset \Re^n$. *Let the parameter update laws be given by (3) and (4). In the presence of system uncertainties and OLAD approximation errors, the state residual* $e_s(k)$ *and the parameter estimation errors,* $\tilde{\theta}_s(k)$ *and* $\tilde{\theta}_y(k)$ *are locally asymptotically stable while the output residual* $e_y(k)$ *is bounded.*

Proof: Refer to Appendix.

It is important to note that a time interval exists from the time of fault occurs to the time when a fault is detected which is termed as fault detection time [8-11]. Subsequently, the OLAD and the robust adaptive terms are initiated. Therefore after the detection time, the output residual bound changes to (A.21).

Remark 8: The above theorem demonstrates that the first difference of the Lyapunov function is negative definite even in the presence of OLAD reconstruction vectors

provided the robust adaptive terms are used in (2). By contrast, a uniformly ultimately bounded (UUB) result is given in the literature [8-11, 29, 33, 34, 43] if the robust adaptive terms are not applied. These robust adaptive terms and Lemma 1 enables one to express the system uncertainties and unmodeled dynamics as a function of state and output residuals as well as parameter estimation errors which when combined with other terms render a negative definite first difference.

In the event that the boundedness of the parameter estimates of the OLADs can only be demonstrated, then the accuracy of obtaining TTF will depend upon the bound on the parameter estimates. Additionally, if the parameters can be tied to physical parameters and used for TTF determination in conjunction with fault isolation, prognostics can be developed. Instead, based on the fault diagnosis scheme introduced in this paper, the parameters of the OLAD that approximates the fault function will be used for the purpose of TTF determination.

In the next section, the TTF scheme development is introduced by using parameter update laws. The algorithm and the mathematical equation used are derived.

V. Prediction Scheme

In this section, parameter-based TTF determination is proposed by asserting the LIP assumption. This analysis can be easily extended to the state estimator based approach. The following assumption holds in deriving the TTF.

Assumption 3: The actual parameter vectors $\hat{\theta}_s(k)$ and $\hat{\theta}_y(k)$ represents the true system parameters.

Remark 9: For many practical systems, for example, in a mass damper system, or in civil infrastructure such as a bridge system, the mass, damping constant and spring constant may be expressed as linear in the unknown parameters (LIP). In the event of a fault, system parameters change, and tend to reach their failure thresholds as defined by the designer. When any one of the parameters attains its corresponding failure threshold, failure is considered to have occurred. Similarly, for the mechanical system like hydraulic pump, the states represent outlet pressure, flow etc which could be utilized for detection and TTF determination.

The TTF is defined as the time elapsed when the first parameter reaches its lower or upper failure threshold. Next the parameter update laws given in (3) and (4) could be used to project the system parameter online and will be used in the following theorem to develop an explicit mathematical equation for deriving TTF. This equation is then used to develop an algorithm for the continuous prediction of TTF at every time instant.

Theorem 4 (Time to Failure Determination-Parameter based Approach): In the presence of a state fault, the TTF for the ij^{th} system parameter at the k^{th} time instant can be determined using

$$k_{s_{fij}} = \frac{\left| \log\left(\left| \frac{\left(\gamma_s \left\| I - \alpha_s \varphi_s \varphi_s^T \right\| \theta_{s_{ij_{\max}}} - \alpha_s \left(\varphi_s e_y^T B \right)_{ij} \right)}{\left(\gamma_s \left\| I - \alpha_s \varphi_s \varphi_s^T \right\| \theta_{s_{ij_0}} - \alpha_s \left(\varphi_s e_y^T B \right)_{ij} \right)} \right| \right) \right|}{\left| \log(1 - \gamma_s \left\| I - \alpha_s \varphi_s \varphi_s^T \right\|) \right|} + k_{s_{0ij}} \tag{12}$$

where $k_{s_{fij}}$ is the estimated TTF, $k_{s_{0ij}}$ is the time instant when the prediction starts (bearing in mind that $k_{s_{dt}}$, is the fault detection time or initial value which increases incrementally), $\theta_{s_{ij_{\max}}}$ is the failure threshold in terms of the maximum value of the

system parameter, and $\theta_{s_{ij_0}}$ is the value of the system parameter at the time instant $k_{s_{0_{ij}}}$. Additionally, $i = 1, ..., l$ and $j = 1, ..., n$.

Similarly, in the presence of an output fault, the TTF for the mq^{th} system parameter at the k^{th} time instant can be determined using

$$k_{y_{f_{mq}}} = \frac{\left| \log\left(\left| \frac{\left(\gamma_y \left\| I - \alpha_y \varphi_y \varphi_y^T \right\| \theta_{y_{mq_{\max}}} - \alpha_y \left(\varphi_y e_y^T \right)_{mq} \right)}{\left(\gamma_y \left\| I - \alpha_y \varphi_y \varphi_y^T \right\| \theta_{y_{mq_0}} - \alpha_y \left(\varphi_y e_y^T \right)_{mq} \right)} \right| \right) \right|}{\left| \log(1 - \gamma_y \left\| I - \alpha_y \varphi_y \varphi_y^T \right\|) \right|} + k_{y_{0mq}} \tag{13}$$

where $k_{y_{f_{mq}}}$ is the estimated TTF, $k_{y_{0mq}}$ is the time instant when the prediction starts (bearing in mind that $k_{y_{dt}}$, is the output fault detection time which increases incrementally), $\theta_{y_{mq_{\max}}}$ is the maximum value of the system parameter, and $\theta_{y_{mq_0}}$ is the system parameter at the time instant $k_{y_{0mq}}$.

Proof: Refer to Appendix.

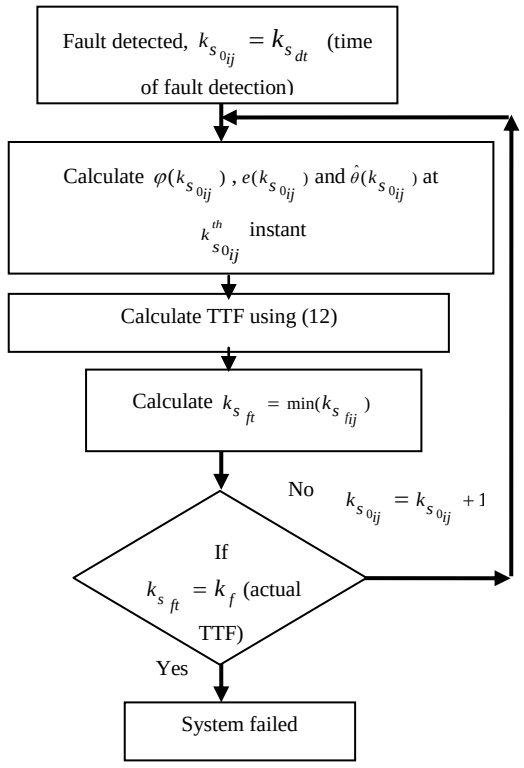

Figure 2: Flow chart indicating the TTF determination.

Figure 2 provides a flow chart to determine TTF ($k_{s_{f_{ij}}}$) for each system parameter in the event of a state fault. The TTF is determined at each time instant starting at the time when a fault is detected until the first system parameter reaches its failure threshold. Therefore, the TTF decreases as the parameter approaches its failure threshold.

Remark 10: The mathematical equation (12) and (13) is derived for the ij^{th} and the mq^{th} system parameter respectively. In general, for a given system with a state fault, the TTF would be $k_{s_{ft}} = \min(k_{s_{fij}}), i = 1, 2, ..., l$, $j = 1, ..., n$, where $l \times n$ are the number of parameters of the system states; for a system with an output fault, the TTF would

be $k_{y_{ft}} = \min(k_{y_{fmq}}), m = 1, 2, ..., p$, $q = 1, 2, ..., h$ where $p \times h$ are the number of output system parameters. The TTF is the time elapsed when the first parameter reaches its limit.

Remark 11: In the development of the FDP scheme, the time interval that is of interest is the interval between the time of fault occurrence to the time of actual failure, which is determined from the failure threshold on the parameter or states of the system. In the event that a state and an output faults occur simultaneously, both the OLAD parameters will be projected to their limits. The OLAD parameter that reaches its corresponding limit first will be utilized for TTF.

Remark 12: The extra terms introduced in the parameter update laws (3) and (4), which are in the form of difference equations, allow the convergence of the parameters. However, for the purpose of fault detection estimator stability, these terms are not required which implies that the stability results in Theorem 3 could be obtained without the extra terms in (3) and (4). The extra terms are required for TTF determination.

Remark 13: Apart from using the parameter trajectories for TTF prediction, the fault detection estimator state trajectory can be utilized for TTF determination. Since the state residual converges to zero asymptotically, the fault detection estimator states converge to the actual system states accurately. Hence the state trajectory based TTF scheme could be used as an alternate method to the parameter trajectory based schemes for systems that do not satisfy LIP provided the states represent physical entities.

It is important to note that the proposed mathematically rigorous approach of TTF determination is more accurate than data-driven methods [40, 53]. In the next section, an example is used to demonstrate the proposed FDP scheme.

VI. Simulation Results

A fourth-order dynamic satellite system is utilized to show the robust FDP scheme. Consider a discrete-time MIMO representation of the satellite system [9] defined by

$$x(k+1) = Ax(k) + \varphi_S(y(k), u(k)) + \eta_S(x(k), u(k)) + g_S(y(k), u(k))$$
$$y(k) = Cx(k) + \eta_y(x(k), u(k)) + g_y(u(k)) \tag{14}$$

where $x(k) = [x_1(k), x_2(k), x_3(k), x_4(k)]^T$ is the state vector, $y = [y_1, y_2]^T$ is the output vector,

$$A = \begin{bmatrix} 1 & 0 & t_s & 0 \\ 0 & 1 & 0 & t_s \\ 0 & 0 & 1 & 0 \\ 0 & 0 & 0 & 1 \end{bmatrix}, \quad \varphi_S(y(k), u(k)) = \begin{bmatrix} 0 \\ 0 \\ t_S\left[\dfrac{-y_1(k)}{(y_1^2(k)+y_2^2(k))^{3/2}}\dfrac{k_c}{m} + \dfrac{u_1(k)y_1(k)+u_2(k)y_2(k)}{(y_1^2(k)+y_2^2(k))^{1/2}}\dfrac{1}{m}\right] \\ t_S\left[\dfrac{-y_2(k)}{(y_1^2(k)+y_2^2(k))^{3/2}}\dfrac{k_c}{m} + \dfrac{u_1(k)y_2(k)-u_2(k)y_1(k)}{(y_1^2(k)+y_2^2(k))^{1/2}}\dfrac{1}{m}\right] \end{bmatrix},$$

and $C = \begin{bmatrix} 1 & 0 & 0 & 0 \\ 0 & 1 & 0 & 0 \end{bmatrix}$.

The mass of the satellite is taken as $m = 200kg$, parameter $k_c = K_E m$, where $K_E = 3.986 \times 10^5 km^3/s^2$. The satellite is first observed in perigee $375km$ above the surface of the earth $r_0 = R_E + 375km$, where $R_E = 6.378 \times 10^3 km$. The initial angular speed ω_{s0} is computed using the orbital mechanics $\omega_{s0} = \sqrt{(e_{orbit}+1)(K_E/r_0^3)}$, where $e_{orbit} = 0.162$ is the eccentricity. Control inputs u_1 and u_2 are the radial and tangential thrust forces, respectively which are taken as $u_1(k) = (y_1^2(k)+y_2^2(k))^{1/2}\left[\dfrac{k_c}{(y_1^2(k)+y_2^2(k))^{3/2}} + 0.0001\sin(0.01k)\right]$ and $u_2(k) = m_1(y_1^2(k)+y_2^2(k))^{1/2}\cos(0.01k)$, where $m_1 = 0.0001m$ and $t_s = 0.01$. The initial conditions of the

satellite system is taken as $x_1(0) = 0, x_2(0) = r_0, x_3(0) = r_0\omega_{s0}$, and $x_4(0) = 0$. To monitor and detect faults in (14), the FD estimator is given by

$$\hat{x}(k+1) = A\hat{x}(k) + \varphi_s(\hat{y}(k), u(k)) - Ke_y(k) + \hat{g}_s(\hat{y}(k), u(k); \hat{\theta}_s(k)) + v_{s_r}(k)$$

$$\hat{y}(k) = C\hat{x}(k) + \hat{g}_y(u(k); \hat{\theta}_y(k)) + v_{y_r}(k) \qquad (15)$$

where $\hat{x}(k) = [\hat{x}_1(k), \hat{x}_2(k), \hat{x}_3(k), \hat{x}_4(k)]^T$ is the estimated system state vector $\varphi_s(\hat{y}(k), u(k)) =$

$$\begin{bmatrix} 0 \\ 0 \\ t_s\left[\dfrac{-\hat{y}_1(k)}{(\hat{y}_1^2(k)+\hat{y}_2^2(k))^{3/2}}\dfrac{k_c}{m} + \dfrac{u_1(k)\hat{y}_1(k)+u_2(k)\hat{y}_2(k)}{(\hat{y}_1^2(k)+\hat{y}_2^2(k))^{1/2}}\dfrac{1}{m}\right] \\ t_s\left[\dfrac{-\hat{y}_2(k)}{(\hat{y}_1^2(k)+\hat{y}_2^2(k))^{3/2}}\dfrac{k_c}{m} + \dfrac{u_1(k)\hat{y}_2(k)-u_2(k)\hat{y}_1(k)}{(\hat{y}_1^2(k)+\hat{y}_2^2(k))^{1/2}}\dfrac{1}{m}\right] \end{bmatrix}, \text{ and } K = \begin{bmatrix} -a_1 & 0 \\ 0 & -a_2 \\ 0 & 0 \\ 0 & 0 \end{bmatrix}.$$

with $a_1 = a_2 = 10^{-3}$. Additionally, the initial conditions of the estimator is taken as $\hat{x}_1(0) = -0.05, \hat{x}_2(0) = r_0, \hat{x}_3(0) = r_0\omega_{s0}$, and $x_4(0) = -0.01$. In this simulation, two different scenarios are presented to show the robustness of the proposed FDP scheme.

Scenario 1-State fault: In this simulation scenario, we consider the state fault as

$g_s(y(k), u(k)) = \theta_s^T(k)\phi_s(y(k), u(k))$,

where $\theta_s(k) = \begin{bmatrix} \theta_{s_1}(k) & 0 & 0 & 0 \\ 0 & \theta_{s_2}(k) & 0 & 0 \\ 0 & 0 & \theta_{s_3}(k) & 0 \\ 0 & 0 & 0 & \theta_{s_4}(k) \end{bmatrix}$, $\phi_s(y(k), u(k)) = \begin{bmatrix} -\cos(\omega_1 y_1(k)) \\ \cos(\omega_2 y_2(k)) \\ \cos(\omega_3 y_2(k)) \\ \sin(\omega_4 y_1(k)) \end{bmatrix}$, $\omega_1 = \omega_3 = 1\times10^{-5}$ and

$\omega_2 = \omega_4 = 1\times10^{-4}$. The fault occurs only in system states $x_3(k)$ and $x_4(k)$. Therefore, $\theta_{s_1}(k) = \theta_{s_2}(k) = 0$ whereas

$$\theta_{s_3}(k) = \begin{cases} 0 & for\ 0 < k < 25\ \text{sec} \\ 1.8(1 - e^{-0.07(k-25)}) & k \geq 25\ \text{sec} \end{cases}$$

and

$$\theta_{s_4}(k) = \begin{cases} 0 & for\ 0 < k < 25\ \text{sec} \\ 0.75(1 - e^{-0.06(k-25)}) & k \geq 25\ \text{sec} \end{cases}$$

Note the state faults could be due to the inadvertent activation of the thrusters in the satellite system and are seeded at the 25th second of system operation. Since only a state fault is considered for this simulation, we have $g_y(u(k)) = [0, 0]^T$. Additionally, the output uncertainty in the system is taken as $\eta_y^T(x(k), u(k)) = [0.04\sin(0.0001k), 0]^T$ whereas the state uncertainty is represented by

$$\eta_s(y(k), u(k)) = \begin{bmatrix} 0 \\ 0 \\ \dfrac{0.000024x_2(k)}{(x_1^2(k) + x_2^2(k))^{3/2}}\dfrac{k_c}{m} - \dfrac{0.06(u_1(k)x_2(k) + u_2(k)x_1(k))}{(x_1^2(k) + x_2^2(k))^{1/2}}\dfrac{1}{0.97m} \\ \dfrac{0.000032x_4(k)}{(x_1^2(k) + x_2^2(k))^{3/2}}\dfrac{k_c}{m} - \dfrac{0.08(u_1(k)x_2(k) + u_2(k)x_1(k))}{(x_1^2(k) + x_2^2(k))^{1/2}}\dfrac{1}{0.97m} \end{bmatrix}$$

The online approximator (OLAD) used in the FD estimator in (15) is given by $\hat{g}_s(\hat{y}(k), u(k); \hat{\theta}_s(k)) = \hat{\theta}_s^T(k)\phi_s(\hat{y}(k), u(k))$, where

$\hat{\theta}_s(k) = \begin{bmatrix} \hat{\theta}_{s_{11}}(k) & \hat{\theta}_{s_{12}}(k) & \hat{\theta}_{s_{13}}(k) & \hat{\theta}_{s_{14}}(k) \\ \hat{\theta}_{s_{21}}(k) & \hat{\theta}_{s_{22}}(k) & \hat{\theta}_{s_{23}}(k) & \hat{\theta}_{s_{24}}(k) \\ \hat{\theta}_{s_{31}}(k) & \hat{\theta}_{s_{32}}(k) & \hat{\theta}_{s_{33}}(k) & \hat{\theta}_{s_{34}}(k) \\ \hat{\theta}_{s_{41}}(k) & \hat{\theta}_{s_{42}}(k) & \hat{\theta}_{s_{43}}(k) & \hat{\theta}_{s_{44}}(k) \end{bmatrix}$ is the estimated parameter matrix, and

$\phi_s^T(\hat{y}(k), u(k)) = \left[-\cos(\omega_1 \hat{y}_1(k)) \quad \cos(\omega_2 \hat{y}_2(k)) \quad \cos(\omega_3 \hat{y}_2(k)) \quad \sin(\omega_4 \hat{y}_1(k))\right]^T$. The parameters are updated using the update law in (3) by taking $\alpha_s = 0.04$ and $\gamma_s = 0.41$. However, their initial values are taken to be zero. The robust adaptive term is defined by $v_{s_r}(k) = \dfrac{\hat{\theta}_s^T(k) B_1}{B_1^T \hat{\theta}_s(k) \hat{\theta}_s^T(k) B_1 + c_s}$, where $B_1^T = \left[0.01 \quad 0.08 \quad -0.42 \quad -0.5\right]$, and $c_s = 0.85$. Since we have only a state fault, $\hat{g}_y^T(u(k); \hat{\theta}_y(k)) = \left[0 \quad 0\right]^T$ and $v_{y_r}^T(k) = \left[0 \quad 0\right]^T$.

To show the performance of the FD estimator, the state residual of the two measurable outputs defined in terms of, $x_1(k)$ and $x_2(k)$, are shown in Figs. 3 and 4. From the figures, it is evident that prior to the fault due to the system uncertainties, the state residuals remain bounded. However, after the fault, the residual converges asymptotically to zero as shown in the Theorem 3 since the OLAD and the robust term are initiated to learn the unknown fault dynamics. However, since the system has coupled dynamics and considering the manuscript length, the residuals of the remaining system states ($x_3(k)$ and $x_4(k)$) have not been shown.

To monitor the chosen system and detect faults, norm of the output residual is generated as shown in Fig. 5. We used a constant threshold of 0.77 unit magnitude ($\varepsilon = \mu_s \tilde{\eta}_s + (\mu_{y_1} + \mu_{y_2}) \tilde{\eta}_y$, for the given value of C, A_0 and, K matrices, we have $\mu_s \approx 1.02$, $\tilde{\eta}_s \approx 0.71$, $\mu_{y_1} \approx 1 \times 10^{-5}$, $\mu_{y_2} = 1$, and $\tilde{\eta}_y = 0.04$, $\varepsilon \approx 0.77$) to avoid false and missed alarms. In the event of a fault, the residual increases and exceeds the threshold as shown in Fig. 5 declaring the presence of a fault.

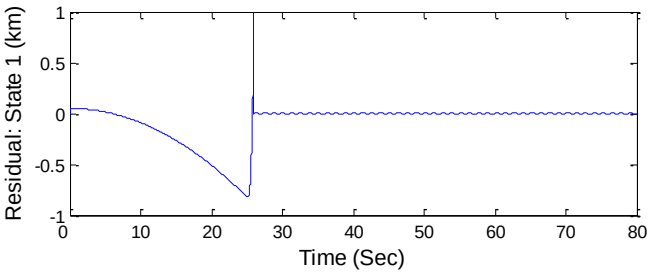

Figure 3: State residual ($e_{S_1}(k) = x_1(k) - \hat{x}_1(k)$).

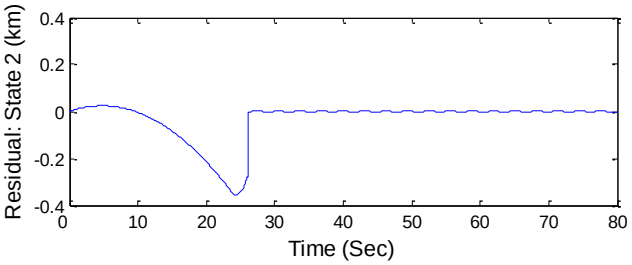

Figure 4: State residual ($e_{S_2}(k) = x_2(k) - \hat{x}_2(k)$).

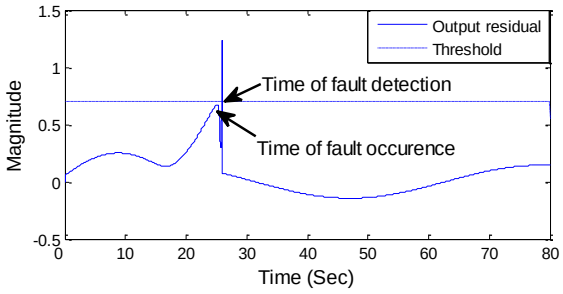

Figure 5: Output residual norm and the detection threshold.

Subsequently, the respective fault parameters are estimated online to learn its evolution as shown in Figs. 6 and 7. Note, in this case of a state fault, the condition (9) of the sensitivity theorem would be satisfied thus initiating the state OLAD. Moreover, from Figs. 6 and 7, it is evident that the parameter estimation error converges asymptotically. Additionally, failure thresholds on each of the parameters are assumed as shown in the figure. Usually, such thresholds could be derived from the design specification or system

operation. The failure thresholds on $\theta_3(k)$ and $\theta_4(k)$ are taken as 1.55 and 0.57 units respectively.

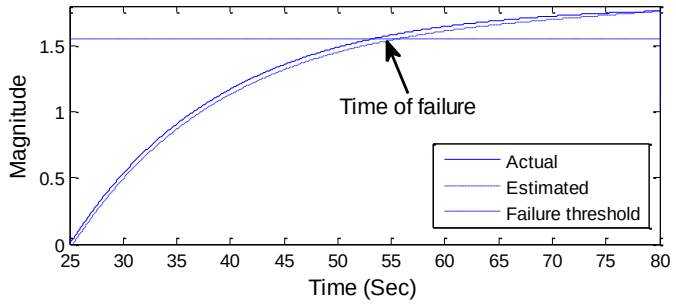

Figure 6: Online estimation of the fault parameter $\theta_3(k)$.

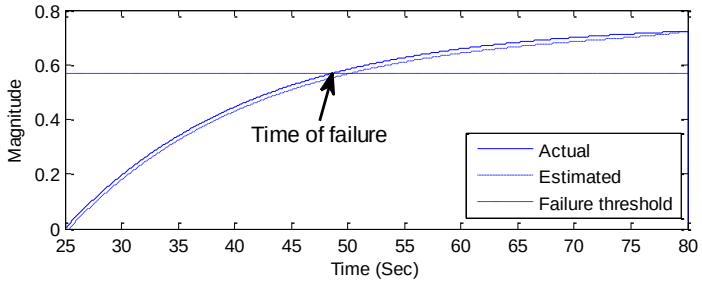

Figure 7: Online estimation of the fault parameter $\theta_4(k)$.

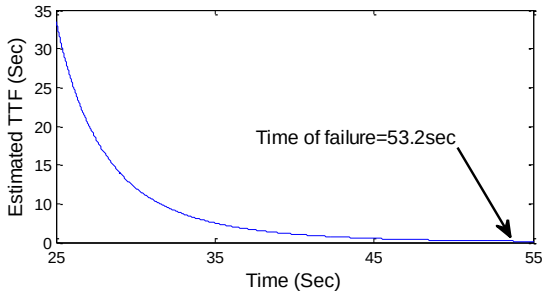

Figure 8: The TTF determination due to the state fault $g_{s_3}(.)$.

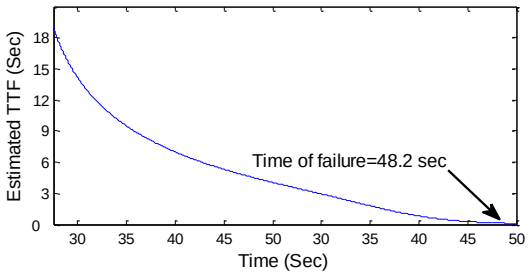

Figure 9: The TTF determination due to the state fault $g_{s_4}(.)$.

Using these failure thresholds on the parameters, we estimate the TTF for each parameter as shown in Figs. 8 and 9. Since we have two parameters, we consider the minimum of both the estimated TTF's at each time instant. Hence by using Figs. 8 and 9 the remaining useful life of the monitored system could be estimated. It is also observed that the TTF prediction coincides with the actual time of failure.

This simulation result demonstrates the fact that the proposed FDP scheme could detect and learn the unknown fault dynamics and predict TTF.

Scenario 2- Output fault: In this simulation scenario, a sensor fault is assumed on the system (14), which is described by $g_y(u(k)) = \theta_y^T(k)\phi_y(u(k))$, where $\phi_y^T(u(k)) = \left[\cos(\omega_y u_1(k)) \quad \sin(\omega_y u_2(k))\right]^T$, $\omega_y = 0.1$, $\theta_y(k) = \begin{bmatrix} \theta_{y_1}(k) & 0 \\ 0 & \theta_{y_2}(k) \end{bmatrix}$. We assume the fault has occurred on the output, $y_1(k)$. Therefore, $\theta_{y_2}(k) = 0$ and $\theta_{y_1}(k) = \begin{cases} 0 & for\, 0 < k < k_0 \\ 25(1 - e^{-0.3(k-k_0)}) & k \geq k_0 \end{cases}$, where the fault is seeded at $k_0 = 23\,\text{sec}$. The output OLAD used for the online learning of the output fault dynamics is given

by $g_y(u(k), \hat{\theta}_y(k)) = \hat{\theta}_y^T(k)\phi_y(u(k))$, where $\hat{\theta}_y(k) = \begin{bmatrix} \hat{\theta}_{y_{11}}(k) & \hat{\theta}_{y_{12}}(k) \\ \hat{\theta}_{y_{21}}(k) & \hat{\theta}_{y_{22}}(k) \end{bmatrix}$ is the estimated parameters matrix. Additionally, the parameter $\hat{\theta}_y(k)$ is tuned online using the update law (4) by taking $\alpha_y = 0.6$ and $\gamma_y = 0.0028$. Also, the initial values of the parameters are assumed to be zero. The robust adaptive term is defined by $v_{y_r}(k) = \dfrac{\hat{\theta}_y^T(k)B_2}{B_2^T\hat{\theta}_y(k)\hat{\theta}_y^T(k)B_2 + c_y}$, where, $B_2^T = [0.23 \quad 0.0001]^T$, and $c_y = 0.7$. For this simulation, the output uncertainty is defined by $\eta_y(x(k), u(k)) = [\sin(0.05k), 0]^T$. In addition, Gaussian/white measurement noise with a magnitude of 0.15 units in the output $y_2(k)$ is introduced. Moreover, we have $\eta_s^T(x(k), u(k)) = [0 \quad 0 \quad 0 \quad 0]^T$, $g_s^T(y(k), u(k)) = [0 \quad 0 \quad 0 \quad 0]^T$, $\hat{g}_s(\hat{y}(k), u(k); \hat{\theta}_s(k)) = [0 \quad 0 \quad 0 \quad 0]^T$, and $v_{s_r}^T(k) = [0 \quad 0 \quad 0 \quad 0]^T$.

Figs. 10 and 11 represent the state residuals where the residuals converge asymptotically to zero with no faults and in the absence of state uncertainties. This implies that the proposed FD estimator follows the actual system accurately under these conditions. Additionally, these results are consistent with the theoretical conclusions. Since, an output uncertainty is considered and to avoid false alarms, a constant threshold of 1.1 unit magnitude (in this case, since there are no state uncertainties, i.e., $\tilde{\eta}_s \approx 0$, additionally, $\mu_{y_1} \approx 1 \times 10^{-5}$, $\mu_{y_2} = 1$, and $\tilde{\eta}_y = 1$, therefore, $\varepsilon \approx 1.1$ is a conservative bound) is used on the output residual as shown in Fig. 12. In the event of a fault, the output residual norm exceeds the threshold. Subsequently, the online estimation of the output fault parameter is shown in Fig. 13 where the fault is found to evolve with time. Here only one parameter estimate and its corresponding threshold are shown due to space constraints.

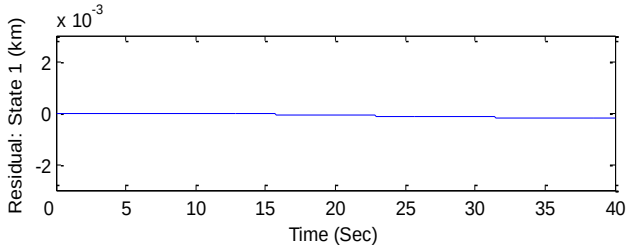

Figure 10: State residual $e_{s_1}(k) = x_1(k) - \hat{x}_1(k)$.

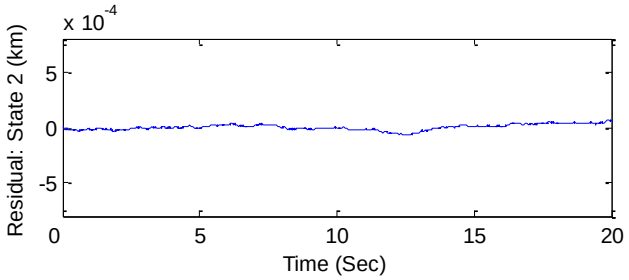

Figure 11: State residual $e_{s_2}(k) = x_2(k) - \hat{x}_2(k)$.

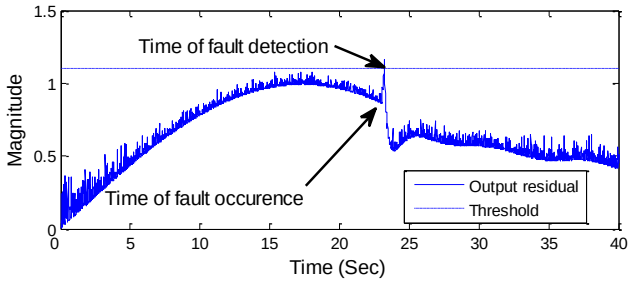

Figure 12: Output residual norm and the detection threshold.

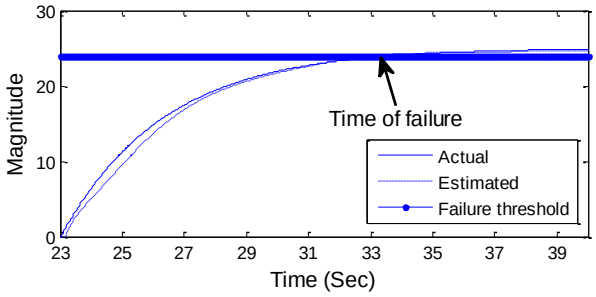

Figure 13: Online estimation of the fault parameter ($\theta_y(k)$).

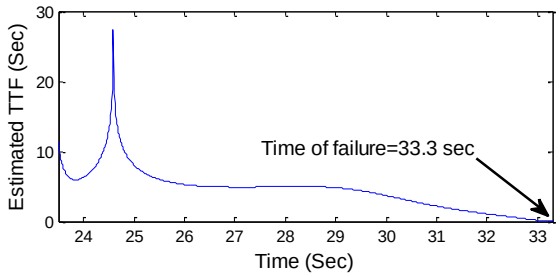

Figure 14: The TTF determination after the output fault.

Using similar arguments from the previous simulation, for an output fault, the condition in (10) of the sensitivity theorem would be satisfied. Therefore, the output OLAD would be appropriate in learning the unknown output fault. However, by assuming a failure threshold limit of 24 units on the output fault parameter, we determine the TTF. Based on this estimate, the TTF due to the output fault is calculated as shown in Fig. 14. The variations in the initial few seconds of the prediction could be attributed to the initial parameter values and adaptation gains. However, as the learning of the unknown fault function improves, the TTF estimation is found to be satisfactory and approaches the actual time of failure.

Through this simulation, the performance of the proposed FDP scheme is demonstrated satisfactorily. Although, the case of simultaneously occurring state and output faults have not been presented here, but by performing a separate simulation, the results were observed to be satisfactory. Thus a unified scheme such as the proposed one could detect an unknown fault, learn its dynamics, and provides the TTF. This information is vital for planning maintenance and thus would avoid catastrophic failures.

VII. Conclusions and Future Work

In this paper, a robust model-based FDP scheme for nonlinear discrete-time MIMO system was developed. Mathematical results show asymptotic stability of the proposed FDP scheme. Improved stability results were obtained by using mild assumptions on the approximation errors and the use of robust adaptive terms which are functions of the OLAD parameters. The conditions under which the state and output faults can be detected are mathematically given and a fault diagnosis scheme is introduced based on the sensitivity theorem and OLAD outputs. Also, a parameter-based TTF scheme was developed and demonstrated. Finally, simulation results illustrate the satisfactory performance of the FDP scheme and the stability results. Future effort includes the development of an online fault prognosis scheme with root-cause analysis for such class of nonlinear MIMO systems. Another future effort includes experimental verification of the proposed detection and prediction scheme.

Appendix

Proof of Theorem 1: During the time interval when the state fault occurs and prior to the OLAD initiation, the state residual dynamics $e_s(k)$ and the output residual dynamics $e_y(k)$ satisfy

$$e_s(k+1) = A_0 e_s(k) + \eta_s(x(k),u(k)) + \tilde{\varphi}_s(k) + \Pi_s(k-T_s) f_s(y(k),u(k)) + K\eta_y(x(k),u(k))$$

$$e_y(k) = Ce_s(k) + \eta_y(x(k),u(k)) \tag{A.1}$$

For anytime $k_s > 0$, the solution of (A.1) is given by

$$e_y(T_s+k_s) = Ce_s(T_s+k_s) + \eta_y(x(T_s+k_s),u(T_s+k_s))$$

$$= \sum_{i=T_s}^{T_s+k_s} CA_0^{(T_s+k_s-i)}(\eta_s(x(i-1),u(i-1)) + \tilde{\varphi}_s(i-1) + K\eta_y(x(i-1),u(i-1))) + \eta_y(x(T_s+k_s),u(T_s+k_s))$$

$$+ \sum_{i=T_s}^{T_s+k_s} CA_0^{(T_s+k_s-i)} \Pi_s(i-T_s) f_s(y(i-1),u(i-1))$$

By using triangle inequality and with some manipulation, we get

$$\left\| e_y(T_s+k_s) \right\| \geq -\varepsilon + \frac{1}{\mu_{y_2}} \left\| \sum_{i=T_s}^{T_s+k_s} CA_0^{(T_s+k_s-i)} \Pi_s(i-T_s) f_s(y(i-1),u(i-1)) \right\|$$

If the condition in (9) is satisfied then a state fault is detected, i.e., $\left\| e_y(T_s+k_s) \right\| \geq \varepsilon$. Next, during the time interval when the output fault occurs and prior to the adaptation of the online approximator, the residuals are given by

$$e_s(k+1) = A_0 e_s(k) + \eta_s(x(k),u(k)) + K\eta_y(x(k),u(k)) + \tilde{\varphi}_s(k) + K\Pi_y(k-T_y) f_y(u(k))$$

$$e_y(k) = Ce_s(k) + \eta_y(x(k),u(k)) + \Pi_y(k-T_y) f_y(u(k)) \tag{A.2}$$

Similarly for anytime $k_y > 0$, the solution of (A.2) is given by

$$e_y(T_y + k_y) = Ce_s(T_y + k_y) + \eta_y(x(T_y + k_y), u(T_y + k_y)) + \Pi_y(k_y) f_y(u(T_y + k_y))$$

$$= \sum_{i=T_y}^{T_y+k_y} CA_0^{(T_y+k_y-i)}[\eta_s(x(i-1), u(i-1)) + \tilde{\varphi}_s(i-1) + K\eta_y(x(i-1), u(i-1))] + \eta_y(x(T_y + k_y), u(T_y + k_y))$$

$$+\Pi_y(k_y) f_y(u(T_y + k_y)) + \sum_{i=T_y}^{T_y+k_y} CA_0^{(T_y+k_y-i)} K\Pi_y(i - T_y) f_y(u(i-1))$$

By using triangle inequality, we have

$$\left\| e_y(T_y + k_y) \right\| \geq -\varepsilon + \frac{1}{\mu_{y_2}} \left\| \Pi_y(k_y) f_y(u(T_y + k_y)) + \sum_{i=T_y}^{T_y+k_y} CA_0^{(T_y+k_y-i)} K\Pi_y(i - T_y) f_y(u(i-1)) \right\|$$

As long as the condition (10) holds, an output fault will be detectable, i.e., $\left\| e_y(T_y + k_y) \right\| \geq \varepsilon$.

Proof of Theorem 2: Let us assume that for a finite time interval $0 < k_1 < T$, $\left\| e_y(k) \right\| < \varepsilon$ for $k < k_1$ and

$$e_y(k_1) = \varepsilon \tag{A.3}$$

From the continuity of $e_y(k)$ and the adaptive laws (3) and (4), the parameters of the OLAD scheme and the robust term will not be updated or adapted in the interval $[0, k_1)$. Hence in the time interval $[0, k_1)$ the residuals $e_s(k)$ and $e_y(k)$ satisfy

$$e_s(k+1) = A_0 e_s(k) + \tilde{\varphi}_s(k) + \eta_s(x(k), u(k)) + Ke_y(k)$$

$$e_y(k) = Ce_s(k) + \eta_y(x(k), u(k))$$

The solution of $e_y(k)$ is given as

$$\left\|e_y(k_1)\right\| = \left\|\sum_{i=0}^{k_1} CA_0^{(k_1-i)}[\eta_s(x(i-1),u(i-1)+\tilde{\varphi}_s(i-1)+K\eta_y(x(i-1),u(i-1))]+\eta_y(x(i-1),u(i-1))\right\|$$

$$< \frac{\left\|C\sum_{j=0}^{k} A_0^{k-j}\right\|}{\left\|C\sum_{j=0}^{k} A_0^{k-j}\right\|(1+c_g)}\tilde{\eta}_s + \frac{\left\|C\sum_{j=0}^{k} A_0^{k-j}K\right\|}{\left\|C\sum_{j=0}^{k} A_0^{k-j}\right\|(1+c_g)}\tilde{\eta}_y + \frac{1}{\left\|C\sum_{j=0}^{k} A_0^{k-j}\right\|(1+c_g)}\tilde{\eta}_y = \mu_s\tilde{\eta}_s + (\mu_{y_1}+\mu_{y_2})\tilde{\eta}_y = \varepsilon$$

Thus the above step contradicts our assumption in (A.3). Hence, we conclude that in the time interval $k \in [0,T)$ the output residual $e_y(k)$ remains within the threshold. Consequently, it can be deduced that the scheme is robust and the output of the OLAD remains zero prior to the fault. This also implies that the robust term would remain zero prior to the fault.

Proof of Lemma 1: Consider the state residual dynamics in (11), which is given by

$$e_s(k+1) = A_0 e_s(k) + \eta_s(x(k),u(k)) + \Psi_s(k) + \varepsilon_s(k) + K\eta_y(x(k),u(k))$$

$$+K\Psi_y(k) + K\varepsilon_y(k) + Kv_y(k) - K\frac{\left(\theta_y^T B_2 - C_4\right)}{B_2^T\hat{\theta}_y(k)\hat{\theta}_y^T(k)B_2 + c_y} + \tilde{\varphi}_s(k) + v_s(k) - \frac{(\theta_s^T B_1 - C_3)}{B_1^T\hat{\theta}_s(k)\hat{\theta}_s^T(k)B_1 + c_s},$$

Solving for $e_s(k)$, we have

$$e_s(k) = A_0^k e_s(0) + \sum_{j=0}^{k} A_0^{k-j}\left[\eta_s(x(j),u(j)) + \tilde{\theta}_s^T(j)\phi_s(j) + \varepsilon_s(j) + K\eta_y(x(j),u(j)) + K\tilde{\theta}_y^T(j)\phi_y(j) + K\varepsilon_y(j) + \tilde{\varphi}_s(j)\right.$$

$$\left.+K\frac{\left(\tilde{\theta}_y^T(j)B_2 - C_4\right)}{B_2^T\hat{\theta}_y(j)\hat{\theta}_y^T(j)B_2 + c_y} + \frac{\left(\tilde{\theta}_s^T(j)B_1 - C_3\right)}{B_1^T\hat{\theta}_s(j)\hat{\theta}_s^T(j)B_1 + c_s} - \frac{(\theta_s^T B_1 - C_3)}{B_1^T\hat{\theta}_s(j)\hat{\theta}_s^T(j)B_1 + c_s} - K\frac{\left(\theta_y^T B_2 - C_4\right)}{B_2^T\hat{\theta}_y(j)\hat{\theta}_y^T(j)B_2 + c_y}\right]$$

The above equation could be written as

$$\sum_{j=0}^{k} A_0^{k-j}\left[\eta_s(x(j),u(j)) + \varepsilon_s(j) + K\eta_y(x(j),u(j)) + K\varepsilon_y(j) + \tilde{\varphi}_s(j)\right]$$

$$= e_s(k) - A_0^k e_s(0) - \sum_{j=0}^{k} A_0^{k-j} \left[\tilde{\theta}_s^T(j)\phi_s(j) + K\tilde{\theta}_y^T(j)\phi_y(j) \right.$$

$$\left. + K\frac{\left(\tilde{\theta}_y^T(j)B_2 - C_4\right)}{B_2^T\hat{\theta}_y(j)\hat{\theta}_y^T(j)B_2 + c_y} + \frac{\left(\tilde{\theta}_s^T(j)B_1 - C_3\right)}{B_1^T\hat{\theta}_s(j)\hat{\theta}_s^T(j)B_1 + c_s} - \frac{(\theta_s^T B_1 - C_3)}{B_1^T\hat{\theta}_s(j)\hat{\theta}_s^T(j)B_1 + c_s} - K\frac{\left(\theta_y^T B_2 - C_4\right)}{B_2^T\hat{\theta}_y(j)\hat{\theta}_y^T(j)B_2 + c_y} \right]$$

Next, we apply the Frobenius norm to get

$$\left\|\sum_{j=0}^{k} A_0^{k-j}\eta_s(x(j),u(j))\right\| + \left\|\sum_{j=0}^{k} A_0^{k-j}\varepsilon_s(j)\right\| + \left\|\sum_{j=0}^{k} A_0^{k-j}K\eta_y(x(j),u(j))\right\| + \left\|\sum_{j=0}^{k} A_0^{k-j}K\varepsilon_y(j)\right\| + \left\|\sum_{j=0}^{k} A_0^{k-j}\tilde{\varphi}_s(j)\right\|$$

$$\leq \left\|e_s(k)\right\| + \left\|A_0^k e_s(0)\right\| + \left\|\sum_{j=0}^{k} A_0^{k-j}\tilde{\theta}_s^T(j)\phi_s(j)\right\| + \left\|\sum_{j=0}^{k} A_0^{k-j}K\tilde{\theta}_y^T(j)\phi_y(j)\right\|$$

$$+ \left\|\sum_{j=0}^{k} A_0^{k-j}K\frac{\tilde{\theta}_y^T(j)B_2}{B_2^T\hat{\theta}_y(j)\hat{\theta}_y^T(j)B_2 + c_y}\right\| + \left\|\sum_{j=0}^{k} A_0^{k-j}\frac{\tilde{\theta}_s^T(j)B_1}{B_1^T\hat{\theta}_s(j)\hat{\theta}_s^T(j)B_1 + c_s}\right\|$$

$$+ \left\|\sum_{j=0}^{k} A_0^{k-j}\frac{\theta_s^T B_1}{B_1^T\hat{\theta}_s(j)\hat{\theta}_s^T(j)B_1 + c_s}\right\| + \left\|\sum_{j=0}^{k} A_0^{k-j}K\frac{\theta_y^T B_2}{B_2^T\hat{\theta}_y(j)\hat{\theta}_y^T(j)B_2 + c_y}\right\| \qquad \text{(A.4)}$$

The summation term in the above equation could be solved as $\left\|\sum_{j=0}^{k} A_0^{k-j}\tilde{\theta}_s^T(j)\phi_s(j)\right\| \leq \frac{\phi_{s_{\max}}\left\|\tilde{\theta}_s(k)\right\|}{(1 - A_{0_{\max}})}$. Constricting $A_{0_{\max}} < 0.5$ in the unit disc (where $A_{0_{\max}} = \lambda_{\max}(A_0)$, is the maximum eigen value), will make the FD scheme even more stable. Then it can be written as $\frac{\phi_{s_{\max}}\left\|\tilde{\theta}_s(k)\right\|}{(1 - A_{0_{\max}})} \leq \frac{\phi_{s_{\max}}\left\|\tilde{\theta}_s(k)\right\|}{A_{0_{\max}}}$. In addition, similar result could be derived for the other terms.

Also, $\frac{\tilde{\theta}_s^T(k)B_1}{B_1^T\hat{\theta}_s(k)\hat{\theta}_s^T(k)B_1 + c_s} \le \tilde{\theta}_s^T(k)B_1$, $\frac{\tilde{\theta}_y^T(k)B_2}{B_2^T\hat{\theta}_y(k)\hat{\theta}_y^T(k)B_2 + c_y} \le \tilde{\theta}_y^T(k)B_2$, and thus (A.4) could be rewritten as

$$\frac{\|\eta_s(x,u)\|}{A_{0_{\max}}} + \frac{\|\varepsilon_s(k)\|}{A_{0_{\max}}} + \frac{\|\eta_y(x,u)\|K_{\max}}{A_{0_{\max}}} + \frac{\|\varepsilon_y(k)\|K_{\max}}{A_{0_{\max}}} + \frac{c_g\|\eta_y(x,u)\|}{A_{0_{\max}}} + \frac{c_g\|\varepsilon_y(k)\|}{A_{0_{\max}}} \le \|e_s(k)\| + \|A_0^k e_s(0)\|$$

$$+ \frac{\|\tilde{\theta}_s(k)\|\phi_{s_{\max}}}{A_{0_{\max}}} + \frac{\|\tilde{\theta}_y(k)\|K_{\max}\phi_{y_{\max}}}{A_{0_{\max}}} + \frac{\|\theta_y\|K_{\max}B_{2_{\max}}}{A_{0_{\max}}}$$

$$+ \frac{\|\tilde{\theta}_y(k)\|K_{\max}B_{2_{\max}}}{A_{0_{\max}}} + \frac{\|Ce_s(k)\|c_g}{A_{0_{\max}}} + \frac{\|\tilde{\theta}_y(k)\|c_g\phi_{y_{\max}}}{A_{0_{\max}}} + \frac{\|\tilde{\theta}_y(k)\|c_gB_{2_{\max}}}{A_{0_{\max}}} + \frac{\|\tilde{\theta}_s(k)\|B_{1_{\max}}}{A_{0_{\max}}} + \frac{\|\theta_s\|B_{1_{\max}}}{A_{0_{\max}}}$$

Square and multiply 6 on both sides of the above equation, we have

$$6\left[\frac{\|\eta_s(x,u)\|}{A_{0_{\max}}} + \frac{\|\varepsilon_s(k)\|}{A_{0_{\max}}} + \frac{\|\eta_y(x,u)\|K_{\max}}{A_{0_{\max}}} + \frac{\|\varepsilon_y(k)\|K_{\max}}{A_{0_{\max}}} + \frac{c_g\|\eta_y(x,u)\|}{A_{0_{\max}}} + \frac{c_g\|\varepsilon_y(k)\|}{A_{0_{\max}}}\right]^2 \le 6\left[\|e_s(k)\| + \|A_0^k e_s(0)\|\right.$$

$$+ \frac{\|\tilde{\theta}_s(k)\|\phi_{s_{\max}}}{A_{0_{\max}}} + \frac{\|\tilde{\theta}_y(k)\|K_{\max}\phi_{y_{\max}}}{A_{0_{\max}}}$$

$$+ \frac{\|\tilde{\theta}_y(k)\|K_{\max}B_{2_{\max}}}{A_{0_{\max}}} + \frac{\|Ce_s(k)\|c_g}{A_{0_{\max}}} + \frac{\|\tilde{\theta}_y(k)\|c_g\phi_{y_{\max}}}{A_{0_{\max}}} + \frac{\|\tilde{\theta}_y(k)\|c_gB_{2_{\max}}}{A_{0_{\max}}} + \frac{\|\tilde{\theta}_s(k)\|B_{1_{\max}}}{A_{0_{\max}}} + \frac{\|\theta_s\|B_{1_{\max}}}{A_{0_{\max}}}$$

$$\left. + \frac{c_g\|\theta_y\|B_{2_{\max}}}{A_{0_{\max}}} + \frac{\|\theta_y\|K_{\max}B_{2_{\max}}}{A_{0_{\max}}}\right]^2$$

Take $d_0 = \|A_0^k e_s(0)\| + \frac{\|\theta_s\|B_{1_{\max}}}{A_{0_{\max}}} + \frac{\|\theta_y\|K_{\max}B_{2_{\max}}}{A_{0_{\max}}} + \frac{c_g\|\theta_y\|B_{2_{\max}}}{A_{0_{\max}}}$,

$d_1 = \frac{c_g C_{\max}}{A_{0_{\max}}} + 1$, $d_2 = \frac{B_{1_{\max}}}{A_{0_{\max}}} + \frac{\phi_{s_{\max}}}{A_{0_{\max}}}$, and $d_3 = \frac{\phi_{y_{\max}} K_{\max}}{A_{0_{\max}}} + \frac{K_{\max} B_{2_{\max}}}{A_{0_{\max}}} + \frac{\phi_{y_{\max}} c_g}{A_{0_{\max}}} + \frac{c_g B_{2_{\max}}}{A_{0_{\max}}}$. Then expand the term on the right hand side of the above equation and factoring $A^2_{0_{\max}}$, we have

$$6\left[\left\|\eta_s(x,u)\right\| + \left\|\varepsilon_s(k)\right\| + \left\|\eta_y(x,u)\right\| K_{\max} + \left\|\varepsilon_y(k)\right\| K_{\max} + c_g \left\|\eta_y(x,u)\right\| + c_g \left\|\varepsilon_y(k)\right\|\right]^2$$

$$\leq 6A^2_{0_{\max}} \left(4d_0^2 + 2d_1^2 \left\|e_s(k)\right\|^2 + 2d_2^2 \left\|\tilde{\theta}_s(k)\right\|^2 + 2d_3^2 \left\|\tilde{\theta}_y(k)\right\|^2 + 2d_1 d_2 \left\|\tilde{\theta}_s(k)\right\| \left\|e_s(k)\right\| + 2d_1 d_3 \left\|\tilde{\theta}_y(k)\right\| \left\|e_s(k)\right\|\right)$$

Taking $\beta_0 = 24A^2_{0_{\max}} d_0^2$, $\beta_1 = 12A^2_{0_{\max}} d_1^2$, $\beta_2 = 12A^2_{0_{\max}} d_2^2$, $\beta_3 = 12A^2_{0_{\max}} d_3^2$, $\beta_4 = 12A^2_{0_{\max}} d_1 d_2$, and $\beta_5 = 12A^2_{0_{\max}} d_1 d_3$, to get

$$6\left[\left\|\eta_s(x,u)\right\| + \left\|\varepsilon_s(k)\right\| + \left\|\eta_y(x,u)\right\| K_{\max} + \left\|\varepsilon_y(k)\right\| K_{\max} + c_g \left\|\eta_y(x,u)\right\| + c_g \left\|\varepsilon_y(k)\right\|\right]^2$$

$$\leq \beta_0 + \beta_1 \left\|e_s(k)\right\|^2 + \beta_2 \left\|\tilde{\theta}_s(k)\right\|^2 + \beta_3 \left\|\tilde{\theta}_y(k)\right\|^2 + \beta_4 \left\|e_s(k)\right\| \left\|\tilde{\theta}_s(k)\right\| + \beta_5 \left\|e_s(k)\right\| \left\|\tilde{\theta}_y(k)\right\|$$

In using this lemma, the system uncertainty and the approximation errors are expressed as a function of the state residual and the parameter estimation errors. This lemma and the robust adaptive terms intuitively lead to the negative definiteness of the first difference of the Lyapunov function during the stability analysis of the proposed scheme.

Proof of Theorem 3: Consider the Lyapunov function candidate as

$$V = \frac{1}{12} e_s^T(k) e_s(k) + \frac{1}{\alpha_s} tr[\tilde{\theta}_s^T(k) \tilde{\theta}_s(k)] + \frac{1}{\alpha_y} tr[\tilde{\theta}_y^T(k) \tilde{\theta}_y(k)]$$

The first difference is given by

$$\Delta V = \frac{1}{12} \underbrace{\left[e_s^T(k+1) e_s(k+1) - e_s^T(k) e_s(k)\right]}_{\Delta V_1} + \underbrace{\frac{1}{\alpha_s} tr[\tilde{\theta}_s^T(k+1) \tilde{\theta}_s(k+1) - \tilde{\theta}_s^T(k) \tilde{\theta}_s(k)]}_{\Delta V_2}$$

$$\underbrace{+\frac{1}{\alpha_y} tr[\tilde{\theta}_y^T(k+1)\tilde{\theta}_y(k+1) - \tilde{\theta}_y^T(k)\tilde{\theta}_y(k)]}_{\Delta V_3} \tag{A.5}$$

Substitute $e_s(k+1)$ from (11) in ΔV_1 of (A.5) to render

$$\Delta V_1 = \frac{1}{12}[A_0 e_s(k) + \eta_s(x(k),u(k)) + \Psi_s(k) + \varepsilon_s(k) + K\eta_y(x(k),u(k)) + K\Psi_y(k) + K\varepsilon_y(k) + Kv_y(k)$$

$$-K\frac{\left(\theta_y^T B_2 - C_4\right)}{B_2^T\hat{\theta}_y(k)\hat{\theta}_y^T(k)B_2 + c_y} + \tilde{\varphi}_s(k) + v_s(k) - \frac{(\theta_s^T B_1 - C_3)}{B_1^T\hat{\theta}_s(k)\hat{\theta}_s^T(k)B_1 + c_s}]^T \times$$

$$[A_0 e_s(k) + \eta_s(x(k),u(k)) + \Psi_s(k) + \varepsilon_s(k) + K\eta_y(x(k),u(k)) + K\Psi_y(k) + K\varepsilon_y(k)$$

$$+Kv_y(k) - K\frac{\left(\theta_y^T B_2 - C_4\right)}{B_2^T\hat{\theta}_y(k)\hat{\theta}_y^T(k)B_2 + c_y} + \tilde{\varphi}_s(k) + v_s(k) - \frac{(\theta_s^T B_1 - C_3)}{B_1^T\hat{\theta}_s(k)\hat{\theta}_s^T(k)B_1 + c_s}] - \frac{1}{12}e_s^T(k)e_s(k)$$

Apply the Cauchy-Schwarz inequality $((a_1 + a_2 + ... + a_n)^T(a_1 + a_2 + ... + a_n) \le n(a_1^T a_1 + a_2^T a_2 + .. + a_n^T a_n))$ in the above equation, to get

$$\Delta V_1 \le e_s^T(k)A_0^T A_0 e_s(k) + \eta_s^T(x(k),u(k))\eta_s(x(k),u(k)) + \Psi_s^T(k)\Psi_s(k) + \eta_y^T(x(k),u(k))K^T K\eta_y(x(k),u(k))$$

$$+\Psi_y^T(k)K^T K\Psi_y(k) + v_y^T(k)K^T Kv_y(k) + \varepsilon_y^T(k)K^T K\varepsilon_y(k) + \varepsilon_s^T(k)\varepsilon_s(k) + \tilde{\varphi}_s^T(k)\tilde{\varphi}_s(k)$$

$$+v_s^T(k)v_s(k) + \frac{(\theta_s^T B_1 - C_3)^T(\theta_s^T B_1 - C_3)}{\left(B_1^T\hat{\theta}_s(k)\hat{\theta}_s^T(k)B_1 + c_s\right)^2} + \frac{\left(\theta_y^T B_2 - C_4\right)^T K^T K\left(\theta_y^T B_2 - C_4\right)}{\left(B_2^T\hat{\theta}_y(k)\hat{\theta}_y^T(k)B_2 + c_y\right)^2} - \frac{1}{12}e_s^T(k)e_s(k) \tag{A.6}$$

Substitute the weight update law (3) in ΔV_2 of (A.5) to render

$$\Delta V_2 = \frac{1}{\alpha_s} tr\{[(I - \gamma_s \left\| I - \alpha_s \phi_s(k)\phi_s^T(k) \right\| I)\tilde{\theta}_s(k) - \alpha_s \phi_s(k) e_y^T(k) B$$

$$+\gamma_s \left\| I - \alpha_s \phi_s(k)\phi_s^T(k) \right\| \theta_s]^T \times [(I - \gamma_s \left\| I - \alpha_s \phi_s(k)\phi_s^T(k) \right\| I)\tilde{\theta}_s(k)$$

$$-\alpha_s \phi_s(k) e_y^T(k) B + \gamma_s \left\| I - \alpha_s \phi_s(k)\phi_s^T(k) \right\| \theta_s] - \tilde{\theta}_s^T(k)\tilde{\theta}_s(k)\}$$

Apply the Cauchy-Schwarz inequality $((a_1 + a_2 + ... + a_n)^T (a_1 + a_2 + ... + a_n) \le n(a_1^T a_1 + a_2^T a_2 + .. + a_n^T a_n))$ in the above equation, to reveal

$$\Delta V_2 \le \frac{1}{\alpha_s} tr\{3(I - \gamma_s \left\| I - \alpha_s \phi_s(k)\phi_s^T(k) \right\| I)\tilde{\theta}_s^T(k)\tilde{\theta}_s(k)(I - \gamma_s \left\| I - \alpha_s \phi_s(k)\phi_s^T(k) \right\| I)$$

$$+3\alpha_s^2 \phi_s(k) e_y^T(k) BB^T e_y(k)\phi_s^T(k) + 3\gamma_s^2 \left\| I - \alpha_s \phi_s(k)\phi_s^T(k) \right\|^2 \theta_s^T \theta_s - \tilde{\theta}_s^T(k)\tilde{\theta}_s(k)\}$$

After some mathematical manipulations, the above equation becomes

$$\Delta V_2 \le tr\left\{ \frac{2}{\alpha_s} \tilde{\theta}_s^T(k)\tilde{\theta}_s(k) - \frac{6}{\alpha_s} \gamma_s \left\| I - \alpha_s \phi_s(k)\phi_s^T(k) \right\| \tilde{\theta}_s^T(k)\tilde{\theta}_s(k) \right.$$

$$+ \frac{3}{\alpha_s} \gamma_s^2 \left\| I - \alpha_s \phi_s(k)\phi_s^T(k) \right\|^2 \tilde{\theta}_s^T(k)\tilde{\theta}_s(k) + \frac{3\gamma_s^2}{\alpha_s} \left\| I - \alpha_s \phi_s(k)\phi_s^T(k) \right\|^2 \theta_s^T \theta_s$$

$$\left. +3\alpha_s \phi_s(k) e_y^T(k) BB^T e_y(k)\phi_s^T(k) \right\} \qquad \text{(A.7)}$$

Substitute the weight update law (4) in ΔV_3 of (A.5) to render

$$\Delta V_3 = \frac{1}{\alpha_y} tr\{[(I - \gamma_y \left\| I - \alpha_y \phi_y(k)\phi_y^T(k) \right\| I)\tilde{\theta}_y(k) - \alpha_y \phi_y(k) e_y^T(k)$$

$$+\gamma_y \left\| I - \alpha_y \phi_y(k)\phi_y^T(k) \right\| \theta_y]^T \times [(I - \gamma_y \left\| I - \alpha_y \phi_y(k)\phi_y^T(k) \right\| I)\tilde{\theta}_y(k)$$

$$-\alpha_y \phi_y(k) e_y^T(k) + \gamma_y \left\| I - \alpha_y \phi_y(k)\phi_y^T(k) \right\| \theta_y] - \tilde{\theta}_y^T(k)\tilde{\theta}_y(k)\}$$

Apply the Cauchy-Schwarz inequality

$((a_1 + a_2 + ... + a_n)^T (a_1 + a_2 + ... + a_n) \le n(a_1^T a_1 + a_2^T a_2 + .. + a_n^T a_n))$ in the above equation, to reveal

$$\Delta V_3 \le \frac{1}{\alpha_y} tr\{3(I - \gamma_y \left\| I - \alpha_y \phi_y(k)\phi_y^T(k) \right\| I)\tilde{\theta}_y^T(k)\tilde{\theta}_y(k)(I - \gamma_y \left\| I - \alpha_y \phi_y(k)\phi_y^T(k) \right\| I) + 3\alpha_y^2 \phi_y(k) e_y^T(k) e_y(k) \phi_y^T(k)$$

$$+3\gamma_y^2 \left\| I - \alpha_y \phi_y(k)\phi_y^T(k) \right\|^2 \theta_y^T \theta_y - \tilde{\theta}_y^T(k)\tilde{\theta}_y(k)\}$$

After some mathematical manipulation, the above equation becomes

$$\Delta V_3 \le tr\left\{ \frac{2}{\alpha_y} \tilde{\theta}_y^T(k)\tilde{\theta}_y(k) - \frac{6}{\alpha_y} \gamma_y \left\| I - \alpha_y \phi_y(k)\phi_y^T(k) \right\| \tilde{\theta}_y^T(k)\tilde{\theta}_y(k) \right.$$

$$\left. + \frac{3}{\alpha_y} \gamma_y^2 \left\| I - \alpha_y \phi_y(k)\phi_y^T(k) \right\|^2 \tilde{\theta}_y^T(k)\tilde{\theta}_y(k) + 3\alpha_y \phi_y(k) e_y^T(k) e_y(k) \phi_y^T(k) + \frac{3\gamma_y^2}{\alpha_y} \left\| I - \alpha_y \phi_y(k)\phi_y^T(k) \right\|^2 \theta_y^T \theta_y \right\} \quad \text{(A.8)}$$

Since $\Delta V = \Delta V_1 + \Delta V_2 + \Delta V_3$, combining (A.6)-(A.8), to get

$$\Delta V \le e_s^T(k) A_0^T A_0 e_s(k) + \eta_s^T(x(k), u(k))\eta_s(x(k), u(k)) + \Psi_s^T(k)\Psi_s(k)$$

$$+\eta_y^T(x(k), u(k)) K^T K \eta_y(x(k), u(k)) + \Psi_y^T(k) K^T K \Psi_y(k) + \tilde{\varphi}_s^T(k)\tilde{\varphi}_s(k)$$

$$+v_y^T(k) K^T K v_y(k) + \varepsilon_y^T(k) K^T K \varepsilon_y(k) + \varepsilon_s^T(k)\varepsilon_s(k) + v_s^T(k) v_s(k)$$

$$+\frac{(\theta_s^T B_1 - C_3)^T (\theta_s^T B_1 - C_3)}{\left(B_1^T \hat{\theta}_s(k)\hat{\theta}_s^T(k) B_1 + c_s\right)^2} + \frac{\left(\theta_y^T B_2 - C_4\right)^T K^T K \left(\theta_y^T B_2 - C_4\right)}{\left(B_2^T \hat{\theta}_y(k)\hat{\theta}_y^T(k) B_2 + c_y\right)^2} - \frac{1}{12} e_s^T(k) e_s(k)$$

$$+tr\left\{ \frac{2}{\alpha_s} \tilde{\theta}_s^T(k)\tilde{\theta}_s(k) - \frac{6}{\alpha_s} \gamma_s \left\| I - \alpha_s \phi_s(k)\phi_s^T(k) \right\| \tilde{\theta}_s^T(k)\tilde{\theta}_s(k) + \frac{3}{\alpha_s} \gamma_s^2 \left\| I - \alpha_s \phi_s(k)\phi_s^T(k) \right\|^2 \tilde{\theta}_s^T(k)\tilde{\theta}_s(k) \right.$$

$$\left. + \underbrace{3\alpha_s \phi_s(k) e_y^T(k) B B^T e_y(k) \phi_s^T(k)}_{1} + \frac{3\gamma_s^2}{\alpha_s} \left\| I - \alpha_s \phi_s(k)\phi_s^T(k) \right\|^2 \theta_s^T \theta_s \right\} + tr\left\{ \frac{2}{\alpha_y} \tilde{\theta}_y^T(k)\tilde{\theta}_y(k) \right.$$

$$-\frac{6}{\alpha_y}\gamma_y\left\|I-\alpha_y\phi_y(k)\phi_y^T(k)\right\|\tilde{\theta}_y^T(k)\tilde{\theta}_y(k)+\frac{3}{\alpha_y}\gamma_y^2\left\|I-\alpha_y\phi_y(k)\phi_y^T(k)\right\|^2\tilde{\theta}_y^T(k)\tilde{\theta}_y(k)$$

$$+\underbrace{3\alpha_y\phi_y(k)e_y^T(k)e_y(k)\phi_y^T(k)}_{1}+\frac{3\gamma_y^2}{\alpha_y}\left\|I-\alpha_y\phi_y(k)\phi_y^T(k)\right\|^2\theta_y^T\theta_y\Bigg\} \tag{A.9}$$

Consider the terms numbered as 1 in the above equation, apply the trace operator and using the Cauchy-Schwarz inequality $((a_1+a_2+...+a_n)^T(a_1+a_2+...+a_n)\le n(a_1^Ta_1+a_2^Ta_2+..+a_n^Ta_n))$, to renders

$$tr\left\{3\alpha_s\phi_s(k)e_y^T(k)BB^Te_y(k)\phi_s^T(k)+3\alpha_y\phi_y(k)e_y^T(k)e_y(k)\phi_y^T(k)\right\}$$

$$\le 18\alpha_s\phi_s^T(k)\phi_s(k)e_s^T(k)C^TBB^TCe_s(k)+18\alpha_s\phi_s^T(k)\phi_s(k)\Psi_y^T(k)BB^T\Psi_y(k)$$

$$+18\alpha_s\phi_s^T(k)\phi_s(k)\eta_y^T(x(k),u(k))BB^T\eta_y(x(k),u(k))+18\alpha_s\phi_s^T(k)\phi_s(k)\frac{\left(\theta_y^TB_2-C_4\right)^TBB^T\left(\theta_y^TB_2-C_4\right)}{\left(B_2^T\hat{\theta}_y(k)\hat{\theta}_y^T(k)B_2+c_y\right)^2}$$

$$+18\alpha_s\phi_s^T(k)\phi_s(k)\varepsilon_y^T(k)BB^T\varepsilon_y(k)+18\alpha_s\phi_s^T(k)\phi_s(k)v_y^T(k)BB^Tv_y(k)$$

$$+18\alpha_y\phi_y^T(k)\phi_y(k)e_s^T(k)C^TCe_s(k)+18\alpha_y\phi_y^T(k)\phi_y(k)$$

$$\frac{\left(\theta_y^TB_2-C_4\right)^T\left(\theta_y^TB_2-C_4\right)}{\left(B_2^T\hat{\theta}_y(k)\hat{\theta}_y^T(k)B_2+c_y\right)^2}+18\alpha_y\phi_y^T(k)\phi_y(k)\eta_y^T(x(k),u(k))\eta_y(x(k),u(k))$$

$$+18\alpha_y\phi_y^T(k)\phi_y(k)v_y^T(k)v_y(k)+18\alpha_y\phi_y^T(k)\phi_y(k)\Psi_y^T(k)\Psi_y(k)+18\alpha_y\phi_y^T(k)\phi_y(k)\varepsilon_y^T(k)\varepsilon_y(k)$$

Incorporating the above modification in (A.9) to render

$$\Delta V\le e_s^T(k)A_0^TA_0e_s(k)+\eta_s^T(x(k),u(k))\eta_s(x(k),u(k))+\Psi_s^T(k)\Psi_s(k)+\eta_y^T(x(k),u(k))K^TK\eta_y(x(k),u(k))+\Psi_y^T(k)K^TK\Psi_y(k)$$

$$+\tilde{\varphi}_s^T(k)\tilde{\varphi}_s(k)+v_y^T(k)K^TKv_y(k)+\varepsilon_y^T(k)K^TK\varepsilon_y(k)+\varepsilon_s^T(k)\varepsilon_s(k)+v_s^T(k)v_s(k)$$

$$+\underbrace{\frac{(\theta_s^T B_1 - C_3)^T(\theta_s^T B_1 - C_3)}{\left(B_1^T\hat{\theta}_s(k)\hat{\theta}_s^T(k)B_1 + c_s\right)^2}}_{1} + \underbrace{\frac{\left(\theta_y^T B_2 - C_4\right)^T K^T K\left(\theta_y^T B_2 - C_4\right)}{\left(B_2^T\hat{\theta}_y(k)\hat{\theta}_y^T(k)B_2 + c_y\right)^2}}_{1} - \frac{1}{12}e_s^T(k)e_s(k)$$

$$+tr\left\{\frac{2}{\alpha_s}\tilde{\theta}_s^T(k)\tilde{\theta}_s(k) - \frac{6}{\alpha_s}\gamma_s\left\|I-\alpha_s\phi_s(k)\phi_s^T(k)\right\|\tilde{\theta}_s^T(k)\tilde{\theta}_s(k) + \frac{3}{\alpha_s}\gamma_s^2\left\|I-\alpha_s\phi_s(k)\phi_s^T(k)\right\|^2\tilde{\theta}_s^T(k)\tilde{\theta}_s(k)\right.$$

$$\left.+\frac{3\gamma_s^2}{\alpha_s}\left\|I-\alpha_s\phi_s(k)\phi_s^T(k)\right\|^2\theta_s^T\theta_s\right\} + tr\left\{\frac{2}{\alpha_y}\tilde{\theta}_y^T(k)\tilde{\theta}_y(k) - \frac{6}{\alpha_y}\gamma_y\left\|I-\alpha_y\phi_y(k)\phi_y^T(k)\right\|\tilde{\theta}_y^T(k)\tilde{\theta}_y(k)\right.$$

$$\left.+\frac{3}{\alpha_y}\gamma_y^2\left\|I-\alpha_y\phi_y(k)\phi_y^T(k)\right\|^2\tilde{\theta}_y^T(k)\tilde{\theta}_y(k) + \frac{3\gamma_y^2}{\alpha_y}\left\|I-\alpha_y\phi_y(k)\phi_y^T(k)\right\|^2\theta_y^T\theta_y\right\}$$

$$+18\alpha_s\phi_s^T(k)\phi_s(k)e_s^T(k)C^T BB^T Ce_s(k) + 18\alpha_s\phi_s^T(k)\phi_s(k)\Psi_y^T(k)BB^T\Psi_y(k)$$

$$+18\alpha_s\phi_s^T(k)\phi_s(k)\eta_y^T(x(k),u(k))BB^T\eta_y(x(k),u(k)) + \underbrace{18\alpha_s\phi_s^T(k)\phi_s(k)\frac{\left(\theta_y^T B_2 - C_4\right)^T BB^T\left(\theta_y^T B_2 - C_4\right)}{\left(B_2^T\hat{\theta}_y(k)\hat{\theta}_y^T(k)B_2 + c_y\right)^2}}_{1}$$

$$+18\alpha_s\phi_s^T(k)\phi_s(k)v_y^T(k)BB^T v_y(k) + 18\alpha_s\phi_s^T(k)\phi_s(k)\varepsilon_y^T(k)BB^T\varepsilon_y(k) + 18\alpha_y\phi_y^T(k)\phi_y(k)e_s^T(k)C^T Ce_s(k)$$

$$+18\alpha_y\phi_y^T(k)\phi_y(k)\eta_y^T(x(k),u(k))\eta_y(x(k),u(k)) + \underbrace{18\alpha_y\phi_y^T(k)\phi_y(k)\frac{\left(\theta_y^T B_2 - C_4\right)^T\left(\theta_y^T B_2 - C_4\right)}{\left(B_2^T\hat{\theta}_y(k)\hat{\theta}_y^T(k)B_2 + c_y\right)^2}}_{1}$$

$$+18\alpha_y\phi_y^T(k)\phi_y(k)v_y^T(k)v_y(k) + 18\alpha_y\phi_y^T(k)\phi_y(k)\Psi_y^T(k)\Psi_y(k) + 18\alpha_y\phi_y^T(k)\phi_y(k)\varepsilon_y^T(k)\varepsilon_y(k) \qquad \text{(A.10)}$$

Consider terms numbered as 1 in (A.10), we have

$$\frac{(\theta_s^T B_1 - C_3)^T(\theta_s^T B_1 - C_3)}{\left(B_1^T\hat{\theta}_s(k)\hat{\theta}_s^T(k)B_1 + c_s\right)^2} \le (\theta_s^T B_1 - C_3)^T(\theta_s^T B_1 - C_3) \le (B_1^T\theta_s\theta_s^T B_1 - 2B_1^T\theta_s C_3 + C_3^T C_3) \qquad \text{(A.11)}$$

$$\frac{\left(\theta_y^T B_2 - C_4\right)^T K^T K \left(\theta_y^T B_2 - C_4\right)}{\left(B_2^T \hat{\theta}_y(k) \hat{\theta}_y^T(k) B_2 + c_y\right)^2} \le \left(B_2^T \theta_y K^T K \theta_y^T B_2 - 2B_2^T \theta_y K^T K C_4 + C_4^T K^T K C_4\right) \quad \text{(A.12)}$$

$$18\alpha_s \phi_s^T(k)\phi_s(k) \frac{\left(\theta_y^T B_2 - C_4\right)^T BB^T \left(\theta_y^T B_2 - C_4\right)}{\left(B_2^T \hat{\theta}_y(k) \hat{\theta}_y^T(k) B_2 + c_y\right)^2} \le 18\alpha_s \phi_s^T(k)\phi_s(k)$$

$$\left(B_2^T \theta_y BB^T \theta_y^T B_2 - 2B_2^T \theta_y BB^T C_4 + C_4^T BB^T C_4\right) \quad \text{(A.13)}$$

$$18\alpha_y \phi_y^T(k)\phi_y(k) \frac{\left(\theta_y^T B_2 - C_4\right)^T \left(\theta_y^T B_2 - C_4\right)}{\left(B_2^T \hat{\theta}_y(k) \hat{\theta}_y^T(k) B_2 + c_y\right)^2} \le 18\alpha_y \phi_y^T(k)\phi_y(k)$$

$$\left(B_2^T \theta_y \theta_y^T B_2 - 2B_2^T \theta_y C_4 + C_4^T C_4\right) \quad \text{(A.14)}$$

Consider terms numbered as 2 in (A.10), we have

$$\frac{\left(\tilde{\theta}_y^T(k) B_2 - C_4\right)^T K^T K \left(\tilde{\theta}_y^T(k) B_2 - C_4\right)}{\left(B_2^T \hat{\theta}_y(k) \hat{\theta}_y^T(k) B_2 + c_y\right)^2}$$

$$\le \left(\tilde{\theta}_y^T(k) B_2 - C_4\right)^T K^T K \left(\tilde{\theta}_y^T(k) B_2 - C_4\right) \le 2B_2^T \tilde{\theta}_y(k) K^T K \tilde{\theta}_y^T(k) B_2 + 2C_4^T K^T K C_4 \quad \text{(A.15)}$$

$$\frac{\left(\tilde{\theta}_s^T(k) B_1 - C_3\right)^T \left(\tilde{\theta}_s^T(k) B_1 - C_3\right)}{\left(B_1^T \hat{\theta}_s(k) \hat{\theta}_s^T(k) B_1 + c_s\right)^2} \le \left(\tilde{\theta}_s^T(k) B_1 - C_3\right)^T \left(\tilde{\theta}_s^T(k) B_1 - C_3\right) \le 2B_1^T \tilde{\theta}_s(k) \tilde{\theta}_s^T(k) B_1 + 2C_3^T C_3 \quad \text{(A.16)}$$

$$18\alpha_s \phi_s^T(k)\phi_s(k) \frac{\left(\tilde{\theta}_y^T(k) B_2 - C_4\right)^T BB^T \left(\tilde{\theta}_y^T(k) B_2 - C_4\right)}{\left(B_2^T \hat{\theta}_y(k) \hat{\theta}_y^T(k) B_2 + c_y\right)^2}$$

$$\le 36\alpha_s \phi_s^T(k)\phi_s(k) B_2^T \tilde{\theta}_y(k) BB^T \tilde{\theta}_y^T(k) B_2 + 36\alpha_s \phi_s^T(k)\phi_s(k) C_4^T BB^T C_4 \quad \text{(A.17)}$$

$$18\alpha_y \phi_y^T(k)\phi_y(k) \frac{\left(\tilde{\theta}_y^T(k) B_2 - C_4\right)^T \left(\tilde{\theta}_y^T(k) B_2 - C_4\right)}{\left(B_2^T \hat{\theta}_y(k) \hat{\theta}_y^T(k) B_2 + c_y\right)^2}$$

$$\le 36\alpha_y \phi_y^T(k)\phi_y(k)B_2^T\tilde{\theta}_y(k)\tilde{\theta}_y^T(k)B_2 + 36\alpha_y \phi_y^T(k)\phi_y(k)C_4^T C_4 \quad \text{(A.18)}$$

Using (A.11)-(A.18) in (A.10), we have

$$\Delta V \le e_s^T(k)A_0^T A_0 e_s(k) + \eta_s^T(x(k),u(k))\eta_s(x(k),u(k)) + \Psi_s^T(k)\Psi_s(k)$$

$$+\eta_y^T(x(k),u(k))K^T K\eta_y(x(k),u(k)) + \Psi_y^T(k)K^T K\Psi_y(k) + \tilde{\varphi}_s^T(k)\tilde{\varphi}_s(k) + \varepsilon_y^T(k)K^T K\varepsilon_y(k) + \varepsilon_s^T(k)\varepsilon_s(k)$$

$$-\frac{1}{12}e_s^T(k)e_s(k) + tr\left\{\frac{2}{\alpha_s}\tilde{\theta}_s^T(k)\tilde{\theta}_s(k) - \frac{6}{\alpha_s}\gamma_s\left\|I-\alpha_s\phi_s(k)\phi_s^T(k)\right\|\tilde{\theta}_s^T(k)\tilde{\theta}_s(k) + \frac{3}{\alpha_s}\gamma_s^2\left\|I-\alpha_s\phi_s(k)\phi_s^T(k)\right\|^2 \cdot\right.$$

$$\left.\tilde{\theta}_s^T(k)\tilde{\theta}_s(k) + \frac{3\gamma_s^2}{\alpha_s}\left\|I-\alpha_s\phi_s(k)\phi_s^T(k)\right\|^2\theta_s^T\theta_s\right\} + tr\left\{\frac{2}{\alpha_y}\tilde{\theta}_y^T(k)\tilde{\theta}_y(k) - \frac{6}{\alpha_y}\gamma_y\left\|I-\alpha_y\phi_y(k)\phi_y^T(k)\right\|\tilde{\theta}_y^T(k)\tilde{\theta}_y(k)\right.$$

$$\left.+\frac{3}{\alpha_y}\gamma_y^2\left\|I-\alpha_y\phi_y(k)\phi_y^T(k)\right\|^2\tilde{\theta}_y^T(k)\tilde{\theta}_y(k) + \frac{3\gamma_y^2}{\alpha_y}\left\|I-\alpha_y\phi_y(k)\phi_y^T(k)\right\|^2\theta_y^T\theta_y\right\} + 18\alpha_s\phi_s^T(k)\phi_s(k)e_s^T(k)C^T BB^T Ce_s(k)$$

$$+18\alpha_s\phi_s^T(k)\phi_s(k)\Psi_y^T(k)BB^T\Psi_y(k) + 18\alpha_s\phi_s^T(k)\phi_s(k)\eta_y^T(x(k),u(k))BB^T\eta_y(x(k),u(k))$$

$$+18\alpha_s\phi_s^T(k)\phi_s(k)\varepsilon_y^T(k)BB^T\varepsilon_y(k) + 18\alpha_y\phi_y^T(k)\phi_y(k)\Psi_y^T(k)\Psi_y(k) + 18\alpha_y\phi_y^T(k)\phi_y(k)e_s^T(k)C^T Ce_s(k)$$

$$+18\alpha_y\phi_y^T(k)\phi_y(k)\varepsilon_y^T(k)\varepsilon_y(k) + 18\alpha_y\phi_y^T(k)\phi_y(k)\eta_y^T(x(k),u(k))\eta_y(x(k),u(k))$$

$$+\left(B_2^T\theta_y K^T K\theta_y^T B_2 - 2B_2^T\theta_y K^T KC_4 + C_4^T K^T KC_4\right) + \left(B_1^T\theta_s\theta_s^T B_1 - 2B_1^T\theta_s C_3 + C_3^T C_3\right)$$

$$+18\alpha_s\phi_s^T(k)\phi_s(k)\left(B_2^T\theta_y BB^T\theta_y^T B_2 - 2B_2^T\theta_y BB^T C_4 + C_4^T BB^T C_4\right) + 18\alpha_y\phi_y^T(k)\phi_y(k)\left(B_2^T\theta_y\theta_y^T B_2 - 2B_2^T\theta_y C_4 + C_4^T C_4\right)$$

$$+2B_2^T\tilde{\theta}_y(k)K^T K\tilde{\theta}_y^T(k)B_2 + 2C_4^T K^T KC_4 + 2C_3^T C_3 + 2B_1^T\tilde{\theta}_s(k)\tilde{\theta}_s^T(k)B_1 + 36\alpha_s\phi_s^T(k)\phi_s(k)B_2^T\tilde{\theta}_y(k)BB^T\tilde{\theta}_y^T(k)B_2$$

$$+36\alpha_s\phi_s^T(k)\phi_s(k)C_4^T BB^T C_4 + 36\alpha_y\phi_y^T(k)\phi_y(k)B_2^T\tilde{\theta}_y(k)\tilde{\theta}_y^T(k)B_2 + 36\alpha_y\phi_y^T(k)\phi_y(k)C_4^T C_4 \quad \text{(A.19)}$$

Next, take the Frobenius norm, use Assumption 3, Lemma 1 (Note: using Lemma 1, the uncertainties are replaced by a bound expressed in terms of the state residual and the parameter estimation errors), and combine similar terms, (A.19) could be rewritten as

$$\Delta V \le -\left(\frac{1}{12} - A_{0_{\max}}^2 - 18\alpha_y \phi_{y_{\max}}^2 C_{\max}^2 - 18\alpha_s \phi_{s_{\max}}^2 C_{\max}^2 K_{\max}^2 - 6c_g^2 C_{\max}^2 \right.$$

$$\left. -2\beta_1 \right) \left\| e_s(k) \right\|^2 - \left(\frac{6}{\alpha_s} \gamma_s \left\| I - \alpha_s \phi_s(k) \phi_s^T(k) \right\| - \phi_{s_{\max}}^2 - \frac{2}{\alpha_s} - \frac{3}{\alpha_s} \gamma_s^2 \left\| I - \alpha_s \phi_s(k) \phi_s^T(k) \right\|^2 - 2B_{1_{\max}}^2 - \frac{3}{2} \beta_2 \right) \left\| \tilde{\theta}_s(k) \right\|^2$$

$$-\left(\frac{6}{\alpha_y} \gamma_y \left\| I - \alpha_y \phi_y(k) \phi_y^T(k) \right\| - K_{\max}^2 \phi_{y_{\max}}^2 - \frac{2}{\alpha_y} - \frac{3}{\alpha_y} \gamma_y^2 \left\| I - \alpha_y \phi_y(k) \phi_y^T(k) \right\|^2 - 18\alpha_y \phi_{y_{\max}}^4 \right.$$

$$-18\alpha_s \phi_{s_{\max}}^2 \phi_{y_{\max}}^2 B_{\max}^2 - 36\alpha_s \phi_{s_{\max}}^2 B_{2_{\max}}^2 B_{\max}^2 - 2B_{2_{\max}}^2 K_{\max}^2 - 6c_g^2 \phi_{y_{\max}}^2 - 12c_g^2 B_{2_{\max}}$$

$$\left. -36\alpha_y \phi_{y_{\max}}^2 B_{2_{\max}}^2 - \frac{3}{2} \beta_3 \right) \left\| \tilde{\theta}_y(k) \right\|^2 + \frac{3}{\alpha_s} \gamma_s^2 \left\| I - \alpha_s \phi_s(k) \phi_s^T(k) \right\|^2 \theta_{s_{\max}}^2 + \frac{3}{\alpha_y} \gamma_y^2 \left\| I - \alpha_y \phi_y(k) \phi_y^T(k) \right\|^2 \theta_{y_{\max}}^2$$

$$+B_{2_{\max}}^2 K_{\max}^2 \theta_{y_{\max}}^2 - 2B_{2_{\min}} \theta_{y_{\min}} K_{\min}^2 C_{4_{\min}} + 3C_{4_{\max}}^2 K_{\max}^2 + B_{1_{\max}}^2 \theta_{s_{\max}}^2 - 2B_{1_{\min}} \theta_{s_{\min}} C_{3_{\min}} + 3C_{3_{\max}}^2$$

$$+18\alpha_s \left\| \phi_s(k) \right\|^2 \left(B_{2_{\max}}^2 B_{\max}^2 \theta_{y_{\max}}^2 - 2B_{2_{\min}} \theta_{y_{\min}} B_{\min}^2 C_{4_{\min}} + C_{4_{\max}}^2 B_{\max}^2 \right) + 18\alpha_y \left\| \phi_y(k) \right\|^2 \left(B_{2_{\max}}^2 \theta_{y_{\max}}^2 \right.$$

$$\left. -2B_{2_{\min}} \theta_{y_{\min}} C_{4_{\min}} + C_{4_{\max}}^2 \right) + 18c_g^2 C_{4_{\max}}^2 + 6c_g^2 \theta_{y_{\max}}^2 B_{2_{\max}}^2 + \beta_0 - 12c_g^2 \theta_{y_{\min}} B_{2_{\min}} C_{4_{\min}}$$

$$+36\alpha_s \phi_{s_{\max}}^2 B_{\max}^2 C_{4_{\max}}^2 + 36\alpha_y \phi_{y_{\max}}^2 C_{4_{\max}}^2$$

Take $B_{1_{\min}} = \dfrac{B_{1_{\max}}^2 \theta_{s_{\max}}^2 + 3C_{3\max}^2 + \beta_0 + \dfrac{3\gamma_s^2}{\alpha_s} \left\| I - \alpha_s \phi_s(k) \phi_s^T(k) \right\|^2 \theta_{s_{\max}}^2}{2C_{3_{\min}} \theta_{s_{\min}}}$ and

$$B_{2_{\min}} = \frac{B_{\max}^2 \theta_{y_{\max}}^2 + C_{4_{\max}}^2 + \dfrac{1}{a_d} \left(\dfrac{3\gamma_y^2}{\alpha_y} \left\| I - \alpha_y \phi_y(k) \phi_y^T(k) \right\|^2 \theta_{y_{\max}}^2 \right.}{2C_{4_{\min}} \theta_{y_{\min}}}$$

$$\frac{\left. +3C_{4_{\max}}^2 K_{\max}^2 + 36\alpha_s \phi_{s_{\max}}^2 B_{\max}^2 C_{4_{\max}}^2 + 36\alpha_y \phi_{y_{\max}}^2 C_{4_{\max}}^2 + 18c_g^2 C_{4_{\max}}^2 \right)}{2C_{4_{\min}} \theta_{y_{\min}}}$$

where

$$a_d = \left\| K \right\|^2 + 18\alpha_s \left\| \phi_s(k) \right\|^2 \left\| B \right\|^2 + 18\alpha_y \left\| \phi_y(k) \right\|^2 + 6c_g^2$$

Then the first difference of the Lyapunov equation is given by

$$\Delta V \le -\left(\frac{1}{12} - A_{0_{\max}}^2 - 18\alpha_y \phi_{y_{\max}}^2 C_{\max}^2 - 18\alpha_s \phi_{s_{\max}}^2 C_{\max}^2 K_{\max}^2 - 6c_g^2 C_{\max}^2 - 2\beta_1\right)\left\|e_s(k)\right\|^2$$

$$-\left(\frac{6}{\alpha_s}\gamma_s\left\|I-\alpha_s\phi_s(k)\phi_s^T(k)\right\| - \phi_{s_{\max}}^2 - \frac{2}{\alpha_s} - \frac{3}{\alpha_s}\gamma_s^2\left\|I-\alpha_s\phi_s(k)\phi_s^T(k)\right\|^2 - 2B_{1_{\max}}^2 - \frac{3}{2}\beta_2\right)\left\|\tilde{\theta}_s(k)\right\|^2$$

$$-\left(\frac{6}{\alpha_y}\gamma_y\left\|I-\alpha_y\phi_y(k)\phi_y^T(k)\right\| - K_{\max}^2\phi_{y_{\max}}^2 - \frac{2}{\alpha_y} - \frac{3}{\alpha_y}\gamma_y^2\left\|I-\alpha_y\phi_y(k)\phi_y^T(k)\right\|^2 - 18\alpha_y\phi_{y_{\max}}^4 - 18\alpha_s\phi_{s_{\max}}^2\phi_{y_{\max}}^2 B_{\max}^2\right.$$

$$\left.-36\alpha_s\phi_{s_{\max}}^2 B_{2_{\max}}^2 B_{\max}^2 - 2B_{2_{\max}}^2 K_{\max}^2 - 6c_g^2\phi_{y_{\max}}^2 - 12c_g^2 B_{2_{\max}} - 36\alpha_y\phi_{y_{\max}}^2 B_{2_{\max}}^2 - \frac{3}{2}\beta_3\right)\left\|\tilde{\theta}_y(k)\right\|^2 \qquad \text{(A.20)}$$

Hence $\Delta V < 0$ in (A.20), if the design parameters are selected

as $\alpha_s = \dfrac{K_{\max}^2}{18\phi_{s_{\max}}^2 B_{\max}^2}$, $\alpha_y = \dfrac{K_{\max}^2}{18\phi_{y_{\max}}^2}$, $\dfrac{3-\sqrt{3-3\alpha_s\left(\phi_{s_{\max}}^2 + 2B_{1_{\max}}^2 + (3/2)\beta_2\right)}}{3\left\|I-\alpha_s\phi_s(k)\phi_s^T(k)\right\|} \le \gamma_s \le 1/\left\|I-\alpha_s\phi_s(k)\phi_s^T(k)\right\|$,

$$\frac{3-\sqrt{3-3\alpha_y a_e}}{3\left\|I-\alpha_y\phi_y(k)\phi_y^T(k)\right\|} \le \gamma_y \le 1/\left\|I-\alpha_y\phi_y(k)\phi_y^T(k)\right\|$$

where $a_e = K_{\max}^2\phi_{y_{\max}}^2 + 18\alpha_y\phi_{y_{\max}}^4 + 18\alpha_s\phi_{s_{\max}}^2\phi_{y_{\max}}^2 B_{\max}^2 + 36\alpha_s\phi_{s_{\max}}^2 B_{2_{\max}}^2 B_{\max}^2$

$+2B_{2_{\max}}^2 K_{\max}^2 + 6c_g^2\phi_{y_{\max}}^2 + 12c_g^2 B_{2_{\max}} + 36\alpha_y\phi_{y_{\max}}^2 B_{2_{\max}}^2 + \frac{3}{2}\beta_3$. In addition, we

take $A_{0_{\max}} \le \dfrac{-24c_g C_{\max} \pm \sqrt{576c_g^2 C_{\max}^2 - 25a_s}}{25}$, where

$a_s = 18\alpha_y\phi_{y_{\max}}^2 C_{\max}^2 + 18\alpha_s\phi_{s_{\max}}^2 C_{\max}^2 K_{\max}^2 + 30c_g^2 C_{\max}^2 - \frac{1}{12}$.

The first difference, $\Delta V < 0$ in (A.20), which shows stability in the sense of Lyapunov provided the gains are selected above. Thus the state residual $e_s(k)$, and the parameter estimation errors $\tilde{\theta}_s(k)$ and $\tilde{\theta}_y(k)$ are bounded, provided $e_s(k_0)$, $\tilde{\theta}_s(k_0)$, and $\tilde{\theta}_y(k_0)$

are bounded in the compact set *S*. Additionally, due to the negative definiteness of the first difference of the Lyapunov function [42], the state residual $\|e_s(k)\|$, and parameter estimation errors $\|\tilde{\theta}_s(k)\|$ and $\|\tilde{\theta}_y(k)\|$ approach zero as $k \to \infty$. Next, consider the output equation

$$e_y(k) = Ce_s(k) + \eta_y(x(k), u(k)) + \Psi_y(k) + \varepsilon_y(k) + \nu_y(k) - \frac{(\theta_y^T B_2 - C_4)}{B_2^T \hat{\theta}_y(k) \hat{\theta}_y^T(k) B_2 + c_y}$$

As $k \to \infty$, we have $\|e_s(k)\| \to 0$, $\|\tilde{\theta}_s(k)\| \to 0$ and $\|\tilde{\theta}_y(k)\| \to 0$. Since $\left\|\Psi_y(k)\right\| = \left\|\tilde{\theta}_y^T(k)\phi_y(u(k))\right\|$, therefore, we have $\left\|\Psi_y(k)\right\| \to 0$. Similarly, we have $\left\|\nu_y(k)\right\| \to 0$. Therefore the output residual remains bounded since

$$\left\|e_y(k)\right\| \le \tilde{\eta}_y + \varepsilon_{y_{\max}} + \theta_{y_{\max}} B_{2_{\max}} + C_{4_{\max}} \tag{A.21}$$

This implies that due to the output uncertainties, the output residual remains upper bounded.

Proof of Theorem 4: Since the TTF equation in (12) and (13) are very similar, proof for (12) is given here whereas (13) can be obtained in a manner similar to (12). Additionally, for deriving the proof, it is considered that only the state faults occur.

For a system satisfying *Assumption 1*, the maximum value of the system parameter in the event of a fault is determined by physical limitations. Thus $\hat{\theta}_{s_{ij}}(k_{s_{f_{ij}}}) = \theta_{s_{ij_{\max}}}$. Equation (12) holds only in the time interval $k \in [k_d, k_f]$. Consequently, the update equation in (3) can be written as $\hat{\theta}_s(k+1) = (I - \gamma_s \left\| I - \alpha_s \varphi_s(k) \varphi_s^T(k) \right\| I)\hat{\theta}_s(k) + \alpha_s \varphi_s(k)\, e_y^T(k) B$ The above equation is a linear

time varying equation expressed as

$$\overline{x}(k+1) = \overline{A}(k).\overline{x}(k) + \overline{B}.\overline{u}(k) \tag{A.22}$$

where $\overline{x}(k+1) = \hat{\theta}_s(k+1)$, $\overline{A}(k) = (I - \gamma_s \left\| I - \alpha_s \varphi_s(k) \varphi_s^T(k) \right\| I)$ is a diagonal matrix, $\overline{B} = \alpha_s I_b$, where I an identity matrix and I_b an identity vector, and $\overline{u}(k) = \varphi_s(k)\, e_y^T(k) B$. Since the above defined $\overline{A}$ matrix is diagonal, (A.22) can be written as

$$\overline{x_{ij}}(k+1) = \overline{a_{ii}}(k)\overline{x_{ij}}(k) + \overline{b}\,\overline{u_{ij}}(k) \tag{A.23}$$

where $\overline{x_{ij}}(k) = \hat{\theta}_{s_{ij}}(k)$, $\overline{a_{ii}}(k) = 1 - \gamma_s \left\| I - \alpha_s \varphi_s(k) \varphi_s^T(k) \right\|$, $\overline{b} = \alpha_s$, and $\overline{u_{ij}}(k) = \left(\varphi_s(k) e_y^T(k) B \right)_{ij}$, a product of the basis function, the output residual and a constant matrix.

The solution of the system defined in (A.23) is given by

$$\overline{x_{ij}}(k) = \prod_{t=k_{s0_{ij}}}^{k} \overline{a_{ii}}(t)\overline{x_{ij}}(k_{0_{ij}}) + \sum_{r=k_{s0_{ij}}}^{k} \left(\prod_{t=r}^{k} \overline{a_{ii}}(t) \right) \overline{b}\,\overline{u_{ij}}(r)$$

Since the ij^{th} system parameter reaches its maximum value at the time of failure, i.e., $k_{s_{fij}}$, then $\hat{\theta}_{s_{ij}}(k_{s_{fij}}) = \theta_{s_{ij_{\max}}}$. Additionally, the value of $\hat{\theta}_{s_{ij}}(k_{0_{ij}}) = \theta_{s_{ij_0}}$; hence the above equation becomes

$$\theta_{s_{ij_{\max}}} = \prod_{t=k_{s0_{ij}}}^{k_{s_{fij}}} \overline{a_{ii}}(t)\theta_{s_{ij_0}} + \sum_{r=k_{s0_{ij}}}^{k_{s_{fij}}} \left(\prod_{t=r}^{k_{s_{fij}}} \overline{a_{ii}}(t) \right) \overline{b}\,\overline{u_{ij}}(r)$$

In the above equation, for the time interval $[k_{s0_{ij}}, k_{s_{fij}}]$, $\overline{a_{ii}}(k)$ and $\overline{u_{ij}}(k)$ are assumed to be constant. This suggests that the system defined above can be considered a linearly time invariant system. This assumption is reasonable since $0 < \overline{a_{ii}} < 1$ and stable while the input $\overline{u_{ij}}(k)$ would be bounded due to the guaranteed stability of the parameter

update law in (3). Also, TTF is continuously updated at each time instant in the interval $k \in [k_d, k_f]$, as explained below. Hence the above equation becomes

$$\theta_{s_{ij_{\max}}} = \overline{a}_{ii}^{(k_{s_{f_{ij}}} - k_{s_{0_{ij}}})} \theta_{s_{ij_0}} + \overline{b}\overline{u}_{ij} \sum_{t=k_{s_{0_{ij}}}+1}^{k_{s_{f_{ij}}}} \overline{a}_{ii}^{(k_{s_{f_{ij}}} - t)} \tag{A.24}$$

Using results of geometric series, the above equation becomes

$$\theta_{s_{ij_{\max}}} = \overline{a}_{ii}^{(k_{s_{f_{ij}}} - k_{s_{0_{ij}}})} \theta_{s_{ij_0}} + \overline{b}\overline{u}_{ij} \left(\frac{1 - \overline{a}_{ii}^{(k_{s_{f_{ij}}} - k_{s_{0_{ij}}})}}{1 - \overline{a}_{ii}} \right)$$

With some simple mathematical manipulation, one obtains

$$\overline{a}_{ii}^{(k_{s_{f_{ij}}} - k_{s_{0_{ij}}})} = \frac{[\theta_{s_{ij_{\max}}} (1 - \overline{a}_{ii}) - \overline{b}\overline{u}_{ij}]}{[\theta_{s_{ij_0}} (1 - \overline{a}_{ii}) - \overline{b}\overline{u}_{ij}]}$$

Finally, after performing some mathematical manipulation, we have

$$k_{s_{f_{ij}}} = \frac{\left| \log\left(\left| \frac{\theta_{s_{ij_{\max}}} (1 - \overline{a}_{ii}) - \overline{b}\overline{u}_{ij}}{\theta_{s_{ij_0}} (1 - \overline{a}_{ii}) - \overline{b}\overline{u}_{ij}} \right| \right) \right|}{\left| \log(\overline{a}_{ii}) \right|} + k_{s_{0_{ij}}}$$

Since $\overline{a}_{ii}(k) = 1 - \gamma_s \left\| I - \alpha_s \varphi_s(k) \varphi_s^T(k) \right\|$, $\overline{b} = \alpha_s$, and $\overline{u}_{ij}(k) = \left(\varphi_s e_y^T B \right)_{ij}$, equation (12) results.

References

[1] J. Chen and R. J. Patton, *Robust Model-Based Fault Diagnosis for Dynamic Systems*, Kluwer Academic publishers, MA, USA, 1999.

[2] S. Dash and V. Venkatasubramanian,"Challenges in the industrial applications of fault diagnostic systems," *Computers and Chemical Engineering*, vol. 24, no. 2-7, pp. 785-791, 2000.

[3] G. C. Luh and W. C. Cheng,"Immune model-based fault diagnosis", *Mathematics and Computers in Simulation*," vol. 67, no. 6, pp. 515 – 539, 2005.

[4] P. M. Frank and L. Keller,"Fault diagnosis in dynamic systems using analytical and knowledge-based redundancy–a survey and some new results," *Automatica*, vol. 26, pp. 459-474, 1990.

[5] J. Gertler,"Survey of model-based failure detection and isolation in complex plants", *IEEE Control Syst. Mag.*," vol. 8, pp. 3-11, 1988.

[6] R. Isermann,"Model-based fault-detection and diagnosis–status and applications," *Annual Reviews in Control*, vol. 29, no.1, pp. 71-85, 2005.

[7] R. Isermann, *Fault-Diagnosis Systems: An Introduction from Fault Detection to Fault Tolerance*, Springer, Germany, 2006.

[8] M. A. Demetriou and M. M. Polycarpou,"Incipient fault diagnosis of dynamical systems using online approximators," *IEEE Trans. on Automatic Control*, vol. 43, no. 11, pp. 1612-1617, 1998.

[9] A. B. Trunov and M. M. Polycarpou,"Automated fault diagnosis in nonlinear multivariable systems using a learning methodology," *IEEE Trans. on Neural Networks*, vol. 11, no. 1, pp. 91-101, 2000.

[10] M. M. Polycarpou and A. J. Helmicki,"Automated fault detection and accommodation: a learning systems approach," *IEEE Trans. on Systems, Man, and Cybernetics*, vol. 25, no. 11, pp. 1447-1458, 1995.

[11] X. Zhang, M. M. Polycarpou and T. Parisini,"A robust detection and isolation scheme for abrupt and incipient faults in nonlinear systems," *IEEE Trans. on Automatic Control*, vol. 47, no. 4, pp. 576-593, 2002.

[12] M. Mahmoud,"Sufficient conditions for the stability of input delayed discrete time fault tolerant control systems," *IEEE International Conference on Control Applications*, pp. 504 -509, 2008.

[13] H. Hammouri, P. Kabore, and M. Kinnaert,"A geometric approach to fault detection and isolation for bilinear systems," *IEEE Trans. on Automatic Control*, vol. 46, no. 9, pp. 1451 – 1455, 2001.

[14] M. Massoumnia, G. C. Verghese, and A. S. Willsky,"Failure detection and identification," *IEEE Trans. on Automatic Control*, vol. 34, no. 3, pp. 316-322, 1989.

[15] C. Edwards, S. K. Spurgeon, and R. J. Patton,"Sliding mode observers for fault detection and isolation," *Automatica*, vol. 36, pp. 541-553, 2000.

[16] T. Li, L. Guo, and L. Wu,"Observer-based optimal fault detection using PDFs for time-delay stochastic systems," *Nonlinear Analysis*, vol. 9, no.5, pp. 2337-2349, 2008.

[17] H. Hammouri, P. Kabore, S. Othman, and J. Biston,"Failure diagnosis and nonlinear observer. application to a hydraulic process," *Journal of the Franklin Institute*, vol. 339, no. 4-5, pp. 455-478, 2002.

[18] C. De Persis and A. Isidori,"A geometric approach to nonlinear fault detection and isolation," *IEEE Trans. on Automatic Control*, vol. 46, no. 6, pp. 853 – 865, 2001.

[19] B. Jiang and F. N. Chowdhury,"Parameter fault detection and estimation of a class of nonlinear systems using observers,"*Journal of the Franklin Institute*, vol. 342, no. 7, pp. 725-736, 2005.

[20] H. A. Talebi, S. Tafazoli, and K. Khorasani,"A recurrent neural-network-based sensor and actuator fault detection and isolation for nonlinear systems with application to the satellite's attitude control subsystem," *IEEE Trans. on Neural Networks*, vol. 20, no.1, pp. 45- 60 , 2009.

[21] X. G. Yan and C. Edwards,"Nonlinear robust fault reconstruction and estimation using a sliding mode observer," *Automatica*, vol. 43, no. 9, pp. 1605-1614, 2007.

[22] Q. Wu and M. Saif,"Robust fault detection and diagnosis in a class of nonlinear systems using a neural sliding mode observer," *International Journal of Systems Science*", vol. 38, no. 11, pp. 881-899, 2007.

[23] C. P. Tan, F. Crusca, and M. Aldeen,"Extended results on robust state estimation and fault detection," *Automatica*, vol. 44, no. 8, pp. 2027-2033, 2008.

[24] X. G. Yan and C. Edwards,"Adaptive sliding-mode-observer-based fault reconstruction for nonlinear systems with parametric uncertainties," *IEEE Trans. on Industrial Electronics*, vol. 55, no. 11, pp. 4029-4036, 2008.

[25] C. J. Lopez-Toribio and R. J. Patton,"Fuzzy observers for nonlinear dynamic systems fault diagnosis," *Proc. of the 37th IEEE Conference on Decision and Control*, vol. 1, pp. 84-89, 1998.

[26] C. J. Lopez-Toribio and R. J. Patton,"Takagi-Sugeno fuzzy fault-tolerant control for a non-linear system," *Proc. of the 38th IEEE Conference on Decision and Control*, vol. 5, pp. 4368-4373, 1999.

[27] W. E. Dixon, I. D. Walker, D. M. Dawson, and J. P. Hartranft,"Fault detection for robot manipulators with parametric uncertainty: a prediction-error-based approach," *IEEE Trans. on Robotics and Automation*, vol. 16, no. 6, pp. 689-699, 2000.

[28] F. Caccavale and L. Villani, *Fault Diagnosis and Fault Tolerance for Mechatronic Systems: Recent Advances*, Springer, UK, 2003.

[29] B. T. Thumati and S. Jagannathan,"An online approximator-based fault detection framework for nonlinear discrete-time systems," *Proc. of the IEEE Conference on Decision and Control (CDC)*, pp. 2608-2613, New Orleans, LA, USA, 2007.

[30] P. Kabore and H. Wang,"Using an equivalent feedback control of the residuals for fault detection and identification," *Proc. of the 38th IEEE Conference on Decision and Control*, vol. 5, pp. 4466 – 4471, 1999.

[31] M. L. McIntyre, W. E. Dixon, D. M. Dawson, and I. D. Walker,"Fault identification for robot manipulators," *IEEE Trans. on Robotics and Automation*, vol. 21, no. 5, pp. 1028-1034, 2005.

[32] D. H. Zhou and P. M. Frank,"Fault diagnostics and fault tolerant control," *IEEE Trans. on Aerospace and Electronic Systems*", vol. 34, no. 2, pp. 420-427, 1998.

[33] F. Caccavale and L. Villani,"An adaptive observer for fault diagnosis in nonlinear discrete-time systems," *Proc. of the American Control Conference*, June 30 -July 2, pp. 2463-2468, Boston, MA, 2004.

[34] G. Antonelli, F. Caccavale and L. Villani,"Adaptive discrete-time fault diagnosis for a class of nonlinear systems: application to a mechanical manipulator," *Proc. of* the *IEEE International Symposium on Intelligent Control*, Oct. 5-8, pp. 667-672, Houston, TX, USA, 2003.

[35] A. Alessandri,"Fault diagnosis for nonlinear systems using a bank of neural estimators," *Computers in Industry*, vol. 52, no. 3, pp. 271-289, 2003.

[36] Q. Zhang,"A new residual generation and evaluation method for detection and isolation of faults in nonlinear systems," *Int. J. Adapt. Control and Signal Process.*, vol. 14, pp.759-773, 2000.

[37] J. Luo, M. Namburu, K. Pattipati, L. Qiao, M. Kawamoto, and S, Chigusa,"Model-based prognostic techniques," *AUTOTESTCON 2003: IEEE Systems Readiness Technology Conference*, Anaheim, California, USA, pp. 330-340, 2003.

[38] J. Luo, A. Bixby, K. Pattipati, L. Qiao, M. Kawamoto, and S. Chigusa,"An interacting multiple model approach to model-based prognostics," *IEEE International Conference on Systems, Man and Cybernetics*, Washington, D.C., USA, vol. 1, pp. 189-194, 2003.

[39] E. Phelps, P. Willett, and T. Kirubarajan,"Useful lifetime tracking via the IMM," *Components and System Diagnostics, Prognostics, and Health Management II, Proc. of SPIE*, vol. 4733, pp. 145-156, 2002.

[40] M. J. Roemer and D. M. Ghiocel,"A probabilistic approach to the diagnosis of gas turbine engine faults," *53rd Machinery Prevention Technologies (MFPT) Conference*, Virginia Beach, VA, USA, pp. 325-336, 1999.

[41] Y. Shao and K. Nezu,"Prognosis of remaining bearing life using neural networks," *Proc. of the Institution of Mechanical Engineers, Part I: Journal of Sys. and Control Engg.*, vol. 214, no. 3, pp. 217-230, 2000.

[42] S. Jagannathan, *Neural Network Control of Nonlinear Discrete–time Systems*, CRC publications, NY, USA, 2006.

[43] F. Cacccavale, F. Pierri, and L. Villani,"Adaptive observer for fault diagnosis in nonlinear discrete-time systems," *ASME Journal of Dynamic Systems, Measurement, and Control*, vol. 130, no. 2, pp. 1-9, 2008.

[44] J. Zhang and A. J. Morris,"On-line process fault diagnosis using fuzzy neural networks," *Intelligent Systems Engineering*, pp. 37-47, 1994.

[45] A. R. Barrron,"Universal approximation bounds for superposition of a sigmoidal function," *IEEE Trans. on Information Theory*, vol. 39, no. 3, pp. 930-945, 1993.

[46] B. Xian, D. M. Dawson, M. S. de Queiroz, and J. Chen,"A continuous asymptotic tracking control strategy for uncertain nonlinear systems," *IEEE Trans. on Automatic Control*, vol. 49, no. 7, pp. 1206-1211, 2004.

[47] J. A. Farrell and M. M Polycarpou, *Adaptive Approximation Based Control-Unifying Neural, Fuzzy and Traditional Adaptive Approximation Approaches*, Wiley Interscience, NJ, USA, 2006.

[48] C. M. Kwan, D. M. Dawson, and F. L. Lewis,"Robust adaptive control of robots using neural network: global tracking stability," *Proc. of the Conf. on Decision and Control*, New Orleans, LA, pp. 1846-1851, 1995.

[49] P. M. Patre, W. MacKunis, K. Kaiser, and W. E. Dixon,"Asymptotic tracking for uncertain dynamics systems via a multilayer NN feed forward and RISE feedback control structure," *Proc. of the American Control Conference*, New York City, NY, USA, pp. 5989-5994, 2007.

[50] S. Huang, K. K. Tan, and T. H. Lee,"Decentralized control design for large-scale systems with strong interconnections using neural networks," *IEEE Trans. on Automatic Control*, vol. 48, no. 5, pp. 805-810, 2003.

[51] D. M. Dawson, Z. Qu, and S. Lim,"Re- thinking the robust control of robot manipulators," *Proc. of the Conference on Decision and Control (CDC),* Brighton, England, pp. 1043-1045, 1991.

[52] F. L. Lewis, S. Jagannathan, and A. Yesilderek, *Neural Network Control of Robotics and Nonlinear Systems*, Taylor and Francis, UK, 1999.

[53] A. Mathur, S. Deb, and K. R. Pattipati,"Modeling and real-time diagnostics in TEAMS-RT," *Proc. of the American Control Conference*, Philadelphia, PA, USA, pp.1610-1614, 1998.

4. A Novel Prognostics Scheme for Nonlinear Discrete-time Systems with Multiple State Faults and Fault Types

Balaje T. Thumati and S. Jagannathan

***Abstract*— In this paper, an online prognostics framework is proposed for a class of nonlinear discrete-time systems with simultaneous and multiple faults. In other words, for an *n*-dimensional system, more than one state could have a fault (multiple state faults) and also more than one fault could occur on the same state (multiple fault types). In this framework, a fault is detected first by using the fault detection (FD) estimator, which consists of an OLAD and a robust adaptive term. Subsequently, the prognostics scheme is activated, where the faults are identified by using the fault isolation (FI) estimator. Each state of the isolation estimator corresponds to a particular type of fault combination. Therefore, the fault isolation is successful when the corresponding FI residual converges to zero thus ensuring that the fault has been successfully identified unlike boundedness result common in the FI literature. In addition, the FI scheme is extended to a class of nonlinear discrete-time systems with multiple fault types. Subsequently, a parameter-based scheme is introduced using the parameter update law of the FI estimator in order to predict time-to-failure (TTF). In the event that a fault cannot be identified or if it is a new fault type, the FD estimator parameters can be utilized for identification.**

Balaje T. Thumati (e-mail: bttr74@mst.edu) and S. Jagannathan (e-mail: sarangap@mst.edu) are with the Department of Electrical & Computer Engineering, Missouri University of Science and Technology (formerly University of Missouri–Rolla), Rolla, MO, 65401, USA. This work was supported in part by NSF I/UCRC on Intelligent Maintenance Systems and Intelligent Systems Center.

Finally, a simulation example is used to demonstrate the proposed prognostics scheme.

I. Introduction

Quantitative methodology-based fault detection (FD) schemes have become popular due to the low implementation cost when compared to other techniques [1]. In the quantitative method, a model representative of the system is used in conjunction with the actual system output for residual generation and fault detection. The system model could be derived from either first principles or borrowed from control scientists/engineers. Normally, a predefined threshold on the residual is utilized to declare the presence of a fault and initiate diagnosis. Although, the selection of the fault detection threshold is important to improve detection while minimizing false alarms, a rigorous analytical procedure is now available to identify the fault detection threshold [1-3].

Many available model-based FD and diagnosis methods [4-13] use some sort of residual signal. Such methods for linear systems use structured and fixed directional residuals [1], parity relations [2], geometric approach [3], and eigenstructure assignment [2] etc. However, the prognostics component is not addressed so far.

Recently, the FD and diagnosis schemes are extended to nonlinear continuous-time systems [4-13]. In particular, in [7, 11, 12], a nonlinear sliding mode observer-based FD design is proposed whereas in [10] a nonlinear diagonal observer method is introduced. On the other hand, in [13], geometric relationship is employed. Moreover, a good survey of fault detection and isolation (FDI) schemes for hydraulic systems, flight controls etc., are given in [14]. On the other hand, a recent survey [15] on model-based

FD techniques presents an excellent overview of the state-of-the art developments. A common issue that has been gaining interest in the literature is stability analysis using Lyapunov theory for the design of FD schemes [7-9]. However, the FD schemes [7-9] render only uniform ultimate boundness (UUB) of the closed-loop signals due to the presence of system uncertainties. By contrast, in the recent work [16], asymptotic convergence of the identification error in continuous-time is demonstrated for robot manipulators with actuator faults. However, the time to failure (TTF) determination is not discussed for prognostics although a TTF scheme is essential for next generation complex dynamic systems.

By contrast, certain TTF schemes using data-driven framework [17-19], assumed a specific degradation model which has been found to be limited to the system or material type under consideration. Another scheme [20] employs a deterministic polynomial and a probabilistic method for prognosis by assuming that certain parameters are affected by the fault while others [21] use a black box approach using neural network (NN) on the failure data. All these schemes [17-21] while being data-driven address only TTF prediction, require offline training, and do not offer performance guarantees. Also, no analytical results are included. Therefore, it is envisioned that a combined FI and TTF determination scheme or else referred to as prognostics would not only provide the remaining useful life but also identify the fault occurred. Besides, analytical performance guarantees of the FI and TTF schemes are normally required.

It is reported in [22-23] that a direct conversion of continuous-time FD schemes [4-13] to discrete-time requires high sampling rate whereas when implemented using low sampled embedded hardware results in stability problems. Therefore, FD of discrete-time

systems is explicitly addressed in [22-24] while ensuring that the detection residual is guaranteed to be bounded. However, prognostics component is not studied. Additionally, to the best knowledge of the authors, there are no previously reported discrete-time schemes that can detect, isolate, and estimate TTF for systems with simultaneous and multiple faults. Hence, in this paper, prognostics framework, in discrete-time with guarantees of asymptotic convergence of the FI residual is introduced for a class of nonlinear discrete-systems with simultaneous and multiple faults.

Simultaneous and multiple faults imply that for an *n*-dimensional system, the fault could occur in more than one state at the same time (multiple faults) and also more than one fault can occur on the same state (multiple fault types). Therefore, in this paper, first, the FD estimator from [24] is revisited for the purpose of fault detection. Subsequently, the online approximator in discrete-time (OLAD) and the robust adaptive term in the FD estimator are initiated to learn the unknown fault dynamics. Upon detection, the fault is identified by using a novel FI estimator. Each state of the FI estimator corresponds to a particular type of fault combination. As a consequence, simultaneous and multiple faults occurring on the states are identified if the corresponding FI residual converges to zero asymptotically. Unlike other schemes [8, 9, 22, 23], asymptotic convergence is guaranteed even in the presence of system uncertainties due to the robust adaptive term in the FI estimator.

Subsequently, after isolating the fault, its magnitude is estimated online using a parameter update law, which is used for determining TTF. A mathematical equation is derived to estimate TTF at each time instant by projecting the current value of the FI

parameters to their corresponding limits. The limits provided by the designer indicate that the system is unsafe to operate beyond these limits. Moreover, for most practical systems, the parameters could be tied to physical quantities that have a safe range of values. Alternatively, the state trajectories could be used for TTF determination due to asymptotic convergence of the residual. Finally, a simulation example is used to demonstrate the performance of the prognostics scheme.

Therefore, the important contributions of this paper include an online prognostics scheme, which includes fault isolation and TTF determination, for a class of nonlinear discrete-time systems with abrupt or incipient faults which can occur simultaneously and more than one fault can occur on the same state. Unlike other schemes [8, 9, 22, 23], the proposed scheme delivers asymptotic stability in discrete-time, which means guaranteed isolation and reliable TTF determination in the presence of unstructured system uncertainties [1, 2, 10].

The paper is organized as follows: Section II introduces the system under investigation whereas Section III revisits the fault detection scheme. In Section IV, the prognostic scheme is introduced. Finally, in Section V, a simulation example is used to illustrate the performance of the proposed prognostics scheme. Section VI presents some concluding remarks and discusses future work.

II. System Description

In this section, the system under investigation is introduced. The classes of faults that can occur on the states are discussed in detail. Consider the following general class of

nonaffine nonlinear discrete-time system

$$x(k+1) = \omega(x(k), u(k)) + \eta(x(k), u(k)) + \Pi(k - k_0)h(x(k), u(k)) \quad (1)$$

where $x \in \Re^n$ is the system state vector, $u \in \Re^m$ is the control input vector, $\omega : \Re^n \times \Re^m \to \Re^n$, $\eta : \Re^n \times \Re^m \to \Re^n$, $h : \Re^n \times \Re^m \to \Re^n$ are smooth vector fields. The term $\omega(x(k), u(k))$ represents the known nonlinear system dynamics whereas $\eta(x(k), u(k))$ denotes the system uncertainty. The fault function $h(x(k), u(k))$ represents a vector of possible faults that can occur and their associated dynamics. Moreover, the fault function $h(x(k), u(k))$ is defined as $h(.) = \left[\theta_1^T f_1(x(k), u(k)), ..., \theta_n^T f_n(x(k), u(k)) \right]^T$ where $\theta_i \in \Re^{l_i}$, $i = 1, 2, ..., n$, is an unknown parameter vector referred to as the magnitude of the fault function and $f_i : \Re^n \times \Re^m \to \Re^{l_i}$ is a known smooth vector field referred to as the fault basis function consisting with the literature on fault isolation [8]. In the above definition, each fault vector is distinct and each f_i represents the fault function of the i^{th} fault affecting the i^{th} state equation. In addition, the unknown parameter θ_i is the magnitude of the i^{th} fault.

Remark 1: In this framework, the number of the faults cannot be greater than the number of system states [10]. However, more faults could be considered, if we relax the assumption of multiple faults and multiple fault types and consider only single faults. In such a case, a bank of FI estimators and decision logic could be used to identify the faults [8]. The time profile $\Pi(k - k_0)$ of the faults are modeled by

$$\Pi(k - k_0) = diag(\Omega_1(k - k_0), \Omega_2(k - k_0), ..., \Omega_n(k - k_0))$$

where

$$\Omega_i(\tau) = \begin{cases} 0, & \text{if } \tau < 0 \\ 1 - e^{-\bar{\kappa}_i \tau}, & \text{if } \tau \geq 0 \end{cases} \quad \text{for } i = 1, 2, \ldots n \tag{2}$$

and $\bar{\kappa}_i > 0$ is an unknown constant that represents the rate at which the fault in the corresponding state x_i occurs. The term $\Omega_i(\tau)$ approaches a step function when $\bar{\kappa}_i$ is large, which in turn represents an abrupt fault. The use of exponential term is only to signify the fault growth rate. However, the nonlinear fault function $h(.)$ denotes the magnitude and type of fault, such as a stuck actuator etc.

Remark 2: Modeling of faults using time profiles is common in FD literature [25] and used extensively by others [8, 9, 22-24].

The type of faults considered in (1) is unstructured and belong to a more general class of faults which include step faults [10] unlike [1, 2]. The following assumption is required in order to proceed.

Assumption 1: The modeling uncertainty is unstructured and bounded above [8, 9, 22, 23], i.e., $|\eta_i(x(k), u(k))| \leq \eta_{i_M}$, $\forall (x, u) \in (\chi \times U)$, $i = 1, 2, \ldots n$ where $\eta_{i_M} \geq 0$ is a known constant.

Remark 3: This assumption is required to distinguish uncertainties from the fault functions.

In the above formulation, the faults are assumed to occur simultaneously, i.e., more than one state could have a fault at a given time instant. However, we next consider a more complex scenario, where multiple faults occur on the same system state and also more than one state could have multiple fault types at a given time. Therefore, the system (1) could be rewritten as

$$
\begin{aligned}
x_1(k+1) &= \omega_1(x(k),u(k)) + \eta_1(x(k),u(k)) + \Pi_1(k-k_0)h_1(x(k),u(k)) \\
x_2(k+1) &= \omega_2(x(k),u(k)) + \eta_2(x(k),u(k)) + \sum_{j=1}^{2} \Pi_j(k-k_0)h_j(x,u) \\
&\vdots \\
x_n(k+1) &= \omega_n(x(k),u(k)) + \eta_n(x(k),u(k)) + \sum_{j=1}^{n} \Pi_j(k-k_0)h_j(x,u)
\end{aligned}
\tag{3}
$$

In the above formulation, the faults are assumed to occur on the system states as stated in (3) where state 1 has only one fault occurring whereas state 2 can have two types of faults occurring simultaneously. Therefore, for isolating multiple fault types, the system under consideration should satisfy the upper triangular or lower triangular property.

Remark 4: In the case of simultaneous faults on the states, the faults function on a particular state may affect other states. For instance, a fault occurring on the first system state can have some influence on the remainder ($n-1$) system states although this effect will not increase the magnitude of the fault function on the first state except it influences the basis function which is assumed to be known a priori. Consequently, the residual on the first state will still converge to zero despite faults occurring on the other states.

The representation given in (3) considers a broad range of fault conditions, which include faults affecting its own state and other states of the system. Such fault conditions were not previously addressed in either continuous time or discrete time fault diagnosis scheme [8-10, 22, 23].

In the previously reported FD schemes [10, 26], the uncertainty is assumed to be structured which in turn helps in decoupling the faults from uncertainties thus simplifying the development of the FD and isolation scheme. However, such assumptions

are relaxed in this paper even with the revised formulation with multiple fault types. In the next section, the FD scheme is revisited first. Subsequently, the prognostics scheme will be studied in detail.

III. Fault Detection Scheme

Since, the system considered could be subjected to multiple faults and multiple fault types, the first step is to detect the faults, and then isolate them by identifying the faults that have occurred and finally use their magnitude to estimate the TTF. The block diagram representation of the proposed prognostics scheme is shown in Fig. 1. As observed in the figure, the FD estimator is used to monitor and detect faults in the given system. Upon detecting a fault, the prognostics scheme is activated. Upon its activation, the fault is isolated, and then the TTF is estimated, thereby rendering remaining useful life.

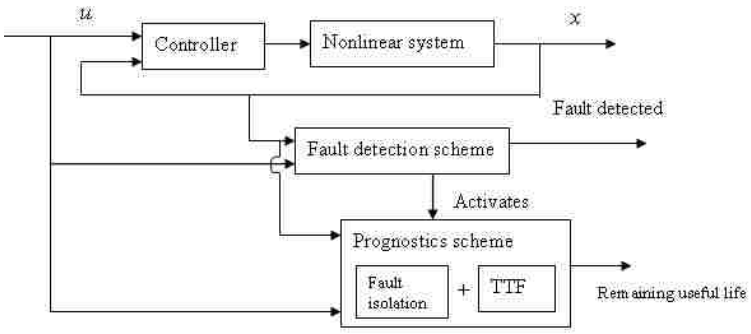

Fig. 1: Overview of the prognostics scheme.

For the purpose of FD, consider the nonlinear FD estimator

$$\hat{\bar{x}}(k+1) = A_d \hat{\bar{x}}(k) + \omega(x(k), u(k)) + \hat{h}_d(x(k), u(k); \hat{\theta}_d(k)) - A_d x(k) - F(k) \quad (4)$$

where $\hat{\bar{x}} \in \Re^n$ is the estimated state vector, $\hat{h}_d : \Re^n \times \Re^m \times \Re^{p\times n} \to \Re^n$ is the detection OLAD output, with $\hat{\theta}_d \in \Re^{p\times n}$ is a set of adjustable parameters of the detection OLAD, $A_d = diag(A_{d_{11}}, A_{d_{22}} ....., A_{d_{nn}})$ is a diagonal matrix chosen by the user, and $F(k)$ is the robust adaptive term to be defined later. Prior to the fault, the initial values of the FD estimator (4) are taken as $\hat{\bar{x}}(0) = \bar{x}_0$, $\hat{\theta}_d(0) = \hat{\theta}_{d_0}$, such that $\hat{h}(x, u, \hat{\theta}_{d_0}) = 0$ for all $x \in \chi$ and $u \in U$.

It is worth mentioning that the FD estimator given in (4) reproduces the real behavior of the nonlinear discrete-time system. Thus the main aim is not to estimate the system states from the input or output measurements, but to generate residuals for FD in the given system [8, 22, 23]. The detection OLAD and robust adaptive term are initiated only upon detection and their outputs are zero prior to detection.

Now define the FD residual as $\bar{e} = x - \hat{\bar{x}}$. Next a dead-zone operator defined by

$$D[\bar{e}_i(k)] = \begin{cases} 0, & \text{if } |\bar{e}_i(k)| \le \rho_i \\ \bar{e}_i(k), & \text{if } |\bar{e}_i(k)| > \rho_i \end{cases} \tag{5}$$

is used for FD to improve robustness by using a threshold where ρ_i is the i^{th} FD threshold since uncertainties are considered in (1). A fault is detected when the FD residual exceeds a predefined threshold. However, the selection of the FD threshold is a challenging task since it provides a trade-off between missed and false alarms. But, analytically, the time varying FD threshold $\rho_i = \dfrac{\beta_i \eta_{i_M}(1-\mu_i^k)}{(1-\mu_i)}$ or a constant threshold $\rho_i = \dfrac{\beta_i \eta_{i_M}}{(1-\mu_i)}$ can be determined using linear control theory [27], where $\beta_i = \beta_{c_i}\mu_i$, μ_i and β_{c_i} are positive constants such that the Frobenius norm $\left\| A_{d_{ii}}^k \right\| \le \beta_{c_i}\mu_i^k < 1$. This intuitively explains that the

fault magnitudes have to be higher than the system uncertainties in order to detect faults.

Remark 5: Upon fault detection, the detection OLAD and the robust adaptive terms in the FD estimator respectively approximate the unknown fault dynamics online and ensure the convergence of the FD residual to zero asymptotically.

Therefore, using the dead-zone operator defined in (5), prior to the fault, *i.e.*, $|\overline{e}_i(k)| \le \rho_i$, $\hat{\theta}_d(k) = \begin{bmatrix} 0 & . & . & . & 0 \\ . & . & . & . & . \\ . & . & . & . & . \\ 0 & . & . & . & 0 \end{bmatrix}_{p\times n}$, which means $\hat{h}_d(x(k), u(k); \hat{\theta}_d(k)) = [0, 0, ..., 0]^T$, and $F(k) = [0, 0, ..., 0]^T$ in the time interval $0 \le k \le T$.

When the residual exceeds the detection threshold, i.e., $|\overline{e}_i(k)| > \rho_i$, a fault is declared active and the OLAD schemes that generate, $\hat{h}_d(.)$ is initiated and tuned online using the following update law

$$\hat{\theta}_d(k+1) = \hat{\theta}_d(k) + \alpha\varphi(k)\mathrm{D}[\overline{e}^T(k+1)] \tag{6}$$

where $\alpha > 0$ is the learning rate and $\varphi(k) = \varphi(x(k), u(k))$ is the basis function such as a RBF, sigmoid etc. The robust adaptive term is defined by $F(k) = \dfrac{\left(\hat{\theta}_d(k)\right)^T B}{B^T\hat{\theta}_d(k)\left(\hat{\theta}_d(k)\right)^T B + c_d}$, where $c_d > 0$ is a user defined constant and $B \in \Re^p$ is a constant vector. The following theorem from [24] is revisited to show asymptotic performance of the FD estimator ((4)-(6)) upon detection.

Theorem 1 (FD Estimator Stability Analysis after Detection): Let the proposed estimator in (4) be used to monitor the system given by (1). Let the update law given in (6) be used for tuning the unknown parameters of the OLAD after detection. In the

presence of bounded uncertainties, the FD residual, $\bar{e}(k)$, and the parameter estimation errors $\tilde{\theta}_{d(k)}$ are locally asymptotically stable**.**

Proof: Refer to [24].

In this theorem, the FD residual and the parameter estimation errors are guaranteed to converge to zero. This guarantees asymptotic tracking of the system states even in the presence of a fault and the system uncertainty. In the next section, the prognostics scheme is introduced.

IV. Prognostics Scheme

After the detection of the fault, as illustrated in Fig. 1, the prognostics scheme is activated. However, to estimate the remaining useful life of the system, the faults in the system have to be isolated and identified, and then the TTF has to be calculated at each time instant. Finally, by taking the minimum of all the estimated TTF's, the remaining useful life of the system is determined. Before proceeding with fault isolation, it is essential to understand some common terminologies. Fault isolation (root-cause analysis) involves with identifying the fault type whereas fault identification involves with estimating the magnitude of the fault [8].

Therefore, fault diagnosis involves fault isolation and identification. Next, in the following text, there are two subsections, where the first subsection considers the case of multiple state faults whereas the second subsection considers multiple fault types. In each of the design, a FI estimator is used for identifying the fault. Every state of the FI estimator has a unique fault function (for multiple faults, the states have a unique combination of fault functions). Subsequently, analytical results are derived to illustrate

the criteria for fault isolation. Next, we present the design of FI estimator for system with multiple faults only.

A. Systems with Multiple Faults

Consider the following FI estimator to identify the simultaneously occurring faults in (1) as

$$\hat{x}(k+1) = G\hat{x}(k) + \omega(x(k), u(k)) + \hat{h}(x(k), u(k); \hat{\theta}(k)) - Gx(k) + v(k) \tag{7}$$

where $\hat{x}(k) = [\hat{x}_1(k), ..., \hat{x}_n(k)]^T$ is the estimated states, $\hat{h}^T(.) = \left[\hat{\theta}_1^T(k) f_1(x(k), u(k)), ..., \hat{\theta}_n^T(k) f_n(x(k), u(k))\right]^T$ is the approximation of the fault function with each $\hat{\theta}_i \in \Re^{l_i}$, $i = 1, 2, ..., n$ is the estimated fault parameter of the i^{th} state variable and $G = diag(g_{11}, g_{22}....., g_{nn})$ with g_{ii} chosen such that all the poles are within the unit disc.

The robust adaptive term for FI is given by

$$v(k) = \left[\frac{\hat{\theta}_1^T(k) b_1}{b_1^T \hat{\theta}_1(k) \hat{\theta}_1^T(k) b_1 + c_1}, ..., \frac{\hat{\theta}_n^T(k) b_n}{b_n^T \hat{\theta}_n(k) \hat{\theta}_n^T(k) b_n + c_n}\right], \text{ where } b_i \in \Re^{l_i \times 1} \text{ is a constant vector,}$$

and c_i, $i = 1, 2, ..., n$ is a scalar constant.

Remark 6: It is very important to note that the fault function is a function of the magnitude of the fault plus the basis function which is unique for a fault type. This basis function is generally a function of all the system states and the input and is considered known. Therefore, a fault on another state will have some influence on the other states through this basis function. However, since the basis function of the proposed FI estimator is same as the basis function of the fault dynamics, isolation of the fault is

possible. Next, define the i^{th} FI residual as $e_i(k) = x_i(k) - \hat{x}_i(k)$. In order to learn the unknown fault parameters, which are required for the TTF determination, the following parameter update law defined as

$$\hat{\theta}_i(k+1) = \hat{\theta}_i(k) + \alpha_i f_i(k) e_i(k+1) - \gamma_i \left\| I - \alpha_i f_i f_i^T \right\| \hat{\theta}_i(k) \tag{8}$$

is proposed, where $\alpha_i > 0$ is the learning rate and $\gamma_i > 0$ is a design parameter.

Remark 7: The update law in (8) is similar to (6) without the dead-zone operator since the FI estimator is initiated only upon detecting a fault. Moreover, (8) has an extra term normally utilized for relaxing the persistency of excitation (PE) condition. This extra term is needed here to render a stable TTF determination and not for FD. By contrast, this term is not utilized in continuous-time FI [8].

Remark 8: It is essential to note that the i^{th} system state FI estimator approximates the i^{th} fault function and is considered to be matched if a fault occurs. Consequently, an i^{th} fault function causes a fault mismatch with other fault functions, $h_1, \ldots, h_{i-1}, h_{i+1}, \ldots h_n$ if it occurs in other states a concept utilized for isolating faults. This idea is also utilized for isolating multiple faults types.

To guarantee the isolation of multiple state faults, we mathematically show the asymptotic convergence of the FI residual and the parameter estimation errors of the matched state of the FI estimator. In other words, in the following theorem, the asymptotic convergence of the i^{th} fault residual of FI estimator is presented. Before we proceed, the following Lemma is needed.

Lemma 1: The bound on the i^{th} component of the system uncertainty ($\eta_i(x(k), u(k))$) could be expressed in terms of the FI residual and the parameter estimation errors as

$$\left(1+5\alpha_i(2+1/\delta_i)f_i^T f_i\right)\eta_i^2(k) \le \eta_{i_M} = \beta_{i_0} + \beta_{i_1}\|e_i(k)\|^2 + \beta_{i_2}\|e_i(k)\|\|\tilde{\theta}_i(k)\| + \beta_{i_3}\|\tilde{\theta}_i(k)\|^2$$

where $\beta_{i_0}, \beta_{i_1}, \beta_{i_2}$ and β_{i_3} are known positive constants.

Proof: Refer to Appendix.

Remark 9: It is important to note that the lemma enables the system uncertainties and the NN reconstruction errors to be expressed a function of the residual and parameter estimation errors. As a consequence, one can include these terms from the NN reconstruction errors and uncertainties along with other negative terms in the first difference of the Lyapunov function making the first difference negative definite. Such results are available in the literature [28-31] for controlling systems in continuous-time. Next the performance of the FI estimator is demonstrated.

Theorem 2 (FI Estimator Performance): Let the proposed FI scheme defined by (7) and (8) be used to identify i^{th} fault function in the i^{th} state of the nonlinear discrete-time system given by (1). Then, in the presence of bounded uncertainties, the i^{th} FI residual, $e_i(k)$, and the i^{th} parameter estimation error, $\tilde{\theta}_i(k)$, converge to zero asymptotically**.**

Proof: Refer to Appendix.

In the above theorem, since $e_i(k) \to 0$ as $k \to \infty$ in the presence of a fault on the i^{th} system state, $\hat{x}_i = x_i$ implies that the i^{th} fault would be isolated by the proposed FI estimator without any adaptive threshold unlike in [8]. An i^{th} fault function occurring on other system states would cause a fault mismatch forcing the other residuals not to converge to zero which can be effectively used to isolate all the *n* distinct faults occurring simultaneously in the system. Similar results can be shown for the ideal case when there

is no uncertainty in the nonlinear discrete-time system without using the robust adaptive term in the FI estimator since asymptotic convergence can be shown.

Unlike in [10], this work also relaxes the additional assumption of separating faults as linear and nonlinear terms to render isolation of multiple faults.

Remark 10: In the event of a new fault, the detection OLAD of the FD estimator could be used for estimating them.

To perform prognostics, it is required that the multiple occurring faults have to be mutually isolable or mutually distinct. In the following theorem, two faults are considered distinguishable if the i^{th} fault function $\left(h_i(x,u)\right)$ and the r^{th} estimated fault function $\left(\hat{h}_r(x,u;\hat{\theta}_r)\right)$ satisfy the condition defined in (9).

In other words, a fault mismatch function can be interpreted as the difference between the r^{th} fault function and the estimated fault function in the i^{th} state equation. This fault mismatch will drive the residual greater than zero which is similar to continuous time FI scheme [8].

Theorem 3: Consider the fault isolation scheme given by (7) and (8). The i^{th} incipient fault in the system is isolable if for each state $r \in \{1,....,n\} \setminus \{i\}$ of the FI estimator there exists a time $k_r > k_d$ such that the following condition is satisfied:

$$\left|\sum_{j=k_d}^{k}\left(g_{rr}\right)^{k-j}\left[(1 - e^{-\bar{\kappa}_1(j-k_0)})\left(\theta_i^T f_i(x,u)\right) - \left(\hat{\theta}_r^T(j) f_r(x,u)\right)\right]\right|$$

$$> \left(g_{rr}\right)^{k-k_d}\left|e_r(k_d)\right| + \sum_{j=k_d}^{k}\left(g_{rr}\right)^{k-j}\left(\eta_{i_M} + \left|v_r(j)\right|\right) \qquad (9)$$

Proof: Refer to Appendix.

When condition (9) is satisfied the isolation residual $\left|e_r(k)\right| > 0$. This implies that the r^{th} fault is excluded. If this condition satisfied, then for each $r \in \{1, ..., n\} \setminus \{i\}$, the faults are distinguishable.

Remark 11: It is noted from Theorem 3 that the fault function of each estimator state is unique. Therefore, the i^{th} fault in the system matches only to the i^{th} fault function of the FI estimator.

A similar condition could be derived for *abrupt faults*. For such class of faults, we have $\bar{\kappa}_i \to \infty$ in the definition of time profile in (2). Therefore, the following corollary is presented to guarantee that each of the abrupt faults is distinguishable.

Corollary 1: Consider the fault isolation scheme given by (7) and (8). The i^{th} abrupt fault in the system is isolable if for each state $r \in \{1, ..., n\} \setminus \{i\}$ of the FI estimator there exists a time $k_r > k_d$ such that the following condition is satisfied:

$$\left|\sum_{j=k_d}^{k} \left(g_{rr}\right)^{k-j} \left[\left(\theta_i^T f_i(x,u)\right) - \left(\hat{\theta}_r^T(j) f_r(x,u)\right)\right]\right| > \left(g_{rr}\right)^{k-k_d} \left|e_r(k_d)\right| + \sum_{j=k_d}^{k} \left(g_{rr}\right)^{k-j} \left(\eta_{i_M} + \left|v_r(j)\right|\right) \qquad (10)$$

Proof: By taking $\bar{\kappa}_i \to \infty$ in the fault time profile, this proof would become identical to the proof of theorem 3. Therefore, one could derive the condition given in (10).

Remark 12: Since the basis function of r^{th} estimated fault is different from the basis function of the i^{th} fault function, the r^{th} robust adaptive term $v_r(k)$ would not be able to compensate the i^{th} fault function. This results in a significant error as reflected in the magnitude since the update law for the r^{th} estimated fault will have a different basis function.

Remark 13: Typically, if only one fault occurs, then it's isolated when the corresponding fault isolation residual converges to zero. However for faults occurring on different states simultaneously, the isolation residuals of more than one estimator state would converge to zero. On the other hand, when multiple fault types occur on a state, then a combination of isolation residuals should be considered. In any case, a priori knowledge about the potential fault types that can occur on a given state needs to be accurately known.

Another important criteria used for evaluating the performance of a FI scheme is the time to taken to identify a fault, which is normally referred to as *fault isolation time*. In the following theorem, we derive an analytical equation to estimate the FI time.

Theorem 4: Consider the fault isolation scheme given by (7) and (8). For each $r \in \{1, ..., n\}$, assume there would exists a time interval $\left[k_d + k_{1r}, k_d + k_{2r}\right]$, such that the maximum fault-isolation time for all the incipient faults is given by

$$k_{i_{isol}} = \max_{r \in \{1,....,n\}} \left\{ k_{1r} + D_r\left(k_{1r}\right) \right\}$$

where $D_r\left(k_{1r}\right)$ is defined as

$D_r\left(k_{1r}\right) = \left(\log\left(C_r\right) / \log\left(g_{rr}^{-1}\right)\right) - 1$. Additionally,

$$C_r = \left\{ 1 + \frac{(1-g_{rr})}{\delta_r} \left(\left(g_{rr}\right)^{(k_{1r}-1)} \left|e_{r(k_d)}\right| + \frac{2}{g_{rr}} \sum_{j=k_d}^{k_d+k_{1r}} \left(g_{rr}\right)^{\left(k_d+k_{1r}-j\right)} \left(\eta_{i_M} + \left|v_r(j)\right|\right) \right) \right\}$$

with $\delta_r > 0$ being a constant.

Proof: Refer to Appendix.

Note the above equation could be used also for calculating fault isolation time for the given system with *abrupt faults*. The above two theorems show that *n*-faults occurring

simultaneously would be isolated in a finite time provided only one fault occurs on a given state. In the following subsection, we extend the above derived results for multiple fault types.

B. Systems with Multiple Fault Types

It is straightforward to see that the above FI design and the theorems could be extended to systems with multiple fault types. Therefore, the FI estimator used for identifying the multiple faults in (1) has to be modified to identity multiple fault types occurring on the same state as

$$\begin{aligned}
\hat{x}_1(k+1) &= \overline{g}_{11}\hat{x}_1(k) + \omega_1(x(k),u(k)) + \hat{h}_1(x(k),u(k);\hat{\theta}_1(k)) - \overline{g}_{11}x_1(k) + \overline{v}_1(k)\\
\hat{x}_2(k+1) &= \overline{g}_{22}\hat{x}_2(k) + \omega_2(x(k),u(k)) + \sum_{j=1}^{2}\hat{h}_j(x(k),u(k);\hat{\theta}_j(k)) - \overline{g}_{22}x_2(k) + \overline{v}_2(k)\\
&\vdots\\
\hat{x}_n(k+1) &= \overline{g}_{nn}\hat{x}_n(k) + \omega_n(x(k),u(k)) + \sum_{j=1}^{n}\hat{h}_j(x(k),u(k);\hat{\theta}_j(k)) - \overline{g}_{nn}x_n(k) + \overline{v}_n(k)
\end{aligned} \tag{11}$$

where $\overline{G} = diag(\overline{g}_{11}, \overline{g}_{22}.....,\overline{g}_{nn})$ with $\overline{g}_{ii}$ chosen such that all the poles are within the unit disc and $\overline{v}_i(k)$, $i = 1, 2, ..., n$ are the robust adaptive terms which are defined later in the text. Alternatively, (11) could be rewritten as

$$\begin{aligned}
\hat{x}_1(k+1) &= \overline{g}_{11}\hat{x}_1(k) + \omega_1(x(k),u(k)) + \hat{\overline{\theta}}_1^T(k)\overline{f}_1(x(k),u(k)) - \overline{g}_{11}x_1(k) + \overline{v}_1(k)\\
\hat{x}_2(k+1) &= \overline{g}_{22}\hat{x}_2(k) + \omega_2(x(k),u(k)) + \hat{\overline{\theta}}_2^T(k)\overline{f}_2(x(k),u(k)) - \overline{g}_{22}x_2(k) + \overline{v}_2(k)\\
&\vdots\\
\hat{x}_n(k+1) &= \overline{g}_{nn}\hat{x}_n(k) + \omega_n(x(k),u(k)) + \hat{\overline{\theta}}_n^T(k)\overline{f}_n(x(k),u(k)) - \overline{g}_{nn}x_n(k) + \overline{v}_n(k)
\end{aligned}$$

where $\hat{\bar{\theta}}_i(k) = \left[\hat{\theta}_i(k), ..., \hat{\theta}_1(k)\right]^T$ and $\bar{f}_i(k) = \left[f_i(k), ..., f_1(k)\right]^T$, $i = 1, 2, ..., n$. This representation is only for the purpose of understanding. However, for all subsequent discussions, we only refer to the FI estimator representation given in (11).

Similar to isolating multiple faults, multiple fault types could also be isolated if the FI residual derived using (3) and (11) converge asymptotically to zero. This implies that if the fault combination in a given system state matches with the fault combination in the corresponding FI estimator estate, then, the multiple fault types would be identified. For the sake of understanding, we derive the i^{th} FI residual for the multiple fault types, which is given by

$$\bar{e}_i(k+1) = \bar{g}_{ii}\bar{e}_i(k) + \sum_{j=1}^{i}\left[(1 - e^{-\bar{\kappa}_1(k-k_0)})\left(\theta_j^T f_j(x(k),u(k))\right) - \left(\hat{\theta}_j^T(k)\, f_j(x(k),u(k))\right)\right] + \eta_i(x(k),u(k)) - v_i(k) \quad (12)$$

Next, to tune the parameters of the FI estimator given in (11), we propose the following parameter update law

$$\hat{\bar{\theta}}_i(k+1) = \hat{\bar{\theta}}_i(k) + \bar{\alpha}_i \bar{f}_i(k)\bar{e}_i(k+1) - \bar{\gamma}_i \left\| I - \bar{\alpha}_i \bar{f}_i(k)\bar{f}_i^T(k)\right\| \hat{\bar{\theta}}_i(k) \quad (13)$$

where $\bar{\alpha}_i > 0$ is the learning rate and $\bar{\gamma}_i > 0$ is a design parameter. Before proceeding any further, the robust terms are defined by

$$\bar{v}(k) = \left[\frac{\hat{\bar{\theta}}_1^T(k)\bar{b}_1}{\bar{b}_1^T\hat{\bar{\theta}}_1(k)\hat{\bar{\theta}}_1^T(k)\bar{b}_1 + \bar{c}_1}, ..., \frac{\hat{\bar{\theta}}_n^T(k)\bar{b}_n}{\bar{b}_n^T\hat{\bar{\theta}}_n(k)\hat{\bar{\theta}}_n^T(k)\bar{b}_n + \bar{c}_n}\right], \text{ where } \bar{b}_i \in \Re^{q_i \times 1}, q_i = l_i + ... + l_1, \text{ is a}$$

constant vector and $\bar{c}_i$ is a scalar constant, $i = 1, 2, ..., n$.

Next, to guarantee the asymptotic convergence, the following corollary is introduced. In this corollary, the FI residual and the parameter estimation errors are mathematically shown to converge asymptotically to zero.

Corollary 2: Let the proposed FI scheme defined by (11) and (13) be used to identify i^{th} combination of fault functions in the i^{th} state of the nonlinear discrete-time system given in (3). Then, in the presence of bounded uncertainties, the i^{th} FI residual, $\overline{e_i}(k)$, and the i^{th} parameter estimation error, $\tilde{\overline{\theta}}_i(k)$, converge asymptotically to zero**.**

Proof: Define the Lyapunov function candidate as

$$\overline{V_i} = \frac{1}{5}\overline{e_i}^2(k) + \frac{1}{\alpha_i}\tilde{\overline{\theta}}_i^T(k)\tilde{\overline{\theta}}_i(k)$$

where $\tilde{\overline{\theta}}_i(k) = \overline{\theta_i} - \hat{\overline{\theta}}_i(k)$, where $\overline{\theta_i} = \left[\theta_i, ..., \theta_1\right]^T$.

Next, taking the first difference of the above defined Lyapunov function, then substitute (12) and (13), after which the proof will be identical to Theorem 2. Therefore, the asymptotic convergence can be proven, i.e., $\overline{V_i} < 0$. Thus we have $\overline{e_i}(k) \to 0$ and $\tilde{\overline{\theta}}_i(k) \to 0$ as $k \to \infty$.

As in the case of multiple faults, similar conditions of fault isolability and fault isolation time could be derived for multiple fault types. For sake of completeness the following corollaries are stated, and moreover the proofs of the following corollaries are straightforward and are similar to the previous case. First the fault isolability condition is introduced and later the fault isolation time is derived.

Corollary 3: Consider the fault isolation scheme given by (11) and (13). The i^{th} *incipient or abrupt fault combination* in the system is isolable if for each state $r \in \{1, ..., n\} \setminus \{i\}$ of the FI estimator there exists a time $k_r > k_d$ such that the following condition is satisfied.

For incipient faults

$$\left|\sum_{m=k_d}^{k}\left(\bar{g}_{rr}\right)^{k-m}\left(\sum_{j=1}^{i}\left[\left(1-e^{-\bar{\kappa}_j(m-k_0)}\right)\left(\theta_j^T f_j(x,u)\right)\right]-\sum_{s=1}^{r}\left(\hat{\theta}_s^T(j) f_s(x,u)\right)\right)\right|$$

$$>\left(\bar{g}_{rr}\right)^{k-k_d}\left|\bar{e}_r(k_d)\right|+\sum_{j=k_d}^{k}\left(\bar{g}_{rr}\right)^{k-j}\left(\eta_{i_M}+\left|\bar{v}_r(j)\right|\right)$$

For abrupt faults

$$\left|\sum_{m=k_d}^{k}\left(\bar{g}_{rr}\right)^{k-m}\left(\sum_{j=1}^{i}\left[\left(\theta_j^T f_j(x,u)\right)\right]-\sum_{s=1}^{r}\left(\hat{\theta}_s^T(j) f_s(x,u)\right)\right)\right|>\left(\bar{g}_{rr}\right)^{k-k_d}\left|\bar{e}_r(k_d)\right|+\sum_{j=k_d}^{k}\left(\bar{g}_{rr}\right)^{k-j}\left(\eta_{i_M}+\left|\bar{v}_r(j)\right|\right)$$

Corollary 4: Consider the fault isolation scheme given by (11) and (13). For each $r\in\{1,\ldots..,n\}$, assume that there exists a time interval $\left[k_d+\bar{k}_{1r}, k_d+\bar{k}_{2r}\right]$, such that the maximum fault-isolation time for all the incipient faults is given by

$$k_{i_{isol}}=\max_{r\in\{1,\ldots..,n\}}\left\{\bar{k}_{1r}+\bar{D}_r\left(\bar{k}_{1r}\right)\right\}$$

where $\bar{D}_r\left(\bar{k}_{1r}\right)$ is defined as

$\bar{D}_r(\bar{k}_{1r})=\left(\log\left(\bar{C}_r\right)/\log\left(\bar{g}_{rr}^{-1}\right)\right)-1$, additionally,

$$\bar{C}_r=\left\{1+\frac{(1-\bar{g}_{rr})}{\bar{\delta}_r}\left(\left(\bar{g}_{rr}\right)^{\left(\bar{k}_{1r}-1\right)}\left|\bar{e}_r(k_d)\right|+\frac{2}{\bar{g}_{rr}}\sum_{j=k_d}^{k_d+\bar{k}_{1r}}\left(\bar{g}_{rr}\right)^{\left(k_d+\bar{k}_{1r}-j\right)}\left(\eta_{i_M}+\left|\bar{v}_r(j)\right|\right)\right)\right\}$$

with $\bar{\delta}_r>0$ being a constant.

Note the same equation is applicable to calculate fault isolation time for systems with multiple fault types that are abrupt in nature.

So far, we have discussed the isolation of multiple occurring faults and the multiple fault types. The next step is to estimate the remaining useful life of the system.

In the following section, a TTF scheme is presented, where an analytical equation is derived, which is used for estimating TTF at each time step after the detection of the fault until the actual failure.

C. TTF Determination

Before presenting the TTF scheme, it is worth noting that the magnitude of the estimated fault parameters associated with the corresponding state of the FI estimator will increase with time upon fault detection. Consequently, the parameters of the matched fault function can be utilized for TTF determination by projecting them at each time instant to their corresponding failure threshold. Initially, the TTF is determined for the case of multiple faults, later extended to multiple fault types. To determine TTF, an explicit mathematical equation is derived, which is based on the online parameter update law (8). This equation is then used to develop an algorithm for the continuous prediction of TTF as given next.

Theorem 5 (TTF Determination for Multiple Faults): In the presence of multiple faults, the TTF for the j^{th} parameter, $j = 1, 2, ..., l_i$ of the i^{th} fault, $i = 1, 2, ..., n$, at the k^{th} time instant can be determined using

$$k_{f_{i_j}} = \frac{\left| \log\left(\left| \frac{\left(\gamma_i \left\| I - \alpha_i f_i f_i^T \right\| \theta_{i_{j_{\max}}} - \alpha_i \left(f_i e_i \right)_j \right)}{\left(\gamma_i \left\| I - \alpha_i f_i f_i^T \right\| \theta_{i_{j_0}} - \alpha_i \left(f_i e_i \right)_j \right)} \right| \right) \right|}{\left| \log(1 - \gamma_i \left\| I - \alpha_i f_i f_i^T \right\|) \right|} + k_{0_{i_j}} \tag{14}$$

where $k_{f_{i_j}}$ is the estimated TTF, $k_{0_{i_j}}$ is the time instant when the prediction starts (bearing in mind that k_d, is the FD time or initial value which increases incrementally),

$\theta_{i_{j\max}}$ is the limiting value of the parameter from the fault function, and $\theta_{i_{j_0}}$ is the value of the parameter at the time instant $k_{0_{i_j}}$.

Proof: Refer to Appendix.

Figure 2 provides a flow chart to determine TTF ($k_{f_{i_j}}$) for each fault parameter. The TTF is determined at each time instant starting when a fault is detected until the parameter reaches its failure threshold. Therefore, TTF decreases as the parameter approaches its limit.

Remark 14: The mathematical equation (14) is derived for the j^{th} parameter, $j = 1, 2, ..., l_i$ of the i^{th} fault. In general, for a given system with *n* possible faults, the TTF would be $k_{sf} = \min(k_{f_{i_j}}),\ j = 1, 2, ..., l_i,\ \ i = 1, 2, ..., n$. The TTF is the time elapsed when the first parameter reaches its limit.

Similar to Theorem 5, the TTF scheme could be derived for multiple fault types. Therefore, the following corollary is introduced, where the explicit equation for determining TTF is given

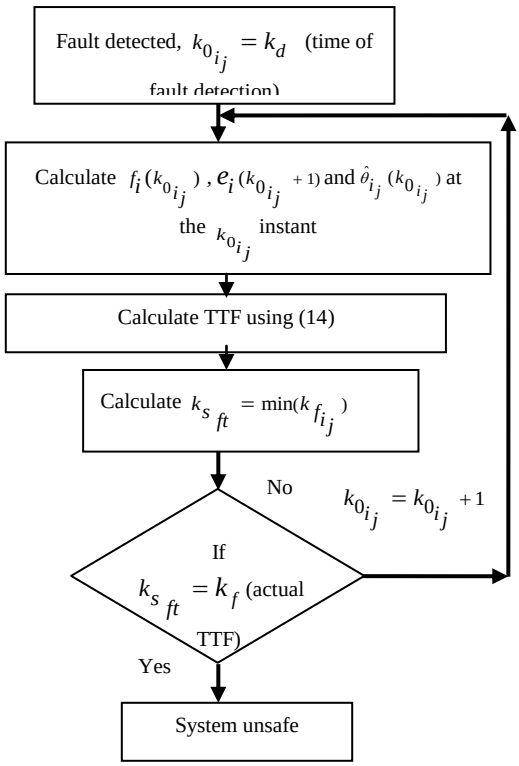

Fig. 2: Flow chart indicating the TTF determination.

Corollary 4 (TTF Determination for Multiple Fault Types): In the presence of multiple fault types, the TTF for the j^{th} parameter, $j = 1, 2, ..., q_i$ of the i^{th} fault combination, $i = 1, 2, ..., n$, at the k^{th} time instant can be determined using

$$\overline{k}_{f_{i_j}} = \frac{\left| \log\left(\left| \frac{\left(\gamma_i \left\| I - \alpha_i \overline{f}_i \overline{f}_i^T \right\| \overline{\theta}_{i_{j_{\max}}} - \alpha_i \left(\overline{f}_i e_i \right)_j \right)}{\left(\gamma_i \left\| I - \alpha_i \overline{f}_i \overline{f}_i^T \right\| \overline{\theta}_{i_{j_0}} - \alpha_i \left(\overline{f}_i e_i \right)_j \right)} \right| \right) \right|}{\left| \log(1 - \gamma_i \left\| I - \alpha_i \overline{f}_i \overline{f}_i^T \right\|) \right|} + \overline{k}_{0_{i_j}} \tag{15}$$

where $\overline{k}_{f_{i_j}}$ is the estimated TTF, $\overline{k}_{0_{i_j}}$ is the time instant when the prediction starts (bearing in mind that k_d , is the FD time or initial value which increases incrementally), $\overline{\theta}_{i_{j\max}}$ is

the limiting value of the parameter from the fault function, and $\bar{\theta}_{i_{j_0}}$ is the value of the parameter at the time instant $\bar{k}_{0_{i_j}}$.

Proof: Using the update law in (13) and following the proof of Theorem 5, it is straightforward to derive equation (15).

Similar to the procedure outlined in Fig. 2, for the case of multiple fault types, the TTF could estimated at each time instant using (15). Therefore, as we approach the failure threshold, the estimated TTF would decrease.

In this section, a TTF scheme is introduced for nonlinear systems with either multiple faults or multiple fault types.

Remark 15: As seen, the proposed prognostics scheme is carried out online and deterministic in contrast with available probabilistic methods in the literature [20].

In the next section, the proposed prognostics scheme is demonstrated using a simulation example.

V. Simulation Results

To verify the proposed prognostics scheme, consider a three-tank system with the following discrete-time model [8]

$$x(k+1) = \omega(x(k), u(k)) + \eta(x(k)) + \Pi(k - k_0)h(x(k))$$

where $x(k) = [x_1(k), x_2(k), x_3(k)]^T$, system uncertainty is taken as $\eta(x(k)) = \left[10^{-3}\sin(0.7k) \quad 10^{-2}\cos(0.8k) \quad 10^{-1}\cos(0.5k)\right]^T$. Note the uncertainty is a time-

varying disturbance. We assume that multiple incipient faults in terms of leakage in tanks 1 and 2 occur. The multiple faults are given by

$\Pi(k-k_0)h(x(k)) = \begin{bmatrix} \theta_1\sqrt{2gx_1(k)} & \theta_2\sqrt{2gx_2(k)} & 0 \end{bmatrix}^T$, where

$\theta_1 = \left(1 - e^{-0.5(k-k_0)}\right)0.0154$ and $\theta_2 = \left(1 - e^{-0.2(k-k_0)}\right)0.0182$. Also, the faults are induced at $k_0 = 25\,\text{sec}$. Finally, the nominal dynamics are described by

$$\omega(x(k),u(k)) = \begin{bmatrix} T\left[\dfrac{-d_1a_p sign(x_1(k)-x_3(k))\sqrt{2g\,|x_1(k)-x_3(k)|}+u_1(k)}{A}\right] \\ +x_1(k) \\ T\left[\dfrac{-d_3a_p sign(x_2(k)-x_3(k))\sqrt{2g\,|x_2(k)-x_3(k)|}}{A}\right. \\ \left.\dfrac{-d_2a_p\sqrt{2gx_2(k)}+u_2(k)}{A}\right]+x_2(k) \\ T\left[\dfrac{d_1a_p sign(x_1(k)-x_3(k))\sqrt{2g\,|x_1(k)-x_3(k)|}}{A}\right. \\ \left.\dfrac{-d_3a_p sign(x_3(k)-x_2(k))\sqrt{2g\,|x_3(k)-x_2(k)|}}{A}\right]+x_3(k) \end{bmatrix}$$

The parameters used for this simulation are given by: $d_1 = 1$, $d_2 = 0.8$, $d_3 = 1$, $a_p = 5\times10^{-5}m^2$, $A = 0.0154m^2$, and $g = 9.8m/s^2$. We use the following FD estimator to detect faults

$$\hat{\bar{x}}(k+1) = A_d\hat{\bar{x}}(k) + \omega(x(k),u(k)) + \hat{h}_d(x(k);\hat{\theta}_d(k)) - A_d x(k) - F(k)$$

where $\hat{\bar{x}}(k) = [\hat{\bar{x}}_1(k), \hat{\bar{x}}_2(k), \hat{\bar{x}}_3(k)]^T$, $A_d = \begin{bmatrix} 0.001 & 0 & 0 \\ 0 & 0.001 & 0 \\ 0 & 0 & 0.001 \end{bmatrix}$, detection OLAD being $\hat{h}_d(x(k);\hat{\theta}_d(k)) = \hat{\theta}_d^T(k)\phi(Vx(k)+B_N)$, with $\hat{\theta}_d \in \Re^{3\times8}$, $\phi(.) \in \Re^{8\times1}$ is a vector of sigmoid

functions. Additionally, v and B_N are chosen randomly. The robust adaptive term is defined as $F(k) = \dfrac{\left(\hat{\theta}_d(k)\right)^T B}{B^T \hat{\theta}_d(k)\left(\hat{\theta}_d(k)\right)^T B + c_d}$, where B is randomly chosen and $c_d = 0.04$. The parameters of the OLAD are tuned online using the update law in (6) with $\alpha = 0.098$.

To detect the faults in the presence of system uncertainty, a constant threshold is selected for all the states by taking $\mu = 0.001$ $\beta = 0.138$, $\eta_M = 0.1$ in $\rho = \dfrac{\beta \eta_M}{(1-\mu)}$, so that $\rho \approx 0.14$. With this detection threshold selection, prior to the fault, the norm of the FD residual remains within the threshold as shown in Fig. 3. However, after the fault has occurred at the 25th second, the residual increases around 27.3th second thus exceeding the threshold. In other words, the detection time appears to be approximately 2.3 seconds. The OLAD and the robust adaptive terms are initiated. As seen in Fig. 3, upon detection, the FD residual drops and converges to zero due to the initiation of the detection OLAD and the robust adaptive term in the FD estimator. This confirms the theoretical results in the previous sections.

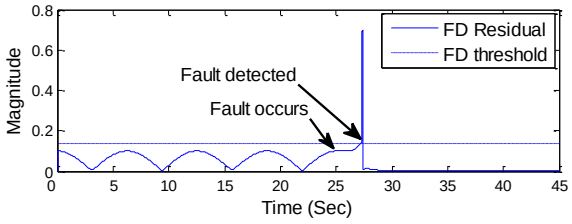

Fig. 3: Residual and the threshold for detecting faults.

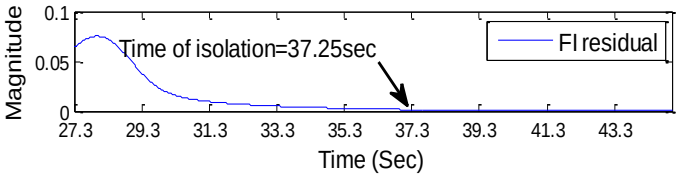

Fig. 4: Convergence of the FI residual ($e_1(k)$).

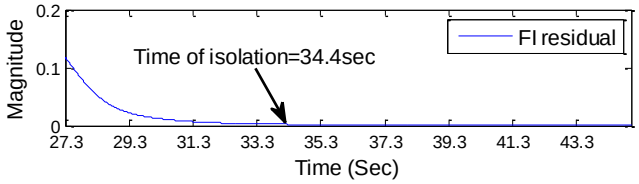

Fig. 5: Convergence of the FI residual ($e_2(k)$).

Next, to identify the fault, consider the following FI estimator

$$\hat{x}(k+1) = G\hat{x}(k) + \omega(x(k), u(k)) + \hat{h}(x(k); \hat{\theta}(k)) - Gx(k) + \nu(k)$$

where $\hat{x}(k) = [\hat{x}_1(k), \hat{x}_2(k), \hat{x}_3(k)]^T$, $G = \begin{bmatrix} 0.001 & 0 & 0 \\ 0 & 0.001 & 0 \\ 0 & 0 & 0.001 \end{bmatrix}$,

$\hat{h}(x(k); \hat{\theta}(k)) = \begin{bmatrix} \hat{\theta}_1(k)\sqrt{2gx_1(k)} & \hat{\theta}_2(k)\sqrt{2gx_2(k)} & 0 \end{bmatrix}^T$, with $\hat{\theta}_1(k)$ and $\hat{\theta}_2(k)$ are estimated using the update law in (8) with $\alpha = 0.38 \times 10^{-4}$ and $\gamma = 0.62 \times 10^{-3}$. As stated in Theorem 2, a fault is isolated if the associated FI residual converges to zero. In fact, the norm of the FI residuals $e_1(k)$ and $e_2(k)$ in Figs. 4 and 5 show asymptotic convergences indicating that the two faults can be isolated correctly. Condition (9) appears to be satisfied. Additionally, from Figs. 4 and 5, we see that both the faults are isolated by 37.25 seconds.

This would roughly be 10 seconds after the fault is detected. Therefore, the two faults are isolated in a finite amount of time.

The accuracy of fault isolation depends on the estimation of the fault magnitudes. This certainly helps in determining the TTF. The fault parameter $\hat{\theta}_1(k)$ and $\hat{\theta}_2(k)$ estimation is shown in Figs. 6 and 7. We set a failure threshold of 0.0155 and 0.017 on the first and the second fault parameter respectively. Additionally, it could be seen that the parameter estimation converges asymptotically.

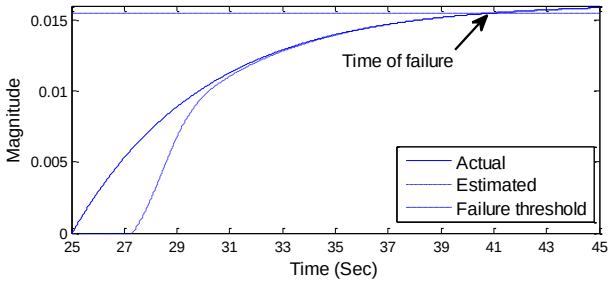

Fig. 6: Online estimation of the fault parameter (θ_1).

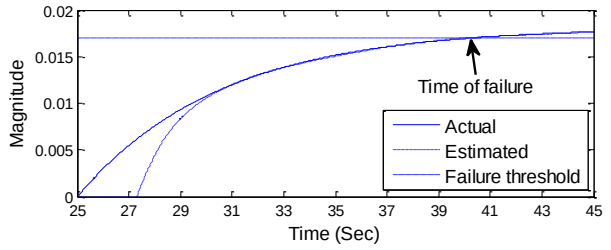

Fig. 7: Online estimation of the fault parameter (θ_2).

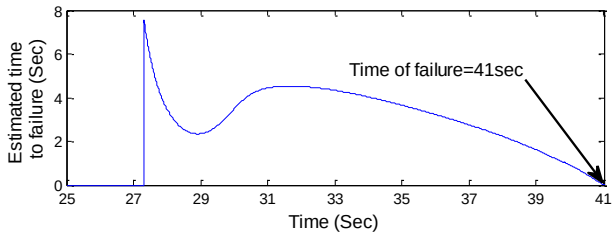

Fig. 8: The TTF determination due to the state fault $h_{1(.)}$.

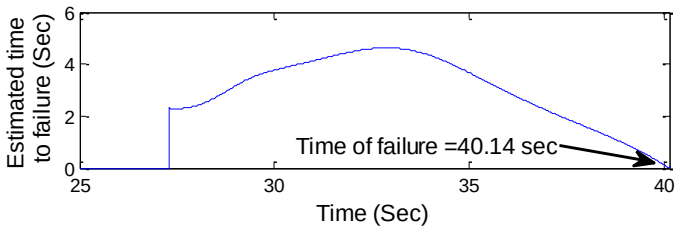

Fig. 9: The TTF determination due to the state fault $h_{2(.)}$.

The TTF is determined for each of the fault parameters as shown in Figs. 8 and 9. In both the cases, the initial change is attributed to the random selection in the adaptation gains of the parameter update law. However, as the fault dynamics are learned, the parameter predictions becomes better and eventually converge indicating the actual time of failures, i.e., 41sec and 40.14 sec respectively. As outlined in Fig. 2, the minimum of the TTF's at each time instant is taken to determine the remaining useful life of the system which in this case will be 40.14 seconds. Thus, the proposed online scheme isolates and identifies a fault, and estimates the TTF without any a priori offline training.

VI. Conclusions

In this paper, a novel prognostics scheme providing online fault isolation and TTF determination for discrete-time systems are introduced for nonlinear systems with simultaneous faults occurring in the system provided the state experiences the expected fault. This approach has been extended to systems with multiple fault types acting on each state. Under certain conditions, it was shown that the multiple faults and fault types can be successfully isolated and identified upon detection.

Initially, the FD scheme is revisited. Upon detection, the asymptotic convergence of the FI residuals and the associated parameter estimation errors show that the FI scheme can isolate and identify multiple fault and multiple fault types. Finally, a simulation example shows that the prognostic scheme successfully isolates the multiple faults and determines the TTF. Future work involves relaxing the state measurement.

Appendix

Proof of Lemma 1: From (1) and (7), the FI residual dynamics are given by

$$e_i(k+1) = g_{ii}e_i(k) + (1 - e^{-\bar{\kappa}_i(k-k_0)})\left(\theta_i^T f_i(x(k),u(k))\right) - \left(\hat{\theta}_i^T(k) f_i(x(k),u(k))\right) + \eta_i(x(k),u(k)) - v_i(k) \tag{A.1}$$

Substitute the robust adaptive term $v_i(k) = \dfrac{\hat{\theta}_i^T(k)b_i}{b_i^T\hat{\theta}_i(k)\hat{\theta}_i^T(k)b_i + c_i}$, add and subtract $\dfrac{\left(\theta_i^T b_i - C_i\right)}{b_i^T\hat{\theta}_i(k)\hat{\theta}_i^T(k)b_i + c_i}$ in (A.1), where C_i is another constant, we have

$$e_i(k+1) = g_{ii}e_i(k) + (1 - e^{-\bar{\kappa}_i(k-k_0)})\left(\theta_i^T f_i(k)\right) - \left(\hat{\theta}_i^T(k) f_i(k)\right) + \eta_i(x,u) + \frac{\left(\tilde{\theta}_i^T(k)b_i - C_i\right)}{b_i^T\hat{\theta}_i(k)\hat{\theta}_i^T(k)b_i + c_i} - \frac{\left(\theta_i^T b_i - C_i\right)}{b_i^T\hat{\theta}_i(k)\hat{\theta}_i^T(k)b_i + c_i} \quad \text{(A.2)}$$

Solve (A.2) to obtain

$$e_i(k) = g_{ii}^k e_i(0) + \sum_{j=0}^{k} g_{ii}^{k-j}\left[(1 - e^{-\bar{\kappa}_i(k-k_0)})\left(\theta_i^T f_i(k)\right) - \left(\hat{\theta}_i^T(k) f_i(k)\right) + \frac{\left(\tilde{\theta}_i^T(j)b_i - C_i\right)}{b_i^T\hat{\theta}_i(j)\hat{\theta}_i^T(j)b_i + c_i} + \eta_i(x,u) + \frac{\left(\tilde{\theta}_i^T(k)b_i - C_i\right)}{b_i^T\hat{\theta}_i(k)\hat{\theta}_i^T(k)b_i + c_i}\right.$$

$$\left. - \frac{\left(\theta_i^T b_i - C_i\right)}{b_i^T\hat{\theta}_i(j)\hat{\theta}_i^T(j)b_i + c_i}\right]$$

The above equation is rewritten as

$$\sum_{j=0}^{k} g_{ii}^{k-j}\eta_i(x,u) = e_i(k) - g_{ii}^k e_i(0) - \sum_{j=0}^{k} g_{ii}^{k-j}\left[(1 - e^{-\bar{\kappa}_i(k-k_0)})\left(\theta_i^T f_i(k)\right) - \left(\hat{\theta}_i^T(k) f_i(k)\right) + \frac{\left(\tilde{\theta}_i^T(k)b_i - C_i\right)}{b_i^T\hat{\theta}_i(k)\hat{\theta}_i^T(k)b_i + c_i}\right.$$

$$\left. - \frac{\left(\theta_i^T b_i - C_i\right)}{b_i^T\hat{\theta}_i(j)\hat{\theta}_i^T(j)b_i + c_i}\right]$$

Using $0 \le 1 - e^{-\bar{\kappa}_i(k-k_0)} \le 1$ and applying Frobenius norm to obtain

$$\left\|\sum_{j=0}^{k} g_{ii}^{k-j}\eta_i(x,u)\right\| \le \left\|e_i(k)\right\| + \left\|g_{ii}^k e_i(0)\right\| + \left\|\sum_{j=0}^{k} g_{ii}^{k-j}\left[\left(\tilde{\theta}_i^T(k) f_i(k)\right)\right.\right.$$

$$\left.\left. + \left\|\sum_{j=0}^{k} g_{ii}^{k-j}\frac{\tilde{\theta}_i^T(j)b_i}{b_i^T\hat{\theta}_i(j)\hat{\theta}_i^T(j)b_i + c_i}\right\| + \left\|\sum_{j=0}^{k} g_{ii}^{k-j}\frac{\theta_i^T b_i}{b_i^T\hat{\theta}_i(j)\hat{\theta}_i^T(j)b_i + c_i}\right\|\right. \quad \text{(A.3)}$$

The summation term in the above equation can be solved as $\left\|\sum_{j=0}^{k} g_{ii}^{k-j}\tilde{\theta}_i^T(j) f_i(j)\right\| \le \frac{f_{i_{\max}}\left\|\tilde{\theta}_i(k)\right\|}{(1 - g_{ii_{\max}})}$. Constricting $g_{ii_{\max}} < 0.5$ within the unit disc makes the

FD scheme stable. Then we obtain $\frac{f_{i_{\max}} \left\| \tilde{\theta}_i(k) \right\|}{(1 - g_{ii_{\max}})} \leq \frac{f_{i_{\max}} \left\| \tilde{\theta}_i(k) \right\|}{g_{ii_{\max}}}$. Similarly bounds could be derived for the other terms in the above equation. Also, $\frac{\tilde{\theta}_i^T(k) b_i}{b_i^T \hat{\theta}_i(j) \hat{\theta}_i^T(j) b_i + c_i} \leq \tilde{\theta}_i^T(k) b_i$,

$\frac{\theta_i^T b_i}{b_i^T \hat{\theta}_i(j) \hat{\theta}_i^T(j) b_i + c_i} \leq \theta_i^T b_i$. Therefore (A.3) could be rewritten as

$$\frac{\left\| \eta_i(k) \right\|}{g_{ii_{\max}}} \leq \left\| e_i(k) \right\| + \left\| g_{ii}^k e_i(0) \right\| + \frac{f_{i_{\max}} \left\| \tilde{\theta}_i(k) \right\|}{g_{ii_{\max}}} + \frac{b_{i_{\max}} \left\| \tilde{\theta}_i(k) \right\|}{g_{ii_{\max}}} + \frac{b_{i_{\max}} \left\| \theta_i \right\|}{g_{ii_{\max}}}$$

Take $b_0 = \left\| g_{ii}^k e_i(0) \right\| + \frac{b_{i_{\max}} \left\| \theta_i \right\|}{g_{ii_{\max}}}$, $b_1 = f_{i_{\max}} + b_{i_{\max}}$, then the above equation could be rewritten as

$$\left\| \eta_i(k) \right\|^2 \leq g_{ii_{\max}}^2 \left(\left\| e_i(k) \right\| + b_0 + \frac{b_1 \left\| \tilde{\theta}_i(k) \right\|}{g_{ii_{\max}}} \right)^2$$

Expanding the square term on the right hand side of the above equation and after some mathematical manipulation, the following equation is obtained as

$$\left\| \eta_i(k) \right\|^2 \leq 3 g_{ii_{\max}}^2 b_0^2 + 2 g_{ii_{\max}}^2 \left\| e_i(k) \right\|^2 + 2 b_1^2 \left\| \tilde{\theta}_i(k) \right\|^2 + 2 g_{ii_{\max}} b_1 \left\| e_i(k) \right\| \left\| \tilde{\theta}_i(k) \right\| \qquad \text{(A.4)}$$

Multiply (A.4) by $\left(1 + 5\alpha_i (2 + 1/\delta_i) f_{i_{\max}}^2\right)$ to render the following equation

$$\left(1 + 5\alpha_i (2 + 1/\delta_i) f_{i_{\max}}^2\right) \left\| \eta_i(k) \right\|^2 \leq 3 \left(1 + 5\alpha_i (2 + 1/\delta_i) f_{i_{\max}}^2\right) g_{ii_{\max}}^2 b_0^2$$

$$+2 \left(1 + 5\alpha_i (2 + 1/\delta_i) f_{i_{\max}}^2\right) g_{ii_{\max}}^2 \left\| e_i(k) \right\|^2 + 2 \left(1 + 5\alpha_i (2 + 1/\delta_i) f_{i_{\max}}^2\right) b_1^2 \left\| \tilde{\theta}_i(k) \right\|^2$$

$$+2\left(1+5\alpha_i(2+1/\delta_i)f_{i_{\max}}^2\right)g_{ii_{\max}}b_1\left\|e_i(k)\right\|\left\|\tilde{\theta}_i(k)\right\|$$

Take $b_{i_0}=3\left(1+5\alpha_i(2+1/\delta_i)f_{i_{\max}}^2\right)g_{ii_{\max}}^2b_0^2$, $b_{i_1}=2\left(1+5\alpha_i(2+1/\delta_i)f_{i_{\max}}^2\right)g_{ii_{\max}}^2$,

$b_{i_2}=2\left(1+5\alpha_i(2+1/\delta_i)f_{i_{\max}}^2\right)g_{ii_{\max}}b_1$, and $b_{i_3}=2\left(1+5\alpha_i(2+1/\delta_i)f_{i_{\max}}^2\right)b_1^2$, would give us

$$\left(1+5\alpha_i(2+1/\delta_i)f_{i_{\max}}^2\right)\eta_i^2(k)\le\eta_{i_M}=\beta_{i_0}+\beta_{i_1}\left\|e_i(k)\right\|^2+\beta_{i_2}\left\|e_i(k)\right\|\left\|\tilde{\theta}_i(k)\right\|+\beta_{i_3}\left\|\tilde{\theta}_i(k)\right\|^2$$

Proof of Theorem 2: Consider the Lyapunov function candidate as

$$V_i=\frac{1}{5}e_i^2(k)+\frac{1}{\alpha_i}\tilde{\theta}_i^T(k)\tilde{\theta}_i(k)$$

whose first difference is given by

$$\Delta V_i=\underbrace{\frac{1}{5}\left[e_i^2(k+1)-e_i^2(k)\right]}_{\Delta V_1}+\underbrace{\frac{1}{\alpha_i}\left[\tilde{\theta}_i^T(k+1)\tilde{\theta}_i(k+1)-\tilde{\theta}_i^T(k)\tilde{\theta}_i(k)\right]}_{\Delta V_2} \tag{A.5}$$

Substituting (A.2) in ΔV_1 of (A.5), the first term is given by

$$\Delta V_1=\frac{1}{5}\Bigg[g_{ii}e_i(k)+(1-e^{-\bar{\kappa}_1(k-k_0)})\left(\theta_i^T f_i(x(k),u(k))\right)-\left(\hat{\theta}_i^T(k)\,f_i(x(k),u(k))\right)+\eta_i(x(k),u(k))+\frac{\left(\tilde{\theta}_i^T(k)b_i-C_i\right)}{b_i^T\hat{\theta}_i(k)\hat{\theta}_i^T(k)b_i+c_i}$$

$$-\frac{\left(\theta_i^Tb_i-C_i\right)}{b_i^T\hat{\theta}_i(k)\hat{\theta}_i^T(k)b_i+c_i}\Bigg]^2-\frac{1}{5}e_i^2(k)$$

Since $0\le 1-e^{-\bar{\kappa}_1(k-k_0)}\le 1$, denote $\Psi_{1_i}(k)=\left(\tilde{\theta}_i^T(k)\,f_i(x(k),u(k))\right)$ and $\Psi_{2_i}(k)=\dfrac{\left(\tilde{\theta}_i^T(k)b_i-C_i\right)}{b_i^T\hat{\theta}_i(k)\hat{\theta}_i^T(k)b_i+c_i}$.

Expand the square term in the above equation to get

$$\Delta V_1\le\left[e_i^2(k)g_{ii}^2+\Psi_{1_i}^2(k)+\eta_i^2(k)+\Psi_{2_i}^2(k)+\frac{\left(\theta_i^Tb_i-C_i\right)^2}{b_i^T\hat{\theta}_i(k)\hat{\theta}_i^T(k)b_i+c_i}\right]-\frac{1}{5}e_i^2(k) \tag{A.6}$$

Next substitute (7) in ΔV_2 of (A.5) to get

$$\Delta V_2 = \frac{1}{\alpha_i}\{[(1-\gamma_i \|I-\alpha_i f_i f_i^T\|)\tilde{\theta}_i(k) - \alpha_i f_i(k) e_i(k+1) + \gamma_i \|I-\alpha_i f_i f_i^T\| \theta_i]^T \times [(1-\gamma_i \|I-\alpha_i f_i f_i^T\|)\tilde{\theta}_i(k)$$

$$-\alpha_i f_i(k) e_i(k+1) + \gamma_i \|I-\alpha_i f_i f_i^T\| \theta_i] - \tilde{\theta}_i^T(k)\tilde{\theta}_i(k)\Big\}$$

Expand terms in the above equation to obtain

$$\Delta V_2 \le \frac{1}{\alpha_i}\{-2\gamma_i \|I-\alpha_i f_i f_i^T\| \tilde{\theta}_i^T(k)\tilde{\theta}_i(k) + \gamma_i^2 \|I-\alpha_i f_i f_i^T\|^2 \tilde{\theta}_i^T(k)\tilde{\theta}_i(k) - 2\alpha_i \tilde{\theta}_i^T(k)(I-\gamma_i \|I-\alpha_i f_i f_i^T\|).$$

$$f_i e_i(k+1) + 2\tilde{\theta}_i^T(k)(I-\gamma_i \|I-\alpha_i f_i f_i^T\|)\gamma_i \|I-\alpha_i f_i f_i^T\| \theta_i + \alpha_i^2 e_i(k+1) f_i^T(k) f_i(k) e_i(k+1)$$

$$+\gamma_i^2 \|I-\alpha_i f_i f_i^T\|^2 \theta_i^T \theta_i - 2\alpha_i e_i(k+1) f_i^T(k)\gamma_i \|I-\alpha_i f_i f_i^T\| \theta_i$$

After some manipulations, we have

$$\Delta V_2 \le -\frac{2(1+2\delta_i)\gamma_i}{\alpha_i}\|I-\alpha_i f_i f_i^T\| \tilde{\theta}_i^T(k)\tilde{\theta}_i(k) + \frac{(1+2\delta_i)\gamma_i^2}{\alpha_i}\|I-\alpha_i f_i f_i^T\|^2 \tilde{\theta}_i^T(k)\tilde{\theta}_i(k) + \frac{2\delta_i}{\alpha_i}\tilde{\theta}_i^T(k)\tilde{\theta}_i(k)$$

$$+5\alpha_i(2+1/\delta_i) f_i^T(k) f_i(k)\left[e_i^2(k) g_{ii}^2 + \Psi_{1_i}^2(k) + \eta_i^2(k) + \Psi_{2_i}^2(k) + \frac{\left(\theta_i^T b_i - C_i\right)^2}{b_i^T \hat{\theta}_i(k)\hat{\theta}_i^T(k) b_i + c_i}\right]$$

$$+\frac{(2+1/\delta_i)\gamma_i^2}{\alpha_i}\|I-\alpha_i f_i f_i^T\|^2 \theta_i^T \theta_i \qquad \text{(A.7)}$$

where $\delta_i > 0$ is a constant. Since $\Delta V_i = \Delta V_1 + \Delta V_2$, combine (A.6) and (A.7). Then, the first difference of the Lyapunov function can be written as

$$\Delta V_i \le \left[e_i^2(k) g_{ii}^2 + \Psi_{1_i}^2(k) + \eta_i^2(k) + \Psi_{2_i}^2(k) + \frac{\left(\theta_i^T b_i - C_i\right)^2}{b_i^T \hat{\theta}_i(k)\hat{\theta}_i^T(k) b_i + c_i}\right]$$

$$-\frac{1}{5}e_i^2(k) - \frac{2(1+2\delta_i)\gamma_i}{\alpha_i}\|I-\alpha_i f_i f_i^T\| \tilde{\theta}_i^T(k)\tilde{\theta}_i(k) + \frac{(1+2\delta_i)\gamma_i^2}{\alpha_i}.$$

$$\left\|I-\alpha_i f_i f_i^T\right\|^2 \tilde{\theta}_i^T(k)\tilde{\theta}_i(k)+\frac{2\delta_i}{\alpha_i}\tilde{\theta}_i^T(k)\tilde{\theta}_i(k)+5\alpha_i(2+1/\delta_i) f_i^T(k) f_i(k)\Big[e_i^2(k)g_{ii}^2+\Psi_{1_i}^2(k)+\eta_i^2(k)$$

$$+\Psi_{2_i}^2(k)+\underbrace{\frac{\left(\theta_i^T b_i-C_i\right)^2}{b_i^T\hat{\theta}_i(k)\hat{\theta}_i^T(k)b_i+c_i}}_{2}\Big]+\frac{(2+1/\delta_i)\gamma_i^2}{\alpha_i}\left\|I-\alpha_i f_i f_i^T\right\|^2\theta_i^T\theta_i$$

Using lemma 1 in the above equation, we have

$$\Delta V_i\le\Big[e_i^2(k)g_{ii}^2+\Psi_{1_i}^2(k)+\underbrace{\Psi_{2_i}^2(k)}_{1}+\underbrace{\frac{\left(\theta_i^T b_i-C_i\right)^2}{b_i^T\hat{\theta}_i(k)\hat{\theta}_i^T(k)b_i+c_i}}_{2}\Big]-\frac{1}{5}e_i^2(k)$$

$$-\frac{2(1+2\delta_i)\gamma_i}{\alpha_i}\left\|I-\alpha_i f_i f_i^T\right\|\tilde{\theta}_i^T(k)\tilde{\theta}_i(k)+\frac{(1+2\delta_i)\gamma_i^2}{\alpha_i}\left\|I-\alpha_i f_i f_i^T\right\|^2\tilde{\theta}_i^T(k)\tilde{\theta}_i(k)+\frac{2\delta_i}{\alpha_i}\tilde{\theta}_i^T(k)\tilde{\theta}_i(k)$$

$$+5\alpha_i(2+1/\delta_i) f_i^T(k) f_i(k)\left[e_i^2(k)g_{ii}^2+\Psi_{1_i}^2(k)+\Psi_{2_i}^2(k)+\underbrace{\frac{\left(\theta_i^T b_i-C_i\right)^2}{b_i^T\hat{\theta}_i(k)\hat{\theta}_i^T(k)b_i+c_i}}_{2}\right]$$

$$+\frac{(2+1/\delta_i)\gamma_i^2}{\alpha_i}\left\|I-\alpha_i f_i f_i^T\right\|^2\theta_i^T\theta_i+\beta_{i_0}+\beta_{i_1}\left\|e_i(k)\right\|^2+\beta_{i_2}\left\|e_i(k)\right\|\left\|\tilde{\theta}_i(k)\right\|+\beta_{i_3}\left\|\tilde{\theta}_i(k)\right\|^2 \qquad \text{(A.8)}$$

Consider terms numbered as (1) in (A.8), we have

$$\left(1+5\alpha_i(2+1/\delta_i) f_i^T f_i\right)\Psi_{2_i}^2(k)\le 2\left(1+5\alpha_i(2+1/\delta_i)\alpha_i f_i^T f_i\right)\left(\tilde{\theta}_i^T(k)b_i b_i^T\tilde{\theta}_i(k)+c_i^T c_i\right) \qquad \text{(A.9)}$$

Next, consider terms numbered as (2) in (A.8), we have

$$\left(1+5\alpha_i(2+1/\delta_i) f_i^T f_i\right)\frac{\left(\theta_i^T b_i-C_i\right)^2}{b_i^T\hat{\theta}_i(k)\hat{\theta}_i^T(k)b_i+c_i}\le\left(1+5\alpha_i(2+1/\delta_i) f_i^T f_i\right)\left(\theta_i^T b_i-C_i\right)^2$$

$$\le\left(1+5\alpha_i(2+1/\delta_i) f_i^T f_i\right)\left(\theta_i^T b_i b_i^T\theta_i-2\theta_i^T b_i c_i+c_i^T c_i\right) \qquad \text{(A.10)}$$

Using (A.9) and (A.10) in (A.8), we have

$$\Delta V_i \le e_i^2(k)g_{ii}^2 + \Psi_{1_i}^2(k) - \frac{1}{5}e_i^2(k) \quad +2\left(1+5\alpha_i(2+1/\delta_i)f_i^T f_i\right)\left(\tilde{\theta}_i^T(k)b_i b_i^T\tilde{\theta}_i(k) + c_i^T c_i\right)$$

$$+\left(1+5\alpha_i(2+1/\delta_i)f_i^T f_i\right)\left(\theta_i^T b_i b_i^T\theta_i - 2\theta_i^T b_i c_i + c_i^T c_i\right)$$

$$-\frac{2(1+2\delta_i)\gamma_i}{\alpha_i}\left\|I-\alpha_i f_i f_i^T\right\|\tilde{\theta}_i^T(k)\tilde{\theta}_i(k) + \frac{(1+2\delta_i)\gamma_i^2}{\alpha_i}\left\|I-\alpha_i f_i f_i^T\right\|^2\tilde{\theta}_i^T(k)\tilde{\theta}_i(k) + \frac{2\delta_i}{\alpha_i}\tilde{\theta}_i^T(k)\tilde{\theta}_i(k)$$

$$+5\alpha_i(2+1/\delta_i)f_i^T(k)f_i(k)\left[e_i^2(k)g_{ii}^2 + \Psi_{1_i}^2(k)\right] + \frac{(2+1/\delta_i)\gamma_i^2}{\alpha_i}\left\|I-\alpha_i f_i f_i^T\right\|^2\theta_i^T\theta_i$$

$$+\beta_{i_0} + \beta_{i_1}\left\|e_i(k)\right\|^2 + \beta_{i_2}\left\|e_i(k)\right\|\left\|\tilde{\theta}_i(k)\right\| + \beta_{i_3}\left\|\tilde{\theta}_i(k)\right\|^2$$

Next, apply Frobenius norm, the first difference of the Lyapunov equation can be written as

$$\Delta V_i \le -\left(\frac{1}{5} - g_{ii_{\max}}^2 - 5\alpha_i(2+1/\delta_i)f_{i_{\max}}^2 g_{ii_{\max}}^2 - \frac{3}{2}\beta_{i_1}\right)\left\|e_i(k)\right\|^2$$

$$-\left(\frac{2(1+2\delta_i)\gamma_i}{\alpha_i}\left\|I-\alpha_i f_i f_i^T\right\| - f_{i_{\max}}^2 - 2(1+5\alpha_i(2+1/\delta_i)f_{i_{\max}}^2)b_{i_{\max}}^2\right.$$

$$\left.-\frac{(1+2\delta_i)\gamma_i^2}{\alpha_i}\left\|I-\alpha_i f_i f_i^T\right\|^2 - \frac{2\delta_i}{\alpha_i} - 5\alpha_i(2+1/\delta_i)f_{i_{\max}}^4 - \frac{3}{2}\beta_{i_3}\right)\left\|\tilde{\theta}_i(k)\right\|^2 + 2\left(1+5\alpha_i(2+1/\delta_i)\left\|f_i(k)\right\|^2\right)c_{i_{\max}}^2$$

$$+\left(1+5\alpha_i(2+1/\delta_i)\left\|f_i(k)\right\|^2\right)\left(\theta_{i_{\max}}^2 b_{i_{\max}}^2 - 2\theta_{i_{\min}}b_{i_{\min}}c_{i_{\min}} + c_{i_{\max}}^2\right)$$

$$+\frac{(2+1/\delta_i)\gamma_i^2}{\alpha_i}\left\|I-\alpha_i f_i f_i^T\right\|^2\theta_{i_{\max}}^2 + \beta_{i_0} \qquad \text{(A.11)}$$

Take $b_{i_{\max}} = \dfrac{\delta_i}{\sqrt{2(1+5\alpha_i(2+1/\delta_i)f_{i_{\max}}^2)}}$ and $b_{i_{\min}} = \dfrac{\left(3C_{i_{\max}}^2 + b_{i_{\max}}^2\theta_{i_{\max}}^2\right)}{2C_{i_{\min}}\theta_{i_{\min}}} +$

$$\frac{\left(\left(\frac{(2+1/\delta_i)\gamma_i^2}{\alpha_i}\left\|I-\alpha_i f_i(k) f_i^T(k)\right\|^2 \theta_{i_{\max}}^2 + b_{i_0}\right)/(1+5\alpha_i(2+1/\delta_i)\left\|f_i(k)\right\|^2)\right)}{2C_{i_{\min}}\theta_{i_{\min}}}$$

. Therefore, (A.11)

could be rewritten as

$$\Delta V_i \le -\left(\frac{1}{5} - g_{ii_{\max}}^2 - 5\alpha_i(2+1/\delta_i) f_{i_{\max}}^2 g_{ii_{\max}}^2 - \frac{3}{2}\beta_{i_1}\right)\left\|e_i(k)\right\|^2$$

$$-\left(\frac{2(1+2\delta_i)\gamma_i}{\alpha_i}\left\|I-\alpha_i f_i f_i^T\right\| - f_{i_{\max}}^2 - 2(1+5\alpha_i(2+1/\delta_i) f_{i_{\max}}^2) b_{i_{\max}}^2\right.$$

$$\left.-\frac{(1+2\delta_i)\gamma_i^2}{\alpha_i}\left\|I-\alpha_i f_i f_i^T\right\|^2 - \frac{2\delta_i}{\alpha_i} - 5\alpha_i(2+1/\delta_i) f_{i_{\max}}^4 - \frac{3}{2}\beta_{i_3}\right)\left\|\tilde{\theta}_i(k)\right\|^2 \qquad \text{(A.12)}$$

Hence $\Delta V_i < 0$ in (A.12) provided the design parameters can be selected as

$$g_{ii_{\max}} \le \sqrt{\frac{(1/5)}{\left(4+20\alpha_i(2+1/\delta_i) f_{i_{\max}}^2\right)}} \quad , \quad 0<\alpha<1 \quad , \quad \frac{1-\sqrt{1-C_{r_i}}}{\left\|I-\alpha_i f_i^T f_i\right\|} \le \gamma_i \le 1/\left\|I-\alpha_i f_i^T f_i\right\|,$$

where $C_{r_i} = \frac{\alpha_i}{(2+1/\delta_i)}\left(\frac{2\delta_i}{\alpha_i} + f_{i_{\max}}^2 + 5\alpha_i(2+1/\delta_i) f_{i_{\max}}^4 + \frac{3\beta_{i_3}}{2} + 2\left(1+5\alpha_i(2+1/\delta_i) f_{i_{\max}}^2\right) b_{i_{\max}}^2\right)$.

The first difference, $\Delta V_i < 0$ in (A.12), indicates stability in the sense of Lyapunov, provided the gains are selected above. Summing both sides of the equation (A.12), and since $\Delta V < 0$, we have $\left|\sum_{k=0}^{\infty}\Delta V(k)\right| = \left|V(\infty)-V(0)\right| < \infty$. Therefore, from [27, 31], taking limits on both sides one has $\left\|e_i(k)\right\| \to 0$ and $\left\|\tilde{\theta}_i(k)\right\| \to 0$ as $k \to \infty$, provided $e_i(k_0)$ and $\tilde{\theta}_i(k_0)$, are selected in the compact set *S*.

Proof of Theorem 3: In the presence of the i^{th} fault, the isolation residual associated with the r^{th} fault isolation scheme is given by

$$e_r(k+1) = g_{rr} e_r(k) + (1 - e^{-\bar{\kappa}_i(k-k_0)})\left(\theta_i^T f_i(x,u)\right) - \left(\hat{\theta}_r^T(k) f_r(x,u)\right) + \eta_i(x(k),u(k)) + v_r(k)$$

Solving the above equation, we have

$$e_r(k) = \left(g_{rr}\right)^{k-k_d} e_r(k_d) + \sum_{j=k_d}^{k} \left(g_{rr}\right)^{k-j} (1 - e^{-\bar{\kappa}_i(j-k_0)})\left(\theta_i^T f_i(x(j),u(j))\right) - \sum_{j=k_d}^{k} \left(g_{rr}\right)^{k-j} \left(\hat{\theta}_r^T(j) f_r(x(j),u(j))\right)$$

$$+ \sum_{j=k_d}^{k} \left(g_{rr}\right)^{k-j} \eta_i(x(j),u(j)) - \sum_{j=k_d}^{k} \left(g_{rr}\right)^{k-j} v_r(j)$$

By using the triangle inequality (if $a = b + c$, then, $|a| \geq |b| - |c|$), the above equation yields

$$\left|e_r(k)\right| \geq \left|\sum_{j=k_d}^{k} \left(g_{rr}\right)^{k-j} (1 - e^{-\bar{\kappa}_i(j-k_0)})\left(\theta_i^T f_i(x(j),u(j))\right)\right|$$

$$- \left|\sum_{j=k_d}^{k} \left(g_{rr}\right)^{k-j} \left(\hat{\theta}_r^T(j) f_r(x(j),u(j))\right)\right| - \left(g_{rr}\right)^{k-k_d} \left|e_r(k_d)\right| - \left|\sum_{j=k_d}^{k} \left(g_{rr}\right)^{k-j} \eta_i(x(j),u(j))\right| - \left|\sum_{j=k_d}^{k} \left(g_{rr}\right)^{k-j} v_r(j)\right|$$

Therefore, when the condition (9) is satisfied, $\left|e_r(k)\right| > 0$. This implies that the r^{th} fault is excluded. If this condition satisfied, then for each $r \in \{1,.....,n\} \setminus \{i\}$, each of the faults is distinguishable.

Proof of Theorem 4: Consider the following definition of a mismatch function for the i^{th} incipient fault and the r^{th} fault isolation scheme

$$p(k) = (1 - e^{-\bar{\kappa}_i(k-k_0)})\left(\theta_i^T f_i(x,u)\right) - \left(\hat{\theta}_r^T(k) f_r(x,u)\right)$$

Assume there exists a time interval $\left[k_d + k_{1r}, k_d + k_{2r}\right]$ and a scalar constant $\delta_r > 0$ for each $r \in \{1,.....,n\}$ such that, for all $k \in \left[k_d + k_{1r}, k_d + k_{2r}\right]$, we define

$$\left|p(k)\right| \geq \eta_{iM} + \left|v_r(k)\right| + \delta_r \tag{A.13}$$

Next, consider the fault isolability condition from theorem 3 for the interval $k \in \left[k_{1r}, k_{2r}\right]$ as

$$\left|\sum_{j=k_d}^{k_d+k} \left(g_{rr}\right)^{\left(k_d+k-j\right)} p(j)\right| > \left(g_{rr}\right)^{k} \left|e_r(k_d)\right| + \left|\sum_{j=k_d}^{k_d+k} \left(g_{rr}\right)^{\left(k_d+k-j\right)} \left(\eta_{i_M} + \left|v_r(j)\right|\right)\right| \tag{A.14}$$

From the inequality

$$\left|\sum_{j=k_d}^{k_d+k} \left(g_{rr}\right)^{\left(k_d+k-j\right)} p(j)\right| \geq \left|\sum_{j=k_d+k_{1r}}^{k_d+k} \left(g_{rr}\right)^{\left(k_d+k-j\right)} p(j)\right| - \left|\sum_{j=k_d}^{k_d+k} \left(g_{rr}\right)^{\left(k_d+k-j\right)} p(j)\right|$$

it follows that a sufficient condition for (A.14) to be satisfied is given by

$$\left|\sum_{j=k_d+k_{1r}}^{k_d+k} \left(g_{rr}\right)^{\left(k_d+k-j\right)} p(j)\right| > \left(g_{rr}\right)^{k} \left|e_r(k_d)\right| + \left|\sum_{j=k_d}^{k_d+k} \left(g_{rr}\right)^{\left(k_d+k-j\right)} \left(\eta_{i_M} + \left|v_r(j)\right|\right)\right|$$

$$+ \left|\sum_{j=k_d}^{k_d+k_{1r}} \left(g_{rr}\right)^{\left(k_d+k_{1r}-j\right)} p(j)\right|$$

The above equation could be rewritten as

$$\left|\sum_{j=k_d+k_{1r}}^{k_d+k} \left(g_{rr}\right)^{\left(k_d+k-j\right)} p(j)\right| > \left(g_{rr}\right)^{k} \left|e_r(k_d)\right| + \left|\sum_{j=k_d+k_{1r}}^{k_d+k} \left(g_{rr}\right)^{\left(k_d+k-j\right)} \left(\eta_{i_M} + \left|v_r(j)\right|\right)\right|$$

$$+ \left(g_{rr}\right)^{\left(k-k_{1r}\right)} \left[\left|\sum_{j=k_d}^{k_d+k_{1r}} \left(g_{rr}\right)^{\left(k_d+k_{1r}-j\right)} p(j)\right| + \sum_{j=k_d}^{k_d+k_{1r}} \left(g_{rr}\right)^{\left(k_d+k_{1r}-j\right)} \left(\eta_{i_M} + \left|v_r(j)\right|\right)\right] \tag{A.15}$$

Next, using (A.13), we obtain

$$\left|\sum_{j=k_d+k_{1r}}^{k_d+k} \left(g_{rr}\right)^{\left(k_d+k-j\right)} p(j)\right| = \sum_{j=k_d+k_{1r}}^{k_d+k} \left(g_{rr}\right)^{\left(k_d+k-j\right)} \left|p(j)\right|$$

$$\geq \sum_{j=k_d+k_{1r}}^{k_d+k} \left(g_{rr}\right)^{\left(k_d+k-j\right)} \left[\eta_{iM} + \left|v_r(k)\right|\right] + \delta_r \frac{(1-g_{rr}^{(k+1-k_{1r})})}{(1-g_{rr})} \qquad \text{(A.16)}$$

Combine (A.15) and (A.16), we have

$$\delta_r \frac{(1-g_{rr}^{(k+1-k_{1r})})}{(1-g_{rr})} \geq \left(g_{rr}\right)^k \left|e_r(k_d)\right| + 2\left(g_{rr}\right)^{(k-k_{1r})} \left[\sum_{j=k_d}^{k_d+k_{1r}} \left(g_{rr}\right)^{\left(k_d+k_{1r}-j\right)} \left(\eta_{i_M} + \left|v_r(j)\right|\right)\right]$$

Therefore, solving the above equation for k , we have

$$(1-g_{rr}^{(k+1-k_{1r})}) \geq \frac{(1-g_{rr})}{\delta_r}\left(\left(g_{rr}\right)^k \left|e_r(k_d)\right| + 2\left(g_{rr}\right)^{(k-k_{1r})} \left[\sum_{j=k_d}^{k_d+k_{1r}} \left(g_{rr}\right)^{\left(k_d+k_{1r}-j\right)} \left(\eta_{i_M} + \left|v_r(j)\right|\right)\right]\right)$$

After some manipulation, we have

$$k = k_{1r} - 1 + \log\left\{ \frac{1 + \frac{(1-g_{rr})}{\delta_r}\left[\left(g_{rr}\right)^{(k_{1r}-1)} \left|e_r(k_d)\right| \right.}{\log(g_{rr}^{-1})} + \frac{\left. \frac{2}{g_{rr}}\left(\sum_{j=k_d}^{k_d+k_{1r}} \left(g_{rr}\right)^{\left(k_d+k_{1r}-j\right)} \left(\eta_{i_M} + \left|v_r(j)\right|\right)\right)\right]}{\log(g_{rr}^{-1})} \right\}$$

Proof of Theorem 5: The TTF is estimated by using the maximum value or threshold, i.e., $\theta_{i_j}(k_{f_{i_j}}) = \theta_{i_{j\max}}$. Equation (14) holds only in the time interval $k \in [k_d, k_f]$. Consequently, the update equation in (8) can be written as

$$\hat{\theta}_{i_j}(k+1) = \left(1 - \gamma_i \left\| I - \alpha_i f_i f_i^T \right\|\right)\hat{\theta}_{i_j}(k) + \alpha_i \left(f_i(k) e_i(k+1)\right)_j$$

The above equation becomes linear time varying system at each time instant by considering other terms being held at the time of prediction as

$$\overline{x}(k+1) = \overline{a}(k)\overline{x}(k) + \overline{b}\overline{u}(k) \qquad \text{(A.17)}$$

where $\overline{x}(k+1) = \hat{\theta}_{i_j}(k+1)$, $\overline{a}(k) = (1 - \gamma_i \| I - \alpha_i f_i f_i^T \|)$, $\overline{b} = \alpha_i$, and $\overline{u}(k) = \left(f_i(k) e_i(k+1) \right)_j$.

Note $\overline{u}(k)$ is the j^{th} product of the i^{th} basis function and the i^{th} fault isolation residual. Therefore, the solution of the system defined in (A.17) is given by

$$\overline{x}(k) = \prod_{t=k_{0_{i_j}}}^{k} \overline{a}(t)\overline{x}(k_{0_i}) + \sum_{r=k_{0_{i_j}}}^{k} \left(\prod_{t=r}^{k} \overline{a}(t) \right) \overline{b}\overline{u}(r)$$

Since the j^{th} system parameter reaches its maximum value at the time of failure, i.e., $k_{f_{i_j}}$, then $\theta_{i_j}(k_{f_{i_j}}) = \theta_{i_{j\max}}$. Additionally, the value of $\theta_{i_j}(k_{0_{i_j}}) = \theta_{i_{j_0}}$; hence the above equation becomes $\theta_{i_{j\max}} = \prod_{t=k_{0_{i_j}}}^{k_{f_{i_j}}} \overline{a}(t)\overline{x}(k_{0_i})\theta_{i_{j_0}} + \sum_{r=k_{0_{i_j}}}^{k_{f_{i_j}}} \left(\prod_{t=r}^{k_{f_{i_j}}} \overline{a}(t) \right) \overline{b}\overline{u}(r)$. In the above equation, for the time interval $[k_{0_{i_j}}, k_{f_{i_j}}]$, $\overline{a}(k)$ and $\overline{u}(k)$ are assumed to be time invariant, scalars. This assumption is reasonable since $0 < \overline{a} < 1$ and the input $\overline{u}(k)$ would be bounded due to the guaranteed stability of the parameter update law in (8) although the input (in this case the residual) is continuously increasing due to the presence of a fault. Consequently, the system defined above can be considered a linearly time-invariant system. Also, TTF is continuously updated at each time instant in the interval $k \in [k_d, k_f]$, as explained below. Hence

$$\theta_{i_{j\max}} = \overline{a}^{(k_{f_{i_j}} - k_{0_{i_j}})} \theta_{i_{j_0}} + \overline{b}\overline{u} \sum_{t=k_{0_{i_j}}+1}^{k_{f_{i_j}}} \overline{a}^{(k_{f_{i_j}} - t)} \qquad \text{(A.18)}$$

Using results of geometric series, (A.18) becomes

$\theta_{i_{j\max}} = \overline{a}^{(k_{f_{i_j}} - k_{0_{i_j}})} \theta_{i_{j_0}} + \overline{b}\overline{u}\left(\frac{1-\overline{a}^{(k_{f_{i_j}} - k_{0_{i_j}})}}{1-\overline{a}}\right)$. With some simple mathematical

manipulation, one obtains

$\overline{a}^{(k_{f_{i_j}} - k_{0_{i_j}})} = \frac{[\theta_{i_{j\max}}(1-\overline{a}) - \overline{b}\overline{u}]}{[\theta_{i_{j_0}}(1-\overline{a}) - \overline{b}\overline{u}]}$. Finally, after performing additional mathematical

manipulation, we have

$k_{f_{i_j}} = \frac{\left|\log\left(\left|\frac{\theta_{i_{j\max}}(1-\overline{a}) - \overline{b}\overline{u}}{\theta_{i_{j_0}}(1-\overline{a}) - \overline{b}\overline{u}}\right|\right)\right|}{\left|\log(\overline{a})\right|} + k_{0_{i_j}}$. Since $\overline{a}$, $\overline{b}$, and $\overline{u}$ are known, therefore equation

(14) results.

References

[1] J. J. Gertler, *Fault Detection and Diagnosis in Engineering Systems*, Marcel Dekker, New York, USA, 1998.

[2] P. M. Frank and L. Keller,"Fault diagnosis in dynamic systems using analytical and knowledge-based redundancy – A survey and some new results," *Automatica*, vol. 26, pp. 459-474, 1990.

[3] M. Massoumnia, G. C. Verghese, and A. S. Willsky,"Failure detection and identification," *IEEE Trans. on Automatic Control*, vol. 34, no. 3, pp. 316-322, 1989.

[4] A. Alessandri,"Fault diagnosis for nonlinear systems using a bank of neural estimators," *Computers in Industry*, vol. 52, no. 3, pp. 271-289, 2003.

[5] R. Martinez-Guerra and A. Luviano-Juarez,"Fault diagnosis of nonlinear systems using reduced-order observers and algebraic observers," *Proc. of the Conference on Decision and Control (CDC)*, San Diego, USA, pp. 544-549, 2006.

[6] A. P. Wang and H. Wang,"Fault diagnosis for nonlinear systems via neural networks and parameter estimation," *International Conference on Control and Automation* (ICCA '05), Budapest, Hungary, vol. 1, pp. 559- 563, 2005.

[7] Q. Wu and M. Saif,"Robust fault detection and diagnosis in a class of nonlinear systems using a neural sliding mode observer," *International Journal of Systems Science*, vol. 38, no. 11, pp. 881-899, 2007.

[8] X. Zhang, M. M. Polycarpou, and T. Parsini,"A robust detection and isolation scheme for abrupt and incipient faults in nonlinear systems," *IEEE Trans. on Automatic Control*, vol. 47, no. 4, pp. 576-593, 2002.

[9] H.A. Talebi, S. Tafazoli, and K. Khorasani,"A recurrent neural-network-based sensor and actuator fault detection and isolation for nonlinear systems with application to the satellite's attitude control subsystem," *IEEE Trans. on Neural Networks*, vol. 20, no.1, pp. 45- 60 , 2009.

[10] S. Narasimhan, P. Vachhani, and R. Rengaswamy,"Nonlinear residual feedback observer for fault diagnosis in nonlinear systems," *Automatica*, vol. 44, no. 9, pp.2222-2229, 2008.

[11] X. G. Yan and C. Edwards,"Nonlinear robust fault reconstruction and estimation using a sliding mode observer," *Automatica*, vol. 43, no. 9, pp. 1605-1614, 2007.

[12] X. G. Yan and C. Edwards,"Adaptive sliding-mode-observer-based fault reconstruction for nonlinear systems with parametric uncertainties," *IEEE Trans. on Industrial Electronics.*, vol. 55, no. 11, pp. 4029-4036, 2008.

[13] C. De Persis and A. Isidori,"A geometric approach to nonlinear fault detection and isolation," *IEEE Trans. on Automatic Control*, vol. 46, no. 6, pp. 853 – 865, 2001.

[14] F. Caccavale and L. Villani, *Fault Diagnosis and Fault Tolerance for Mechatronic Systems: Recent Advances*, Springer, UK, 2003.

[15] R. Isermann,"Model-based fault-detection and diagnosis–status and applications," *Annual Reviews in Control*, vol. 29, no.1, pp. 71-85, 2005.

[16] M. L. McIntyre, W. E. Dixon, D. M. Dawson, and I. D. Walker,"Fault identification for robot manipulators," *IEEE Trans. on Robotics and Automation*, vol. 21, no. 5, pp. 1028-1034, 2005.

[17] J. Luo, M. Namburu, K. Pattipati, L. Qiao, M. Kawamoto, and S, Chigusa,"Model-based prognostic techniques," *AUTOTESTCON 2003: IEEE Systems Readiness Technology Conference*, Anaheim, California, USA, pp. 330-340, 2003.

[18] J. Luo, A. Bixby, K. Pattipati, L. Qiao, M. Kawamoto, and S. Chigusa,"An interacting multiple model approach to model-based prognostics," *IEEE International Conference on Systems, Man and Cybernetics*, Washington, D.C., USA, vol. 1, pp. 189-194, 2003.

[19] E. Phelps, P. Willett, and T. Kirubarajan,"Useful lifetime tracking via the IMM," *Components and System Diagnostics, Prognostics, and Health Management II, Proc. of SPIE*, vol. 4733, pp. 145-156, 2002.

[20] M. J. Roemer and D. M. Ghiocel,"A probabilistic approach to the diagnosis of gas turbine engine faults," *53rd Machinery Prevention Technologies (MFPT) Conference*, Virginia Beach, VA, USA, pp. 325-336, 1999.

[21] Y. Shao and K. Nezu,"Prognosis of remaining bearing life using neural networks," *Proc. of the Institution of Mechanical Engineers, Part I: Journal of Syst. and Control Eng.*, vol. 214, no. 3, pp. 217-230, 2000.

[22] F. Cacccavale, F. Pierri, and L. Villani,"Adaptive observer for fault diagnosis in nonlinear discrete-time systems," *ASME Journal of Dynamic Syst., Meas., and Control*, vol. 130, no. 2, pp. 1-9, 2008.

[23] F. Caccavale and L. Villani,"An adaptive observer for fault diagnosis in nonlinear discrete-time systems," *Proc. of the American Control Conference*, pp. 2463-2468, Boston, MA, 2004.

[24] B. T. Thumati and S. Jagannathan,"A model based fault detection and accommodation scheme for nonlinear discrete-time systems with asymptotic stability guarantee," *Proc. of American Controls Conference,* St. Louis, MO, pp. 4988 – 4993, 2009.

[25] J. Zhang and A. J. Morris,"On-line process fault diagnosis using fuzzy neural networks," *Intelligent Syst. Engineering*, pp. 37-47, 1994.

[26] C. Edwards, S. K. Spurgeon, and R. J. Patton,"Sliding mode observers for fault detection and isolation," *Automatica,* vol. 36, pp. 541-553, 2000.

[27] C. T. Chen, *Linear System Theory and Design*, 3rd Ed., Oxford University Press, New York, 1999.

[28] F. L. Lewis, S. Jagannathan, and A. Yesilderek, *Neural Network Control of Robotics and Nonlinear Systems*, Taylor & Francis, UK, 1999.

[29] P. M. Patre, W. MacKunis, K. Kaiser, and W. E. Dixon,"Asymptotic tracking for uncertain dynamics systems via a multilayer NN feed forward and RISE feedback

control structure," *Proc. of the American Control Conference*, New York City, NY, USA, pp. 5989-5994, 2007.

[30] S. Huang, K. K. Tan, and T. H. Lee,"Decentralized control design for large-scale systems with strong interconnections using neural networks," *IEEE Trans. on Automatic Control*, vol. 48, no. 5, pp. 805-810, 2003.

[31] D. M. Dawson, Z. Qu, and S. Lim,"Re- thinking the robust control of robot manipulators," *Proc. of the Conference on Decision and Control (CDC)*, Brighton, England, pp. 1043-1045, 1991.

[32] S. Jagannathan, *Neural Network Control of Nonlinear Discrete–time Systems*, CRC publications, New York, USA, 2006.

5. An Asymptotically Stable Online Fault Detection and Accommodation Scheme for Nonlinear Discrete-time Systems

Balaje T. Thumati and S. Jagannathan

Abstract- In this paper, a FDA framework is developed for non-affine nonlinear discrete-time systems by using online approximators. A residual signal is generated by comparing the measured system states with the output of a nonlinear fault detection estimator. A fault is declared active when the residual exceeds a mathematically derived threshold which is defined using the upper bounds on the system uncertainties. Subsequently, an online approximator and a novel robust term, which is defined as a function of online approximator parameter vector, are activated in the nonlinear fault estimator. The online approximator reconstructs the unknown fault dynamics. Next, a novel controller design is introduced in order to accommodate the unknown fault by using a second online approximator and a different robust term. Stable adaptation laws in discrete-time are developed to tune the parameter vector of the online approximators used for both constructing the unknown fault dynamics and the reconfiguring of the controller. By using Lyapunov theory, asymptotic performance of the detection and the accommodation schemes is demonstrated. Finally, a simulation example is utilized to illustrate the performance of the proposed FDA scheme.

Keywords**:** Fault Detection, Fault Accommodation, Asymptotic Stability, and Lyapunov Theory.

1. Introduction

In this paper, a model based FDA scheme is developed as they are considered more robust when compared to qualitative based techniques (Frank and Keller, 1990; Chen and Patton, 1999). In the past literature (Frank and Keller, 1990; Chen and Patton, 1999; Gertler, 1988), FDA schemes are developed by assuming: 1) a linear model of the system, 2) sensor faults, and 3) system uncertainties and fault modes are decoupled. Since in most scenarios, practical systems are nonlinear in nature, the above discussed schemes (Frank and Keller, 1990; Chen and Patton, 1999; Gertler, 1988) have not been applied extensively.

Now, with the development of adaptive control theory, different FDA schemes were developed (Polycarpou, 2001; Polycarpou and Helmicki, 1995; Jiang and Chowdhury, 2005; Chen and Saif, 2001) for nonlinear systems. Such schemes are capable of detecting both abrupt and incipient faults. In addition, the stability, robustness, and sensitivity of the schemes are studied extensively. However, the drawbacks of the nonlinear FDA scheme (Polycarpou, 2001; Polycarpou and Helmicki, 1995; Jiang and Chowdhury, 2005; Chen and Saif, 2001) include: 1) bounded performance guarantees of the FDA technique and 2) applicability to nonlinear continuous time systems. It is well-known in the literature that continuous-time development (Lewis *et al.*, 1999) cannot be easily converted directly into discrete-time for hardware implementation due primarily to the fact that Lyapunov first difference is quadratic with respect to the states whereas first derivative of the Lyapunov function is linear. In addition, by increasing the sampling rates alone, one cannot ensure stability of nonlinear systems for discrete-time implementation even if the continuous-time counterpart is stable.

Therefore, Caccavale and Villani (2004) introduced a fault detection scheme in discrete-time by using the stringent persistent of excitation (PE) condition, which is very difficult to verify or guarantee. Therefore, in our previous work (Thumati and Jagannathan, 2007), a fault detection scheme using online approximators (OLA) is introduced by relaxing the PE requirement. However, uniform ultimate boundedness of all the signals is demonstrated similar to the case of fault detection algorithms in continuous-time.

By contrast, in this paper, a novel FDA scheme is introduced for detecting and accommodating faults in nonlinear discrete-time system in non-affine form. First, a nonlinear fault detection estimator comprising of a nonlinearly parameterized online approximator in discrete time (OLAD) using multilayer neural network (MNN) and a robust term is used for detecting and learning unknown nonlinear fault dynamics. In contrast, the FDA schemes in continuous-time use linearly parameterized approximators. The purpose of the fault detection estimator is to generate residuals for fault detection. Later, a novel online fault accommodation strategy is developed by reconfiguring the controller. The design of the corrective control for an unknown fault dynamics is acheived by using linearly parameterized and nonlinearly parameterized online approximators. Finally, the stability of the FDA scheme is analyzed extensively using the Lyapunov theory. It is obsereved that for a linearly parameterized approximator, the FDA scheme renders asymptotic stability of the closed loop systems, whereas, for a nonlinearly parameterized approximator, the FDA scheme renders asymptotic convergence of the residual and tracking error while parameters of the approximators remain bounded.

These improved performance results obtained in this paper are possible due to the introduction of the robust term and making some mild assumptions on the uncertainities.

In summary, the major contribution of this paper is the introduction of a novel multilayer-based fault detection and accommodation scheme for non-affine nonlinear discrete-time system. The proposed scheme renders asymptotic performance guarantees in the presence of NN reconstruction errors. To best of our knowledge there is no previously reported FDA scheme for such class of systems that renders asymptotic performance. In the next section, the system under investigation is explained.

2. Problem Statement

To address a wide range of physical systems, the following general class of nonlinear discrete-time system is considered as

$$x(k+1) = \omega(x(k), u(k)) + \eta(x(k), u(k)) + h(x(k), u(k)) \tag{1}$$

where $x \in \Re^n$ is the system state vector, $u \in \Re^m$ is the control input vector, and $\omega : \Re^n \times \Re^m \to \Re^n$, $\eta : \Re^n \times \Re^m \to \Re^n$, $h : \Re^n \times \Re^m \to \Re^n$ are smooth vector fields. The term $\omega(x(k), u(k))$ represents the known nonlinear system dynamics while $\eta(x(k), u(k))$ denotes system uncertainty. The unknown function $h(x(k), u(k)) = \Pi(k - k_0) f(x(k), u(k))$, represents the fault function where $f(x(k), u(k))$ represents the unknown fault dynamics with $\Pi(k - k_0)$ being a $n \times n$ square matrix function representing the time profiles of the faults, and $k_0 \geq 0$ is the starting time.

Typically, the time profiles of the faults are modeled by

$$\Pi(k - k_0) = diag(\Omega_1(k - k_0), \Omega_2(k - k_0), ..., \Omega_n(k - k_0))$$

where

$$\Omega_i(\tau) = \begin{cases} 0, & \text{if } \tau < 0 \\ 1 - e^{-\bar{\kappa}_i \tau}, & \text{if } \tau \geq 0 \end{cases} \quad \text{for } i = 1, 2, \ldots n \tag{2}$$

and $\bar{\kappa}_i > 0$ is an unknown constant representing the rate at which the fault in the corresponding state x_i occurs. The term $\Omega_i(\tau)$ approaches a step function when $\bar{\kappa}_i$ is large, which in turn represents an abrupt fault. The primary focus of this paper is on the abrupt faults; however, some aspects of incipient faults are considered as well.

Remark 1: Modeling faults using the above time profile is quite common in the fault detection literature as given in Zhang and Morris (1994), and used extensively by researchers (Polycarpou, 2001; Caccavale and Villani, 2004; Demetriou and Polycarpou, 1998).

The first step in any FDA scheme is fault detection. In this paper, for the purpose of fault detection, a MNN-based online approximator is introduced whereas for the purpose of accommodation both a single layer and MNN based approximators will be used. Next, the following assumption is borrowed from the fault detection literature.

Assumption 1: The modeling uncertainty is unstructured and bounded (Polycarpou, 2001; Caccavale and Villani, 2004; Demetriou and Polycarpou, 1998; Polycarpou and Helmicki, 1995), i.e.,

$$\left\| \eta(x(k), u(k)) \right\| \leq \eta_M, \ \forall (x, u) \in (\chi \times U)$$

where $\eta_M \geq 0$ is a known constant.

Remark 2: This assumption is required to distinguish uncertainties from the fault functions.

In the previously reported fault detection schemes (Frank and Keller, 1990; Chen and Patton, 1999; Gertler, 1988), the type of uncertainty assumed is structured and/or parametric. This may not be true for most physical system in an industrial setting and therefore in this paper, such assumptions are relaxed unlike other schemes where simple sensor faults (Caccavale and Villani, 2004) are considered. In the next section, the fault detection scheme is introduced.

3. Fault Detection Scheme

The nonlinear estimator presented below comprises of the OLAD and a novel adaptive robust term. It is worth noting that the purpose of the fault detection estimator is not to estimate the system states since they are measured, but to use the estimated states to generate residuals. This is in contrast with a state estimator or an observer that is normally used for controller design.

A. Nonlinear Estimator Dynamics

Based on the system representation (1), a nonlinear fault estimator is given by

$$\hat{x}(k+1) = A_0\hat{x}(k) + \omega(x(k),u(k)) + \hat{h}(x(k),u(k);\hat{\theta}(k)) - A_0x(k) + v(k) \tag{3}$$

where $\hat{x} \in \Re^n$ is the estimated state vector, $\hat{h}: \Re^n \times \Re^m \times \Re^{l\times n} \to \Re^n$ is the online approximation in discrete-time (OLAD), $\hat{\theta} \in \Re^{l\times n}$ is a set of adjustable parameters of the OLAD, A_0 is a constant $n\times n$ design matrix chosen by the user, and $v(k)$ is the robust term, which is to be defined later. Prior to the occurrence of the fault, the initial values for the fault detection estimator (3) are taken as $\hat{x}(0) = x(0)$, $\hat{\theta}(0) = \hat{\theta}_0$, such that $\hat{h}(x,u,\hat{\theta}_0) = 0$ for all $x \in \chi$ and $u \in U$.

Remark 3: Only upon the detection of a fault, the OLAD and the robust term are initiated.

Define the residual as $e = x - \hat{x}$. From (1) and (3) prior to the fault, the residual dynamics is written as

$$e(k+1) = A_0 e(k) + \eta(x(k), u(k)) \tag{4}$$

In order to detect faults in the system, the residual is compared against a known threshold by using a dead-zone operator in order to improve robustness (Frank and Keller, 1990). The dead-zone operator is defined as $D[\cdot]$ as

$$D[e(k)] = \begin{cases} 0, & \text{if } \|e(k)\| \le \rho \\ e(k), & \text{if } \|e(k)\| > \rho \end{cases} \tag{5}$$

where $\rho > 0$ is the threshold. The selection of the threshold size ρ clearly provides a tradeoff between reducing the possibility of false alarms (robustness) and improving the sensitivity of the faults.

Remark 4: A threshold is widely used in existing fault detection schemes (Polycarpou, 2001; Caccavale and Villani, 2004; Polycarpou and Helmicki, 1995; Thumati and Jagannathan, 2007). To minimize false alarms, this threshold on the residual is normally selected based on the bound on the system uncertainties and approximation errors.

Prior to the fault, the residual, $e(k)$, will remain within the threshold. But, in the event of a fault, the residual increases and exceeds the threshold declaring a fault is active. The selection of an appropriate value for ρ is addressed next.

B. Performance of the Detection Scheme

For selecting an appropriate threshold, consider the residual dynamics defined in (4) prior to the fault. The solution of equation (4) can be obtained from standard linear

control theory (Chen, 1999) which is given by $e(k) = \sum_{j=0}^{k-1} A_0^{k-1-j} \eta(x(j), u(j))$ for zero initial conditions. Since the matrix A_0 satisfies the Schur's criterion (Chen, 1999), there exist two positive constants μ and β_c such that the Frobenius norm $\left\| A_0^k \right\| \le \beta_c \mu^k < 1$. Therefore, $\|e(k)\| \le \beta \eta_M \frac{(1-\mu^k)}{(1-\mu)}$, where $\beta = \beta_c \mu$. This implies that if the size of the dead-zone is selected as $\rho = \frac{\beta \eta_M}{(1-\mu)}$, then the residual $e(k)$ would remain within the threshold for all $k \ge k_0$. Under these conditions, the OLAD and the robust term are not initiated.

Normally, a linearly parameterized OLAD is used for learning the unknown fault dynamics after the detection. In contrast, in this paper, a nonlinearly parameterized OLAD or a MNN is used as OLAD since a MNN is more accurate than a linearly parameterized approximator (Jagannathan, 2006). Hence the fault dynamics in (1) could be written as

$$h(x(k), u(k)) = \theta_3^T \varphi_3(\theta_2^T \varphi_2(\theta_1^T \varphi_1(x(k), u(k)))) + \varepsilon_1(k) \tag{6}$$

where θ_1, θ_2, and θ_3 are the target weights of the MNN-based OLAD and $\varepsilon_1(k)$ being the reconstruction errors. By appropriate selection of the MNN size, the approximation error could be made small (Barron, 1993). Additionally, the target weights are considered to be bounded $\|\theta_1\| \le \theta_{1\max}$, $\|\theta_2\| \le \theta_{2\max}$ and $\|\theta_3\| \le \theta_{3\max}$ and $\varphi_1(.)$, $\varphi_2(.)$ and $\varphi_3(.)$ are the activation functions of the first, second and third layer of the NN respectively.

Also, the OLAD output in (3) is expressed as

$$\hat{h}(x(k), u(k), \hat{\theta}(k)) = \hat{\theta}_3^T(k) \hat{\varphi}_3(\hat{\theta}_2^T(k) \hat{\varphi}_2(\hat{\theta}_1^T(k) \hat{\varphi}_1(x(k), u(k)))) \tag{7}$$

where $\hat{\theta}_1(k)$, $\hat{\theta}_2(k)$, and $\hat{\theta}_3(k)$ are the actual weights of the first, second and third layers of the MNN OLAD and $\hat{\varphi}_1(x(k))$ represent input layer activation function. Then $\hat{\varphi}_2(\hat{\theta}_1^T(k)\hat{\varphi}_1(x(k),u(k)))$, $\hat{\varphi}_3(\hat{\theta}_2^T(k)\hat{\varphi}_2(\hat{\theta}_1^T(k)\hat{\varphi}_1(x(k),u(k))))$ denote the hidden layer and output layers activation function respectively at the k^{th} instant. For a multilayer function approximation, the activation function vector need not form a basis function (Jagannathan, 2006). Define the weight or parameter estimation errors as

$\tilde{\theta}_1(k) = \theta_1 - \hat{\theta}_1(k)$, $\tilde{\theta}_2(k) = \theta_2 - \hat{\theta}_2(k)$ and $\tilde{\theta}_3(k) = \theta_3 - \hat{\theta}_3(k)$.

Next the following fact can be stated.

Fact 1: The activation functions for a MNN are bounded by known positive values such that

$\|\hat{\varphi}_1(k)\| \le \varphi_{1_{\max}}$, $\|\hat{\varphi}_2(k)\| \le \varphi_{2_{\max}}$ and $\|\hat{\varphi}_3(k)\| \le \varphi_{3_{\max}}$.

Define activation function vector error as

$\tilde{\varphi}_1(k) = \varphi_1 - \hat{\varphi}_1(k)$, $\tilde{\varphi}_2(k) = \varphi_2 - \hat{\varphi}_2(k)$ and $\tilde{\varphi}_3(k) = \varphi_3 - \hat{\varphi}_3(k)$.

Using the definitions in (6) and (7), the residual dynamics from (1) and (3) upon detection would become

$$e(k+1) = A_0 e(k) + \eta(x(k),u(k)) + \Psi_1(k) + \varepsilon_1(k) + \theta_3^T \tilde{\varphi}_3(x(k)) - \frac{\hat{\theta}_3^T(k) B_v}{B_v^T \hat{\theta}_3(k) \hat{\theta}_3^T(k) B_v + c_m} \tag{8}$$

where $\Psi_1(k) = \tilde{\theta}_3^T(k)\hat{\varphi}_3(x(k))$, and $v(k) = \frac{\hat{\theta}_3^T(k) B_v}{B_v^T \hat{\theta}_3(k) \hat{\theta}_3^T(k) B_v + c_m}$ being the robust term, with $c_m > 0$ is a constant and B_v is an appropriate dimensioned constant vector, to be defined

later. Next by adding and subtracting $\frac{\theta_3^T B_v - C_v}{B_v^T \hat{\theta}_3(k)\hat{\theta}_3^T(k) B_v + c_m}$ in (8), where C_v is an appropriate dimensioned constant vector, would result in the following equation

$$e(k+1) = A_0 e(k) + \Psi_1(k) + \Psi_2(k) + \varepsilon(k) - \frac{(\theta_3^T B_v - C_v)}{B_v^T \hat{\theta}_3(k)\hat{\theta}_3^T(k) B_v + c_m} \tag{9}$$

where $\varepsilon(k) = \eta(x(k), u(k)) + \varepsilon_1(k) + \theta_3^T \tilde{\varphi}_3(x(k))$, $\Psi_2(k) = \frac{\tilde{\theta}_3^T(k) B_v - C_v}{B_v^T \hat{\theta}_3(k)\hat{\theta}_3^T(k) B_v + c_m}$.

Next, the following theorem is introduced to guarantee the asymptotic stability of the residual in the fault detection scheme with the nonlinear MNN-based OLAD. Before we proceed, the following Lemma is needed.

Lemma 1: The term (ε), and the ideal weights of the MNN OLAD are assumed to be bounded above by a smooth nonlinear function of the residual and the last layer NN weights (Patre et. al, 2007; Kwan et. al, 1995; Lewis et. al, 1999) as

$$\frac{\sum_{i=1}^{2} \theta_{i_{\max}}^2 \left\|\hat{\varphi}_i(k)\right\|^2}{(2 - \alpha_i \left\|\hat{\varphi}_i(k)\right\|^2)} + (5\alpha_3 \hat{\varphi}_3^T \hat{\varphi}_3 + 4)\varepsilon^T(k)\varepsilon(k) \le \beta_0 + \beta_1 \left\|e(k)\right\|^2 + \beta_2 \left\|\tilde{\theta}_3(k)\hat{\varphi}_3(k)\right\|^2 + \beta_3 \left\|e(k)\right\| \left\|\tilde{\theta}_3(k)\hat{\varphi}_3(k)\right\|$$

where $\beta_0, \beta_1, \beta_2,$ and β_3 are computable positive constants.

Proof: Refer to Appendix.

Theorem 1 (Fault Detection Estimator Performance): Let the proposed estimator in (3) comprising of a nonlinearly parameterized OLAD be used to monitor the system given by (1). Considering bounded system uncertainties and under Assumptions 1-2, let the MNN based OLAD weight tuning be provided by

$$\hat{\theta}_1(k+1) = \hat{\theta}_1(k) - \alpha_1 \hat{\varphi}_1(k)[\hat{y}_1(k) + B_1 A_0 e(k)]^T \tag{10}$$

$$\hat{\theta}_2(k+1) = \hat{\theta}_2(k) - \alpha_2\ \hat{\varphi}_2(k)[\hat{y}_2(k) + B_2 A_0 e(k)]^T \tag{11}$$

with $\hat{y}_i(k) = \hat{w}_i^T(k)\ \hat{\varphi}_i(k)$ and $\|B_i\| \le \kappa_i$, $i = 1, 2$. Let the weight update law for the third layer be

$$\hat{\theta}_3(k+1) = \hat{\theta}_3(k) + \alpha_3\ \hat{\varphi}_3(k) e^T(k+1) \tag{12}$$

where $\alpha_i > 0$, $\forall i = 1, 2, 3$, denotes the learning rate or adaptation gains. Then, the residual, $e(k)$, is locally asymptotically stable, while the MNN OLAD weight estimation errors $\tilde{\theta}_1(k)$, $\tilde{\theta}_2(k)$ and $\tilde{\theta}_3(k)$ are bounded.

Remark 5: Theorem 1 guarantees the asymptotic stability of the residual in the proposed fault detection scheme after the fault has occurred by using a nonlinearly parameterized OLAD. Such results using nonlinearly parameterized OLAD for continuous-time and for nonlinear discrete-time systems are currently not available. By contrast, in continuous-time (Caccavale and Villani, 2004; Demetriou and Polycarpou, 1998; Polycarpou and Helmicki, 1995), a bounded residual is only shown even with a linearly parameterized OLAD.

Remark 6: The purpose of the fault detection estimator is to generate the residual signal. This is in contrast with the state estimators normally used in the controller designs.

In the next section, the fault accommodation scheme is introduced.

4. Fault Accommodation Scheme

Fault accommodation involves the reconfiguration of the control input to compensate the unknown fault function (Polycarpou 2001). Here, the problem is more complicated since the fault $h(.)$ is unknown and non-affine in nature. Prior to the fault detection, any bounded controller derived for non-affine systems can be used (see, Young et *al.*,

2006)) and one such control design is presented later in this section.

Next, the nonlinear system (1) with the fault function is expressed as

$$x(k+1) = \omega(x(k), u(k)) + \eta(x(k), u(k)) + h(x(k), u(k))$$

This system could be transformed into affine-like form by using the technique from Yang et *al.* (2008) as

$$x(k+1) = \eta_f(x(k)) + \eta_g(x(k))\Delta u(k) \tag{13}$$

where $\eta_f, \eta_g : \Re^n \to \Re^n$ are unknown smooth vector fields due to the presence of unknown fault function and system uncertainties included along with the known nominal dynamics, and $\Delta u(k) = u(k) - u(k-1)$, with $\Delta u(0) = 0$. Before introducing the fault accommodation control law, the following standard assumption is needed (Jagannathan, 2006).

Assumption 2: The term $\eta_g(x(k)) \in \Re^{n \times n}$ is a positive definite invertible diagonal matrix for each $\chi \subset \Re^n$. Further, assume $\eta_{\min} \in \Re$ and $\eta_{\max} \in \Re$ represent the minimum and the maximum eigenvalues of the matrix $\eta_g(x(k))$ such that $0 < \eta_{\min} \le \eta_{\max}$ (see, Yang et. *al* 2008).

Next, select the control input change after detection as

$$\Delta u(k) = \frac{1}{\eta_g(x(k))}(x_d(k+1) - \eta_f(x(k))) + le_t(k) + v_c(k) \tag{14}$$

where e_t is the tracking error, $x_d(k)$ is the desired trajectory, $v_c(k)$ is another robust adaptive term to be defined later and l is a user selectable design matrix.

Since η_f and η_g are not known in (14), this problem is overcome by utilizing another OLAD. Initially, a linearly parameterized NN is used, i.e.,

$$\Delta u(k) = W^T \phi(x(k), x_d(k+1)) + \varepsilon_t(k) + le_t(k) + v_C(k)$$

where $W \in \Re^{n \times p}$ is the target weight matrix and $\phi(.) \in \Re^{p \times 1}$ is the basis function such as RBF, sigmoid function, with $\varepsilon_t(k)$ is the NN approximation error. In addition, as seen in the previous section, the approximation error is considered to be bounded above such that $\|\varepsilon_t(k)\| \le \varepsilon_{tM}$. Therefore, the output of the linearly parameterized NN is given by

$$\Delta u(k) = \hat{W}^T(k)\phi(x(k), x_d(k+1)) + le_t(k) + v_C(k)$$

Next, define the robust term $v_c(k)$ as

$v_c(k) = \dfrac{\hat{W}^T(k) B_{1t}}{B_{1t}^T \hat{W}(k) \hat{W}^T(k) B_{1t} + c_t}$, where $B_{1t} \in \Re^{p \times 1}$ is a constant vector and $c_t > 0$ is a constant. Therefore, the tracking error dynamics after detecting a fault becomes

$$e_t(k+1) = \eta_g(x(k))\left(le_t(k) + \Psi_{1t}(k) + \varepsilon_{mt}(k) - \Psi_{2t}(k) + \frac{W^T B_{1t}}{B_{1t}^T \hat{W}(k) \hat{W}^T(k) B_{1t} + c_t} \right) \quad (15)$$

where $\Psi_{1t}(k) = (\tilde{W}^T(k)\phi(k))$, $\varepsilon_{mt}(k) = (-\varepsilon_t(k) + (W^T(k)\tilde{\phi}(k))$, and $\Psi_{2t}(k) = \dfrac{\left(\tilde{W}^T(k) B_{1t} - C_{1t}\right)}{B_{1t}^T \hat{W}(k) \hat{W}^T(k) B_{1t} + c_t}$,

$C_{1t} \in \Re^{n \times 1}$ is a constant vector.

Next, the following lemma is required before proceeding any further.

Lemma 2: The term, $\varepsilon_t(k)$, can be expressed as a function of tracking and the NN weight estimation error bounds (Patre *et al.*, 2007; Kwan *et al.*, 1995; Lewis *et al.*, 1999), i.e.,

$$\left(1 + 15\alpha_c \phi^T \phi\right) \varepsilon_t^T(k) \varepsilon_t(k) \le \varepsilon_{tM} = b_0 + b_1 \|e_t(k)\|^2 + b_2 \|e_t(k)\| \|\tilde{W}(k)\| + b_3 \|\tilde{W}(k)\|^2 \quad (16)$$

where $b_0, b_1, b_2,$ and b_3 are computable positive constants.

Proof: Refer to Thumati and Jagannathan (2009).

Next, we present the following theorem, which guarantees the asymptotic stability of the closed loop system.

***Theorem 2 (Fault Accommodation Scheme)*:** Consider the system (1) with the proposed fault detection scheme described in the previous section with a linear online approximator such as a single-layer NN. Upon detection of the fault, let the control signal be augmented with $\Delta u(k) = \hat{W}^T(k)\phi(x(k), x_d(k+1)) + le_t(k) + v_c(k)$. Let the NN weight tuning be provided by

$$\hat{W}(k+1) = \hat{W}(k) + \alpha_c \phi(k) e_t^T(k+1) - \gamma_c \left\| I - \alpha_c \phi^T(k)\phi(k) \right\| \hat{W}(k) \tag{17}$$

where $\alpha_c > 0$ is the learning rate and $\gamma_c > 0$ is the adaptation rate. Then the tracking error $e_t(k)$ and the weight estimation error $\tilde{W}(k)$ are locally asymptotically stable.

***Proof*:** Refer to Thumati and Jagannathan (2009).

In addition to using a linearly parameterized NN for approximating the unknown input, a MNN could also be used to approximate the corrective control law as given below

$$\Delta u(k) = w_3^T \varphi_{m_3}(w_2^T \varphi_{m_2}(w_1^T \varphi_{m_1}(z(k)))) + \varepsilon_2(k) + le_t(k) + v_c(k)$$

where $z(k) = [x(k), x_d(k+1)]^T$, W_1, W_2, and W_3 represent target weights and $\varepsilon_2(k)$ being the MNN approximation error. Additionally, the target weights are considered to be bounded $\|W_1\| \le W_{1\max}$, $\|W_2\| \le W_{2\max}$ and $\|W_3\| \le W_{3\max}$ and $\varphi_{m_1}(.)$, $\varphi_{m_2}(.)$ and $\varphi_{m_3}(.)$ are the activation functions of the first, second and third layer of the MNN respectively. Therefore, the output of the MNN is given by

$$\Delta u(k) = \hat{w}_3^T(k)\hat{\varphi}_{m_3}(\hat{w}_2^T(k)\hat{\varphi}_{m_2}(\hat{w}_1^T(k)\hat{\varphi}_{m_1}(z(k)))) + le_t(k) + v_c(k)$$

where $\hat{w}_3(k), \hat{w}_2(k), \hat{w}_1(k)$ are the actual NN weights of the third, second and first layer respectively and $\hat{\varphi}_{m_1}(x(k))$ represent the input layer activation function. Then $\hat{\varphi}_{m_2}(.)$, $\hat{\varphi}_{m_3}(.)$ denote the hidden layer and output layers activation function respectively at the k^{th} instant.

Define the weight estimation errors as $\tilde{W}_1(k) = W_1 - \hat{W}_1(k)$, $\tilde{W}_2(k) = W_2 - \hat{W}_2(k)$, and $\tilde{w}_3(k) = w_3 - \hat{w}_3(k)$. Next the following fact can be stated.

Fact 2: Similar to Fact 1, we have $\left\|\hat{\varphi}_{m_1}(k)\right\| \le \varphi_{m_{1\max}}$, $\left\|\hat{\varphi}_{m_2}(k)\right\| \le \varphi_{m_{2\max}}$ and $\left\|\hat{\varphi}_{m_3}(k)\right\| \le \varphi_{m_{3\max}}$.

Additionally, $\tilde{\varphi}_{m_1}(k) = \varphi_{m_1} - \hat{\varphi}_{m_1}(k)$, $\tilde{\varphi}_{m_2}(k) = \varphi_{m_2} - \hat{\varphi}_{m_2}(k)$, and $\tilde{\varphi}_{m_3}(k) = \varphi_{m_3} - \hat{\varphi}_{m_3}(k)$.

It is essential to note that the control input change prior and after the fault is summarized as

$$\Delta u(k) = \begin{cases} -(1/\beta_d)(g(k) f(k)) + le_t(k) & for\, k < k_d \\ \hat{W}^T(k)\phi(.) + le_t(k) + v_c(k) (or) \hat{w}_3^T(k)\hat{\varphi}_{m_3}(.) + le_t(k) + v_c(k) & for\, k \ge k_d \end{cases}$$

where $\beta_d > 0$ is an user-defined constant, $g(k) = \partial\omega(x,u)/\partial u$, and $f(k) = \omega(x,u) - x_d(k+1)$ are known smooth vector fields obtained from the known nonaffine nominal dynamics. Finally, k_d is defined as the fault detection time. Using the above equation, $u(k)$ can be obtained.

Next, define $v_c(k) = \dfrac{\hat{W}_3^T(k) B_m}{B_m^T \hat{W}_3(k) \hat{W}_3^T(k) B_m + c_v}$, where B_m is an appropriate dimensioned constant vector, and $c_v > 0$, is a constant. Therefore, the tracking error dynamics after detecting a fault becomes

$$e_t(k+1) = \eta_g(x(k))\left(le_t(k) + \Psi_{1mt}(k) + \varepsilon_{mt}(k) - \Psi_{2mt}(k) + \frac{\left(W_3^T B_m - C_{mt}\right)}{B_m^T \hat{W}_3(k)\hat{W}_3^T(k) B_m + c_v}\right) \tag{18}$$

where $\Psi_{1mt}(k) = (\tilde{W}_3^T(k)\hat{\varphi}_{m_3}(k))$, $\varepsilon_{mt}(k) = (-\varepsilon_2(k) + W_3^T\tilde{\varphi}_{m_3}(k))$, and $\Psi_{2mt}(k) = \frac{\left(\tilde{W}_3^T(k) B_m - C_{mt}\right)}{B_m^T \hat{W}_3(k)\hat{W}_3^T(k) B_m + c_v}$, $C_{mt} \in \Re^{n\times 1}$ is a constant vector. Next, the following lemma is required before proceeding any further.

Lemma 3: The approximation error term, $\varepsilon_{mt}(k)$ of the NN can be expressed as a smooth nonlinear function of the tracking error and the MNN weight estimation errors as

$$\frac{2\sum_{i=1}^{2} W_{i_{\max}}^2 \left(\left\| \hat{\varphi}_{m_i}(k)\right\|^2\right)}{\left(2 - \alpha_{m_i}\left\|\hat{\varphi}_{m_i}(k)\right\|^2\right)} + \left(\gamma_2 B_{m_3}^T \eta_g(k) B_{m_3} + 1 + 5\alpha_{m_3}\hat{\varphi}_{m_3}^T \hat{\varphi}_{m_3} B_{m_3}^T \eta_g(k)\eta_g^T(k) B_{m_3}\right)\varepsilon_{mt}^T(k)\varepsilon_{mt}(k)$$

$$\leq p_0 + p_1\left\|e_t(k)\right\|^2 + p_2\left\|e_t(k)\right\|\left\|\tilde{W}_3(k)\hat{\varphi}_{m_3}(k)\right\| + p_3\left\|\tilde{W}_3(k)\hat{\varphi}_{m_3}(k)\right\|^2 \tag{19}$$

where p_0, p_1, p_2, and p_3 are computable positive constants.

Proof: Similar to Lemma 1.

Next, the following theorem on the asymptotic stability of the tracking error after a fault is introduced.

Theorem 3: Consider the hypothesis presented in Theorem 1, and upon detecting the fault, let the control input change be given by $\Delta u(k) = \hat{W}_3^T(k)\hat{\varphi}_{m_3}(.) + le_t(k) + v_c(k)$, where the MNN weight tuning be provided by

$$\hat{W}_1(k+1) = \hat{W}_1(k) - \alpha_{m_1}\ \hat{\varphi}_{m_1}(k)[\hat{y}_1(k) + B_{m_1} le_t(k)]^T \tag{20}$$

$$\hat{W}_2(k+1) = \hat{W}_2(k) - \alpha_{m_2}\ \hat{\varphi}_{m_2}(k)[\hat{y}_2(k) + B_{m_2} le_t(k)]^T \tag{21}$$

with $\hat{y}_i(k) = \hat{W}_i^T(k)\ \hat{\varphi}_{m_i}(k)$. Let the weight update law for the third layer be provided by

$$\hat{W}_3(k+1) = \hat{W}_3(k) + \alpha_{m_3}\ \hat{\varphi}_{m_3}(k) e_t^T(k+1) B_{m_3} \tag{22}$$

where $\alpha_{m_i} > 0$, $\left\| B_{m_i} \right\| \le \kappa_{m_i}$, $\forall i = 1, 2, 3$, denotes the learning rate or adaptation gains. Then, the tracking error, $e_t(k)$, is locally asymptotically stable, whereas the MNN weight estimation errors $\tilde{w}_1(k)$, $\tilde{w}_2(k)$ and $\tilde{w}_3(k)$ are bounded.

Proof: Refer to Appendix.

Remark 7: It is important to note that the objective of the OLAD in the case of FD is to learn the fault dynamics whereas during fault accommodation it approximates the fault dynamics plus any system uncertainties. Additionally, the update laws in (10)-(12) and (20)-(22) relaxes the need for PE without the extra term (Jagannathan 2006).

Remark 8: With the addition of the robust term, the persistency of excitation (PE) condition is not required in contrast with the past discrete-time controls literature where the PE condition is normally asserted for boundedness of the weights under the NN reconstruction errors.

In the next section, we present a simulation example to study the performance of the proposed FDA scheme.

5. Simulation Results

Consider the nonaffine nonlinear discrete system (Yang *et al.*, 2008) described in the state space form as

$$x_1(k+1) = x_2(k)$$

$$x_2(k+1) = x_3(k)$$

$$x_3(k+1) = 0.2\cos(0.8(x_2(k) + x_1(k))) + 0.4\sin(0.8(x_2(k) + x_1(k)) + 2u(k) + u(k-1)) + 0.1(9 + x_2(k) + x_1(k))$$

$$+\frac{2(u(k)+u(k-1))}{1+\cos(x_2(k))}+d(k)+h(k)u(k),\ y(k)=x_2(k) \tag{23}$$

where $x(k)=[x_1(k),x_2(k),x_3(k)]^T$ is the state vector, $y(k)$ is the output, $u(k)$ is the control input, and $d(k)$ is a bounded disturbance acting on the system, which is taken as $d(k)=0.035\sin(0.1k)+d_1(k)$, with $d_1(k)$ being a white noise with a magnitude of 0.003, and the sampling time is taken as 0.02sec. An incipient actuator fault is seeded in the system which is given by

$$h(k)=\begin{cases}(1-e^{-0.5(k-50)})0.5 & fork\geq 50\sec\\ 0 & fork<50\sec\end{cases}.$$ Moreover,

$$\frac{\partial\omega}{\partial u}=g(k)=0.8\cos(0.8(x_2(k)+x_1(k))+2u(k)+u(k-1))+{}^{2}\!\Big/\!_{(1+\cos(x_2(k)))}$$

Using the above equation, one can observe that Assumption 2 holds. A reference trajectory is defined for tracking purposes as

$$y_d(k)=\begin{cases}0.8+0.05(\sin(\pi k/50)+\sin(\pi k/100)+\sin(\pi k/150)) & fork>0\\ 0 & fork\leq 0\end{cases}$$

The initial conditions on the state vector is given by $x(0)=[0,0,0]^T$, with the nominal control law prior to the fault is defined as $\Delta u(k)=-(1/7)(g(k)f(k))+le_t(k)$, where $l=0.0001$, and

$$f(k)=0.2\cos(0.8(x_2(k)+x_1(k)))+0.4\sin(0.8(x_2(k)+x_1(k))+2u(k)$$

$$+u(k-1))+0.1(9+x_2(k)+x_1(k))+\frac{2(u(k)+u(k-1))}{1+\cos(x_2(k))}-y_d(k+1)$$

Note, this nominal controller guarantees a stable tracking performance prior to the fault as shown in the following simulation results.

Next to detect faults, the following FD estimator described by

$$\hat{x}_1(k+1) = \hat{x}_2(k) + 0.5(x_1(k) - \hat{x}_1(k))$$

$$\hat{x}_2(k+1) = \hat{x}_3(k) + 0.7(x_2(k) - \hat{x}_2(k))$$

$$\hat{x}_3(k+1) = 0.2\cos(0.8(\hat{x}_2(k) + \hat{x}_2(k))) + 0.4\sin(0.8(\hat{x}_2(k) + \hat{x}_2(k)) + 2u(k) + u(k-1)) + 0.1(9 + \hat{x}_2(k) + \hat{x}_1(k))$$

$$+ \frac{2(u(k) + u(k-1))}{1 + \cos(\hat{x}_2(k))} + h(u(k), \hat{\theta}(k)) + 0.6(x_3(k) - \hat{x}_3(k)) \tag{24}$$

is employed where $\hat{x}(k) = [\hat{x}_1(k), \hat{x}_2(k), \hat{x}_3(k)]^T$ is the vector of estimated states. The OLAD $\hat{h}(u(k), \hat{\theta}(k))$ is chosen to be a three layer NN with 4, 6, 6 sigmoid neurons in the first, second, and third layers respectively. Additionally, the weights of the MNN OLAD are tuned online using (10)-(12) with $\alpha_1 = 0.58$, $\alpha_2 = 0.21$, and $\alpha_3 = 0.12$. Parameters of the robust term, $v(k)$, is taken as $c_m = 0.02$ with B_v being a randomly chosen constant vector.

Due to system uncertainties, a threshold is chosen to avoid missed or false alarms. By taking $\beta = 1.13$, $\eta_M = 0.035$, $\mu = 0.01$, we have $\rho \approx 0.04$, which is a constant threshold. As observed in Fig. 1, the norm of the residual stays within the threshold prior to the fault although it is bounded. However, after the fault occurs, the residual exceeds this threshold thus indicating the presence of a fault. Moreover, the OLAD is initiated to learn the unknown fault dynamics online while the robust term ensures asymptotic tracking. Therefore, the residual drops and converges asymptotically to zero. This verifies the theoretical results presented in this paper.

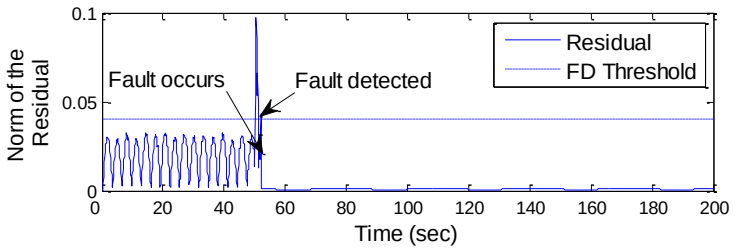

Fig. 1: Residual norm and fault detection threshold.

Next, the tracking performance of the controller without the fault accommodation scheme is shown in Fig. 2.

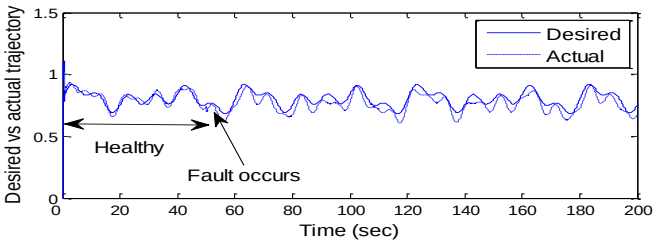

Fig. 2: Tracking performance w/o fault accommodation.

From the figure, one can observe that the tracking performance of the system deteriorates after the fault occurs. The change in the control input is summarized as

$$\Delta u(k) = \begin{cases} -(1/7)(g(k)f(k)) + le_t(k) & for k < k_d \\ \hat{u}_{ac}(k) & for k \geq k_d \end{cases}$$

where $\hat{u}_{ac}(k) = \hat{W}_3^T(k)\hat{\varphi}_{m_3}(.) + le_t(k) + v_c(k)$ by using a MNN. The MNN is chosen to be a three-layer network with 6, 8, 3, sigmoid neurons and tuned online using the update law in (20)-(22) with $\alpha_{m_1} = 0.049$, $\alpha_{m_2} = 0.039$, and $\alpha_{m_3} = 0.28$. Additionally, the parameters of the

robust adaptive term are taken as $c_v = 0.085$, with B_m randomly chosen constant vector.

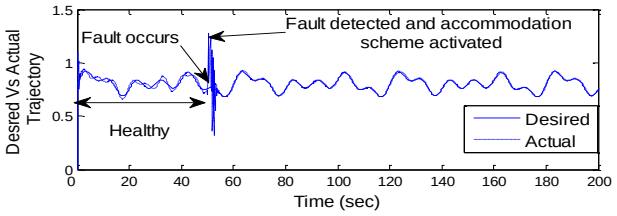

Fig. 3: Tracking performance with fault accommodation.

Fig. 3 illustrates the fault accommodation scheme upon detection which clearly demonstrates the regained tracking performance. Therefore, this simulation demonstrates the satisfactory performance of the proposed FDA scheme.

6. Conclusions

In this paper, a FDA scheme comprising of a nonlinearly parameterized approximator for nonaffine nonlinear discrete-time system is introduced. The proposed fault detection scheme quickly detects and learns the unknown faults online. Subsequently, an online fault accommodation stragtegy was introduced, where the corrective control is derived using both a linearly and nonlinearly parameterized approximators. The scheme renders asymptotic stability by introducing a robust term and under mild assumptions on the system uncertainites. In addition, the stability is verified mathematically and also in simulation. Since the accommodation uses the measured states of the system, in the future, the state measurability will be relaxed.

Appendix

Proof of Lemma 1: Consider (8), solve, and apply the Frobenius norm. Additionally, note $A_{0_{\max}} < (1 - A_{0_{\max}})$ if $A_{0_{\max}} \leq 0.5$ (where $A_{0_{\max}}$ is the maximum singular value of A_0), also define $b_0 = \left\| A_0^k e(0) \right\| + \frac{B_{v_{\max}} \left\| \theta \right\|}{A_{0_{\max}}}$ with the vector B_v could chosen in such a way, such that $\frac{\left\| \tilde{\theta}_3(k) B_v \right\|}{A_{0_{\max}}} \leq \frac{\left\| \tilde{\theta}_3(k) \hat{\varphi}_3(k) \right\|}{A_{0_{\max}}}$. Define $b_1 = \frac{2}{A_{0_{\max}}}$. Then using (8), we have

$$\left\| \varepsilon(k) \right\|^2 \leq A_{0_{\max}}^2 \left[b_0^2 + \left\| e(k) \right\|^2 + \frac{b_1^2 \left\| \tilde{\theta}_3(k) \hat{\varphi}_3(k) \right\|^2}{A_{0_{\max}}^2} + \underbrace{2 \left\| e(k) \right\| b_0}_{1} + \underbrace{\frac{2 b_0 b_1 \left\| \tilde{\theta}_3(k) \hat{\varphi}_3(k) \right\|}{A_{0_{\max}}}}_{1} + \frac{2 b_1 \left\| e(k) \right\| \left\| \tilde{\theta}_3(k) \hat{\varphi}_3(k) \right\|}{A_{0_{\max}}} \right]$$

Apply Cauchy-Schwarz inequality to terms numbered as 1 in the above equation, pre-multiply $(5\alpha_3 \hat{\varphi}_3^T \hat{\varphi}_3 + 4)$ and add $\frac{2 \sum_{i=1}^{2} \theta_{i_{\max}}^2 \left\| \hat{\varphi}_i(k) \right\|^2}{(2 - \alpha_i \left\| \hat{\varphi}_i(k) \right\|^2)}$, take $\beta_0 = \frac{2 \sum_{i=1}^{2} \theta_{i_{\max}}^2 \left\| \hat{\varphi}_i(k) \right\|^2}{(2 - \alpha_i \left\| \hat{\varphi}_i(k) \right\|^2)}$ $+3 A_{0_{\max}}^2 b_0^2 (5\alpha_3 \hat{\varphi}_3^T \hat{\varphi}_3 + 4)$, $\beta_1 = 2 A_{0_{\max}}^2 (5\alpha_3 \hat{\varphi}_3^T \hat{\varphi}_3 + 4)$, $\beta_2 = 2 b_1^2 (5\alpha_3 \hat{\varphi}_3^T \hat{\varphi}_3 + 4)$, and $\beta_3 = 2 A_{0_{\max}} b_1 (5\alpha_3 \hat{\varphi}_3^T \hat{\varphi}_3 + 4)$, will yield (9).

Proof of Theorem 1: Consider a Lyapunov candidate as

$$V = e^T(k) e(k) + \frac{1}{\alpha_1} tr[\tilde{\theta}_1^T(k) \tilde{\theta}_1(k)] + \frac{1}{\alpha_2} tr[\tilde{\theta}_2^T(k) \tilde{\theta}_2(k)] + \frac{1}{\alpha_3} tr[\tilde{\theta}_3^T(k) \tilde{\theta}_3(k)]$$

whose first difference is given by

$$\Delta V = \underbrace{e^T(k+1) e(k+1) - e^T(k) e(k)}_{\Delta V_1} + \underbrace{\frac{1}{\alpha_1} tr[\tilde{\theta}_1^T(k+1) \tilde{\theta}_1(k+1) - \tilde{\theta}_1^T(k) \tilde{\theta}_1(k)]}_{\Delta V_2}$$

$$\underbrace{+\frac{1}{\alpha_2}tr[\tilde{\theta}_2^T(k+1)\tilde{\theta}_2(k+1)-\tilde{\theta}_2^T(k)\tilde{\theta}_2(k)]}_{\Delta V_3}+\underbrace{\frac{1}{\alpha_3}tr[\tilde{\theta}_3^T(k+1)\tilde{\theta}_3(k+1)-\tilde{\theta}_3^T(k)\tilde{\theta}_3(k)]}_{\Delta V_4} \quad \text{(A.1)}$$

Substitute (8) in ΔV_1 of (A.1) and perform some mathematical manipulations to yield

$$\Delta V_1 = e^T(k)A_0^TA_0e(k)+2e^T(k)A_0^T\Psi_1(k)+2e^T(k)A_0^T\Psi_2(k)+2e^T(k)A_0^T\varepsilon(k)-2\frac{e^T(k)A_0^T(\theta_3^TB_v-C_v)}{B_v^T\hat{\theta}_3(k)\hat{\theta}_3^T(k)B_v+c_m}+\Psi_1^T(k)\Psi_1(k)$$

$$-2\frac{\Psi_1^T(k)(\theta_3^TB_v-C_v)}{B_v^T\hat{\theta}_3(k)\hat{\theta}_3^T(k)B_v+c_m}+2\Psi_1^T(k)\Psi_2(k)+2\Psi_1^T(k)\varepsilon(k)+\Psi_2^T(k)\Psi_2(k)-\frac{2\Psi_2^T(k)(\theta_3^TB_v-C_v)}{B_v^T\hat{\theta}_3(k)\hat{\theta}_3^T(k)B_v+c_m}$$

$$-\frac{2\varepsilon^T(k)(\theta_3^TB_v-C_v)}{B_v^T\hat{\theta}_3(k)\hat{\theta}_3^T(k)B_v+c_m}+\frac{(\theta_3^TB_v-C_v)^T(\theta_3^TB_v-C_v)}{\left(B_v^T\hat{\theta}_3(k)\hat{\theta}_3^T(k)B_v+c_m\right)^2}+2\Psi_2^T(k)\varepsilon(k)+\varepsilon^T(k)\varepsilon(k)-e^T(k)e(k) \quad \text{(A.2)}$$

Substituting (10) in ΔV_2 of (A.1) and performing some mathematical manipulations to render

$$\Delta V_2 \le -(2-\alpha_1\hat{\varphi}_1^T(k)\hat{\varphi}_1(k))\left\|\tilde{\theta}_1^T(k)\hat{\varphi}_1(k)-\frac{(1-\alpha_1\hat{\varphi}_1^T(k)\hat{\varphi}_1(k))}{(2-\alpha_1\hat{\varphi}_1^T(k)\hat{\varphi}_1(k))}\times(\theta_1^T\hat{\varphi}_1(k)+B_1A_0e(k))\right\|^2+\frac{\theta_{1\max}^2\left\|\hat{\varphi}_1(k)\right\|^2}{(2-\alpha_1\left\|\hat{\varphi}_1(k)\right\|^2)}$$

$$+\frac{A_{0\max}^2\left\|e(k)\right\|^2\kappa_1^2}{(2-\alpha_1\hat{\varphi}_1^T(k)\hat{\varphi}_1(k))}+\frac{2A_{0\max}\left\|e(k)\right\|\kappa_1\varphi_{1\max}\theta_{1\max}}{(2-\alpha_1\hat{\varphi}_1^T(k)\hat{\varphi}_1(k))} \quad \text{(A.3)}$$

Substituting (11) in ΔV_3 of (A.1) and after performing mathematical manipulations to arrive at

$$\Delta V_3 \le -(2-\alpha_2\hat{\varphi}_2^T(k)\hat{\varphi}_2(k))\left\|\tilde{\theta}_2^T(k)\hat{\varphi}_2(k)-\frac{(1-\alpha_2\hat{\varphi}_2^T(k)\hat{\varphi}_2(k))}{(2-\alpha_2\hat{\varphi}_2^T(k)\hat{\varphi}_2(k))}\times(\theta_2^T\hat{\varphi}_2(k)+B_2A_0e(k))\right\|^2+\frac{\theta_{2\max}^2\left\|\hat{\varphi}_2(k)\right\|^2}{(2-\alpha_2\left\|\hat{\varphi}_2(k)\right\|^2)}$$

$$+\frac{A_{0\max}^2\left\|e(k)\right\|^2\kappa_2^2}{(2-\alpha_2\hat{\varphi}_2^T(k)\hat{\varphi}_2(k))}+\frac{2A_{0\max}\left\|e(k)\right\|\kappa_2\varphi_{2\max}\theta_{2\max}}{(2-\alpha_2\hat{\varphi}_2^T(k)\hat{\varphi}_2(k))} \quad \text{(A.4)}$$

Substituting (12) in ΔV_4 of (A.1) and performing some mathematical manipulation would

result in the following equation

$$\Delta V_4 \le -2e^T(k)A_0^T\Psi_1(k) - 2\Psi_1^T(k)\Psi_1(k) - 2\Psi_1^T(k)\Psi_2(k) - 2\Psi_1^T(k)\varepsilon(k)$$

$$+2\frac{\Psi_1^T(k)(\theta_3^T B_v - C_v)}{B_v^T\hat{\theta}_3(k)\hat{\theta}_3^T(k)B_v + c_m} + 5\alpha_3\hat{\varphi}_3^T\hat{\varphi}_3 e^T(k)A_0^T A_0 e(k) + 5\alpha_3\hat{\varphi}_3^T\hat{\varphi}_3\Psi_1^T(k)\Psi_1(k)$$

$$+5\alpha_3\hat{\varphi}_3^T\hat{\varphi}_3\Psi_2^T(k)\Psi_2(k) + 5\alpha_3\hat{\varphi}_3^T\hat{\varphi}_3\varepsilon^T(k)\varepsilon(k) + 5\alpha_3\hat{\varphi}_3^T\hat{\varphi}_3\frac{(\theta_3^T B_v - C_v)^T(\theta_3^T B_v - C_v)}{\left(B_v^T\hat{\theta}_3(k)\hat{\theta}_3^T(k)B_v + c_m\right)^2} \qquad \text{(A.5)}$$

Since $\Delta V = \Delta V_1 + \Delta V_2 + \Delta V_3 + \Delta V_4$, combining (A.2)-(A.5), and performing some mathematical manipulations, the first difference of the Lyapunov candidate is expressed as

$$\Delta V \le 4e^T(k)A_0^T A_0 e(k) + \underbrace{4\Psi_2^T(k)\Psi_2(k)}_{1} + \underbrace{4\frac{(\theta_3^T B_v - C_v)^T(\theta_3^T B_v - C_v)}{\left(B_v^T\hat{\theta}_3(k)\hat{\theta}_3^T(k)B_v + c_m\right)^2}}_{2} + 4\varepsilon^T(k)\varepsilon(k) - \Psi_1^T(k)\Psi_1(k) - e^T(k)e(k)$$

$$-(2-\alpha_1\hat{\varphi}_1^T(k)\hat{\varphi}_1(k))\left\|\tilde{\theta}_1^T(k)\hat{\varphi}_1(k) - \frac{(1-\alpha_1\hat{\varphi}_1^T(k)\hat{\varphi}_1(k))}{(2-\alpha_1\hat{\varphi}_1^T(k)\hat{\varphi}_1(k))}\times(\theta_1^T\hat{\varphi}_1(k) + B_1A_0e(k))\right\|^2$$

$$+\frac{\theta_{1\max}^2\left\|\hat{\varphi}_1(k)\right\|^2}{(2-\alpha_1\left\|\hat{\varphi}_1(k)\right\|^2)} + \frac{A_{0_{\max}}^2\left\|e(k)\right\|^2\kappa_1^2}{(2-\alpha_1\left\|\hat{\varphi}_1(k)\right\|^2)} + \frac{A_{0_{\max}}^2\left\|e(k)\right\|^2\kappa_1^2}{(2-\alpha_1\left\|\hat{\varphi}_1(k)\right\|^2)}$$

$$+\frac{\theta_{1\max}^2\left\|\hat{\varphi}_1(k)\right\|^2}{(2-\alpha_1\left\|\hat{\varphi}_1(k)\right\|^2)} - (2-\alpha_2\hat{\varphi}_2^T(k)\hat{\varphi}_2(k))\left\|\tilde{\theta}_2^T(k)\hat{\varphi}_2(k) - \frac{(1-\alpha_2\hat{\varphi}_2^T(k)\hat{\varphi}_2(k))}{(2-\alpha_2\hat{\varphi}_2^T(k)\hat{\varphi}_2(k))}\times(\theta_2^T\hat{\varphi}_2(k) + B_2A_0e(k))\right\|^2$$

$$+\frac{\theta_{2\max}^2\left\|\hat{\varphi}_2(k)\right\|^2}{(2-\alpha_2\left\|\hat{\varphi}_2(k)\right\|^2)} + \frac{A_{0_{\max}}^2\left\|e(k)\right\|^2\kappa_2^2}{(2-\alpha_2\left\|\hat{\varphi}_2(k)\right\|^2)} + \frac{A_{0_{\max}}^2\left\|e(k)\right\|^2\kappa_2^2}{(2-\alpha_2\left\|\hat{\varphi}_2(k)\right\|^2)} + \frac{\theta_{2\max}^2\left\|\hat{\varphi}_2(k)\right\|^2}{(2-\alpha_2\left\|\hat{\varphi}_2(k)\right\|^2)}$$

$$+5\alpha_3\hat{\varphi}_3^T\hat{\varphi}_3 e^T(k)A_0^T A_0 e(k) + 5\alpha_3\hat{\varphi}_3^T\hat{\varphi}_3\Psi_1^T(k)\Psi_1(k) + \underbrace{5\alpha_3\hat{\varphi}_3^T\hat{\varphi}_3\Psi_2^T(k)\Psi_2(k)}_{1} + 5\alpha_3\hat{\varphi}_3^T\hat{\varphi}_3\varepsilon^T(k)\varepsilon(k)$$

$$\underbrace{+5\alpha_3\hat{\varphi}_3^T\hat{\varphi}_3\frac{(\theta_3^T B_v - C_v)^T(\theta_3^T B_v - C_v)}{\left(B_v^T\hat{\theta}_3(k)\hat{\theta}_3^T(k)B_v + c_m\right)^2}}_{2} \qquad \text{(A.6)}$$

Consider only terms numbered as ‘1’ in (A.6) as

$$(4+5\alpha_3\hat{\varphi}_3^T\hat{\varphi}_3)\Psi_2^T(k)\Psi_2(k) = (4+5\alpha_3\hat{\varphi}_3^T\hat{\varphi}_3)\left(\frac{\tilde{\theta}_3^T(k)B_v - C_v}{B_v^T\hat{\theta}_3(k)\hat{\theta}_3^T(k)B_v + c_m}\right)^T \times \left(\frac{\tilde{\theta}_3^T(k)B_v - C_v}{B_v^T\hat{\theta}_3(k)\hat{\theta}_3^T(k)B_v + c_m}\right)$$

$$\leq 2(4+5\alpha_3\hat{\varphi}_3^T\hat{\varphi}_3)(B_v^T\tilde{\theta}_3(k)\tilde{\theta}_3^T(k)B_v + C_v^TC_v) \quad \text{(A.7)}$$

Next, consider only terms numbered as '2' in (18), to render

$$(4+5\alpha_3\hat{\varphi}_3^T\hat{\varphi}_3)\frac{(\theta_3^TB_v - C_v)^T(\theta_3^TB_v - C_v)}{\left(B_v^T\hat{\theta}_3(k)\hat{\theta}_3^T(k)B_v + c_m\right)^2}$$

$$\leq (4+5\alpha_3\hat{\varphi}_3^T\hat{\varphi}_3)(B_v^T\theta_3\theta_3^TB_v - 2B_v^T\theta_3C_v + C_v^TC_v) \quad \text{(A.8)}$$

Use the modifications suggested in (A.7), (A.8), and Lemma 1 in (A.6), the first difference can be rewritten as

$$\Delta V \leq 4e^T(k)A_0^TA_0e(k) - \Psi_1^T(k)\Psi_1(k) - e^T(k)e(k)$$

$$-(2-\alpha_1\hat{\varphi}_1^T(k)\hat{\varphi}_1(k))\left\|\tilde{\theta}_1^T(k)\hat{\varphi}_1(k) - \frac{(1-\alpha_1\hat{\varphi}_1^T(k)\hat{\varphi}_1(k))}{(2-\alpha_1\hat{\varphi}_1^T(k)\hat{\varphi}_1(k))} \times(\theta_1^T\hat{\varphi}_1(k) + B_1A_0e(k))\right\|^2 + \frac{2A_{0_{\max}}^2\left\|e(k)\right\|^2\kappa_1^2}{(2-\alpha_1\left\|\hat{\varphi}_1(k)\right\|^2)}$$

$$-(2-\alpha_2\hat{\varphi}_2^T(k)\hat{\varphi}_2(k))\left\|\tilde{\theta}_2^T(k)\hat{\varphi}_2(k) - \frac{(1-\alpha_2\hat{\varphi}_2^T(k)\hat{\varphi}_2(k))}{(2-\alpha_2\hat{\varphi}_2^T(k)\hat{\varphi}_2(k))} \times(\theta_2^T\hat{\varphi}_2(k) + B_2A_0e(k))\right\|^2$$

$$+\frac{2A_{0_{\max}}^2\left\|e(k)\right\|^2\kappa_2^2}{(2-\alpha_2\left\|\hat{\varphi}_2(k)\right\|^2)} + 5\alpha_3\hat{\varphi}_3^T\hat{\varphi}_3\Psi_1^T(k)\Psi_1(k) + 5\alpha_3\hat{\varphi}_3^T\hat{\varphi}_3e^T(k)A_0^TA_0e(k)$$

$$+2(4+5\alpha_3\hat{\varphi}_3^T\hat{\varphi}_3)(B_v^T\tilde{\theta}_3(k)\tilde{\theta}_3^T(k)B_v + C_v^TC_v)$$

$$+(4+5\alpha_3\hat{\varphi}_3^T\hat{\varphi}_3)(B_v^T\theta_3\theta_3^TB_v - 2B_v^T\theta_3C_v + C_v^TC_v)$$

$$+\beta_0 + \beta_1\left\|e(k)\right\|^2 + \beta_2\left\|\tilde{\theta}_3(k)\hat{\varphi}_3(k)\right\|^2 + \beta_3\left\|e(k)\right\|\left\|\tilde{\theta}_3(k)\hat{\varphi}_3(k)\right\|$$

Take $B_v = \frac{\sqrt{\alpha_3}\hat{\varphi}_3(k)}{\sqrt{(8+10\alpha_3\left\|\hat{\varphi}_3(k)\right\|^2)}}$ and apply Frobenius norm, we have

$$\Delta V \le -\left(1-4A_{0_{\max}}^2-\gamma A_{0_{\max}}^2-\frac{3}{2}\beta_1\right)\|e(k)\|^2-(2-\alpha_1\hat{\varphi}_1^T(k)\hat{\varphi}_1(k))\left\|\tilde{\theta}_1^T(k)\hat{\varphi}_1(k)-\frac{(1-\alpha_1\hat{\varphi}_1^T(k)\hat{\varphi}_1(k))}{(2-\alpha_1\hat{\varphi}_1^T(k)\hat{\varphi}_1(k))}\right.$$

$$\left.\times(\theta_1^T\hat{\varphi}_1(k)+B_1A_0e(k))\right\|^2-(2-\alpha_2\hat{\varphi}_2^T(k)\hat{\varphi}_2(k))\left\|\tilde{\theta}_2^T(k)\hat{\varphi}_2(k)-\frac{(1-\alpha_2\hat{\varphi}_2^T(k)\hat{\varphi}_2(k))}{(2-\alpha_2\hat{\varphi}_2^T(k)\hat{\varphi}_2(k))}\times(\theta_2^T\hat{\varphi}_2(k)+B_2A_0e(k))\right\|^2$$

$$-(1-5\alpha_3\|\hat{\varphi}_3(k)\|^2-\alpha_3-\beta_2-\beta_4)\|\tilde{\theta}_3(k)\hat{\varphi}_3(k)\|^2$$

$$+2(4+5\alpha_3\|\hat{\varphi}_3(k)\|^2)C_{v_{\max}}^2+\beta_0+(4+5\alpha_3\|\hat{\varphi}_3(k)\|^2)(B_{v_{\max}}^2\theta_{3_{\max}}^2-2B_{v_{\min}}\theta_{3_{\min}}C_{v_{\min}}+C_{v_{\max}}^2)$$

where $\gamma=\dfrac{\sum_{i=1}^{2}2\kappa_i^2}{(2-\alpha_i\|\hat{\varphi}_i(k)\|^2)}+5\alpha_3\|\hat{\varphi}_3(k)\|^2$. Take $C_{v_{\min}}=\dfrac{B_{v_{\max}}^2\theta_{3_{\max}}^2+3C_{v_{\max}}^2+(\beta_0/(4+5\alpha_3\hat{\varphi}_3{}^T\hat{\varphi}_3))}{2B_{v_{\min}}\theta_{3_{\min}}}$, then first difference of the Lyapunov function is given by

$$\Delta V \le -\left(1-4A_{0_{\max}}^2-\gamma A_{0_{\max}}^2-3A_{0_{\max}}^2(5\alpha_3\hat{\varphi}_3{}^T\hat{\varphi}_3+4)\right)\|e(k)\|^2$$

$$-(2-\alpha_1\hat{\varphi}_1^T(k)\hat{\varphi}_1(k))\left\|\tilde{\theta}_1^T(k)\hat{\varphi}_1(k)-\frac{(1-\alpha_1\hat{\varphi}_1^T(k)\hat{\varphi}_1(k))}{(2-\alpha_1\hat{\varphi}_1^T(k)\hat{\varphi}_1(k))}\times(\theta_1^T\hat{\varphi}_1(k)+B_1A_0e(k))\right\|^2$$

$$-(2-\alpha_2\hat{\varphi}_2^T(k)\hat{\varphi}_2(k))\left\|\tilde{\theta}_2^T(k)\hat{\varphi}_2(k)-\frac{(1-\alpha_2\hat{\varphi}_2^T(k)\hat{\varphi}_2(k))}{(2-\alpha_2\hat{\varphi}_2^T(k)\hat{\varphi}_2(k))}\times(\theta_2^T\hat{\varphi}_2(k)+B_2A_0e(k))\right\|^2$$

$$-(1-5\alpha_3\|\hat{\varphi}_3(k)\|^2-\alpha_3-\frac{3}{2}\beta_2)\|\tilde{\theta}_3(k)\hat{\varphi}_3(k)\|^2 \qquad \text{(A.9)}$$

The first difference, $\Delta V \le 0$ in (A.9), which shows stability in the sense of Lyapunov provided the gains are selected as

$A_{0_{\max}} \le \sqrt{\dfrac{1}{4+\gamma+3(5\alpha_3\hat{\varphi}_3{}^T\hat{\varphi}_3+4)}}$, $\alpha_3=\dfrac{\left(1-\frac{3}{2}\beta_2\right)}{1+5\|\hat{\varphi}_3(k)\|^2}$, and $\frac{3}{2}\beta_2 \le 1$. Hence $e(k)$, $\tilde{\theta}_3(k)$, $\tilde{\theta}_2(k)$, and $\tilde{\theta}_1(k)$ are bounded, provided $e(k_0)$, $\tilde{\theta}_3(k_0)$, $\tilde{\theta}_2(k_0)$, and $\tilde{\theta}_1(k_0)$ are bounded. Additionally summing

both sides of the equation (A.9), and since $\Delta V \le 0$, we have $\left|\sum_{k=0}^{\infty} \Delta V(k)\right| = \left|V(\infty) - V(0)\right| < \infty$. Taking limits on both sides of this equation, and using Lin and Narendra (1980), it can be concluded that the residual $\|e(k)\| \to 0$ as $k \to \infty$.

***Proof of Theorem 2*:** Consider the following Lyapunov candidate function

$$J = \frac{1}{5\eta_{g_{\max}}^2} e_t^T(k) e_t(k) + \sum_{i=1}^{3} \frac{1}{\alpha_{m_i}} tr[\tilde{W}_i^T(k) \tilde{W}_i(k)]$$

whose first difference is given by

$$\Delta J = \underbrace{\frac{1}{5\eta_{g_{\max}}^2}\left[e_t^T(k+1)e_t(k+1) - e_t^T(k)e_t(k)\right]}_{\Delta J_1} + \underbrace{\frac{1}{\alpha_{m_1}} tr[\tilde{W}_1^T(k+1)\tilde{W}_1(k+1) - \tilde{W}_1^T(k)\tilde{W}_1(k)]}_{\Delta J_2}$$

$$+ \underbrace{\frac{1}{\alpha_{m_2}} tr[\tilde{W}_2^T(k+1)\tilde{W}_2(k+1) - \tilde{W}_2^T(k)\tilde{W}_2(k)]}_{\Delta J_3} + \underbrace{\frac{1}{\alpha_{m_3}} tr[\tilde{W}_3^T(k+1)\tilde{W}_3(k+1) - \tilde{W}_3^T(k)\tilde{W}_3(k)]}_{\Delta J_4} \quad \text{(A.10)}$$

Substitute tracking error dynamics (18) in ΔJ_1 of (A.10), we have

$$\Delta J_1 = \frac{1}{5\eta_{g_{\max}}^2}\left\{\left[\eta_g(x(k))\left(le_t(k) + \Psi_{1mt}(k) + \varepsilon_{mt}(k) - \Psi_{2mt}(k) + \frac{(W_3^T B_m - C_{mt})}{B_m^T \hat{W}_3(k)\hat{W}_3^T(k) B_m + c_v}\right)\right]^T \times \right.$$

$$\left.\left[\eta_g(x(k))\left(le_t(k) + \Psi_{1mt}(k) + \varepsilon_{mt}(k) - \Psi_{2mt}(k) + \frac{(W_3^T B_m - C_{mt})}{B_m^T \hat{W}_3(k)\hat{W}_3^T(k) B_m + c_v}\right)\right] - e_t^T(k)e_t(k)\right\}$$

Apply Cauchy-Schwarz to the first term in the above equation, and then we have

$$\Delta J_1 \le \left[\left(e_t^T(k) l^T l e_t(k) + \Psi_{1mt}^T(k)\Psi_{1mt}(k) + \varepsilon_{mt}^T(k)\varepsilon_{mt}(k) + \Psi_{2mt}^T(k)\Psi_{2mt}(k) + \frac{(W_3^T B_m - C_{mt})^T (W_3^T B_m - C_{mt})}{\left(B_m^T \hat{W}_3(k)\hat{W}_3^T(k) B_m + c_v\right)^2}\right)\right]$$

$$-\frac{1}{5\eta_{g_{\max}}^{2}} e_t^T(k) e_t(k) \tag{A.11}$$

Substitute (20) in ΔJ_2 of (A.10) and perform some mathematical manipulation to yield

$$\Delta J_2 \le -(2-\alpha_{m_1}\hat{\varphi}_{m_1}^T(k)\hat{\varphi}_{m_1}(k))\left\|\tilde{W}_1^T(k)\hat{\varphi}_{m_1}(k) - \frac{(1-\alpha_{m_1}\hat{\varphi}_{m_1}^T(k)\hat{\varphi}_{m_1}(k))}{(2-\alpha_{m_1}\hat{\varphi}_{m_1}^T(k)\hat{\varphi}_{m_1}(k))}\times(W_1^T\hat{\varphi}_{m_1}(k) + B_{m_1} l e_t(k))\right\|^2 + \frac{W_{1\max}^2\left\|\hat{\varphi}_{m_1}(k)\right\|^2}{(2-\alpha_{m_1}\left\|\hat{\varphi}_{m_1}(k)\right\|^2)}$$

$$+\frac{l_{\max}^2\left\|e_t(k)\right\|^2\kappa_{m_1}^2}{(2-\alpha_{m_1}\hat{\varphi}_{m_1}^T(k)\hat{\varphi}_{m_1}(k))} + \frac{2l_{\max}\left\|e_t(k)\right\|\kappa_{m_1}\left\|\hat{\varphi}_{m_1}\right\|W_{1\max}}{(2-\alpha_{m_1}\hat{\varphi}_{m_1}^T(k)\hat{\varphi}_{m_1}(k))} \tag{A.12}$$

Substitute (21) in ΔJ_3 of (A.10) and perform some mathematical manipulation to arrive at

$$\Delta J_3 \le -(2-\alpha_{m_2}\hat{\varphi}_{m_2}^T(k)\hat{\varphi}_{m_2}(k))\left\|\tilde{W}_2^T(k)\hat{\varphi}_{m_2}(k) - \frac{(1-\alpha_{m_2}\hat{\varphi}_{m_2}^T(k)\hat{\varphi}_{m_2}(k))}{(2-\alpha_{m_2}\hat{\varphi}_{m_2}^T(k)\hat{\varphi}_{m_2}(k))}\times(W_2^T\hat{\varphi}_{m_2}(k) + B_{m_2} l e_t(k))\right\|^2 + \frac{W_{2\max}^2\left\|\hat{\varphi}_{m_2}(k)\right\|^2}{(2-\alpha_{m_2}\left\|\hat{\varphi}_{m_2}(k)\right\|^2)}$$

$$+\frac{l_{\max}^2\left\|e_t(k)\right\|^2\kappa_{m_2}^2}{(2-\alpha_{m_2}\hat{\varphi}_{m_2}^T(k)\hat{\varphi}_{m_2}(k))} + \frac{2l_{\max}\left\|e_t(k)\right\|\kappa_{m_2}\left\|\hat{\varphi}_{m_2}\right\|W_{2\max}}{(2-\alpha_{m_2}\hat{\varphi}_{m_2}^T(k)\hat{\varphi}_{m_2}(k))} \tag{A.13}$$

Substitute (22) in ΔJ_4 of (A.10) to render

$$\Delta J_4 = \frac{1}{\alpha_{m_3}} tr\left\{\left[\tilde{W}_3(k) - \alpha_{m_3}\ \hat{\varphi}_{m_3}(k) e_t^T(k+1) B_{m_3}\right]^T \times \left[\tilde{W}_3(k) - \alpha_{m_3}\ \hat{\varphi}_{m_3}(k) e_t^T(k+1) B_{m_3}\right] - \tilde{W}_3^T(k)\tilde{W}_3(k)\right\}$$

Expand the terms in the above equation, we have

$$\Delta J_4 = \frac{1}{\alpha_{m_3}} tr\left[-2\alpha_{m_3}\ \tilde{W}_3^T(k)\hat{\varphi}_{m_3}(k) e_t^T(k+1) B_{m_3} + \alpha_{m_3}^2\ B_{m_3}^T e_t(k+1)\hat{\varphi}_{m_3}^T(k)\hat{\varphi}_{m_3}(k) e_t^T(k+1) B_{m_3}\right]$$

Substitute the tracking error dynamics in the above equation and solve further to yield

$$\Delta J_4 \le \frac{\hat{\varphi}_{m_3}^T(k)\hat{\varphi}_{m_3}(k)\eta_g(k)\tilde{W}_3^T(k)\tilde{W}_3(k)}{\gamma_1} + tr\left[\gamma_1 B_{m_3}^T \eta_g(k) l e_t(k) e_t^T(k) l^T B_{m_3}\right] + \frac{\hat{\varphi}_{m_3}^T(k)\hat{\varphi}_{m_3}(k)\eta_g(k)\tilde{W}_3^T(k)\tilde{W}_3(k)}{\gamma_2}$$

$$+tr\left[\gamma_2 B_{m_3}^T \eta_g(k)\varepsilon_{mt}(k)\varepsilon_{mt}^T(k)B_{m_3}\right]+\frac{\hat{\varphi}_{m_3}^T(k)\hat{\varphi}_{m_3}(k)\eta_g(k)\tilde{W}_3^T(k)\tilde{W}_3(k)}{\gamma_3}+tr\left[\gamma_3 B_{m_3}^T\eta_g(k)\frac{(W_3^T B_m-C_{mt})(W_3^T B_m-C_{mt})^T}{\left(B_m^T\hat{W}_3(k)\hat{W}_3^T(k)B_m+c_v\right)^2}B_{m_3}\right]$$

$$-2\tilde{W}_3^T(k)\hat{\varphi}_{m_3}(k)\eta_g(k)\tilde{W}_3^T(k)\hat{\varphi}_{m_3}(k)B_{m_3}+2\tilde{W}_3^T(k)\hat{\varphi}_{m_3}(k)\eta_g(k)\tilde{W}_3^T(k)\hat{\varphi}_{m_3}(k)B_m B_{m_3}+tr\left[\gamma_4 B_{m_3}^T\eta_g(k)C_{mt}C_{mt}^T B_{m_3}\right]$$

$$+\frac{\hat{\varphi}_{m_3}^T(k)\hat{\varphi}_{m_3}(k)\eta_g(k)\tilde{W}_3^T(k)\tilde{W}_3(k)}{\gamma_4}+5\alpha_{m_3}\hat{\varphi}_{m_3}^T(k)\hat{\varphi}_{m_3}(k)B_{m_3}^T\eta_g(k)le_t(k)e_t^T(k)l^T\eta_g^T(k)B_{m_3}$$

$$+5\alpha_{m_3}\hat{\varphi}_{m_3}^T(k)\hat{\varphi}_{m_3}(k)B_{m_3}^T\eta_g(k)\tilde{W}_3^T(k)\hat{\varphi}_{m_3}(k)\hat{\varphi}_{m_3}^T(k)\tilde{W}_3(k)\eta_g^T(k)B_{m_3}+5\alpha_{m_3}\hat{\varphi}_{m_3}^T(k)\hat{\varphi}_{m_3}(k)B_{m_3}^T\eta_g(k)\varepsilon_{mt}(k)\varepsilon_{mt}^T(k)\eta_g^T(k)B_{m_3}$$

$$+5\alpha_{m_3}\hat{\varphi}_{m_3}^T(k)\hat{\varphi}_{m_3}(k)B_{m_3}^T\eta_g(k)\Psi_{2mt}(k)\Psi_{2mt}^T(k)\eta_g^T(k)B_{m_3}$$

$$+5\alpha_{m_3}\hat{\varphi}_{m_3}^T(k)\hat{\varphi}_{m_3}(k)B_{m_3}^T\eta_g(k)\frac{(W_3^T B_m-C_{mt})(W_3^T B_m-C_{mt})^T}{\left(B_m^T\hat{W}_3(k)\hat{W}_3^T(k)B_m+c_v\right)^2}\eta_g^T(k)B_{m_3} \qquad \text{(A.14)}$$

where $\gamma_i>0$, $\forall i=1,2,3,4$ is a constant. Since $\Delta J=\Delta J_1+\Delta J_2+\Delta J_3+\Delta J_4$, combining (A.11)-(A.14), the first difference of the Lyapunov candidate is expressed as

$$\Delta J\le e_t^T(k)l^T le_t(k)+\Psi_{1mt}^T(k)\Psi_{1mt}(k)+\varepsilon_{mt}^T(k)\varepsilon_{mt}(k)+\underbrace{\Psi_{2mt}^T(k)\Psi_{2mt}(k)}_{1}+\underbrace{\frac{(W_3^T B_m-C_{mt})^T(W_3^T B_m-C_{mt})}{\left(B_m^T\hat{W}_3(k)\hat{W}_3^T(k)B_m+c_v\right)^2}}_{2}$$

$$-\frac{1}{5\eta_{g_{\max}}^2}e_t^T(k)e_t(k)-(2-\alpha_{m_1}\hat{\varphi}_{m_1}^T(k)\hat{\varphi}_{m_1}(k))\left\|\tilde{W}_1^T(k)\hat{\varphi}_{m_1}(k)-\frac{(1-\alpha_{m_1}\hat{\varphi}_{m_1}^T(k)\hat{\varphi}_{m_1}(k))}{(2-\alpha_{m_1}\hat{\varphi}_{m_1}^T(k)\hat{\varphi}_{m_1}(k))}\times(W_1^T\hat{\varphi}_{m_1}(k)+B_{m_1}le_t(k))\right\|^2$$

$$+\frac{W_{1\max}^2\left\|\hat{\varphi}_{m_1}(k)\right\|^2}{(2-\alpha_{m_1}\left\|\hat{\varphi}_{m_1}(k)\right\|^2)}+\frac{l_{\max}^2\left\|e_t(k)\right\|^2\kappa_{m_1}^2}{(2-\alpha_{m_1}\hat{\varphi}_{m_1}^T(k)\hat{\varphi}_{m_1}(k))}+\frac{2l_{\max}\left\|e_t(k)\right\|\kappa_{m_1}\left\|\hat{\varphi}_{m_1}\right\|W_{1\max}}{(2-\alpha_{m_1}\hat{\varphi}_{m_1}^T(k)\hat{\varphi}_{m_1}(k))}$$

$$-(2-\alpha_{m_2}\hat{\varphi}_{m_2}^T(k)\hat{\varphi}_{m_2}(k))\left\|\tilde{W}_2^T(k)\hat{\varphi}_{m_2}(k)-\frac{(1-\alpha_{m_2}\hat{\varphi}_{m_2}^T(k)\hat{\varphi}_{m_2}(k))}{(2-\alpha_{m_2}\hat{\varphi}_{m_2}^T(k)\hat{\varphi}_{m_2}(k))}\times(W_2^T\hat{\varphi}_{m_2}(k)+B_{m_2}le_t(k))\right\|^2$$

$$+\frac{W_{2\max}^2\left\|\hat{\varphi}_{m_2}(k)\right\|^2}{(2-\alpha_{m_2}\left\|\hat{\varphi}_{m_2}(k)\right\|^2)}+\frac{l_{\max}^2\left\|e_t(k)\right\|^2\kappa_{m_2}^2}{(2-\alpha_{m_2}\hat{\varphi}_{m_2}^T(k)\hat{\varphi}_{m_2}(k))}+\frac{2l_{\max}\left\|e_t(k)\right\|\kappa_{m_2}\left\|\hat{\varphi}_{m_2}\right\|W_{2\max}}{(2-\alpha_{m_2}\hat{\varphi}_{m_2}^T(k)\hat{\varphi}_{m_2}(k))}$$

$$+\frac{\hat{\varphi}_{m_3}^T(k)\hat{\varphi}_{m_3}(k)\eta_g(k)\tilde{W}_3^T(k)\tilde{W}_3(k)}{\gamma_1}+tr\left[\gamma_1 B_{m_3}^T\eta_g(k)le_t(k)e_t^T(k)l^T B_{m_3}\right]+\frac{\hat{\varphi}_{m_3}^T(k)\hat{\varphi}_{m_3}(k)\eta_g(k)\tilde{W}_3^T(k)\tilde{W}_3(k)}{\gamma_2}$$

$$+tr\left[\gamma_2 B_{m_3}^T\eta_g(k)\varepsilon_{mt}(k)\varepsilon_{mt}^T(k)B_{m_3}\right]+\frac{\hat{\varphi}_{m_3}^T(k)\hat{\varphi}_{m_3}(k)\eta_g(k)\tilde{W}_3^T(k)\tilde{W}_3(k)}{\gamma_3}+\underbrace{tr\left[\gamma_3 B_{m_3}^T\eta_g(k)\frac{(W_3^TB_m-C_{mt})(W_3^TB_m-C_{mt})^T}{\left(B_m^T\hat{W}_3(k)\hat{W}_3^T(k)B_m+c_v\right)^2}B_{m_3}\right]}_{2}$$

$$-2\tilde{W}_3^T(k)\hat{\varphi}_{m_3}(k)\eta_g(k)\tilde{W}_3^T(k)\hat{\varphi}_{m_3}(k)B_{m_3}+2\tilde{W}_3^T(k)\hat{\varphi}_{m_3}(k)\eta_g(k)\tilde{W}_3^T(k)\hat{\varphi}_{m_3}(k)B_mB_{m_3}$$

$$+\frac{\hat{\varphi}_{m_3}^T(k)\hat{\varphi}_{m_3}(k)\eta_g(k)\tilde{W}_3^T(k)\tilde{W}_3(k)}{\gamma_4}+tr\left[\gamma_4 B_{m_3}^T\eta_g(k)C_{mt}C_{mt}^TB_{m_3}\right]+5\alpha_{m_3}\hat{\varphi}_{m_3}^T(k)\hat{\varphi}_{m_3}(k)B_{m_3}^T\eta_g(k)le_t(k)e_t^T(k)l^T\eta_g^T(k)B_{m_3}$$

$$+5\alpha_{m_3}\hat{\varphi}_{m_3}^T(k)\hat{\varphi}_{m_3}(k)B_{m_3}^T\eta_g(k)\tilde{W}_3^T(k)\hat{\varphi}_{m_3}(k)\hat{\varphi}_{m_3}^T(k)\tilde{W}_3(k)\eta_g^T(k)B_{m_3}$$

$$+\underbrace{5\alpha_{m_3}\hat{\varphi}_{m_3}^T(k)\hat{\varphi}_{m_3}(k)B_{m_3}^T\eta_g(k)\Psi_{2mt}(k)\Psi_{2mt}^T(k)\eta_g^T(k)B_{m_3}}_{1}$$

$$+5\alpha_{m_3}\hat{\varphi}_{m_3}^T(k)\hat{\varphi}_{m_3}(k)B_{m_3}^T\eta_g(k)\varepsilon_{mt}(k)\varepsilon_{mt}^T(k)\eta_g^T(k)B_{m_3}$$

$$\underbrace{+5\alpha_{m_3}\hat{\varphi}_{m_3}^T(k)\hat{\varphi}_{m_3}(k)B_{m_3}^T\eta_g(k)\frac{(W_3^TB_m-C_{mt})(W_3^TB_m-C_{mt})^T}{\left(B_m^T\hat{W}_3(k)\hat{W}_3^T(k)B_m+c_v\right)^2}\eta_g^T(k)B_{m_3}}_{2} \tag{A.15}$$

Consider only terms numbered as 1 in (A.15), we have

$$\Psi_{2mt}^T(k)\Psi_{2mt}(k)+5\alpha_{m_3}\hat{\varphi}_{m_3}^T(k)\hat{\varphi}_{m_3}(k)B_{m_3}^T\eta_g(k)\Psi_{2mt}(k)\Psi_{2mt}^T(k)\eta_g^T(k)B_{m_3}=\frac{\left(\tilde{W}_3^T(k)B_m-C_{mt}\right)^T\left(\tilde{W}_3^T(k)B_m-C_{mt}\right)}{\left(B_m^T\hat{W}_3(k)\hat{W}_3^T(k)B_m+c_v\right)^2}$$

$$+5\alpha_{m_3}\hat{\varphi}_{m_3}^T(k)\hat{\varphi}_{m_3}(k)B_{m_3}^T\eta_g(k)\frac{\left(\tilde{W}_3^T(k)B_m-C_{mt}\right)^T\left(\tilde{W}_3^T(k)B_m-C_{mt}\right)}{\left(B_m^T\hat{W}_3(k)\hat{W}_3^T(k)B_m+c_v\right)^2}\eta_g^T(k)B_{m_3}$$

$$\le 2\left(B_m^T\tilde{W}_3(k)\tilde{W}_3^T(k)B_m+C_{mt}^TC_{mt}\right)+10\alpha_{m_3}\hat{\varphi}_{m_3}^T(k)\hat{\varphi}_{m_3}(k)B_{m_3}^T\eta_g(k)\left(\tilde{W}_3^T(k)B_mB_m^T\tilde{W}_3(k)+C_{mt}^TC_{mt}\right)\eta_g^T(k)B_{m_3} \tag{A.16}$$

Next, consider only terms numbered as 2 in (A.15), we have

$$\frac{(W_3^T B_m - C_{mt})^T (W_3^T B_m - C_{mt})}{\left(B_m^T \hat{W}_3(k)\hat{W}_3^T(k) B_m + c_v\right)^2} + tr\left[\gamma_3 B_{m_3}^T \eta_g(k) \frac{(W_3^T B_m - C_{mt})(W_3^T B_m - C_{mt})^T}{\left(B_m^T \hat{W}_3(k)\hat{W}_3^T(k) B_m + c_v\right)^2} B_{m_3}\right]$$

$$+5\alpha_{m_3} \hat{\varphi}_{m_3}^T(k)\hat{\varphi}_{m_3}(k) B_{m_3}^T \eta_g(k) \frac{(W_3^T B_m - C_{mt})(W_3^T B_m - C_{mt})^T}{\left(B_m^T \hat{W}_3(k)\hat{W}_3^T(k) B_m + c_v\right)^2} \eta_g^T(k) B_{m_3}$$

$$\le \left(B_m^T W_3 W_3^T B_m - 2W_3^T B_m C_{mt} + C_{mt}^T C_{mt}\right) + tr\left[\gamma_3 B_{m_3}^T \eta_g(k)\left(W_3^T B_m B_m^T W_3 - 2W_3^T B_m C_{mt} + C_{mt}^T C_{mt}\right) B_{m_3}\right]$$

$$+5\alpha_{m_3} \hat{\varphi}_{m_3}^T(k)\hat{\varphi}_{m_3}(k) B_{m_3}^T \eta_g(k)\left(W_3^T B_m B_m^T W_3 - 2W_3^T B_m C_{mt} + C_{mt}^T C_{mt}\right) \eta_g^T(k) B_{m_3} \qquad \text{(A.17)}$$

Use (A.16), (A.17), and Lemma 2 in (A.15), then the first difference of the Lyapunov function can be rewritten as

$$\Delta J \le e_t^T(k) l^T l e_t(k) + \Psi_{1mt}^T(k)\Psi_{1mt}(k) - \frac{1}{5\eta_{g_{\max}}^2} e_t^T(k) e_t(k) + \frac{2l_{\max}^2 \left\|e_t(k)\right\|^2 \kappa_{m_1}^2}{(2 - \alpha_{m_1} \hat{\varphi}_{m_1}^T(k)\hat{\varphi}_{m_1}(k))}$$

$$-(2 - \alpha_{m_1} \hat{\varphi}_{m_1}^T(k)\hat{\varphi}_{m_1}(k)) \left\| \tilde{W}_1^T(k)\hat{\varphi}_{m_1}(k) - \frac{(1 - \alpha_{m_1} \hat{\varphi}_{m_1}^T(k)\hat{\varphi}_{m_1}(k))}{(2 - \alpha_{m_1} \hat{\varphi}_{m_1}^T(k)\hat{\varphi}_{m_1}(k))} \times (W_1^T \hat{\varphi}_{m_1}(k) + B_{m_1} l e_t(k)) \right\|^2$$

$$-(2 - \alpha_{m_2} \hat{\varphi}_{m_2}^T(k)\hat{\varphi}_{m_2}(k)) \left\| \tilde{W}_2^T(k)\hat{\varphi}_{m_2}(k) - \frac{(1 - \alpha_{m_2} \hat{\varphi}_{m_2}^T(k)\hat{\varphi}_{m_2}(k))}{(2 - \alpha_{m_2} \hat{\varphi}_{m_2}^T(k)\hat{\varphi}_{m_2}(k))} \times (W_2^T \hat{\varphi}_{m_2}(k) + B_{m_2} l e_t(k)) \right\|^2$$

$$+\frac{2l_{\max}^2 \left\|e_t(k)\right\|^2 \kappa_{m_2}^2}{(2 - \alpha_{m_2} \hat{\varphi}_{m_2}^T(k)\hat{\varphi}_{m_2}(k))} + \frac{\hat{\varphi}_{m_3}^T(k)\hat{\varphi}_{m_3}(k)\eta_g(k)\tilde{W}_3^T(k)\tilde{W}_3(k)}{\gamma_3}$$

$$+\frac{\hat{\varphi}_{m_3}^T(k)\hat{\varphi}_{m_3}(k)\eta_g(k)\tilde{W}_3^T(k)\tilde{W}_3(k)}{\gamma_1} + tr\left[\gamma_1 B_{m_3}^T \eta_g(k) l e_t(k) e_t^T(k) l^T B_{m_3}\right]$$

$$+\frac{\hat{\varphi}_{m_3}^T(k)\hat{\varphi}_{m_3}(k)\eta_g(k)\tilde{W}_3^T(k)\tilde{W}_3(k)}{\gamma_2} - 2\tilde{W}_3^T(k)\hat{\varphi}_{m_3}(k)\eta_g(k)\tilde{W}_3^T(k)\hat{\varphi}_{m_3}(k) B_{m_3} + 2\tilde{W}_3^T(k)\hat{\varphi}_{m_3}(k)\eta_g(k)\tilde{W}_3^T(k)\hat{\varphi}_{m_3}(k) B_m B_{m_3}$$

$$+\frac{\hat{\varphi}_{m_3}^T(k)\hat{\varphi}_{m_3}(k)\eta_g(k)\tilde{W}_3^T(k)\tilde{W}_3(k)}{\gamma_4} + tr\left[\gamma_4 B_{m_3}^T \eta_g(k) C_{mt} C_{mt}^T B_{m_3}\right] + 5\alpha_{m_3} \hat{\varphi}_{m_3}^T(k)\hat{\varphi}_{m_3}(k) B_{m_3}^T \eta_g(k) l e_t(k) e_t^T(k) l^T \eta_g^T(k) B_{m_3}$$

$$+5\alpha_{m_3}\hat{\varphi}_{m_3}^T(k)\hat{\varphi}_{m_3}(k)B_{m_3}^T\eta_g(k)\tilde{W}_3^T(k)\hat{\varphi}_{m_3}(k)\hat{\varphi}_{m_3}^T(k)\tilde{W}_3(k)\eta_g^T(k)B_{m_3}+2\left(B_m^T\tilde{W}_3(k)\tilde{W}_3^T(k)B_m+C_{mt}^TC_{mt}\right)$$

$$+10\alpha_{m_3}\hat{\varphi}_{m_3}^T(k)\hat{\varphi}_{m_3}(k)B_{m_3}^T\eta_g(k)\left(\tilde{W}_3^T(k)B_mB_m^T\tilde{W}_3(k)+C_{mt}^TC_{mt}\right)\eta_g^T(k)B_{m_3}+\left(B_m^TW_3W_3^TB_m-2W_3^TB_mC_{mt}+C_{mt}^TC_{mt}\right)$$

$$+tr\left[\gamma_3B_{m_3}^T\eta_g(k)\left(W_3^TB_mB_m^TW_3-2W_3^TB_mC_{mt}+C_{mt}^TC_{mt}\right)B_{m_3}\right]+5\alpha_{m_3}\hat{\varphi}_{m_3}^T(k)\hat{\varphi}_{m_3}(k)B_{m_3}^T\eta_g(k)\left(W_3^TB_mB_m^TW_3-2W_3^TB_mC_{mt}+C_{mt}^TC_{mt}\right).$$

$$\eta_g^T(k)B_{m_3}+p_0+p_1\left\|e_t(k)\right\|^2+p_2\left\|e_t(k)\right\|\left\|\tilde{W}_3(k)\hat{\varphi}_{m_3}(k)\right\|+p_3\left\|\tilde{W}_3(k)\hat{\varphi}_{m_3}(k)\right\|^2$$

Apply Frobenius norm and Let

$$B_{m_{\min}}=\frac{B_{m_{\max}}^2W_{3_{\max}}^2+C_{mt_{\max}}^2}{2W_{3_{\min}}C_{mt_{\min}}}+\frac{\left(p_0+\gamma_4B_{m_{3_{\max}}}^2\eta_{g_{\max}}C_{mt_{\max}}^2+2C_{mt_{\max}}^2+10\alpha_{m_3}\left\|\hat{\varphi}_{m_3}(k)\right\|^2B_{m_{3_{\max}}}^2\eta_{g_{\max}}^2C_{mt_{\max}}^2\right)}{2W_{3_{\min}}C_{mt_{\min}}\left(1+\gamma_3\left\|B_{m_3}\right\|^2\left\|\eta_g(k)\right\|+5\alpha_{m_3}\left\|\hat{\varphi}_{m_3}(k)\right\|^2\left\|B_{m_3}\right\|^2\left\|\eta_g(k)\right\|^2\right)}$$

and $B_{m_{\max}}=\alpha_{m_3}\left\|\hat{\varphi}_{m_3}(k)\right\|$, therefore, the first difference of the Lyapunov function is given by

$$\Delta J\le-\left(\frac{1}{5\eta_{g_{\max}}^2}-l_{\max}^2-\gamma_1B_{m_{3_{\max}}}^2l_{\max}^2\eta_{g_{\max}}-5\alpha_{m_3}\left\|\hat{\varphi}_{m_3}(k)\right\|^2B_{m_{3_{\max}}}^2\eta_{g_{\max}}^2l_{\max}^2-\frac{3}{2}p_1-\frac{2l_{\max}^2\kappa_{m_1}^2}{(2-\alpha_{m_1}\left\|\hat{\varphi}_{m_1}(k)\right\|^2)}\right)\left\|e_t(k)\right\|^2$$

$$-\left(2\eta_{g_{\min}}B_{m_{3_{\min}}}-\frac{\eta_{g_{\max}}}{\gamma}-2\alpha_{m_3}\eta_{g_{\max}}B_{m_{3_{\max}}}-5\alpha_{m_3}\left\|\hat{\varphi}_{m_3}(k)\right\|^2B_{m_{3_{\max}}}^2\eta_{g_{\max}}^2-2\alpha_{m_3}^2-10\alpha_{m_3}^4\left\|\hat{\varphi}_{m_3}(k)\right\|^2B_{m_{3_{\max}}}^2\eta_{g_{\max}}^2-\frac{3}{2}p_3\right).$$

$$\left\|\tilde{W}_3(k)\hat{\varphi}_{m_3}(k)\right\|^2-(2-\alpha_{m_1}\hat{\varphi}_{m_1}^T(k)\hat{\varphi}_{m_1}(k))\left\|\tilde{W}_1^T(k)\hat{\varphi}_{m_1}(k)-\frac{(1-\alpha_{m_1}\hat{\varphi}_{m_1}^T(k)\hat{\varphi}_{m_1}(k))}{(2-\alpha_{m_1}\hat{\varphi}_{m_1}^T(k)\hat{\varphi}_{m_1}(k))}\times(W_1^T\hat{\varphi}_{m_1}(k)+B_{m_1}le_t(k))\right\|^2$$

$$-(2-\alpha_{m_2}\hat{\varphi}_{m_2}^T(k)\hat{\varphi}_{m_2}(k))\left\|\tilde{W}_2^T(k)\hat{\varphi}_{m_2}(k)-\frac{(1-\alpha_{m_2}\hat{\varphi}_{m_2}^T(k)\hat{\varphi}_{m_2}(k))}{(2-\alpha_{m_2}\hat{\varphi}_{m_2}^T(k)\hat{\varphi}_{m_2}(k))}\times(W_2^T\hat{\varphi}_{m_2}(k)+B_{m_2}le_t(k))\right\|^2 \qquad \text{(A.18)}$$

From (A.18), $\Delta J\le 0$, which shows stability in the sense of Lyapunov provided the gains are selected as

$l_{\max}\le\sqrt{\frac{\left(1/5\eta_{g_{\max}}^2\right)}{d_t}}$, where

$$d_t = \frac{5}{2} + \gamma_1 B_{m_{3\max}}^2 \eta_{g\max} + \frac{3}{2}\gamma_2 \eta_{g\max} B_{m_{3\max}} + 5\alpha_{m_3} \left\|\hat{\varphi}_{m_3}(k)\right\|^2 B_{m_{3\max}}^2 \eta_{g\max}^2$$

$$+ \frac{15}{2}\alpha_{m_3} \left\|\hat{\varphi}_{m_3}(k)\right\|^2 B_{m_{3\max}}^2 \eta_{g\max}^2 + \frac{2\kappa_{m_1}^2}{(2 - \alpha_{m_1}\left\|\hat{\varphi}_{m_1}(k)\right\|^2)} \quad \text{and} \quad 0 < \alpha_i << 1, \forall i = 1,2,3,4.$$

Hence $e_t(k)$, $\tilde{w}_1(k)$, $\tilde{w}_2(k)$ and $\tilde{w}_3(k)$ are bounded, provided $e_t(k_0)$, $\tilde{w}_1(k_0)$, $\tilde{w}_2(k_0)$ and $\tilde{w}_3(k_0)$ are bounded. Additionally summing both sides of the equation (A.18), and using $\Delta J \le 0$, we have $\left|\sum_{k=0}^{\infty} \Delta J(k)\right| = \left|J(\infty) - J(0)\right| < \infty$. Taking limits and using Lin and Narendra (1980), it can be shown that the residual $\left\|e_t(k)\right\| \to 0$ as $k \to \infty$.

References

Barron, A. R. (1993). Universal approximation bounds for superposition of a sigmoidal function. *IEEE Trans. on Information Theory*, 39(3), 930-945.

Caccavale, F. and Villani, L. (2004). An Adaptive Observer for Fault Diagnosis in Nonlinear Discrete-Time Systems. *Proceeding of the 2004 American Control Conference* (pp. 2463- 2468).

Chen, C. T. (1999). *Linear System Theory and Design, 3rd Ed.* New York: Oxford University Press.

Chen, J. and Patton, R. J. (1999). *Robust Model-based Fault Diagnosis for Dynamic Systems*. Massachusetts, USA: Kluwer Academic publishers.

Chen, W. and Saif, M. (2001). An iterative learning observer-based approach to fault detection and accommodation in nonlinear systems. *Proc. of 40th IEEE Conference on Decision and Control (CDC)* (pp. 4469-4474).

Demetriou, M. A. and Polycarpou, M. M. (1998). Incipient fault diagnosis of dynamical systems using online approximators. *IEEE Trans. on Automatic Control*, 43 (11), 1612-1617.

Frank, P. M. and Keller, L. (1990). Fault diagnosis in dynamic systems using analytical and knowledge-based redundancy – A survey and some new results. *Automatica*, 26, 459-474.

Gertler, J. (1988). Survey of model-based failure detection and isolation in complex plants. *IEEE Control Syst. Mag*., 8, 3-11.

Jagannathan, S. (2006). *Neural Network Control of Nonlinear Discrete–time Systems*. New York: CRC publications.

Jiang, B. and Chowdhury, F. N. (2005). Fault estimation and accommodation for linear MIMO discrete-time systems. *IEEE Trans. on Control Systems Technology*, 13 (3), 493-499.

Jiang, B., Staroswiecki, M. and Cocquempot, V. (2006). Fault accommodation for nonlinear dynamic systems. *IEEE Trans. on Automatic Control*, 51 (9), 1578-1583.

Kwan, C. M., Dawson, D. M., and Lewis, F. L. (1995). Robust adaptive control of robots using neural network: global tracking stability. *Proc. of the 34th conference on Decision and Control* (1846-1851).

Lewis, F. L., Jagannathan, S., and Yesilderek, A. (1999). *Neural network control of robotics and nonlinear systems*. United Kingdom: Taylor and Francis.

Lin, Y. H., and Narendra, K. S. (1980). A new error model for adaptive systems. *IEEE Trans. on Automatic Control*, vol. AC-25 (3), 585-587.

Patre, P. M., MacKunis, W., Kaiser, K., and Dixon, W. E. (2007). Asymptotic tracking for uncertain dynamics systems via a multilayer NN feed forward and RISE feedback control structure. *Proc. of the 2007 American Control conference* (pp. 5989-5994).

Polycarpou, M. M. (2001). Fault accommodation of a class of multivariable nonlinear dynamical systems using a learning approach. *IEEE Trans. on Automatic Control*, 46 (5), 736-742.

Polycarpou, M. M. and Helmicki, A. J. (1995). Automated fault detection and accommodation: a learning systems approach. *IEEE Trans. on Systems, Man, and Cybernetics*, 25 (11), 1447-1458.

Thumati, B. T. and Jagannathan, S. (2007). An online approximator-based fault detection framework for nonlinear discrete-time systems. *Proc. of 46th IEEE Conference on Decision and Control (CDC)* (pp. 2608-2613).

Thumati, B. T. and Jagannathan, S. (2009). A model based fault detection and accommodation scheme for nonlinear discrete-time systems with asymptotic stability guarantee", *Proc. of American Controls Conference* (pp. 4988 – 4993).

Yang, Q., Vance, J. B., and Jagannathan, S. (2008). Control of non-affine nonlinear discrete-time systems using reinforcement-learning-based linearly parameterized neural networks. *IEEE Trans. on Systems, Man, and Cybernetics—Part B: Cybernetics*, 38 (4), 994-1001.

Young, A., Chengyu, C., Hovakimyan, N., and Lavretsky E. (2006). Control of a nonaffine double-pendulum system via dynamic inversion and time-scale separation. *Proc. of the 2006 American Control conference* (pp. 1820-1825).

Zhang, J. & Morris, A. J. (1994). On-line process fault diagnosis using fuzzy neural networks. *Intelligent Systems Engineering*, 37-47.

6. A Novel Fault Detection and Prediction Scheme in Discrete-time Using a Nonlinear Observer and Artificial Immune System as an Online Approximator

Gary R. Halligan, Balaje T. Thumati, and S. Jagannathan

Abstract—In this paper, an observer-based fault detection and prediction (FDP) scheme using artificial immune system (AIS) as an online approximator is introduced for a class of nonlinear discrete-time systems. Traditionally, AIS was considered as an offline tool for fault detection in an ad hoc manner. However, in this paper, the AIS utilized as an online approximator in discrete-time (OLAD) is considered while its parameters are tuned online. A nonlinear observer comprising of the AIS and a robust adaptive term is used for detecting faults in the given nonlinear system. A fault is detected by comparing the residual against *apriori* chosen threshold, which is obtained by comparing the output of the nonlinear estimator to that of the given system. Upon detection, the AIS and the robust adaptive term are initiated in the observer, where the AIS parameters are tuned online using a suitable update law for learning the unknown fault dynamics. Additionally, this update law is used to estimate the time-to-failure (TTF), which is considered as a first step for prognostics On the other hand, the robust term, which is a function of the AIS parameter vector, is used to deliver asymptotic convergence of the residual unlike bounded stability in other schemes. The performance of the proposed FDP scheme is first demonstrated on a two-link robot

Gary R. Halligan (halligan@mst.edu), Balaje T. Thumati (e-mail: bttr74@mst.edu), and S. Jagannathan (e-mail: sarangap@mst.edu) are with the Department of Electrical & Computer Engineering, Missouri University of Science and Technology (formerly University of Missouri–Rolla), Rolla, MO, 65401, USA. Research supported in part by NSF I/UCRC on Intelligent Maintenance Systems and Intelligent Systems Center.

arm and an axial piston pump in simulation and subsequently on an axial piston pump test bed.

I. Introduction

Modern engineering systems require early fault detection and warning system to render safe and reliable service. Therefore, numerous efforts have been under taken in addressing the problem of fault detection and prediction (FDP). Due to the presence of noise and system uncertainties, the problem of fault detection (FD) is complex thus requiring robustness. The commonly used FD methods include quantitative or model-based [1] and qualitative or data-driven based techniques [2]. The qualitative based techniques are found to be expensive [1] due to the need for large quantities of data and are dependent upon region of operation. However, quantitative methods require a suitable representation of the nonlinear discrete-time systems. Typically, an observer is utilized to represent the nonlinear system.

In the past literature, FD efforts are limited to linear systems [1-5], by using a sliding mode observer [3], geometric approach [4], and parity relations [2] etc. Typically, in the observer based approach, a residual is generated by comparing the observer output with that of the actual system. Moreover, a fault is detected by comparing the generated residual against *apriori* chosen threshold. However, selection of the threshold is a challenging task due to the presence of uncertainties, but an analytical procedure has been developed to identify thresholds [5] analytically.

In the recent years, with better understanding of nonlinear control system theory, the techniques proposed for linear systems have been extended to nonlinear systems. Such

schemes include the sliding mode observers [6], geometric approach [7], adaptive and diagonal observers [5, 8, 9] and so on. A recent survey on the various FD schemes for nonlinear systems can be found in [10]. Another aspect that is of interest to the FD community is the stability and the robustness of the FD schemes. Recently, various FD schemes [5- 9] have been proven to be stable. However, most of the developments are in continuous-time and not much has been accomplished in the discrete-time.

Another important feature in general unavailable in the previously reported schemes [3-9] is the time-to-failure determination (TTF) since TTF is the first step for prognostics assessment. Some TTF schemes like the data-driven approaches [11-13], assumed a specific degradation model which has been found to be limited to the system or material type under consideration. Another scheme [14] employs a deterministic polynomial and a probabilistic method for prognosis by assuming that certain parameters are affected by the fault while others [15] use a black box approach using neural network (NN) on the failure data. All these schemes [11-15] while being data-driven address only TTF prediction, require offline training and do not offer performance guarantees. Therefore, it is envisioned that a unified FDP scheme will be necessary to alert an impending failure and provide the remaining useful life.

Discrete-time development is important due to the stability problems incurred in the direct conversion of the continuous time FD schemes to discrete-time [16]. Recent developments in discrete-time include [16, 17], where a FD scheme is introduced by using the persistent of excitation (PE) condition. Since it is very difficult to verify or guarantee PE, in our previous work [18], a FD scheme using linearly parameterized online approximators is introduced by relaxing the PE requirement. However, bounded stability of

all the signals is demonstrated similar to the case of fault detection algorithms in continuous-time.

In contrast, in this paper a FDP scheme for nonlinear discrete-time systems with guarantees of asymptotic stability is introduced by using an observer. To best of our knowledge not many FDP schemes in discrete-time render asymptotic stability. However, in [19], asymptotic stability of a continuous time FD scheme for robotic systems with specific actuator faults is undertaken. The FD scheme proposed in this paper comprises of a nonlinear observer, which is used for detecting faults in the given system. Additionally, the nonlinear observer comprises of an online approximator in discrete-time (OLAD) and a robust adaptive term generated by the OLAD parameter vector. The OLAD and the robust adaptive term are initiated only after the detection of a fault. Moreover, a fault is detected by comparing the generated residual against *apriori* chosen threshold. The residual is generated by comparing the outputs of the nonlinear system with that of the observer. By using a suitable update law, the parameters of the OLAD are tuned online to learn the unknown fault dynamics. Additionally, the robust adaptive term is used to guarantee the asymptotic convergence of the residual and the parameter estimation errors after the occurrence of the fault and in the presence of the uncertainties.

Most of the previously proposed FD scheme [5, 9, 16-18] uses neural networks or fuzzy systems as online approximators. However, in this paper, we use an artificial immune system (AIS) as the OLAD since biological immune systems detect external virus and protect the human body. Conventionally, AIS has been considered as an offline tool for applications such as classification, pattern recognition and detection. Additionally, offline data based training schemes are proposed to obtain AIS [20-30] parameters. However, in

this paper a new online adaptive law is introduced for tuning the AIS parameter vector online while demonstrating that the AIS is an online approximator.

In general, AIS draws inspiration from the biological immune system. In the event of a disease causing antigen (such as virus, bacteria etc.) attacking the human body, the immune system detects the foreign bodies and responds to the antigen by releasing suitable antibodies. Based on the affinity between the released antibody and the antigen, the disease causing antigen is destroyed. Moreover, the immune system memorizes the type of antibodies utilized to kill the antigen, so that in future attacks it ensures a quick release of antibody to overcome the antigen. The inherent advantage of the immune system in detecting anomalies makes it as a natural candidate for system identification [21], FD [25-29] and control [30] when compared to neural networks (NNs) which are derived from neurological system.

However, existing AIS-based methods [22, 25-30] are data driven, ad hoc and require extensive offline training to tune the AIS parameter vector. Therefore, in this paper, AIS is used as an OLAD, which is a part of the nonlinear FD observer. Moreover, the AIS parameter vector is tuned online without any *apriori* offline training. Moreover, mathematically, the asymptotic convergence of the residual and the parameter estimation errors of the FD scheme after the occurrence of the fault is shown by using Lyapunov analysis.

Using the parameter update, mathematically a method is proposed to derive the TTF by projecting the current value of the parameter to its limit provided the limiting parameter value is defined by the designer. This process is iteratively performed to continuously predict TTF up to the failure threshold beyond which the system is considered

unsafe. For most practical systems, the unknown parameters could be tied to physical entities thus making the parameter-based TTF determination very useful. Alternatively, the state trajectories from the FD estimator can be utilized for TTF determination due to asymptotic convergence. Finally, simulation examples and experimental results are presented to show the performance of the proposed FDP scheme.

The important contribution of this paper is the asymptotic stability of the FD scheme for nonlinear discrete time systems using the robust adaptive term and the AIS as an OLAD. Addition of the robust adaptive term complicates the stability analysis whereas the Lyapunov proof is still offered. In addition, the time to failure determination is introduced by using the AIS parameter vector. Finally, the online fault detection and prediction is verified on an experimental test bed.

This paper is organized as follows: Section II provides background on the AIS. Section III introduces the system under investigation whereas Section IV explains the FD scheme and the stability analysis. Section V introduces the prediction scheme whereas Section VI provides simulation results and Section VII explains the experimental results. In Section VIII conclusions and future work are given.

II. Artificial Immune System as Function Approximators

In biological organisms, the function of the immune system is to protect the body from invasion by foreign objects, called antigens. This is done by lymphocytes, which comprises of the two main types of white blood cells: T-cells and B-cells. There are two classes of T-cells: killer T-cells and helper T-cells. When an infection is detected, the killer T-cells destroys the infected cells whereas the helper T-cells assist in engulfing and

destroying the invading pathogens. In addition, the helper T-cells stimulates B-cells to produce clones of antibodies to attack the pathogen. The B-cells fine tunes the antibodies to increase their affinities to the antigen being encountered. The higher the affinity is, the stronger the immune response will be. Additionally, more antibodies will be released to mitigate the antigen. Antibodies with highest affinity are retained while a feedback is provided to the T-cells to store in memory the type of antibody required for a particular antigen. This would help in mitigating future attacks by the similar antigen. Interested readers for further reading could refer to [20].

Based on this understanding, a recent work on AIS can be found in [21, 23] wherein the AIS is utilized to solve engineering problems. For instance, in [24], AIS is used for identification of nonlinear systems. In this method, an offline data based training scheme is proposed for the nonlinear system identification. However, an interesting contribution is the definition of a mathematical equation to describe the function of the AIS for system identification

$$\hat{f}(x_j) = \sum_{i=1}^{N} m_{ij} a_i = \frac{\sum_{i=1}^{N} a_i e^{-\beta_i d_{ij}}}{\sum_{i=1}^{N} e^{-\beta_i d_{ij}}} \tag{1}$$

where $i = 1,...,N$ is the number of antibodies, $j = 1,...,N_s$ is the number of data sets, m_{ij} is the ij^{th} affinity function, β_i is the shape parameter, a_i is the appropriate immune response, $d_{ij} = \|x_j - p_i\|$ is the Euclidean distance between the j^{th} antigen epitope vector (x_j) and the i^{th} antibody receptor vector p_i.

For engineering problems, the artificial immune response considers the unknown data as antigen, and the output is the net response of all the antibodies (i.e., output of equation (1)). Therefore, by calculating the error between the estimated and the actual value, the parameters of the AIS function are updated. However, the AIS training is an iterative process and is performed offline. Therefore, in this paper, a new online tuning mechanism is proposed to tune the parameters of the AIS online by using adaptive control techniques. Moreover, we use the same mathematical equation as that given in [24] to describe the function of the AIS and exploit the function approximation property.

To guarantee that the AIS scheme could be utilized for approximating any unknown function over the compact set, in the following theorem we show that indeed an AIS possesses function approximation properties. This enables AIS to be an OLAD similar to an artificial neural network, fuzzy logic and other online approximators. However, AIS is preferred for FD due to its natural affinity of detecting and preventing antigen attacks when compared to other online approximators.

Theorem 1: For every continuous smooth function f , every AIS basis function ϕ, every probability measure σ , and every $n_a \geq 1$, there exists a linear combination of AIS functions $\hat{f}_a(x)$, such that

$$\sum_B \left(f(x) - \hat{f}_a(x) \right)^2 \sigma \leq \frac{(2C)^2}{n_a} \tag{2}$$

where $C > 0$, B is a compact set, and n_a is the number of antibodies or the size of the AIS function.

Proof: Follow steps similar to [31].

As shown in this theorem, the use of AIS in approximating unknown functions is valid. Therefore, similar to neural networks, the unknown function ($f(x)$) and the estimate of AIS could be written as

$$f(x) = \overline{a}^T \varphi(x) + \varepsilon(k),$$

$$\hat{f}_a(x) = \overline{a}^T(k)\varphi(x), \quad \hat{f}_a \in \Re^{n\times 1} \tag{3}$$

where $\overline{a} \in \Re^{l\times n}$ is the unknown ideal immune response, $\varepsilon(k)$ is the approximation error and bounded by a known constant, i.e., $\left\|\varepsilon(k)\right\| \le \varepsilon_a$. Also, $\overline{a}(k) \in \Re^{l\times n}$ is a matrix of estimated immune response, $\varphi(x) \in \Re^{l\times 1}$ is the basis function which is given by

$$\varphi(x) = \left[\frac{e^{-\beta_1 d_1}}{\sum_{i=1}^{l} e^{-\beta_i d_{ij}}}, ..., \frac{e^{-\beta_l d_l}}{\sum_{i=1}^{l} e^{-\beta_i d_{ij}}} \right]^T$$

where β_i, $\forall i = 1, ..., l$ is a positive randomly chosen shape parameter, $d_i = \left\|x - p_i\right\|$, where $x \in \Re^{n\times 1}$ is the input to the AIS basis function, $p_i \in \Re^{n\times 1}$, $\forall i = 1, ..., l$ is a randomly chosen constant vector.

With this understanding on AIS, we next proceed with the discussion on the system under investigation.

III. Problem Statement

Consider the following general class of nonlinear discrete-time systems described by

$$x(k+1) = \omega(x(k), u(k)) + \eta(x(k), u(k)) + h(x(k), u(k)) \tag{4}$$

where $x \in \Re^n$ is the system state vector, $u \in \Re^m$ is the control input vector, $\omega : \Re^n \times \Re^m \to \Re^n$,

$\eta : \Re^n \times \Re^m \to \Re^n$, $h : \Re^n \times \Re^m \to \Re^n$ are smooth vector fields. The term $\omega(x(k), u(k))$ represents the known nonlinear system dynamics while $\eta(x(k), u(k))$ is the system uncertainty. The unknown fault function $h(x(k), u(k)) = \Pi(k - k_0) f(x(k), u(k))$ with $f(x(k), u(k))$ representing the unknown fault dynamics while $\Pi(k - k_0)$ being a $n \times n$ square matrix function representing the time profiles of faults, and $k_0 \geq 0$ is the initial time.

Typically, the time profile of the faults are modeled by

$$\Pi(k - k_0) = diag(\Omega_1(k - k_0), \Omega_2(k - k_0), ..., \Omega_n(k - k_0))$$

where

$$\Omega_i(\tau) = \begin{cases} 0, & \text{if } \tau < 0 \\ 1 - e^{-\bar{\kappa}_i \tau}, & \text{if } \tau \geq 0 \end{cases} \quad \text{for } i = 1, 2, ...n \tag{5}$$

and $\bar{\kappa}_i > 0$ is an unknown constant that represents the rate at which the fault in the corresponding state x_i occurs. The term $\Omega_i(\tau)$ approaches a step function when $\bar{\kappa}_i$ is large, which in turn represents an abrupt fault whereas a small value of $\bar{\kappa}_i$ implies incipient faults. It is important to understand that the exponential time profile is only used to classify the faults as incipient or abrupt. However, $f(x(k), u(k))$ represents the magnitude and the type of the fault. Since the fault function is expressed as a nonlinear function of the system states and the inputs, therefore, it represents a wide range of faults that can potentially occur in a given system. For example, such faults could be a piston wear in a compressor or an actuator fault.

Remark 1: The known nominal dynamics in (4) is in nonaffine form. However, for affine systems, the known nominal dynamics could be written

as $\omega(x(k),u(k)) = \omega_f(x(k)) + \omega_g(x(k))u(k)$, where, $\omega_f \in \Re^{n\times 1}$ and $\omega_g \in \Re^{n\times m}$ are known smooth functions. However, the system uncertainty and the faults still be expressed in nonaffine form and are functions of the system states and the input. It is important to note that the following discussion for nonaffine systems is also applicable to affine systems.

Remark 2: Modeling faults using the above time profile is quite common in the FD literature [32], and is used extensively by researchers [5, 9, 16-18].

Before proceeding any further, we propose the following assumption.

Assumption 1: The modeling uncertainty is unstructured and bounded [5, 9, 16-18] above satisfying $\|\eta(x(k),u(k))\| \le \eta_M,\ \forall (x,u) \in (\chi \times U)$ where $\eta_M \ge 0$ is a known constant.

Remark 3: The uncertainties have to be bounded above in order to identify faults from system uncertainties.

In certain previously reported FD schemes [3, 8], the system uncertainty is assumed to structured, which helps to simplify the development of the FD scheme. In other schemes [1-3], structured faults are assumed, which also simplifies the development of the FD scheme. However, such assumptions are not considered in this paper.

In this paper, we consider a general framework for nonlinear systems with unknown system uncertainty. However, this complicates the design of a FD scheme, but is still undertaken in this paper. In the next section, the fault detection scheme is introduced by using a novel nonlinear observer using AIS as the online approximator. Additionally, using Lyapunov theory, the asymptotic performance of the proposed FD scheme is shown.

IV. Fault Detection Scheme

In this FD scheme, a nonlinear observer is designed to monitor and detect faults in the given system described in (4). It is essential to understand that the purpose of the FD observer is not to estimate the system states [16, 17] whereas to obtain residual for the purpose of detection.

A. Observer Dynamics

Consider the nonlinear observer described by

$$\hat{x}(k+1) = A_0\hat{x}(k) + \omega(x(k), u(k)) + \hat{h}(x(k), u(k); \hat{\theta}(k)) - A_0 x(k) + v(k) \tag{6}$$

where $\hat{x} \in \Re^n$ is the estimated state vector, A_0 is a constant $n \times n$ design matrix chosen by the user, $\hat{h} : \Re^n \times \Re^m \times \Re^{q \times n} \to \Re^n$ is the online approximator in discrete-time (OLAD) [18], $\hat{\theta} \in \Re^{q \times n}$ is a set of adjustable immune system parameters, and $v(k)$ is the robust adaptive term, which is to be defined later. Prior to the fault, the initial values for the estimated model (6) are taken as $\hat{x}(0) = x(0)$, $\hat{\theta}(0) = \hat{\theta}_0$, so that $\hat{h}(x, u, \hat{\theta}_0) = 0$ for all $x \in \chi$ and $u \in U$. Typically, the commonly used OLAD's are neural networks, fuzzy systems etc. However, in this paper, we consider AIS as an OLAD. Therefore, the AIS based OLAD is defined by using (3) as

$$\hat{h}(z, \hat{\theta}) = \hat{\theta}^T(k)\varphi(z) \tag{7}$$

where $z = [x, u]^T$ is the input vector, $\hat{\theta}(k) \in \Re^{l \times n}$ is a tunable immune system response, and $\varphi(z)$ is the AIS basis function as defined in (3).

Remark 4: Upon the detection of the fault, the OLAD and the robust adaptive term are initiated.

Now define the detection residual or state estimation error as $e = x - \hat{x}$. Then from (4) and (6) prior to the fault the residual dynamics are given by

$$e(k+1) = A_0 e(k) + \eta(x(k), u(k)) \tag{8}$$

In order to detect faults in the given system, the residual is compared against a known threshold via a dead-zone operator. The selection of the threshold is a challenging task; however a mathematical procedure is developed for selecting it by using (8). It is important to note that by using a threshold, the robustness of the fault detection scheme can be improved [1, 2, 5, 16-18].

Prior to the fault, the residual, $e(k)$, remains within the threshold. However, in the event of a fault, the residual increases and crosses the threshold and therefore a fault is declared active. We define the threshold operator as $D[\cdot]$

$$D[e(k)] = \begin{cases} 0, & \text{if } \|e(k)\| \le \rho \\ e(k), & \text{if } \|e(k)\| > \rho \end{cases} \tag{9}$$

where $\rho > 0$ is the threshold. The selection of the dead-zone size ρ clearly provides a tradeoff between reducing the possibility of false alarms (robustness) and improving the sensitivity of the faults. The selection of an appropriate value for ρ is addressed next.

B. Fault Detection Threshold Selection

A suitable threshold is selected by solving the residual dynamics (8) through standard linear control theory as $e(k) = \sum_{j=0}^{k-1} A_0^{k-1-j} \eta(x(k), u(k))$. Since the matrix A_0 is stable with its poles chosen inside the unit disc, there exists two positive constants μ and β_c such that the Frobenius norm [33] $\|A_0^k\| \le \beta_c \mu^k \le 1$. Therefore, $\|e(k)\| \le \beta \eta_M \frac{(1-\mu^k)}{(1-\mu)}$, where $\beta = \beta_c \mu$.

This implies that the threshold can be selected as a constant value $\rho = \frac{\beta\eta_M}{(1-\mu)}$ or a time-varying function as $\rho = \frac{\beta\eta_M(1-\mu^k)}{(1-\mu)}$. As a consequence, the residual $e(k)$ remains within the threshold for all $k \geq k_0$ and the OLAD and the robust adaptive terms stay at zero.

The dead-zone operator is utilized to turn the OLAD and robust adaptive terms online. Prior to the fault, *i.e.*, $\|e(k)\| \leq \rho$, $\hat{\theta}(k) = \begin{bmatrix} 0 & . & . & . & 0 \\ . & . & . & . & . \\ . & . & . & . & . \\ 0 & . & . & . & 0 \end{bmatrix}_{l\times n}$, $0 \leq k \leq T$, and $v(k) = [0, 0, ..., 0]^T$. This means $\hat{h}(x(k), u(k); \hat{\theta}(k)) = [0, 0, ..., 0]^T$, in the time interval $0 \leq k \leq T$ prior to a state or output fault.

When the residual exceeds the detection threshold, i.e., $\|e(k)\| > \rho$, a fault is declared active and the OLAD schemes that generate, $\hat{h}(.)$ is initiated. A standard delta-based parameter tuning algorithm [34] can be utilized whereas it is slower in convergence. To overcome this problem, the following parameter update law is used

$$\hat{\theta}(k+1) = \hat{\theta}(k) + \alpha\varphi(k)\mathrm{D}[e^T(k+1)] - \gamma \left\| I - \alpha\varphi(k)\varphi^T(k) \right\| \hat{\theta}(k) \tag{10}$$

is proposed where $\alpha > 0$ is the learning rate, $\gamma > 0$ is the adaptation rate, and $\varphi(k)$ is the OLAD basis function. Now using Theorem 1 and equation (3), we rewrite the fault dynamics in (4) as

$$h(x(k), u(k)) = \theta^T \varphi(x(k), u(k)) + \varepsilon_1(k) \tag{11}$$

where $\theta \in \Re^{l\times n}$ is the target parameter matrix such that the approximation error $\varepsilon_1(k)$ is bounded above and $\varphi(x(k), u(k))$ is the known basis function of the AIS. By appropriate

selection of the antibodies in the AIS scheme, the approximation error can be decreased. The output of the OLAD is given by

$$\hat{h}(x(k),u(k);\hat{\theta}(k)) = \hat{\theta}(k)^{T}\varphi(x(k),u(k)) \tag{12}$$

where $\hat{\theta}(k) \in \Re^{l\times n}$ is the estimated AIS parameter matrix.

With this understanding of the proposed observer design, the stability of the proposed fault detection scheme will be studied next. By using (4) and (6), the residual dynamics after the fault is given by

$$e(k+1) = A_0 e(k) + \eta(x(k),u(k)) + h(x(k),u(k)) - \hat{h}(x(k),u(k);\hat{\theta}(k)) - v(k)$$

where the robust adaptive term is defined as $v(k) = \dfrac{\hat{\theta}^{T}(k)B_1}{B_1^{T}\hat{\theta}(k)\hat{\theta}^{T}(k)B_1 + c_c}$, with $B_1 \in \Re^{l\times 1}$ is a constant vector and $c_c > 0$ a constant. Next using (11) and (12), the residual dynamics is rewritten as

$$e(k+1) = A_0 e(k) + \tilde{\theta}^{T}(k)\varphi(x,u) - \frac{\hat{\theta}^{T}(k)B_1}{B_1^{T}\hat{\theta}(k)\hat{\theta}^{T}(k)B_1 + c_c} + \varepsilon(k) \tag{13}$$

where $\varepsilon(k) = \varepsilon_1(k) + \eta(x(k),u(k))$ with the parameter estimation error defined as $\tilde{\theta}(k) = \theta - \hat{\theta}(k)$.

Next, add and subtract $\dfrac{\left(\theta^{T}B_1 - C_1\right)}{B_1^{T}\hat{\theta}(k)\hat{\theta}^{T}(k)B_1 + c_c}$, in (13), where $C_1 \in \Re^{n\times 1}$ is a constant vector. The residual dynamics become

$$e(k+1) = A_0 e(k) + \Psi_1(k) + \Psi_2(k) + \varepsilon(k) - \frac{\left(\theta^{T}B_1 - C_1\right)}{B_1^{T}\hat{\theta}(k)\hat{\theta}^{T}(k)B_1 + c_c} \tag{14}$$

where $\Psi_1(k) = \tilde{\theta}^T(k)\varphi(x,u)$ and $\Psi_2(k) = \dfrac{\left(\tilde{\theta}^T(k)B_1 - C_1\right)}{B_1^T\hat{\theta}(k)\hat{\theta}^T(k)B_1 + c_c}$. Next the following lemma is needed in order to proceed.

Lemma 1: The term, $\varepsilon(k)$, comprising of the approximation error, $\varepsilon_1(k)$, and the system uncertainty, $\eta(x(k),u(k))$ are bounded above according to

$$\varepsilon^T(k)\varepsilon(k) \le \varepsilon_M = d_0 + d_1\left\|\tilde{\theta}(k)\right\|^2 + d_2\left\|e(k)\right\|\left\|\tilde{\theta}(k)\right\| + d_3\left\|e(k)\right\|^2 \tag{15}$$

where $d_0, d_1, d_2,$ and d_3 are computable positive constants.

Proof: Refer to Appendix.

Remark 5: This lemma is necessary similar to the case of continuous-time [38] while such results are not available for discrete-time systems. This result is very mild [35-38] when compared to the case where the approximation error is considered bounded above by a known constant.

Next, the following theorem guarantees the asymptotic stability of the proposed FD scheme after a fault occurs. Additionally, it is clear that prior to the fault the system remains stable for a bounded system uncertainty $\eta(x(k),u(k))$. This is evident from (8) since A_0 has eigen values within the unit disc.

Theorem 2 (FD Observer Performance upon Detection): Let the proposed nonlinear observer in (6) be used to monitor the system given in (4). Let the update law given in (10) be used for tuning the immune response of the AIS based OLAD. In the presence of a fault and bounded system uncertainties, the detection residual, $e(k)$, and the parameter estimation errors $\tilde{\theta}(k)$ are locally asymptotically stable provided:

(a) $$A_{0_{\max}} \le \sqrt{\frac{(1/5)}{\left(4 + 20\alpha(2 + 1/\delta)\varphi_{\max}^2\right)}}\ , \quad 0 < \alpha < 1 \tag{16}$$

(b) $$\frac{1 - \sqrt{1 - C_r}}{\left\|I - \alpha\varphi(k)\varphi^T(k)\right\|} \le \gamma \le 1 \Big/ \left\|I - \alpha\varphi(k)\varphi^T(k)\right\| \tag{17}$$

and

(c) $$0 < \lambda_s < 0.5\ ,\ 0 < \delta < 1 \tag{18}$$

where $\|A_0\| \le A_{0_{\max}}$, $\|\varphi(k)\| \le \varphi_{\max}$, and $C_r > 0$ is a constant.

Proof: Refer to Appendix.

Remark 6: Theorem 2 guarantees the asymptotic stability of the proposed FD scheme after a fault occurs. In other words, the proposed OLAD will characterize the faults accurately in comparison with the detection schemes in continuous-time where a bounded residual is demonstrated [5, 9].

In the next section, the prediction scheme is introduced.

V. Prediction Scheme

Thus far, a new FD estimator design using the AIS as online approximator was introduced and its stability was studied rigorously. Now TTF can be determined using the behavior of the immune system parameter trajectories before and after the occurrence of a fault. The following assumption holds in deriving the TTF.

Assumption 2: The parameter vector $\hat{\theta}(k)$ is an estimate of the actual system parameters.

Remark 7: This assumption is satisfied when a system can be expressed as linear in the unknown parameters (LIP). For example, in a mass damper system, or in civil

infrastructure such as a bridge, the mass, damping constant and spring constant may be expressed as linear in the unknown parameters. In the event of a fault, system parameters change, and tend to reach their limits. When any one of the parameters exceeds its limit, operation is considered unsafe. TTF is defined as the time elapsed when the first parameter reaches its limit. The TTF can also be analyzed with lower limits.

In this section, to develop an explicit mathematical equation for predicting TTF, we use the parameter update law given in (10). Subsequently, by using this equation, we develop an algorithm for the continuous prediction of TTF iteratively at every time instant. Alternatively, estimated state trajectories can be employed as well if the states can be related to physical quantities. Next, the mathematical equation is presented in the following theorem.

Theorem 3 (Time to Failure): If the system in (4) can be expressed as LIP, the TTF for the ij^{th} system parameter at the k^{th} time instant can be determined using

$$k_{f_{ij}} = \frac{\left| \log\left(\left| \frac{\left(\gamma \left\| I - \alpha\phi\phi^T \right\| \theta_{ij_{\max}} - \alpha\left(\phi e^T\right)_{ij} \right)}{\left(\gamma \left\| I - \alpha\phi\phi^T \right\| \theta_{ij_0} - \alpha\left(\phi e^T\right)_{ij} \right)} \right| \right) \right|}{\left| \log(1 - \gamma \left\| I - \alpha\phi\phi^T \right\|) \right|} + k_{0_{ij}} \tag{19}$$

where $k_{f_{ij}}$ is the TTF, $k_{0_{ij}}$ is the time instant when the prediction starts (bearing in mind that k_{dt} was the initial value, which increases incrementally), $\theta_{ij_{\max}}$ is the maximum value of the system parameter, and θ_{ij_0} is the value of the system parameter at the time instant $k_{0_{ij}}$.

Proof: Refer to [39].

Remark 8: The mathematical equation (19) presents the TTF for the ij^{th} system parameter. In general, for a given system with a parameter vector, the TTF would

be $k_{ft} = \min(k_{f_{ij}}), i = 1, 2, ...l$, $j = 1, ..., n$, where $l \times n$ are the number of system parameters.

The TTF is defined as the time elapsed when the first parameter reaches its limit. The speed at which the actual parameters approach their target values is dictated by the learning rate or adaptation gain and the design constant in the parameter update law (10). A small value for the learning rate implies slower convergence which further means that the TTF is not as accurate when the learning rate is higher. However, a large value of the learning rate can speed up the convergence. Increasing the learning rate can cause hunting problems which will result in inaccurate prediction of TTF.

Remark 9: Although the proposed prediction scheme is based on the parameter trajectory, estimated system states could also be used for prediction since asymptotic stability is proven. A relationship similar to (19) can be derived for TTF using (6). However, for brevity, no further discussions on the use of state trajectories for prediction are included in this paper.

Remark 10: The proposed prediction scheme could be applied to unknown systems that satisfy LIP. It could also be applied to systems with partial information that satisfy LIP. Such systems were addressed in Section III.

Figure 1 provides a flow chart of the iterative algorithm to determine TTF (k_{ft}) for each system parameter. The TTF is calculated at each time instant starting when a fault is detected until the system parameter reaches its maximum value (threshold). Therefore, it is logical that the TTF decreases as the parameters approach their corresponding limits. The simulation results presented below will indeed show that the performance of the FDP scheme as indicated in the theorems can be demonstrated in simulation. By tuning the

system parameter estimate ($\hat{\theta}_i(k)$) to update the TTF recursively, the system could be more accurately monitored than would be possible with other methods [13, 14]. In fact, the TTF will not be accurate when the parameter estimate vector is just started. Over time when the parameter vector starts converging to its true values, the TTF prediction starts improving. Additionally, no prior offline training is required to estimate the system parameters, which significantly reduces the burden of collecting data.

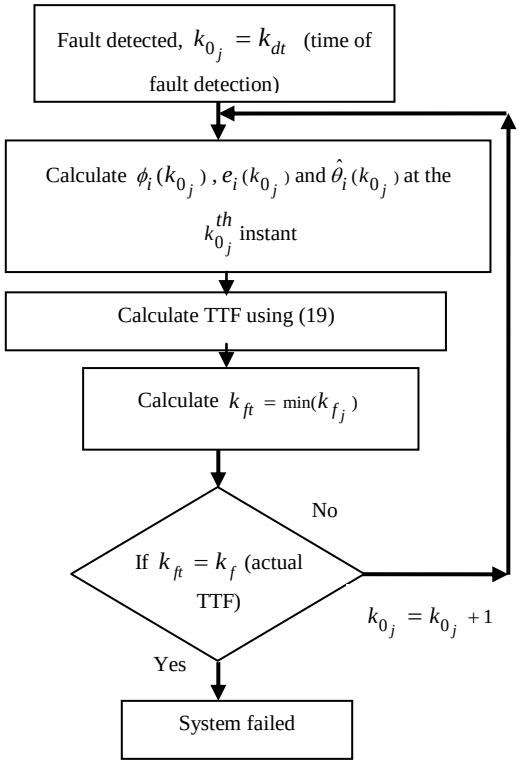

Figure 1: Flow chart indicating the TTF determination.

In the next section, we present some simulation example and later some experimental study to illustrate the proposed FDP scheme.

VI. Simulation Results

In this section, two different simulation examples are presented to demonstrate the proposed fault detection scheme. Initially, a two link manipulator is considered followed by an axial piston pump. Subsequently, in the next section, the proposed FDP scheme is verified on a pump test bed.

A. Two Link Robot Manipulator

A schematic of a two degree of freedom manipulator is shown in Fig. 2 and its dynamics model is given below [24]

$$\tau = M(\theta)\ddot{\theta} + V(\theta,\dot{\theta}) + G(\theta) + F(\dot{\theta}) \tag{20}$$

where $\theta = [\theta_1, \theta_2]^T$ is the vector of angular positions and $\dot{\theta} = [\dot{\theta}_1, \dot{\theta}_2]^T$ is the vector of angular velocity of links 1 and 2 respectively. Additionally, $M(\theta)$ is the inertia matrix, $V(\theta,\dot{\theta})$ is the coriolis or centripetal matrix, $G(\theta)$ is the gravity vector, and $F(\dot{\theta})$ is the friction vector. Moreover, τ is a vector of torque input applied to the two link manipulator.

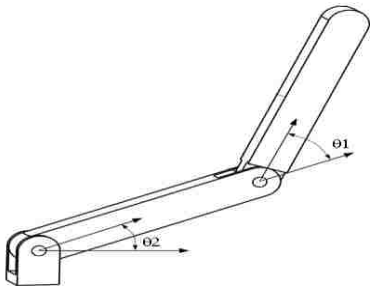

Fig. 2: Schematic of a two link manipulator.

For convenience, we express (20) in the following discrete-time state space form

$$x_1(k+1) = Tx_2(k) + x_1(k)$$

$$x_3(k+1) = Tx_4(k) + x_3(k)$$

$$\begin{bmatrix} x_2(k+1) \\ x_4(k+1) \end{bmatrix} = T\left(M^{-1}\begin{pmatrix} x_1 \\ x_3 \end{pmatrix}\left(\begin{vmatrix} \tau_1 \\ \tau_2 \end{vmatrix} - V\left(\begin{bmatrix} x_1 \\ x_3 \end{bmatrix}, \begin{bmatrix} x_2 \\ x_4 \end{bmatrix}\right) - G\left(\begin{bmatrix} x_1 \\ x_3 \end{bmatrix}\right) - F\left(\begin{bmatrix} x_3 \\ x_4 \end{bmatrix}\right)\right)\right) + \begin{bmatrix} x_2(k) \\ x_4(k) \end{bmatrix}$$

where $x = [x_1, x_2, x_3, x_4]^T$ is the system state vector. We assume an actuator fault, which is expressed as $h(k) = [0, 1.8(1-e^{-0.05(k-40)})\tau_1(k), 0, 0]^T$. The fault is induced at the 40$^{\text{th}}$ second of system operation with a growth rate of 0.05. Moreover, we assume the sampling time for this simulation is taken as $T = 10m\sec$. Additionally, a white noise is introduced in this simulation with a magnitude of 0.004 units and a constant uncertainty of 0.5 units. To monitor and detect faults in the given system, we use the following FD estimator

$$\hat{x}_1(k+1) = Tx_2(k) + x_1(k) + 0.005(\hat{x}_1(k) - x_1(k))$$

$$x_3(k+1) = Tx_4(k) + x_3(k) + 0.005(\hat{x}_3(k) - x_3(k))$$

$$\begin{bmatrix} x_2(k+1) \\ x_4(k+1) \end{bmatrix} = T\left(M^{-1}\begin{pmatrix} x_1 \\ x_3 \end{pmatrix}\left(\begin{vmatrix} \tau_1 \\ \tau_2 \end{vmatrix} - V\left(\begin{bmatrix} x_1 \\ x_3 \end{bmatrix}, \begin{bmatrix} x_2 \\ x_4 \end{bmatrix}\right) - G\left(\begin{bmatrix} x_1 \\ x_3 \end{bmatrix}\right) - F\left(\begin{bmatrix} x_3 \\ x_4 \end{bmatrix}\right)\right)\right) + \begin{bmatrix} x_2(k) \\ x_4(k) \end{bmatrix} + \begin{vmatrix} 0.005(\hat{x}_2(k) - x_2(k)) \\ 0.005(\hat{x}_4(k) - x_4(k)) \end{vmatrix} \quad (21)$$

where $\hat{x} = [\hat{x}_1, \hat{x}_2, \hat{x}_3, \hat{x}_4]^T$ is the estimated state vector, the OLAD is taken as $\hat{h}(k) = [0, \hat{\theta}(k)\tau_1(k), 0, 0]^T$. Next, using (20) and (21), we generate the norm of the residual as shown in Fig. 3. Since we assumed some disturbances, therefore, we need a threshold to improve the robustness of the proposed fault detection scheme. The threshold is derived by taking $\beta = 1.03$, $\mu = 0.01$, and $\eta_M \approx 0.5$, we have $\rho \approx 0.52$. As seen in Fig. 3, the residual remains within the threshold prior to the fault, however, after the fault occurs, the residual exceeds the threshold. Subsequently, the OLAD and the robust adaptive terms are initiated

to learn the unknown fault dynamics. This is evidenced by the fact the residual quickly drops after initiating the OLAD and the robust adaptive term. Additionally, the asymptotic convergence of the residual after the fault is guaranteed as seen in Fig. 3. Therefore, the theoretical results presented in this paper are validated.

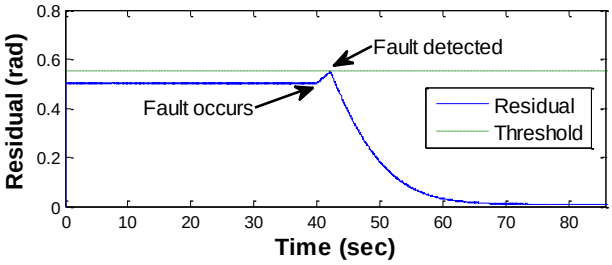

Fig. 3: Residual and the FD threshold.

Next, the online estimation of the fault magnitude using the proposed OLAD scheme is shown in Fig. 4. As seen in the figure, the online learning is found to be satisfactory. The parameter of the OLAD is tuned online using the update law in (9) with $\alpha = 0.034$ and $\gamma = 0.1$. Using the online estimation of the parameters, we estimate TTF as shown in Fig. 5. From the figure, it's evident that the TTF prediction is satisfactory. However, it is noted that the first few seconds of TTF prediction after the fault detection didn't render reliable results therefore, is not presented. This could be attributed to the random selection in the gains of the weight update law. However, after the 50^{th} second of the system operation, the TTF prediction seems to be reasonable and converges to the actual time of failure, which is 79.43 sec.

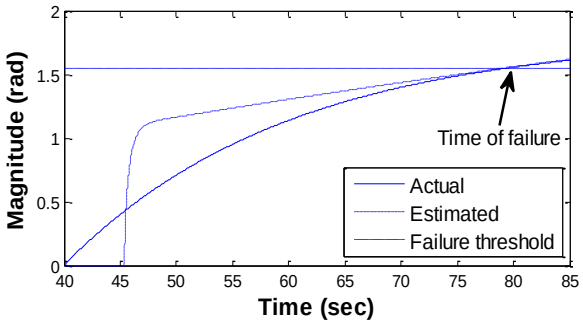

Fig. 4: Online estimation of the fault magnitude.

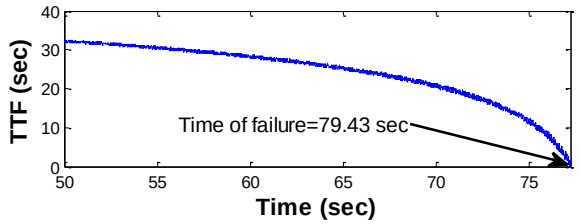

Fig. 5: The TTF determination due to the incipient actuator fault.

To show that the proposed scheme is generic, next, an axial piston pump example is considered in simulation.

B. Axial Piston Pump

A discrete-time dynamic representation of the axial piston pump derived in [40] is given as

$$x_i(k+1) = \frac{BT}{C - A_p S_{pi}}\left(Q_{kpi}(k) - Q_{pi}(k) - Q_{lpi}(k)\right) + x_i(k), i = 1,..,9$$

$$x_{10}(k+1) = \frac{TBC}{V_c}\left(Q_p(k) - Q_s(k)\right) + x_{10}(k)$$

$$y(k) = x_{10}(k) \tag{22}$$

where, $x_i(k)$, $i=1,...,9$ are the system states. Additionally, $[x_1(k),.....,x_9(k)]^T$ is the pressure in the nine pistons, x_{10} is the pump outlet pressure, B is the bulk modulus of the hydraulic fluid, T is the sample timing, V_c is the theoretical volume of flow, and A_p is the piston area. Moreover, S_{pi}, Q_{kpi}, Q_{pi}, Q_{lpi}, and Q_s are the i^{th} piston stroke length, kinematical flow from the piston chamber to the discharge chamber, internal leakage from piston to the case chamber, and the outlet flow of the pump respectively. Additionally, they are obtained using the following equation

$$Q_{kpi}(k) = \frac{\omega \pi d^2 R_p}{4} \tan\beta_c . \sin(\omega k - (i-1)\alpha_p)$$

$$Q_{lpi}(k) = \frac{\pi r h_g^3}{6\mu L}(x_i(k) - P_c)$$

$$Q_{pi}(k) = C_{d1} A_{di} \sqrt{\frac{2|x_i(k) - x_{10}(k)|}{\rho_c}} sign(x_i(k) - x_{10}(k)) \text{ , } i = 1,..,9$$

$$Q_p(k) = \sum_{i=1}^{9} Q_{pi}(k)$$

$$Q_s(k) = C_{d2} A_v \sqrt{\frac{2x_{10}(k)}{\rho_c}}$$

$$S_{pi}(k) = R_p \tan\beta_c (1 - \cos(\omega k - (i-1)\alpha_c))$$

where ω is the angular velocity of the pump drive shaft (rad/s), d is the diameter of the piston (m), R_p is the piston pitch radius on barrel, β_c is the angle of swash plate, α_p is the phase delay (rad), r is the radius of piston (m), h_g is the radial clearance between piston and cylinder bore (m), μ is the absolute fluid viscosity (N sec/m^2), L is the length of leakage passage (m), C_{d1} is the flow discharge coefficient of the discharge areas for piston

port opening to discharge chamber, ρ_c is the flow density (kg/m^3), A_{di} is the i^{th} discharge area for piston port opening to the discharge chamber in valve plate (m^2), C_{d2} is the discharge coefficient of needle valve orifice, and A_v is the orifice area of the needle valve (m^2). The values of the parameters used in this simulation are taken from [40] and we use a sampling interval of $T = 10m\sec$. To monitor and detect faults in (22), we use the following FD estimator

$$\hat{x}_i(k+1) = \frac{BT}{C - A_p S_{pi}}\left(Q_{kpi}(k) - Q_{pi}(k) - Q_{lpi}(k)\right) + x_i(k) + A_{0_i}(\hat{x}_i(k) - x_i(k)) \qquad , i = 1,..,9$$

$$\hat{x}_{10}(k+1) = \frac{TBC}{V_C}\left(Q_p(k) - Q_s(k)\right) + x_{10}(k) + A_{0_{10}}(\hat{x}_{10}(k) - x_{10}(k)) \;\; \hat{y}(k) = \hat{x}_{10}(k) \tag{23}$$

where, $\hat{x}_i(k)$, $i = 1,...,10$ are the estimated system states. Also, $A_0 = 10^{-4}\, diag(0.0630, 0.1796, 0.8, 0.0305, 0.1431, 0.1683, 0.1567, 0.1996, 0.1172, 0.0001)$ is the estimator gain matrix. For this simulation, two different faults, i.e., piston wear fault and pressure sensor fault are seeded. First, we discuss the piston wear fault.

B.1) Piston Wear Fault

An incipient piston wear fault described by

$$h(k) = [0,0,0,0,0,0,0,0,0,34\left(1 - e^{-0.02(k-100)}\right)]^T$$

is induced at the 100th minute of system operation. Additionally, a constant uncertainty of 30 units is considered in the simulation. Next to detect the fault online, we generate norm of the residual (i.e., $|e(k)| = |x_{10}(k) - \hat{x}_{10}(k)|$) from (22) and (23) as shown in Fig. 6. Due to the presence of system uncertainties, a threshold is needed to guarantee robustness. Therefore, by taking $\beta = 1.15$, $\mu = 0.01$, and $\eta_M = 30$, we have $\rho \approx 35$, a constant threshold as shown

in Fig. 6. From the figure, we see that the fault is detected at 105^{th} minute. After the detection, the OLAD is initiated to learn online the magnitude of the unknown fault dynamics as shown in Fig. 7. Additionally, parameters of the OLAD are tuned online using the update law in (9) with $\alpha = 0.1$ and $\gamma = 0.001$. From the figure, it is observed that the online learning of the fault by the OLAD is satisfactory.

Subsequently, the TTF is determined using the scheme outlined in Section IV and is shown in Fig. 8. From the figure, the initial TTF prediction and the oscillatory behavior in the prediction is attributed to the random selection of the gains. However, as the online estimation of the fault parameter improves, the TTF prediction improves and concurs with the actual time of failure, which 251 min.

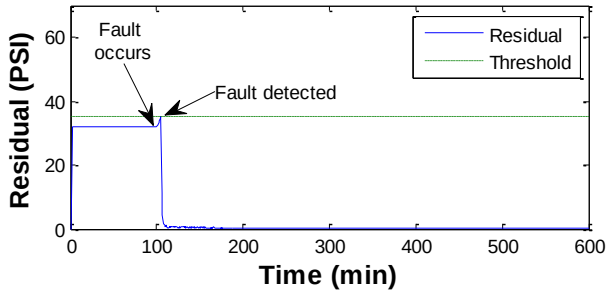

Fig. 6: Residual and the FD threshold- Piston wear fault.

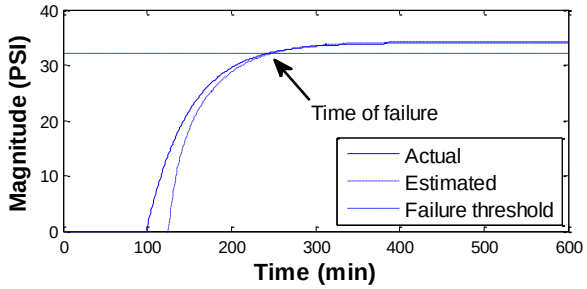

Fig. 7: Online estimation of the piston wear fault magnitude.

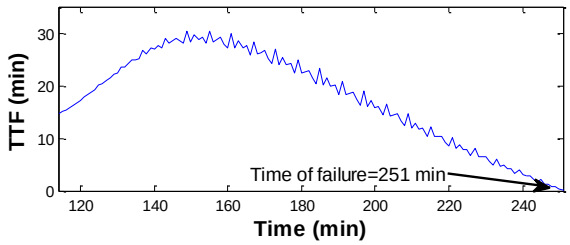

Fig. 8: The TTF determination due to the piston wear fault.

B.2) Outlet Pressure Sensor Fault

Next, a pressure sensor fault is induced, which may be due to loose wiring. Mathematically, the fault is described by

$$h_o(k) = \begin{cases} 0 & for\, k < 100 \text{ min} \\ -0.4(k-99) & \text{for } 100 < k < 300 \text{ min} \\ -1390 & \text{for } k >= 300 \text{ min} \end{cases}$$

For sake of completeness, we assumed a time varying disturbance of 1 unit magnitude. Therefore, we need a threshold to avoid missed or false alarms. Thus by taking $\beta = 1.48$, $\mu = 0.01$ and $\eta_M = 1$, we have $\rho \approx 1.5$. The fault is induced at the 100th minute of system operation. After the fault is initiated, the norm of the residual tends to increase as observed in Fig. 9. Therefore, the fault is detected when the residual exceeds the threshold. Subsequently, the OLAD $\hat{h}_o(k) = \hat{\theta}(k)\varphi(k)$ is initiated to learn online the unknown fault dynamics. Moreover, the OLAD parameter is tuned online using (9) with $\alpha = 0.61$ and $\gamma = 0.001$. Although, the fault begins at 100 minutes, the fault tends to grow and has a sudden increase in the magnitude, which is similar to a step fault. Therefore, we see that the magnitude of the fault changes to a large value, which increases the residual to a large value as seen at around 300 minutes in Fig. 9. However, as the OLAD continues to learn the fault online, eventually the residual converges to zero as seen in the figure.

Next, the online learning of the fault dynamics by the OLAD is given in Fig. 10 and it is found to be satisfactory.

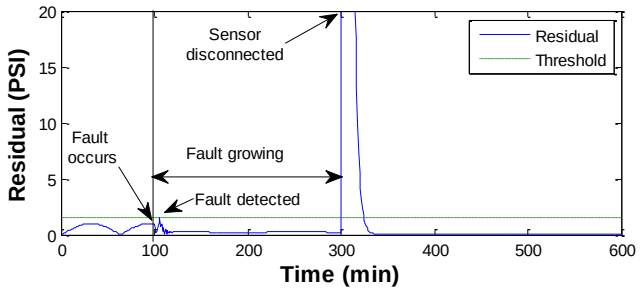

Fig. 9: Residual and the FD threshold- Output sensor fault.

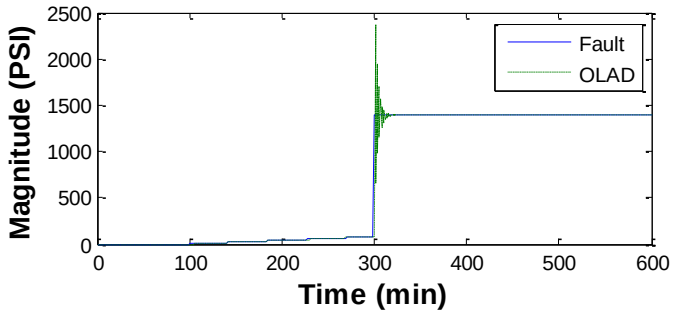

Fig. 10: Evolution of the pressure sensor fault and the OLAD learning.

Till now, we presented two examples in simulation to verify the proposed scheme. However, in the next section, we verify the proposed FD scheme on an axial piston pump test bed. Additionally, the two faults, i.e., piston wear and pressure sensor faults are induced through accelerated testing as detailed below.

VII. Experimental Results

The performance of the proposed FDP scheme is evaluated on a pump test bed. In addition, the two faults assumed in the simulation are used in the experimental study. The piston wear fault was induced by creating cavitation in the axial piston pump test stand, which shown in Fig. 11. In addition, the sensor fault was due to the loosing wiring. In the test stand shown, we have a 10.5cc variable displacement axial piston pump with nine pistons. On the test stand, the inlet, outlet, and case drain pressures were recorded continuously at 1 kHz using NI cDAQ 9172 hardware. Additionally, the case drain flow, outlet flow, reservoir temperature, case drain temperature, and pump temperature were also recorded.

The estimator model derived in (22) is used again for detecting faults in the pump. Moreover, from the model given in (22), we could see that only the output pressure is measurable. Therefore, we use the measured outlet pressure for detecting faults in the pump. Before using the data, due to the measurement noise, therefore, to attenuate them, we use a 10^{th} order band-pass pass Butterworth filter with a cut-off frequency of 250 Hz and 300Hz. A snapshot of the raw data and the filtered data for the outlet pressure signal is shown in Figs. 12 and 13, respectively. As seen in Fig. 13, the raw data is filtered using the above defined filter and averaged over a one second fixed time window. Subsequently, the filtered data was used for the verification of the FDP scheme.

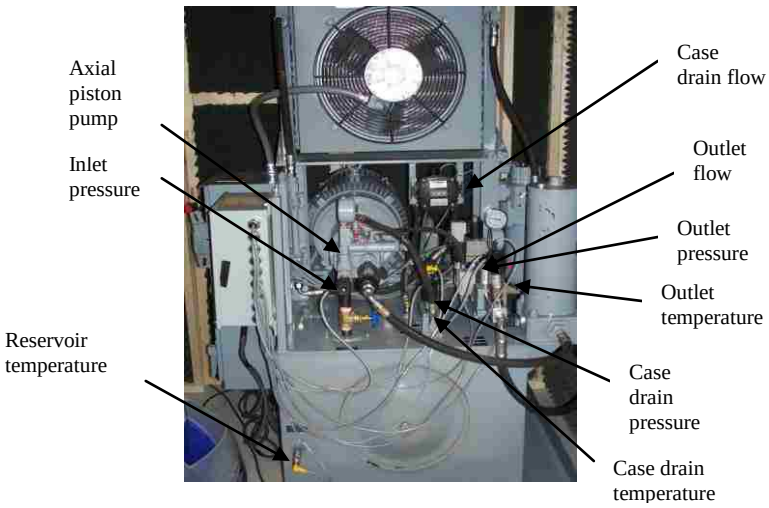

Fig. 11: Picture of the axial piston pump test bed.

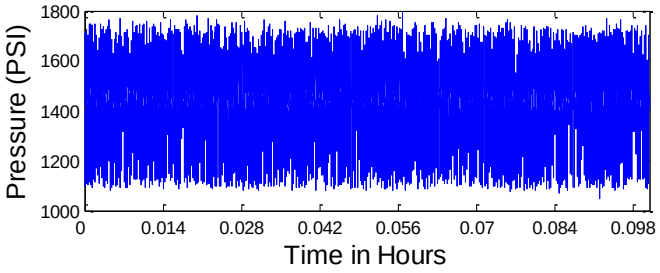

Fig. 12: Raw outlet pressure signal.

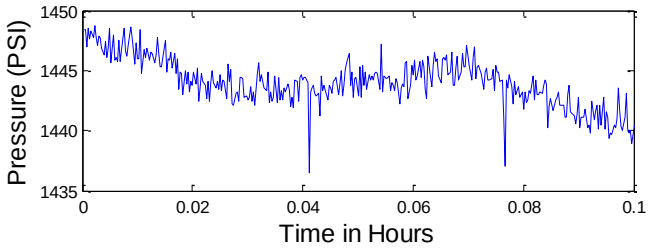

Fig. 13: Processed outlet pressure signal.

Therefore, the FD estimator in (23) is used for monitoring and detecting fault in the pump test bed. The residual generated by comparing the experimental outlet pressure with

that of the estimated outlet pressure from the FD estimator is shown in Fig. 14. In this case, the threshold is obtained by taking $\beta = 1.1$, $\mu = 0.01$ and $\eta_M \approx 25$, we have $\rho \approx 28$. As seen in the figure, the residual remains bounded for the healthy system operation. However, as the fault occurs due to the accelerated testing, the residual tends to increase and thus exceeds the threshold. Subsequently, the fault is detected and the OLAD and robust term are initiated.

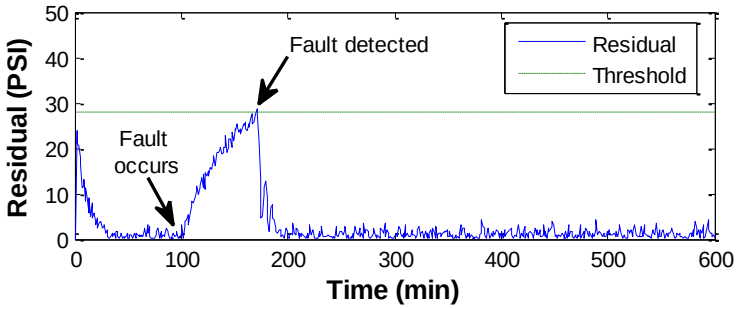

Fig. 14: Residual and the FD threshold- Piston wear fault (experimental results).

Moreover, the OLAD is tuned online using (9) with $\alpha = 0.2$ and $\gamma = 0.03$. From Fig. 15, we could see the satisfactory estimation of the fault magnitude by the OLAD. It is noted that the fluctuations in the magnitude of the OLAD response were reduced to demonstrate the learning. Subsequently, using the online estimation of the fault magnitude, the TTF prediction is determined as shown in Fig. 16. Since the initial online estimation of the fault magnitude was not accurate and also due the random selection in the gains, the TTF prediction was not accurate. However, as the learning improved and approached the actual failure, the TTF prediction was satisfactory. Therefore, in Fig. 16, the TTF prediction is shown only for the last few minutes before the failure.

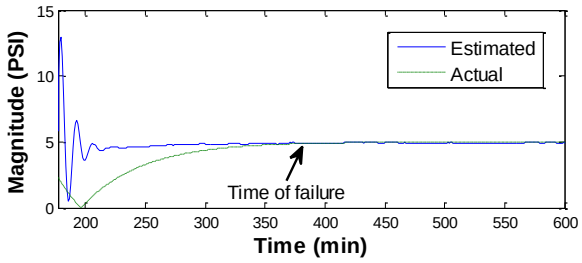

Fig. 15: Online estimation of the piston wear fault magnitude (experimental results).

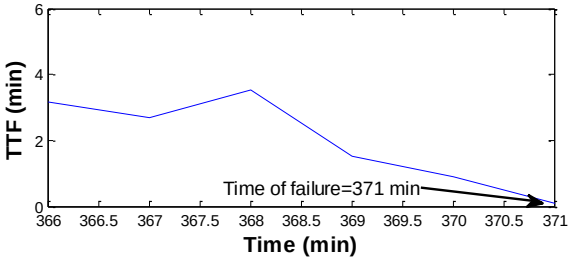

Fig. 16: The TTF determination due to the piston wear fault.

In the next case, we assume a pressure sensor fault on the axial piston pump. The norm of the residual used for detecting the fault is shown in Fig. 17. Here again, the residual shown is the difference in the estimated and the experimental outlet pressure. Also, the threshold is obtained by taking $\beta = 1.11$, $\mu = 0.01$ and $\eta_M = 16$, we have a constant FD threshold of $\rho \approx 18$. From the figure, the fault occurs at the 100^{th} min of operation, where, the sensor fault is due to the loosening of the connect pin, and has a unique behavior. The fault grows with time and at around 300 minutes; the connecting pin is detached completely off the sensor. Therefore, we see a sharp increase in the residual as seen in Fig. 17. Although, the OLAD and the robust term were activated the first time the residual

exceeded the threshold, however, the residual converges to zero only after the second spike as in the figure.

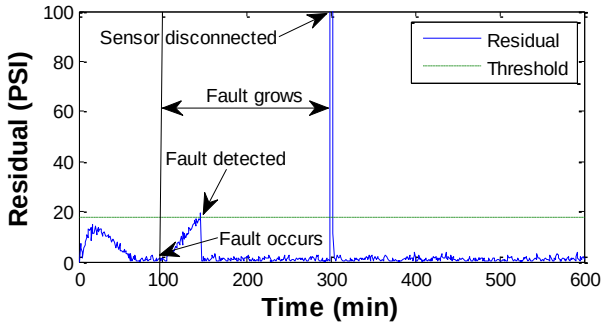

Fig. 17: Residual and the FD threshold- Pressure sensor fault (experimental results).

Moreover, the learning of the fault by the OLAD is shown in Fig. 18, and is found to be highly satisfactory. Similar to the previous case, the OLAD is tuned online using (9) with $\alpha = 0.9$ and $\gamma = 1 \times 10^{-9}$.

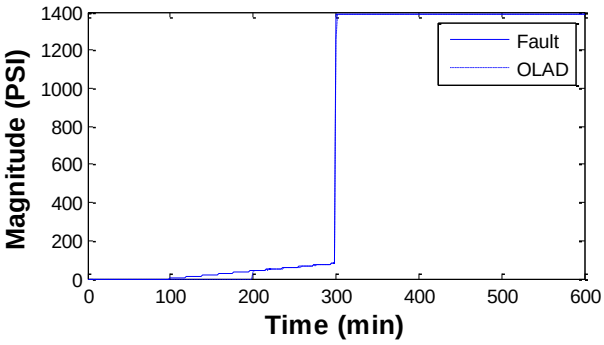

Fig. 18: Evolution of the pressure sensor fault and the OLAD learning (experimental results).

Therefore, from the simulation and experimental verification, one could see that the proposed scheme detects and learns both the incipient and abrupt faults online without any

apriori offline training. Moreover, the experimental results show the feasibility in the implementing the proposed scheme on an experimental hardware. Therefore, the proposed FDP scheme renders a stable performance both in simulation and in practice.

VIII. Conclusions

In this paper, an online fault detection scheme using a new online approximator using AIS is proposed for a class of nonaffine nonlinear discrete-time systems. An asymptotic estimator is designed to monitor and detect faults in the given system. The scheme could detect both the abrupt and incipient faults. Mathematical asymptotic stability results of the proposed fault detection scheme are derived. Moreover, initially two simulation examples were presented to demonstrate the asymptotic stability and the online learning capabilities of the proposed AIS based FD estimator. Later, the FD scheme was verified on an axial-piston pump test bed. From the experimental results, the FD scheme is found to successful in detecting and learning online both the incipient and abrupt faults. Therefore, the proposed FD scheme renders asymptotic performance both in simulation and in experiment.

Appendix

Proof of Lemma 1: Consider (14) and solving it would render

$$e(k) = A_0^k e(0) + \sum_{j=0}^{k} A_0^{k-j} \left[\tilde{\theta}^T(j)\varphi(j) + \frac{\tilde{\theta}^T(j)B_1 - C_1}{B_1^T \hat{\theta}(j)\hat{\theta}^T(j)B_1 + c_c} + \varepsilon(j) - \frac{\left(\theta^T B_1 - C_1\right)}{B_1^T \hat{\theta}(j)\hat{\theta}^T(j)B_1 + c_c} \right]$$

The above equation is rewritten as

$$\sum_{j=0}^{k} A_0^{k-j}\varepsilon(j) = e(k) - A_0^k e(0) - \sum_{j=0}^{k} A_0^{k-j}\tilde{\theta}^T(j)\varphi(j)$$

$$-\sum_{j=0}^{k} A_0^{k-j}\frac{\left(\tilde{\theta}^T(j)B_1 - C_1\right)}{B_1^T\hat{\theta}(j)\hat{\theta}^T(j)B_1 + c_c} + \sum_{j=0}^{k} A_0^{k-j}\frac{\left(\theta^T B_1 - C_1\right)}{B_1^T\hat{\theta}(j)\hat{\theta}^T(j)B_1 + c_c}\Bigg]$$

Take the Frobenius norm to render

$$\left\|\sum_{j=0}^{k} A_0^{k-j}\varepsilon(j)\right\| \le \left\|e(k)\right\| + \left\|A_0^k e(0)\right\| + \left\|\sum_{j=0}^{k} A_0^{k-j}\tilde{\theta}^T(j)\varphi(j)\right\|$$

$$+\left\|\sum_{j=0}^{k} A_0^{k-j}\frac{\tilde{\theta}^T(j)B_1}{B_1^T\hat{\theta}(j)\hat{\theta}^T(j)B_1 + c_c}\right\| + \left\|\sum_{j=0}^{k} A_0^{k-j}\frac{\theta^T B_1}{B_1^T\hat{\theta}(j)\hat{\theta}^T(j)B_1 + c_c}\right\|$$

The summation term in the above equation could be solved using [33] as $\left\|\sum_{j=0}^{k} A_0^{k-j}\tilde{\theta}^T(j)\varphi(j)\right\| \le \frac{\varphi_{\max}\left\|\tilde{\theta}(k)\right\|}{(1-A_{0_{\max}})}$, where $A_{0_{\max}}$ is the maximum singular value of A_0. Additionally, $A_{0_{\max}} < (1 - A_{0_{\max}})$ if $A_{0_{\max}} \le \lambda_s$, where λ_s is a positive constant, therefore, we have $\frac{\varphi_{\max}\left\|\tilde{\theta}(k)\right\|}{(1-A_{0_{\max}})} \le \frac{\varphi_{\max}\left\|\tilde{\theta}(k)\right\|}{A_{0_{\max}}}$. Similar result could be derived for the other terms for instance, $\frac{\tilde{\theta}^T(k)B_1}{B_1^T\hat{\theta}(k)\hat{\theta}^T(k)B_1 + c_c} \le \tilde{\theta}^T(k)B_1$, $\frac{\theta^T B_1}{B_1^T\hat{\theta}(k)\hat{\theta}^T(k)B_1 + c_c} \le \theta^T B_1$. The above equation could be rewritten as

$$\frac{\left\|\varepsilon(k)\right\|}{A_{0_{\max}}} \le \left\|e(k)\right\| + \left\|A_0^k e(0)\right\| + \frac{\varphi_{\max}\left\|\tilde{\theta}(k)\right\|}{A_{0_{\max}}} + \frac{B_{1_{\max}}\left\|\tilde{\theta}(k)\right\|}{A_{0_{\max}}} + \frac{B_{1_{\max}}\left\|\theta\right\|}{A_{0_{\max}}}$$

Squaring both side and factoring $A_{0_{\max}}^2$ would give us

$$\left\|\varepsilon(k)\right\|^2 \le A_{0_{\max}}^2 \left(\left\|e(k)\right\| + \left\|A_0^k e(0)\right\| + \frac{\varphi_{\max}\left\|\tilde{\theta}(k)\right\|}{A_{0_{\max}}} + \frac{B_{1_{\max}}\left\|\tilde{\theta}(k)\right\|}{A_{0_{\max}}} + \frac{B_{1_{\max}}\left\|\theta\right\|}{A_{0_{\max}}} \right)^2$$

Take $b_0 = \left\|A_0^k e(0)\right\| + \frac{B_{1_{\max}}\left\|\theta\right\|}{A_{0_{\max}}}$, $b_1 = \varphi_{\max} + B_{1_{\max}}$, then the above equation could be rewritten as

$$\left\|\varepsilon(k)\right\|^2 \le A_{0_{\max}}^2 \left(\left\|e(k)\right\| + b_0 + \frac{b_1\left\|\tilde{\theta}(k)\right\|}{A_{0_{\max}}} \right)^2$$

Expand the term on the right hand side of the above equation, we have

$$\left\|\varepsilon(k)\right\|^2 \le A_{0_{\max}}^2 \left[b_0^2 + \left\|e(k)\right\|^2 + \frac{b_1^2\left\|\tilde{\theta}(k)\right\|^2}{A_{0_{\max}}^2} + \underbrace{2\left\|e(k)\right\| b_0}_{1} + \underbrace{\frac{2b_0 b_1\left\|\tilde{\theta}(k)\right\|}{A_{0_{\max}}}}_{1} + \frac{2b_1\left\|e(k)\right\|\left\|\tilde{\theta}(k)\right\|}{A_{0_{\max}}} \right]$$

Apply Cauchy-Schwarz inequality to terms numbered as 1 in the above equation, and combine similar terms, we would have the following equation

$$\left\|\varepsilon(k)\right\|^2 \le 3A_{0_{\max}}^2 b_0^2 + 2A_{0_{\max}}^2\left\|e(k)\right\|^2 + 2b_1^2\left\|\tilde{w}(k)\right\|^2 + 2A_{0_{\max}} b_1\left\|e(k)\right\|\left\|\tilde{\theta}(k)\right\|$$

Taking $\overline{d}_0 = 3A_{0_{\max}}^2 b_0^2$, $\overline{d}_1 = 2A_{0_{\max}}^2$, $\overline{d}_2 = 2b_1^2$, and $\overline{d}_3 = 2A_{0_{\max}} b_1$, would reveal equation (15).

Proof of Theorem 2: Consider the Lyapunov function candidate

$$V = e^T(k)e(k) + \frac{1}{\alpha} tr[\tilde{\theta}^T(k)\tilde{\theta}(k)]$$

whose first difference is given by

$$\Delta V = \underbrace{e^T(k+1)e(k+1) - e^T(k)e(k)}_{\Delta V_1} \underbrace{+ \frac{1}{\alpha} tr[\tilde{\theta}^T(k+1)\tilde{\theta}(k+1) - \tilde{\theta}^T(k)\tilde{\theta}(k)]}_{\Delta V_2} \qquad \text{(A.1)}$$

Substitute (14) in ΔV_1 of (A.1), therefore, we have

$$\Delta V_1 = \left(A_0 e(k) + \Psi_2(k) + \Psi_1(k) + \varepsilon(k) - \frac{(\theta^T B_1 - C_1)}{B_1^T\hat{\theta}(k)\hat{\theta}^T(k)B_1 + c_c}\right)^T \times$$

$$(A_0 e(k) + \Psi_2(k) + \Psi_1(k) + \varepsilon(k) - \frac{(\theta^T B_1 - C_1)}{B_1^T \hat{\theta}(k)\hat{\theta}^T(k) B_1 + c_c}) - e^T(k)e(k)$$

Perform some mathematical manipulations to render

$$\Delta V_1 = e^T(k) A_0^T A_0 e(k) + 2e^T(k) A_0^T \Psi_1(k) + 2e^T(k) A_0^T \Psi_2(k) + 2e^T(k) A_0^T \varepsilon(k) - 2\frac{e^T(k) A_0^T (\theta^T B_1 - C_1)}{B_1^T \hat{\theta}(k)\hat{\theta}^T(k) B_1 + c_c} + \Psi_1^T(k)\Psi_1(k)$$

$$-2\frac{\Psi_1^T(k)(\theta^T B_1 - C_1)}{B_1^T \hat{\theta}(k)\hat{\theta}^T(k) B_1 + c_c} + 2\Psi_1{}^T(k)\Psi_2(k) + 2\Psi_1{}^T(k)\varepsilon(k) + \Psi_2^T(k)\Psi_2(k) - \frac{2\Psi_2^T(k)(\theta^T B_1 - C_1)}{B_1^T \hat{\theta}(k)\hat{\theta}^T(k) B_1 + c_c}$$

$$-\frac{2\varepsilon^T(k)(\theta^T B_1 - C_1)}{B_1^T \hat{\theta}(k)\hat{\theta}^T(k) B_1 + c_c} + \frac{(\theta^T B_1 - C_1)^T(\theta^T B_1 - C_1)}{\left(B_1^T \hat{\theta}(k)\hat{\theta}^T(k) B_1 + c_c\right)^2} + 2\Psi_2^T(k)\varepsilon(k) + \varepsilon^T(k)\varepsilon(k) - e^T(k)e(k) \qquad \text{(A.2)}$$

Next substitute the parameter update law (10) in ΔV_2 of (A.1), to obtain

$$\Delta V_2 = \frac{1}{\alpha} tr\left\{\left[\left(I - \gamma\left\|I - \alpha\varphi(k)\varphi^T(k)\right\| I\right)\tilde{\theta}(k) - \alpha\varphi(x(k))e^T(k+1)\right.\right.$$

$$\left.+\gamma\left\|I - \alpha\varphi(k)\varphi^T(k)\right\|\theta)\right]^T \times\left[\left(I - \gamma\left\|I - \alpha\varphi(k)\varphi^T(k)\right\| I\right)\tilde{\theta}(k)\right.$$

$$\left.\left.-\alpha\varphi(x(k))e^T(k+1) + \gamma\left\|I - \alpha\varphi(k)\varphi^T(k)\right\|\theta)\right] - \tilde{\theta}^T(k)\tilde{\theta}(k)\right\}$$

After some mathematical manipulation, the above equation could be rewritten as

$$\Delta V_2 = \frac{1}{\alpha} tr\{-2\gamma\left\|I - \alpha\varphi(k)\varphi^T(k)\right\|\tilde{\theta}^T(k)\tilde{\theta}(k) + \gamma^2\left\|I - \alpha\varphi(k)\varphi^T(k)\right\|^2\tilde{\theta}^T(k)\tilde{\theta}(k)$$

$$\underbrace{-2\alpha\tilde{\theta}^T(k)\left(I - \gamma\left\|I - \alpha\varphi(k)\varphi^T(k)\right\| I\right)\varphi(k)e^T(k+1)}_{1} \underbrace{+2\gamma\left\|I - \alpha\varphi(k)\varphi^T(k)\right\|\tilde{\theta}^T(k)\left(I - \gamma\left\|I - \alpha\varphi(k)\varphi^T(k)\right\| I\right)\theta}_{1}$$

$$+\alpha^2 e(k+1)\varphi^T(x(k))\varphi(x(k))e^T(k+1) \underbrace{-2\alpha\gamma\left\|I - \alpha\varphi(k)\varphi^T(k)\right\| r(k+1)\varphi^T(x(k))\theta}_{1} + \gamma^2\left\|I - \alpha\varphi(k)\varphi^T(k)\right\|^2\theta^T\theta\}$$

Apply Cauchy-Schwarz inequality ($2ab \le a^2 + b^2$) to terms numbered as 1 in the above equation would reveal

$$\Delta V_2 \le \frac{1}{\alpha} tr\{-2\gamma \left\| I - \alpha\varphi(k)\varphi^T(k) \right\| \tilde{\theta}^T(k)\tilde{\theta}(k) + \gamma^2 \left\| I - \alpha\varphi(k)\varphi^T(k) \right\|^2 \tilde{\theta}^T(k)\tilde{\theta}(k) + 2\delta\alpha\tilde{\theta}^T(k)\left(I - \gamma \left\| I - \alpha\varphi(k)\varphi^T(k) \right\| I \right).$$

$$\left(I - \gamma \left\| I - \alpha\varphi(k)\varphi^T(k) \right\| I \right)\tilde{\theta}(k) + (2 + 1/\delta)\gamma^2 \left\| I - \alpha\varphi(k)\varphi^T(k) \right\|^2 \theta^T\theta + \underbrace{(2 + 1/\delta)\alpha^2 e(k+1)\varphi^T(x(k))\varphi(x(k))e^T(k+1)}_{1} \Bigg\}$$

where $\delta > 0$ is a constant. Next, substitute the residual dynamics (14) to the term numbered as 1 in the above equation and apply the Cauchy-Schwarz inequality $((a_1 + a_2 + ... + a_n)^T(a_1 + a_2 + ... + a_n) \le n(a_1^T a_1 + a_2^T a_2 + .. + a_n^T a_n))$ to the same term and perform some mathematical manipulation to render the following equation

$$\Delta V_2 \le \frac{1}{\alpha} tr\Big[-2(2+\delta)\gamma \left\| I - \alpha\varphi(k)\varphi^T(k) \right\| \tilde{\theta}^T(k)\tilde{\theta}(k)$$

$$+(1 + 2\delta)\gamma^2 \left\| I - \alpha\varphi(k)\varphi^T(k) \right\|^2 \tilde{\theta}^T(k)\tilde{\theta}(k) + 2\delta\tilde{\theta}^T(k)\tilde{\theta}(k) \Big]$$

$$+5(2 + 1/\delta)\alpha\varphi^T\varphi e^T(k)A_0^T A_0 e(k) + 5(2 + 1/\delta)\alpha\varphi^T\varphi\Psi_1^T(k)\Psi_1(k)$$

$$+5(2 + 1/\delta)\alpha\varphi^T\varphi\varepsilon^T(k)\varepsilon(k) + 5(2 + 1/\delta)\alpha\varphi^T\varphi \frac{(\theta^T B_1 - C_1)^T(\theta^T B_1 - C_1)}{\left(B_1^T\hat{\theta}(k)\hat{\theta}^T(k)B_1 + c_C \right)^2} + 5(2 + 1/\delta)\alpha\varphi^T\varphi\Psi_2^T(k)\Psi_2(k)$$

$$+(2 + 1/\delta)\frac{\gamma^2}{\alpha} \left\| I - \alpha\varphi(k)\varphi^T(k) \right\|^2 tr\left(\theta^T\theta \right) \qquad \text{(A.3)}$$

Next, the overall first difference of the Lyapunov function candidate, $\Delta V = \Delta V_1 + \Delta V_2$, can be obtained from (A.2) and (A.3) as

$$\Delta V \le \Big[e^T(k) k_v^T k_v e(k) + \Psi_1^T(k)\Psi_1(k) + \varepsilon^T(k)\varepsilon(k) + \underbrace{\Psi_2^T(k)\Psi_2(k)}_{1}$$

$$+ \underbrace{\frac{(\theta^T B_1 - C_1)^T (\theta^T B_1 - C_1)}{\left(B_1^T \hat{\theta}(k)\hat{\theta}^T(k) B_1 + c_C\right)^2}}_{2} \Big] - \frac{1}{5} e^T(k) e(k) + \frac{1}{\alpha} tr\Big[-2(2+\delta)\gamma \left\| I - \alpha\varphi(k)\varphi^T(k) \right\| \tilde{\theta}^T(k)\tilde{\theta}(k)$$

$$+ (1+2\delta)\gamma^2 \left\| I - \alpha\varphi(k)\varphi^T(k) \right\|^2 \tilde{\theta}^T(k)\tilde{\theta}(k) + 2\delta\tilde{\theta}^T(k)\tilde{\theta}(k) \Big] + 5(2+1/\delta)\alpha\varphi^T\varphi e^T(k) A_0^T A_0 e(k)$$

$$+ 5(2+1/\delta)\alpha\varphi^T\varphi\varepsilon^T(k)\varepsilon(k) + \underbrace{5(2+1/\delta)\alpha\varphi^T\varphi \frac{(\theta^T B_1 - C_1)^T (\theta^T B_1 - C_1)}{\left(B_1^T \hat{\theta}(k)\hat{\theta}^T(k) B_1 + c_C\right)^2}}_{2} + 5(2+1/\delta)\alpha\varphi^T\varphi\Psi_1^T(k)\Psi_1(k)$$

$$+ \underbrace{5(2+1/\delta)\alpha\varphi^T\varphi\Psi_2^T(k)\Psi_2(k)}_{1} + (2+1/\delta)\frac{\gamma^2}{\alpha} \left\| I - \alpha\varphi(k)\varphi^T(k) \right\|^2 tr\left(\theta^T\theta\right) \qquad \text{(A.4)}$$

Consider only terms numbered as 1 in (A.4), we have the following equation

$$\left(1 + 5(2+1/\delta)\alpha\varphi^T\varphi\right)\Psi_2^T(k)\Psi_2(k) = \left(1 + 5(2+1/\delta)\alpha\varphi^T\varphi\right)\frac{\left(\tilde{\theta}^T(k)B_1 - C_1\right)^T\left(\tilde{\theta}^T(k)B_1 - C_1\right)}{\left(B_1^T\hat{\theta}(k)\hat{\theta}^T(k)B_1 + c_C\right)^2}$$

$$\le \left(1 + 5\alpha(2+1/\delta)\varphi^T\varphi\right)\left(\tilde{\theta}^T(k)B_1 - C_1\right)^T\left(\tilde{\theta}^T(k)B_1 - C_1\right)$$

$$\le 2\left(1 + 5\alpha(2+1/\delta)\varphi^T\varphi\right)\left[B_1^T\tilde{\theta}(k)\,\tilde{\theta}^T(k)B_1 + C_1^T C_1\right] \qquad \text{(A.5)}$$

Next, consider only terms numbered as 2 in (A.4), we have the following equation

$$\left(1 + 5\alpha(2+1/\delta)\varphi^T\varphi\right)\frac{(\theta^T B_1 - C_1)^T(\theta^T B_1 - C_1)}{\left(B_1^T\hat{\theta}(k)\hat{\theta}^T(k)B_1 + c_C\right)^2} \le$$

$$\left(1 + 5\alpha(2+1/\delta)\varphi^T\varphi\right)\left[B_1^T\theta\theta^T B_1 - 2C_1^T\theta^T B_1 + C_1^T C_1\right] \qquad \text{(A.6)}$$

Consider Lemma 1 and multiply $\left(1 + 5\alpha(2+1/\delta)\varphi^T\varphi\right)$ throughout (14) and using it along with

(A.5) and (A.6) in (A.4), would render the following equation

$$\Delta V \le \left[e^T(k) A_0^T A_0 e(k) + \Psi_1^T(k)\Psi_1(k) \right] - \frac{1}{5} e^T(k) e(k)$$

$$+ \frac{1}{\alpha} tr \left[-2(2+\delta)\gamma \left\| I - \alpha\varphi(k)\varphi^T(k) \right\| \tilde{\theta}^T(k)\tilde{\theta}(k) \right.$$

$$\left. + (1+2\delta)\gamma^2 \left\| I - \alpha\varphi(k)\varphi^T(k) \right\|^2 \tilde{\theta}^T(k)\tilde{\theta}(k) + 2\delta\tilde{\theta}^T(k)\tilde{\theta}(k) \right]$$

$$+ \left(1 + 5\alpha(2+1/\delta)\varphi^T\varphi \right) \varphi^T\varphi e^T(k) A_0^T A_0 e(k) + \left(1 + 5\alpha(2+1/\delta)\varphi^T\varphi \right) \Psi_1^T(k)\Psi_1(k)$$

$$+ (2+1/\delta)\frac{\gamma^2}{\alpha} \left\| I - \alpha\varphi(k)\varphi^T(k) \right\|^2 tr\left(\theta^T\theta\right) + 2\left(1 + 5\alpha(2+1/\delta)\varphi^T\varphi \right) \left[B_1^T \tilde{\theta}(k)\tilde{\theta}^T(k) B_1 + C_1^T C_1 \right]$$

$$+ \left(1 + 5\alpha(2+1/\delta)\varphi^T\varphi \right) \left[B_1^T \theta\theta^T B_1 - 2C_1^T \theta^T B_1 + C_1^T C_1 \right] + d_0 + d_1 \left\| e(k) \right\|^2 + d_2 \left\| \tilde{\theta}(k) \right\|^2 + \underbrace{d_3 \left\| e(k) \right\| \left\| \tilde{\theta}(k) \right\|}_{1} \quad \text{(A.7)}$$

where $d_0 = \left(1 + 5\alpha(2+1/\delta)\varphi^T\varphi \right) \overline{d}_0$, $d_1 = \left(1 + 5\alpha(2+1/\delta)\varphi^T\varphi \right) \overline{d}_1$, $d_2 = \left(1 + 5\alpha(2+1/\delta)\varphi^T\varphi \right) \overline{d}_2$, and $d_3 = \left(1 + 5\alpha(2+1/\delta)\varphi^T\varphi \right) \overline{d}_3$. Apply Cauchy-Schwarz inequality ($ab \le a^2 + b^2$) to the term numbered as 1 in (A.7), then, take Frobenius norm in the above equation, therefore, the first difference of the Lyapunov function is given by

$$\Delta V \le -\delta_{1m} \left\| e(k) \right\|^2 - \delta_{2m} \left\| \tilde{\theta}(k) \right\|^2$$

$$+ 2\left(1 + 5\alpha(2+1/\delta)\varphi^T\varphi \right) C_{1_{\max}}^2 + \left(1 + 5\alpha(2+1/\delta)\varphi^T\varphi \right) \left(B_{1_{\max}}^2 \theta_{\max}^2 - 2C_{1_{\min}} \theta_{\min} B_{1_{\min}} + C_{1_{\max}}^2 \right) + d_0$$

$$+ (2+1/\delta)\frac{\gamma^2}{\alpha} \left\| I - \alpha\varphi(k)\varphi^T(k) \right\|^2 tr\left(\theta^T\theta\right) \quad \text{(A.8)}$$

where $\delta_{1m} = \left(\frac{1}{5} - A_{0_{\max}}^2 - 5\alpha\varphi_{\max}^2 (2+1/\delta) A_{0_{\max}}^2 - \frac{3d_1}{2} \right)$ and

$\delta_{2m} = \left(\frac{2(2+\delta)\gamma}{\alpha} \left\| I - \alpha\varphi(k)\varphi^T(k) \right\| - \frac{(1+2\delta)\gamma^2}{\alpha} \left\| I - \alpha\varphi(k)\varphi^T(k) \right\|^2 \right.$

$\left. -\varphi_{\max}^2 - \frac{2\delta}{\alpha} - 5\alpha(2+1/\delta)\varphi_{\max}^4 - 2\left(1 + 5\alpha(2+1/\delta)\varphi_{\max}^2\right) B_{1_{\max}}^2 - \frac{3d_2}{2} \right)$. Next, take $B_{1_{\min}} =$

$\frac{\left(\left(d_0 + \frac{(2+1/\delta)\gamma^2}{\alpha} \left\| I - \alpha\varphi(k)\varphi^T(k) \right\|^2 \theta_{\max}^2 \right) / \left(1 + 5\alpha(2+1/\delta) \left\| \varphi(k) \right\|^2 \right) \right)}{2C_{1_{\min}} \theta_{\min}} + \frac{\left(3C_{1_{\max}}^2 + \theta_{\max}^2 B_{1_{\max}}^2 \right)}{2C_{1_{\min}} \theta_{\min}}$,

$B_{1_{\max}} = \frac{\delta}{\sqrt{2\left(1 + 5\alpha(2+1/\delta)\varphi_{\max}^2\right)}}$, also define $C_r = \frac{\alpha}{(2+1/\delta)} \left(\frac{2\delta}{\alpha} + \varphi_{\max}^2 + 5\alpha(2+1/\delta)\varphi_{\max}^4 + \frac{3d_2}{2} \right.$

$\left. +2\left(1 + 5\alpha(2+1/\delta)\varphi_{\max}^2\right) B_{1_{\max}}^2 \right)$

then, equation (A.8) could be rewritten as

$$\Delta V \le -\delta_{1m} \left\| e(k) \right\|^2 - \delta_{2m} \left\| \tilde{\theta}(k) \right\|^2 \qquad \text{(A.9)}$$

As long as the gains in (16)-(18) are satisfied, therefore, $\Delta V \le 0$ in (A.9), which shows stability in the sense of Lyapunov. Hence $e(k)$ and $\tilde{\theta}(k)$ are bounded, provided if $e(k_0)$ and $\tilde{\theta}(k_0)$ are bounded in the compact set *S*. Hence $e(k)$ and $\tilde{\theta}(k)$ converges to zero asymptotically. □

References

[1] P. M. Frank and L. Keller,"Fault diagnosis in dynamic systems using analytical and knowledge-based redundancy – A survey and some new results," *Automatica*, vol. 26, pp. 459-474, 1990.

[2] J. Chen and R. J. Patton, *Robust Model-based Fault Diagnosis for Dynamic Systems*, Kluwer Academic publishers, MA, USA, 1999.

[3] C. Edwards, S. K. Spurgeon, and R. J. Patton,"Sliding mode observers for fault detection and isolation," *Automatica*, vol. 36, pp. 541-553, 2000.

[4] M. Massoumnia, G. C. Verghese, and A. S. Willsky,"Failure detection and identification," *IEEE Trans. on Automatic Control*, vol. 34, no. 3, pp. 316-322, 1989.

[5] M. A. Demetriou and M. M. Polycarpou,"Incipient fault diagnosis of dynamical systems using online approximators," *IEEE Trans. on Automatic Control*, vol. 43, no. 11, pp. 1612-1617, 1998.

[6] X. G. Yan and C. Edwards,"Nonlinear robust fault reconstruction and estimation using a sliding mode observer," *Automatica*, vol. 43, no. 9, pp. 1605-1614, 2007.

[7] C. De Persis and A. Isidori,"A geometric approach to nonlinear fault detection and isolation", *IEEE Trans. on Automatic Control*, vol. 46, no. 6, pp. 853 – 865, 2001.

[8] S. Narasimhan, P. Vachhani, and R. Rengaswamy,"Nonlinear residual feedback observer for fault diagnosis in nonlinear systems," *Automatica*, vol. 44, no. 9, pp.2222-2229, 2008.

[9] H. A. Talebi, S. Tafazoli, and K. Khorasani,"A recurrent neural-network-based sensor and actuator fault detection and isolation for nonlinear systems with application to the satellite's attitude control subsystem," *IEEE Trans. on Neural Networks*, vol. 20, no.1, pp. 45- 60 , 2009.

[10] R. Isermann,"Model-based fault-detection and diagnosis–status and applications," *Annual Reviews in Control*, vol. 29, no.1, pp. 71-85, 2005.

[11] J. Luo, M. Namburu, K. Pattipati, L. Qiao, M. Kawamoto, and S, Chigusa,"Model-based prognostic techniques," *AUTOTESTCON 2003: IEEE Systems Readiness Technology Conference*, Anaheim, California, USA, pp. 330-340, 2003.

[12] J. Luo, A. Bixby, K. Pattipati, L. Qiao, M. Kawamoto, and S. Chigusa,"An interacting multiple model approach to model-based prognostics," *IEEE International Conference on Systems, Man and Cybernetics*, Washington, D.C., USA, vol. 1, pp. 189-194, 2003.

[13] E. Phelps, P. Willett, and T. Kirubarajan,"Useful lifetime tracking via the IMM," *Components and System Diagnostics, Prognostics, and Health Management II, Proc. of SPIE*, vol. 4733, pp. 145-156, 2002.

[14] M. J. Roemer and D. M. Ghiocel,"A probabilistic approach to the diagnosis of gas turbine engine faults," *53rd Machinery Prevention Technologies (MFPT) Conference*, Virginia Beach, VA, USA, pp. 325-336, 1999.

[15] Y. Shao and K. Nezu,"Prognosis of remaining bearing life using neural networks," *Proc. of the Institution of Mechanical Engineers, Part I: Journal of Syst. and Control Engg.*, vol. 214, no. 3, pp. 217-230, 2000.

[16] F. Caccavale and L. Villani,"An adaptive observer for fault diagnosis in nonlinear discrete-time systems," *Proc. of the American Control Conference*, Boston, MA, June 30 -July 2, 2004.

[17] F. Cacccavale, F. Pierri, and L. Villani,"Adaptive observer for fault diagnosis in nonlinear discrete-time systems," *ASME Journal of Dynamic Systems, Measurement, and Control*, vol. 130, no. 2, pp. 1-9, 2008.

[18] B. T. Thumati and S. Jagannathan,"An online approximator-based fault detection framework for nonlinear discrete-time systems," *Proc. of 46th IEEE Conference on Decision and Control (CDC)*, New Orleans, LA, USA, pp. 2608-2613, 2007.

[19] M. L. McIntyre, W. E. Dixon, D. M. Dawson, and I. D. Walker,"Fault identification for robot manipulators," *IEEE Trans. on Robotics and Automation*, vol. 21, no. 5, pp. 1028-1034, 2005.

[20] D. Dasgupta, *Artificial Immune Systems and Their Applications*, Springer, NY, 1998.

[21] J. Timmis,"Artifical immune systems-today and tomorrow," *Nat. Comput.*, vol. 6, pp.1-19, 2007.

[22] D. Dasgupta,"Artificial neural networks and artificial immune systems: similarities and differences," *Proc. of the IEEE International Conference on Systems, Man, and Cybernetics*, Orlando, FL, USA, vol. 1, pp.873-878, 1997.

[23] D. Dasgupta,"Advances in artificial immune systems," *IEEE Computational Intelligence Magazine*, vol. 1, no. 4, pp. 40-49, 2006.

[24] C. C. Luh and W. C. Cheng,"Non-linear system identification using an artificial immune system," *Proc. Inst. Mech. Engrs.*, vol. 215, part I, pp. 569- 585, 2001.

[25] J. Gomez, F. Gonzalez, and D. Dasgupta,"An immuno-fuzzy approach to anomaly detection," *The 12th IEEE International Conference on Fuzzy Systems (FUZZ)*, pp. 1219-1224, 2003.

[26] C. C. Luh and W. C. Cheng,"Immune model-based fault diagnosis," *Mathematics and Computers in Simulation*, vol. 67, pp. 515-539, 2005.

[27] L. Shulin, Z. Jiazhong, S. Wengang, and H. Wenhu,"Negative-selection algorithm based approach for fault diagnosis of rotary machinery," *Proc. of the American Control Conference*, Anchorage, AK, USA, pp. 3955-3960, 2002.

[28] I. Aydin, M. Karakose, and E. Akin,"Artificial immune based support vector machine algorithm for fault diagnosis of induction motors," *International Aegean Conference on Electrical Machines and Power Electronics (ACEMP)*, pp. 217-221, 2007.

[29] P. J. Costa Branco, J. A. Dente, and R. Vilela Mendes,"Using immunology principles for fault detection," *IEEE Trans. on Industrial Electronics*, vol. 50, no. 2, pp.362-373, 2003.

[30] R. R. Sumar, A. A. R. Coelho, and L. dos S. Coelho,"Use of an artificial immune network optimization approach to tune the parameters of a discrete variable structure controller," *Expert Systems with Applications*, vol. 36, pp. 5009–5015, 2009.

[31] A. R. Barrron,"Universal approximation bounds for superposition of a sigmoidal function," *IEEE Trans. on Information Theory*, vol. 39, no. 3, pp. 930-945, 1993.

[32] J. Zhang and A. J. Morris,"On-line process fault diagnosis using fuzzy neural networks," *Intelligent Systems Engineering*, pp. 37-47, 1994.

[33] R. G. Bartle and D. R. Sherbert, *Introduction to Real Analysis*, Wiley, NY, USA, 1982.

[34] S. Jagannathan, *Neural Network Control of Nonlinear Discrete –time Systems*, CRC publications, NY, 2006.

[35] C. M. Kwan, D. M. Dawson, and F. L. Lewis,"Robust adaptive control of robots using neural network: global tracking stability," *Proc. of the 34th conference on Decision and Control*, New Orleans, LA, pp. 1846-1851, 1995.

[36] P. M. Patre, W. MacKunis, K. Kaiser, and W. E. Dixon,"Asymptotic tracking for uncertain dynamics systems via a multilayer NN feed forward and RISE feedback control structure," *Proc. of the American Control Conference*, New York City, NY, USA, pp. 5989-5994, 2007.

[37] D. M. Dawson, Z. Qu, and S. Lim,"Re-thinking the robust control of robot manipulators," *Proc. of the Conference on Decision and Control (CDC),* Brighton, England, pp. 1043-1045, 1991.

[38] F. L. Lewis, S. Jagannathan, and A. Yesilderek, *Neural Network Control of Robotics and Nonlinear Systems*, Taylor and Francis, UK, 1999.

[39] B. T. Thumati and S. Jagannathan,"A model based fault detection and prognostic scheme for uncertain nonlinear discrete-time systems," *Proc. of 47th IEEE Conference on Decision and Control (CDC)*, Cancun, Mexico, pp. 392 - 397, 2008.

[40] Z. Li,"*Condition Monitoring of Axial Piston Pump*," MS Thesis, 2005; http://library2.usask.ca/theses/available/etd-11252005-202705 /unrestricted/EricLithesis 2005NovA.pdf.

SECTION

2. CONCLUSIONS AND FUTURE WORK

In this dissertation, online learning techniques are used to develop robust model-based fault prognostics and accommodation schemes for a class of nonlinear discrete-time systems. A novel discrete-time estimator design guaranteed fault detection and isolation. Using the estimator parameters, a stable and reliable parameter based time to failure (TTF) prediction scheme was introduced. Consequently, by combining the fault isolation with TTF, prognostics schemes were introduced. In addition, for fault accommodation, a novel controller reconfiguration design guaranteed asymptotic performance for a class of nonaffine nonlinear system. The proposed fault prognostics and accommodation framework is able to detect and diagnose both the commonly classified incipient and abrupt fault types satisfactorily. Stability was guaranteed in the presence of system uncertainties, approximation errors and unknown fault dynamics. Additionally, the robustness and sensitivity of the fault detection scheme were demonstrated. Further, both a linearly parameterized approximator such as single layer NN and nonlinearly parameterized approximator such as multi-layer neural network (MN) were proposed for detection and accommodation.

2.1 CONCLUSIONS

In the first paper, a fault detection and prediction (FDP) scheme was developed for a class of multivariable nonlinear discrete-time system with state or process faults. The novel FD estimator design comprises of a robust adaptive term and an online approximator. After the detection, the unknown fault dynamics was learned online using

a suitable online approximator and it is observed that the fault learning is satisfactory. In addition, unlike other FD methods, the proposed update law relaxed the need of persistency of excitation (PE) condition. Using Lyapunov theory, the residual and the parameter estimation errors are shown to converge asymptotically. This result was achieved by using the robust adaptive term in the FD estimator, which is a function of the parameters of the online approximator. In addition, a TTF scheme using the parameter update law renders a satisfactory estimation of the remaining useful life. Finally, simulation results illustrate the satisfactory performance of the proposed FDP scheme. However, this FDP scheme assumes that all the states are available for measurement.

Therefore, this assumption was relaxed in the second paper. In addition, the robustness and sensitivity of the FDP scheme proposed was analyzed mathematically while the parameter update law of the online approximator was modified to take into account the output signals. Stability results guarantee the asymptotic convergence of the fault detection residual and parameter estimation errors. The TTF scheme was modified to consider the output signals and still rendered a satisfactory performance. However, this FDP scheme addressed only state faults.

Therefore, in the third paper, the FDP scheme was extended to a multi-input-multi-output (MIMO) nonlinear system with both state and sensor faults. A novel design of FDP scheme was proposed to successfully characterize both the state and the sensor faults. In addition, the sensitivity and the robustness were also addressed adequately. Using Lyapunov theory, asymptotic stability of the closed loop system was achieved by using the robust term design and making mild assumptions on the system uncertainties and online approximator reconstruction errors. The stability proof was complicated as the

residual and the parameter estimation errors of two online approximators were shown to converge asymptotically. The purpose of the two online approximators was to learn the state and sensor fault dynamics respectively. Individual TTF schemes for the process and sensor faults rendered satisfactory performance. Additionally, simulation results demonstrated the satisfactory performance in detecting and learning state and sensor faults.

The first three papers discussed only fault detection and not fault isolation (root-cause analysis). Thus in the fourth paper, a fault isolation scheme for a class of nonlinear system with state faults was introduced. Different fault conditions were considered, i.e., states with multiple faults and more than one fault type could effect the same state. Such fault conditions were not addressed in the previously reported isolation schemes. Unlike other schemes using adaptive thresholds for fault isolation, in this approach, a fault is successfully isolated if the corresponding fault isolation residual converges to zero. Such results were demonstrated in the presence of system uncertainties. Since fault isolation is combined with the parameter based TTF scheme, a stable prognostic scheme was developed.

Using Lyapunov analysis, the scheme is guaranteed to be asymptotically stable in terms of fault isolation residual and the parameter estimation error. In addition to the stability analysis, the fault isolability and fault isolation time guaranteed the isolation of faults in a finite amount of time. The simulation results demonstrated the successful isolation of the multiple faults in the given system. Additionally, the results rendered a satisfactory estimation of the remaining useful life when there is more than one fault parameter affecting the system.

In the fifth paper, a fault accommodation scheme for a class of nonlinear discrete time system with unknown state or process fault dynamics was proposed. Both a linearly and nonlinearly parameterized online approximators were used for designing the corrective control. In this design, the fault accommodation is achieved by reconfiguring the controller after the detection of fault. The tracking performance after the fault is verified through rigorous stability analysis, where the tracking and the parameter estimation errors converge asymptotically to zero for a linearly parameterized approximator. However, for a nonlinearly parameterized approximator only boundness of the parameter is shown while the tracking error still converges to zero. Additionally, the simulation results verify the theoretical conjectures.

Finally, in the sixth paper, a new artificial immune system (AIS) as an online approximator was used in the fault detection scheme. Unlike conventional offline based tuning methods, a new online adaptive parameter update law relaxing PE condition was proposed to tune AIS. Asymptotic convergence of the fault detection residual and the AIS parameter estimation error are demonstrated using Lyapunov theory. The proposed scheme demonstrates asymptotic performance both in simulation and experimentally. For the experimental results, a Caterpillar axial piston pump hydraulic test bed was used to demonstrate the satisfactory performance of the online learning and TTF determination.

2.2 FUTURE WORK

As part of the future work, the fault isolation scheme proposed could be extended to a nonlinear discrete system with state and sensor faults. This would complicate the

design and proving stability might be a challenge. In addition, deriving fault isolability condition and fault isolation time might require rigorous effort. However, the benefit is relaxing the requirement of all states measurability in using the isolation scheme. Additionally, this would help in simultaneous isolation of both the state and sensor faults.

Another possibility would be to extend the proposed fault accommodation scheme to a multivariable system with state and sensor faults. This would require the design of a suitable strategy for modifying the control law. The design would certainly be complicated as the control law depends upon the output signals alone. Additionally, the stability of the fault accommodation scheme using a single layer NN or MNN for such a class of nonlinear system should be addressed. Finally, the tracking performance by using the fault accommodation in the presence of both the state and sensor faults has to be shown.

In the context of AIS as online approximator, at present only one parameter of the AIS scheme is assumed tunable. However, in the future work the remaining other parameters could also be tuned. This would render better learning performance, but, verifying the stability of the parameters update law would be interesting and challenging. Additionally, with this online tuning capability, other possible application of AIS could be explored. Such areas could be control of nonlinear systems, system identification etc. However, deriving stability results for different applications of AIS might be an interesting area to explore.

VITA

Balaje Thandavamoorthy Thumati was born September 24, 1982 in Chennai, India. He earned the Bachelor of Engineering degree in instrumentation and control from University of Madras, India, in 2003 and Master of Science degree in measurement and control engineering from Idaho State University, ID, USA, in 2005. He is a member of IEEE – Institute of Electrical and Electronics Engineers. Balaje received the degree of Doctor of Philosophy in December 2009.